

**SELECTIVE OESTROGEN RECEPTOR MODULATORS  
Mechanisms of Action in the Reproductive Tract**

Thesis submitted for the degree of  
Doctor of Philosophy at the University of Leicester

**By Emma Parrott BSc (Hons)**  
Centre for The Mechanisms of Human Toxicity  
University of Leicester

October 2001

UMI Number: U149540

All rights reserved

INFORMATION TO ALL USERS

The quality of this reproduction is dependent upon the quality of the copy submitted.

In the unlikely event that the author did not send a complete manuscript and there are missing pages, these will be noted. Also, if material had to be removed, a note will indicate the deletion.



UMI U149540

Published by ProQuest LLC 2013. Copyright in the Dissertation held by the Author.  
Microform Edition © ProQuest LLC.

All rights reserved. This work is protected against  
unauthorized copying under Title 17, United States Code.



ProQuest LLC  
789 East Eisenhower Parkway  
P.O. Box 1346  
Ann Arbor, MI 48106-1346

## Table of contents

Table of contents .....	2
Abstract.....	12
Thesis associated publications .....	13
Acknowledgements.....	14
List of Abbreviations .....	15
<b>Chapter 1: General introduction.....</b>	<b>18</b>
<b>1.1 Breast cancer .....</b>	<b>19</b>
1.1.1 Hereditary breast cancer.....	19
1.1.2 Hormonal breast cancer.....	20
<b>1.2 Oestrogens.....</b>	<b>22</b>
1.2.1 Oestrogen metabolism .....	24
1.2.2 Oestrogen induced cell proliferation.....	25
<b>1.3 The oestrogen receptor.....</b>	<b>25</b>
1.3.1 Oestrogen receptor protein structure .....	26
1.3.2 Oestrogen receptor mode of action.....	29
1.3.3 Cell surface oestrogen receptor .....	30
1.3.4 Oestrogen receptor subtypes .....	31
1.3.5 Oestrogen receptor coactivators and corepressors.....	34

1.3.6 AP-1 pathway .....	38
1.3.7 Oestrogen receptor dimer formation .....	38
1.3.8 Oestrogen receptor variants .....	39
1.3.9 Oestrogen receptor knockout mice .....	40
1.3.10 Oestrogen receptor $\gamma$ .....	41
<b>1.4 Tamoxifen .....</b>	<b>42</b>
1.4.1 Uterotrophic effects .....	42
1.4.2 Carcinogenic effects of tamoxifen in rodents .....	44
1.4.3 Tamoxifen resistance .....	46
1.4.4 Tamoxifen's affinity for the oestrogen receptor .....	47
<b>1.5 Uterine histology .....</b>	<b>47</b>
<b>1.6 Endometrial cancer .....</b>	<b>49</b>
<b>1.7 Selective oestrogen receptor modulators .....</b>	<b>51</b>
1.7.1 Toremifene .....	51
1.7.2 Raloxifene .....	52
1.7.3 SERM clinical trials .....	53
1.7.4 Aromatase inhibitors .....	54
<b>1.8 Anti-oestrogens .....</b>	<b>55</b>
<b>1.9 Rodent models for oestrogen receptor regulation .....</b>	<b>56</b>
1.9.1 The rat model .....	56
1.9.2 The mouse model .....	57
1.9.3 The neonatal mouse model .....	58

1.9.4	Tumour formation.....	59
1.9.5	The role of oestrogen receptor expression in cell proliferation.....	60
<b>1.10</b>	<b>Uterotrophic responses to SERMs in adult rodents.....</b>	<b>62</b>
<b>1.11</b>	<b>Degradation pathways of the oestrogen receptor .....</b>	<b>62</b>
1.11.1	Proteasome-mediated degradation.....	63
<b>1.12</b>	<b>Aims .....</b>	<b>67</b>
<b>Chapter 2: Materials and Methods .....</b>		<b>69</b>
<b>2.1</b>	<b>Materials and Methods .....</b>	<b>70</b>
2.1.1	Animals and treatments .....	70
2.1.2	Chemicals and reagents .....	71
<b>2.2</b>	<b>Localisation of ER mRNA by <i>in situ</i> hybridisation.....</b>	<b>75</b>
2.2.1	Oligonucleotide probes for <i>in situ</i> hybridisation.....	76
2.2.2	Purification and quantification of oligonucleotide probes .....	77
	Table 2.1 Mouse ER $\alpha$ oligonucleotide probe sequences for <i>in situ</i> hybridisation .....	78
	Table 2.2 Mouse ER $\beta$ oligonucleotide probe sequences for <i>in situ</i> hybridisation .....	78
	Table 2.3 Rat ER $\alpha$ oligonucleotide probe sequences for <i>in situ</i> hybridisation .....	79
	Table 2.4 Rat ER $\beta$ oligonucleotide probe sequences for <i>in situ</i> hybridisation .....	79

2.2.3	Allyl amine labelling of oligonucleotides with digoxigenin at 5' and 3'	80
2.2.4	Dot blot hybridisation to test labelling efficiency	81
2.2.5	Aminopropyl triethoxysilane (APES) coated slides	82
2.2.6	Siliconised coverslips	82
2.2.7	Histology	83
2.2.8	Preparation of sections	83
2.2.9	Hybridisation of sections	84
2.2.10	Detection of hybridised probes	85
2.2.11	<i>In situ</i> hybridisation controls	85
<b>2.2.12</b>	<b>RT-PCR study to confirm <i>in situ</i> hybridisation probe specificity</b>	<b>86</b>
2.2.12.1	RNA extraction for RT-PCR	86
2.2.12.2	cDNA synthesis	88
2.2.12.3	RT-PCR amplification of rat ER $\alpha$ and ER $\beta$ full length transcripts	88
	Table 2.5 Rat ER $\alpha$ oligonucleotide primers for PCR	89
	Table 2.6 Rat ER $\beta$ oligonucleotide primers for PCR	89
2.2.12.4	Sequence confirmation by restriction enzyme digestion	90
2.2.12.5	Approximate quantification of PCR products using ethidium bromide	90
2.2.12.6	<sup>32</sup> P labelling of oligonucleotide cocktails	91
2.2.12.7	Column purification of labelled oligonucleotides	91
2.2.12.8	Dot blot hybridisation of PCR products and oligonucleotide cocktails	92
2.2.12.9	Hybridisation and detection	93

<b>2.3</b>	<b>Immunochemical methods of ER protein localisation .....</b>	<b>93</b>
2.3.1	Immunohistochemistry .....	93
2.3.1.1	Preparation of sections for ER $\alpha$ and ER $\beta$ detection .....	93
2.3.1.2	Antibody detection of ER $\alpha$ .....	94
2.3.1.3	Antibody detection of ER $\beta$ .....	94
2.3.1.4	Oil red O staining of fat deposits .....	95
2.3.2	Western blotting .....	95
2.3.2.1	Protein concentration determination .....	95
2.3.2.2	SDS-polyacrylamide gel electrophoresis and Western blotting.....	96
2.3.2.3	Detection .....	97
<b>2.4</b>	<b>Cell culture .....</b>	<b>98</b>
2.4.1	Cell culture .....	98
2.4.2	Subcultures .....	99
2.4.3	Preparing cells for storage in liquid nitrogen .....	99
2.4.4	Preparation of dextran charcoal stripped serum .....	100
2.4.5	Treatment of cells.....	100
2.4.6	Estimation of cell viability by trypan blue exclusion .....	101
2.4.7	Preparation of cell lysates for Western blotting.....	101
2.4.8	Fluorescence based determination of proteasome activity using Suc-LLVY-AMC .....	102
<b>2.5</b>	<b>Clontech Mouse 1.2 cDNA microarray analysis .....</b>	<b>103</b>
2.5.1	Total RNA extraction for cDNA arrays.....	103
2.5.2	DNase treatment of total RNA.....	104
2.5.3	Preparation of cDNA probes .....	104

2.5.4	Purification of labelled cDNA probes.....	105
2.5.5	Hybridisation of labelled cDNA to the Atlas Array .....	106
2.5.6	Post hybridisation washes and exposure .....	107
2.5.7	Stripping cDNA probes from Atlas Array .....	107
2.5.8	Analysis of Atlas cDNA Expression Array .....	108
2.5.9	Corroboration of Atlas Array results by semi-quantitative RT-PCR	108
	Table 2.7 Mouse primer sequences .....	110
<b>Chapter 3: ER protein degradation: response of the ER to oestradiol and related SERMs <i>in vitro</i>..... 111</b>		
<b>3.1</b>	<b>Introduction.....</b>	<b>112</b>
<b>3.2</b>	<b>Methods and Results.....</b>	<b>115</b>
3.2.1	Preparation of cell lysates for Western blotting.....	115
3.2.2	Western blot controls and recombinant protein concentrations .....	115
3.2.3	MCF-7 and Ishikawa ER expression .....	117
	Table 3.1 ER $\alpha$ and ER $\beta$ protein levels calculated from the density of the recombinant proteins .....	120
3.2.4	Growth curves with SERMs.....	121
3.2.5	Response of ER $\alpha$ expression to oestradiol and tamoxifen .....	123
3.2.6	Effect of proteasome inhibitors on cell viability.....	125
3.2.7	Effect of proteasome inhibitors on ER expression .....	127
<b>3.3</b>	<b>Discussion.....</b>	<b>137</b>

<b>Chapter 4: Localisation of ER<math>\alpha</math> and ER<math>\beta</math> in the ovariectomised rat and mouse uterus: visualised by <i>in situ</i> hybridisation and immunohistochemistry .....</b>	<b>141</b>
<b>4.1 Introduction.....</b>	<b>142</b>
<b>4.2 Methods and Results.....</b>	<b>145</b>
4.2.1 Morphological changes in ovariectomised rat uterus following treatment .....	145
4.2.2 ER $\alpha$ and ER $\beta$ mRNA localisation in the ovariectomised rat uterus	147
Table 4.1 Representative data for purified rat ER $\alpha$ oligonucleotides following purification .....	147
4.2.2.1 <i>In situ</i> hybridisation of ER $\alpha$ and ER $\beta$ mRNA in the ovariectomised adult rat uterus .....	149
4.2.3 ER $\alpha$ and ER $\beta$ protein localisation in the ovariectomised adult rat uterus .....	151
4.2.4 Morphological changes in ovariectomised mouse uterus following treatment .....	155
4.2.5 ER $\alpha$ and ER $\beta$ mRNA localisation in the ovariectomised adult mouse uterus .....	157
4.2.5.1 <i>In situ</i> hybridisation of ER $\alpha$ and ER $\beta$ mRNA in the ovariectomised adult mouse uterus.....	157
4.2.6 ER $\alpha$ and ER $\beta$ protein localisation in the ovariectomised adult mouse uterus .....	158

4.2.6.1	Immunohistochemical detection of ER $\alpha$ and ER $\beta$ protein in the ovariectomised adult mouse uterus.....	160
4.2.7	<i>In situ</i> hybridisation controls .....	162
4.2.7.1	Reverse transcriptase polymerase chain reaction (RT-PCR) confirmation of oligonucleotide probe specificity .....	164
4.2.7.2	Approximate quantification of PCR products using ethidium bromide .....	168
4.2.7.3	Dot blot hybridisation of ER $\alpha$ and ER $\beta$ PCR products and detection with $\alpha^{32}\text{P}$ labelled oligonucleotide cocktails.....	168
<b>4.3</b>	<b>Discussion.....</b>	<b>170</b>
<b>Chapter 5: The neonatal mouse model: uterine pathological changes and microarray identification of genes altered in response to oestradiol and related SERMs.....</b>		
<b>176</b>		
<b>5.1</b>	<b>Introduction .....</b>	<b>177</b>
<b>5.3</b>	<b>Results.....</b>	<b>180</b>
5.3.1	Pathological changes in the neonatal uterus.....	180
5.3.1.1	Adult animals.....	181
5.3.1.2	Neonatal animals .....	181
5.3.2	Uterine weights.....	183
	Table 5.1 Effects on animal and uterine weights of treatment with SERMs .....	185
5.3.3	Localisation of ER protein .....	186
5.3.4	Protein staining of fat cells .....	186

5.3.5 RNA extraction data .....	186
5.3.6 Clontech Atlas™ cDNA microarrays .....	188
5.3.7 Microarray data and gene analysis .....	188
Table 5.2 Total RNA yield from pooled neonatal mouse uterine tissues following DNase treatment.....	189
Table 5.3 Total radioactivity of <sup>32</sup> P labelled cDNA probes for microarray analysis.....	189
Table 5.4 Major changes in gene expression that occurred in common following either tamoxifen or toremifene treatment, compared with controls .....	194
5.3.8 PCR verification of altered gene expression .....	197
Table 5.5 Gene changes found only following oestradiol treatment when compared with control.....	198
Table 5.6 Gene changes occurring only following raloxifene treatment when compared with control .....	200
<b>5.4 Discussion.....</b>	<b>201</b>
<b>Chapter 6: General discussion .....</b>	<b>209</b>
<b>6.1 General discussion.....</b>	<b>210</b>
6.1.1 <i>In vitro</i> cell line model for ER degradation.....	210
6.1.2 Use of animal models for studying human endometrial cancers....	211
6.1.3 Adult ovariectomised rodent models .....	213
6.1.4 The neonatal mouse model.....	214
6.1.5 Conclusions.....	215

<b>Appendix 1.....</b>	<b>217</b>
<b>Appendix 2.....</b>	<b>241</b>
<b>Appendix 3.....</b>	<b>242</b>
<b>Reference List.....</b>	<b>243</b>

## Abstract

The increased incidence of endometrial cancers in women treated with tamoxifen, an adjuvant treatment for breast cancer, has led to the search for more tissue selective oestrogen agonists. The potential of the oestrogen receptor to regulate the response to oestrogen, tamoxifen and related compounds in the uterus has been investigated. The control of oestrogen receptor degradation was investigated in Ishikawa (endometrial) and MCF-7 (breast) cell lines. Results show that proteasome-mediated oestrogen receptor alpha and oestrogen receptor beta degradation was ligand dependent. The effects of selective oestrogen receptor modulators on the expression of oestrogen receptor alpha or oestrogen receptor beta were investigated in the uterus of ovariectomised Wistar (Han) rats and CD-1 mice using *in situ* hybridisation and immunohistochemistry. Results showed that both mRNA and protein were localised in the epithelial cells of the lumen and glands for both species. Treatment with oestradiol and tamoxifen caused an increase in expression of oestrogen receptor alpha and oestrogen receptor beta mRNA and protein throughout many cell types, compared to ovariectomised controls. The increase in oestrogen receptor expression, in combination with uterotrophic effects, suggests a role in cell proliferation. To further investigate the mechanisms of endometrial tumours, a neonate mouse model was used. It was shown for the first time that oral dosing of neonate CD-1 mice on days 2 to 5 after birth with tamoxifen or toremifene gave rise to adenomyosis by 3 months of age. An investigation into the accompanying changes of gene expression, by cDNA microarray analysis suggested nerve growth factor alpha, insulin-like growth factor 2 and preadipocyte factor 1 as candidate genes associated with the development of this condition.

## Thesis associated publications

**EL Parrott**, M Butterworth, AR Green, INH White and P Greaves (2001)

Adenomyosis - a result of disordered stromal differentiation *American*

*Journal of Pathology* 159:623-630

AR Green, **EL Parrott**, M Butterworth, PS Jones, P Greaves and INH White

(2001) Comparisons of the effects of tamoxifen, toremifene and

raloxifene on enzyme and gene expression in the rat uterus *Journal of*

*Endocrinology* 170:555-564

PS Jones, **EL Parrott** & INH White (1999) Activation of

transcription by estrogen receptor  $\alpha$  and  $\beta$  is cell type and promoter

dependent *Journal of Biological Chemistry* 274:32008-32014

## **Acknowledgements**

I would like to thank my supervisor, Dr Ian White for his invaluable guidance and encouragement during the completion of this thesis. I am also grateful to Andy Green, Michael Butterworth, Paul Jones, Nihal Razvi, Anna Simpson, Richard and Jenny Edwards for their contributions to this work. I would also like to thank Dr Peter Greaves for his expert help and advice.

## List of Abbreviations

AF-1	transcriptional activation function 1
AIB1	amplified in breast cancer 1
APES	aminopropyl triethoxysilane
BCPT	breast cancer prevention trial
BERKO	ER $\beta$ knockout mouse
bFGF	basic fibroblast growth factor
BLAST	Basic Local Alignment Search Tool
bp	base pair
BRCA ( <i>brca</i> )	breast cancer susceptibility gene
BSA	bovine serum albumin
CBP	cAMP response element binding protein
cDNA	complementary DNA
cpm	counts per minute
DAB	3, 3'-diaminobenzidine tetrahydrochloride
DEPC	diethyl pyrocarbonate
DES	diethylstilbestrol
dH <sub>2</sub> O	distilled water
DIG-NHS	digoxygenin 3-O-methylcarbonyl- $\epsilon$ -aminocaproic acid N-hydroxysuccinimide ester
DMEM	Dulbecco's Modified Eagle's Medium
DMSO	dimethylsulfoxide
DNA	deoxyribonucleic acid
dNTP	dideoxy nucleoside triphosphate

DTT	dithiotheitol
E <sub>1</sub>	oestrone
E <sub>2</sub>	17 $\beta$ -oestradiol
ECL	Enhanced Chemiluminescence
EDTA	ethylenediaminetetraacetic acid tetrasodium salt
EGF ( <i>egf</i> )	epidermal growth factor
EGR-1 ( <i>egr-1</i> )	early growth response protein 1
ER ( <i>er</i> )	oestrogen receptor/s
ERE	oestrogen response element
ERKO	ER $\alpha$ knockout mouse
ERK	extracellular-signal related kinase
ERR	oestrogen-related receptor
FBS	foetal bovine serum
GAPdh ( <i>gapdh</i> )	glyceraldehyde-3-phosphate dehydrogenase
GRIP	glucocorticoid receptor interacting protein 1
HRP	horseradish peroxidase
IGF-2 ( <i>igf-2</i> )	insulin-like growth factor 2
IMS	industrial methylated spirits
LCM	laser capture micro-dissection
MAPK	mitogen activated protein kinase
MEK	mitogen-activated protein kinase kinase
mRNA	messenger RNA
NBF	neutral buffered formalin
N-CoR	nuclear receptor corepressor
ND	not determined

NGF- $\alpha$ ( <i>ngfa</i> )	7S nerve growth factor alpha
PAGE	polyacrylamide gel electrophoresis
PBS	phosphate buffered saline
PCR	polymerase chain reaction
PNACL	Protein and Nucleic Acid Sequencing Laboratory
PR	progesterone receptor
PREF-1 ( <i>pref-1</i> )	preadipocyte factor 1
RAC3	receptor coactivator 3
RNA	ribonucleic acid
RT	room temperature
RT-PCR	reverse transcriptase polymerase chain reaction
SDS	sodium dodecyl sulfate
SERM	selective oestrogen receptor modulator
SMRT	silencing mediator of retinoid and thyroid hormone receptor
SRC-1	steroid receptor coactivator
ss	single stranded
TBS	tris buffered saline
TdT	terminal deoxynucleotide transferase
TGF ( <i>tgf</i> )	transforming growth factor
TIF2	transcriptional intermediary factor
T <sub>m</sub>	melting temperature
UP	ultra pure
VEGF	vascular epidermal growth factor

## **Chapter 1: General introduction**

## 1.1 Breast cancer

Breast cancer is one of the most frequent malignancies in women. Each year over 35 370 new cases are being diagnosed in the UK, which accounts for 1 in 4 female cancers. In the general population, the cumulative lifetime risk of developing breast cancer is estimated at 10%: approximately 75% of breast cancers are found in postmenopausal women over the age of 50 (Osteoporosis Int., 1997). In 1996, 13 198 died from the disease in the UK (Cancer Research Campaign, 2000). However, there was a substantial decrease in breast cancer death rates in the UK between 1987 and 1997, and mortality figures continue to decrease. The annual breast cancer death rate for women between the ages of 20-49, 50-69 and 70-79 has decreased by 22%, 22% and 12% respectively (Peto *et al.*, 2000). These dramatic changes in breast cancer mortality rates are due both to changes in the way the disease is diagnosed and treated (Peto *et al.*, 2000; Blanks *et al.*, 2000).

### 1.1.1 Hereditary breast cancer

A family history of breast cancer is one of the risk factors of the disease. If a woman has a first-degree relative with breast cancer (i.e. a mother or sister) her risk of developing the disease doubles, comparatively her risk will increase by five fold if she has two first-degree relatives with the disease (Claus *et al.*, 1991). In the US and European populations, 5-10% of breast cancers are hereditary. Hereditary breast cancers are characterised by an early onset of the cancer, transmission of the cancer through successive generations and an association with ovarian, colon and prostate cancers (Yang *et al.*, 1999).

Hereditary breast cancers are accounted for by several genes including *BRCA1* and *BRCA2* (Yang *et al.*, 1999). *BRCA1* was first associated with inherited breast cancer in 1990 and mapped to chromosome 17q21 (Hall *et al.*, 1990), this was followed by the identification of *BRCA2*, which was mapped, to chromosome 13q12-13 in 1994 (Wooster *et al.*, 1994). Mutations within these genes predispose women to early onset breast cancer (Easton *et al.*, 1993) and their isolation allows direct screening for mutations and identification of women at risk of hereditary breast cancer. *BRCA1* has been associated with ovarian cancer (Easton *et al.*, 1993) however; the incidence of *BRCA* related breast cancer is not known to be associated with endometrial cancer. Both genes are thought to be tumour suppressor genes associated with response to DNA damage including checkpoint activation, gene transcription and DNA repair (Bhattacharyya *et al.*, 2000). *BRCA1* has recently been shown to activate the androgen receptor in breast cancer cell lines, an action mediated through the NH<sub>2</sub>-terminal activation function of the receptor: thus *BRCA1* may be involved in androgen regulated proliferation (Park *et al.*, 2000). A recent study describes a role for *BRCA2* in human cell division: mutation of *BRCA2* dramatically slows the cells ability to pass through mitosis, suggesting a unique role for *BRCA2* in the progress of the cell cycle (Futamura *et al.*, 2000).

### **1.1.2 Hormonal breast cancer**

Hormone related cancers have a different mechanism of carcinogenesis from, for example, genotoxic carcinogens whereby the ability of both the endogenous and exogenous hormone to drive cell proliferation increases the number of cell

divisions and thus the possibility of random genetic errors. The introduction of genetic errors during replication eliminates the need for a specific initiator although the stimulation provided by the hormone is required throughout progression. A break in the hormonal stimulation, provided by the appropriate hormone antagonist, can slow the progression of the cancer (Henderson *et al.*, 2000).

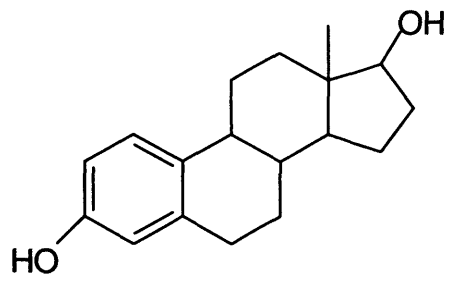
There is a large amount of evidence implicating oestrogens in the aetiology of breast cancer (Fishman *et al.*, 1995). Oestrogens have been shown to cause tumours in the mammary glands of rodents and the removal of the ovary, or treatment with the appropriate oestrogen antagonist, has the opposite effect (Nandi *et al.*, 1995). Figures recently reviewed show that women who are postmenopausal, and have subsequently developed breast cancer, have a 15% higher level of serum oestrogens than women who are not affected by the disease (Henderson *et al.*, 2000).

Breast cancer risk factors can be taken as measures of the cumulative dose of oestrogen the responsive tissue is exposed to over time. These risk factors include increased oestrogen exposure by early menarche and/or late menopause. Post-menopausal obesity increases a woman's risk by 50% and hormone replacement therapy also slightly increases risk. Women will have an increased risk if they do not have children, or if they bear their first child after the age of 30 (Imperial Cancer Research Fund, 2000). Factors which may protect women from the disease include decreased hormone exposure by a young age at first full term pregnancy, prolonged lactation and exercise.

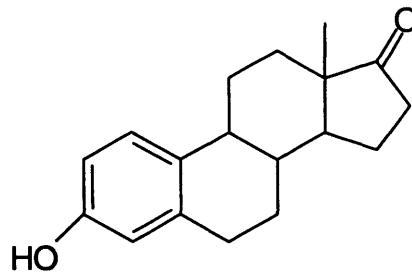
## 1.2 Oestrogens

Oestrogens are members of the steroid hormone superfamily and primarily regulate female reproductive functions. The predominantly occurring endogenous oestrogens are oestrone ( $E_1$ ) and  $17\beta$ -oestradiol ( $E_2$ ) (Figure 1.1). The most biologically active form in pre-menopausal women is  $E_2$ . Oestrogens regulate the development and maintenance of female primary and secondary sexual characteristics. They are additionally involved in the cardiovascular system, the central nervous system and the remodelling of the skeleton. In postmenopausal women, biosynthesis of oestrogen in the ovary dramatically declines causing a range of physiological effects in steroidogenic target tissues. The decrease in circulating oestrogen in postmenopausal women has been implicated in osteoporosis (Lindsay *et al.*, 1991), coronary heart disease (Bush *et al.*, 1990) and Alzheimer's disease (Henderson *et al.*, 1994; 1997). Although oestrogen is considered to be a 'female' hormone, it occurs in males and sexual distinctions arise as a result only from quantitative divergence in hormone concentrations and differential expression of steroid hormone receptors (Hess *et al.*, 1997).

Oestrogens mediate their effects by regulating gene expression in target cells of which the endometrium is one of the primary target tissues. Oestrogens are also important endocrine factors influencing the growth and development of the normal breast epithelium. The hormone controls the expression of genes to adapt the tissue functions to the stages of reproduction. Therefore an important mechanism in modulating target tissue growth, differentiation and function is the regulation of oestrogen levels.



17β-Oestradiol



Oestrone

**Figure 1.1** Chemical structures of 17β-oestradiol and oestrone

### 1.2.1 Oestrogen metabolism

Oestrogen biosynthesis occurs primarily in the ovarian granulosa cells of premenopausal women and within adipose tissue of postmenopausal women (Simpson *et al.*, 1989). In the ovary, oestradiol is synthesised from testosterone (Pearlstone *et al.*, 1999), by the aromatase enzyme complex. This enzyme complex includes aromatase cytochrome P-450 (Simpson *et al.*, 1989), which is encoded by the CYP19 gene (Toda *et al.*, 1995). Most oestrone is produced in the ovary but some is produced in the liver from oestradiol and in adipose tissue, from the principle oestrogen precursor androstenedione. Oestrogens are a major causative factor of endometrial cancer in postmenopausal women and have been implicated in the pathogenesis of some types of breast cancer (Simpson *et al.*, 1989).

Intracellular metabolism of oestrogens is critical in altering their effects on target cells. Oestrogens are eliminated from the body by conversion to hormonally less active, or inactive, water-soluble molecules that are excreted. Metabolism of oestrogens for excretion from the body may result in some oestrogenic action from the formation of active oestrogen metabolites (Zhu *et al.*, 1998). Oestradiol is metabolised into 2-hydroxyoestradiol and 4-hydroxyoestradiol: these metabolites can react with DNA (Tsutsui *et al.*, 1997) and it has been suggested that these may have a role in the carcinogenic effects of oestrogen in responsive tissues (Service, 1998; Zhu *et al.*, 1998; Liehr *et al.*, 2000).

### 1.2.2 Oestrogen induced cell proliferation

In the appropriate target tissues, oestrogen and some of its metabolites are powerful stimulators of cell proliferation and may contribute to the progression of tumours in the breast and uterus. The hormone can modify the production of intracellular growth factors and their receptors, such as transforming growth factor alpha (TGF- $\alpha$ ) (Simpson *et al.*, 1998), vascular epidermal growth factor (VEGF) (Hyder *et al.*, 1996) and basic fibroblast growth factor (bFGF) (Rider *et al.*, 1997), inducing a cascade of transcriptional events altering cell physiology.

### 1.3 The oestrogen receptor

Oestrogens mediate their effects in target tissues through the oestrogen receptor/s (ER) first identified by Gorski *et al.*, (1968) and Jensen *et al.*, (1972). The ER is a member of the superfamily of steroid nuclear hormone receptors and was cloned and sequenced by Greene *et al.*, in 1986. This superfamily includes receptors for the steroid hormones, thyroid hormones, vitamin D and also retinoic acid, as well as orphan receptors that respond to as yet unidentified ligands. Orphan receptors include the oestrogen-related receptors (ERR $\alpha$ , ERR $\beta$ ) and the recently identified ERR $\gamma$ , these receptors have a high level of sequence homology to the ER and can bind to functional oestrogen response elements (Coward *et al.*, 2001). ER are ligand activated transcription factors which transduce extracellular signals into transcriptional responses.

Activating ligands include oestrogens, of which E<sub>2</sub> has the highest binding affinity. Other steroids, such as androgen, can also bind and activate the ER

although biological activity is minimal (Ekena *et al.*, 1998). A large number of aromatic synthetic oestrogens, for example diethylstilbestrol (DES) and its derivatives, bind ER and transactivate oestrogen responsive genes (Chae *et al.*, 1991; 1998). The naturally occurring, dietary phytoestrogens: coumestrol and genistein also bind to and activate the ER (Kuiper *et al.*, 1998; Nikov *et al.*, 2000) acting as oestrogen agonists *in vitro* (Makela *et al.*, 1994) and may trigger responses mediated by physiological oestrogens.

The human gene for the ER, which is approximately 140kb long, is located on chromosome 6 (Evans *et al.*, 1988). The ER gene is transcribed from three different promoters producing proteins with unique 5' untranslated regions and identical coding regions. Two of the transcripts were found in the uterus and breast, and the other predominantly in the liver (Grandien *et al.*, 1997). The ER gene encodes a protein of 595 amino acids (66kDa) whose X-ray crystalline structure has been reported (Brzozowski *et al.*, 1997). Helices H3 to H12 of the ER ligand-binding domain are folded into an  $\alpha$ -helical sandwich flanked by a  $\beta$ -pleated sheet, in a similar manner to other nuclear receptors crystal structure. E<sub>2</sub> binds the ER diagonally across the cavity between H11, H3 and H6: the structure of the receptor allows it to bind wide variety of compounds which, to be effective, must have an aromatic ring (Brzozowski *et al.*, 1997).

### 1.3.1 Oestrogen receptor protein structure

As with most steroid nuclear receptors, the ER gene has 8 exons coding 6 functional domains labelled A-F (Figure 1.2). The **A/B domain**, coding the

amino terminal domain of the protein, is not conserved between receptors. This domain contains an independent transcriptional activation function 1 (AF-1) that can activate transcription when linked to a DNA binding domain. Phosphorylation of serine 118 is important for the action of AF-1 (Ali *et al.*, 1993). The cysteine rich DNA binding domain (**domain C**, spanning exons 2 and 3) is approximately 70 amino acids and contains two zinc finger-like motifs that direct the sequence specific binding of the ER to the oestrogen response element (ERE) (Schwabe *et al.*, 1990). The ERE consists of a specific 13 base pair DNA palindrome GGTCAnnnTGACC; the consensus sequence is an inverted repeat with the three central nucleotides acting as a spacer between the palindromic half-sites of the ERE. The C domain also contains a nuclear localisation signal enabling the protein to be targeted to the nucleus after translation. **Domain D** contains the hinge region. Ligand binding is located within **domain E** (spanning exons 4-8) with the AF-2 whose activity is ligand dependent. Dimerisation and further nuclear localisation functions are located in **domain F** (Ferguson *et al.*, 1997) as well as a role in distinguishing between agonist and antagonist binding to the ER (Pavao *et al.*, 2001).

A conserved function of steroid hormone receptors is the auto-regulation of their gene expression. In human cell lines, oestrogen is the primary regulator for ER stability and *in vitro* down regulates the half-life of ER mRNA by approximately 6 fold (Saceda *et al.*, 1998); also decreasing ER transcription rates by 40% (Lee *et al.*, 1998).

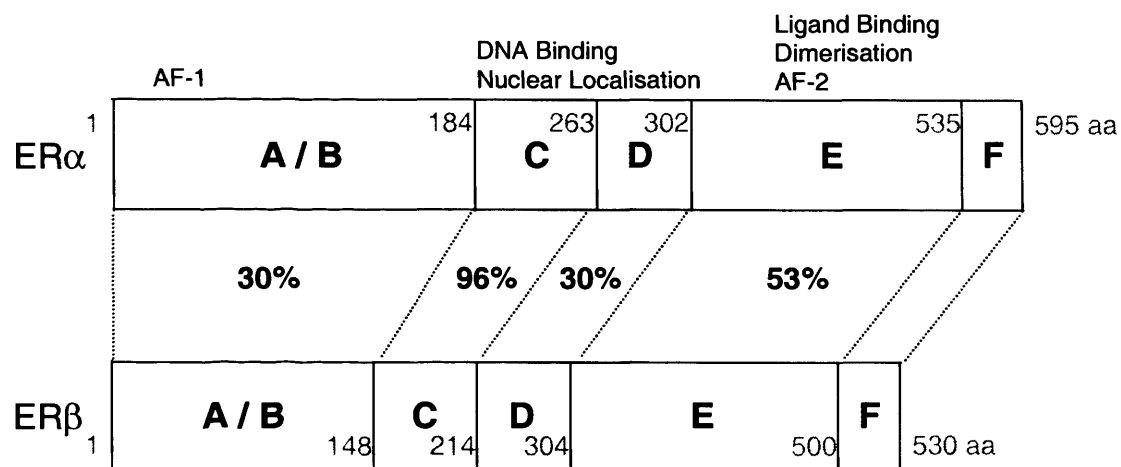


**Figure 1.2** Comparison of human ER $\alpha$  and ER $\beta$  protein domains (adapted from Ogawa *et al.*, 1998 and Pavao *et al.*, 2001).

Early studies in MCF-7 human breast cancer cells demonstrated down regulation of ER in the presence of oestrogen where ER protein was localised within the cytoplasmic and nucleic fractions of the cells. Within 30min of oestradiol treatment, and for the following 3-5h, nuclear ER was depleted by 70% before stabilising; 30% depletion was observed following the addition of tamoxifen (Horwitz *et al.*, 1978).

### 1.3.2 Oestrogen receptor mode of action

Heat shock protein, HSP 90, disables transactivation of the ER whilst no ligand is bound and keeps it in a high affinity hormone-binding conformation (Fliss *et al.*, 2000). Upon binding, the ligand induces conformational changes that expose areas of the receptor and enable it to bind DNA and recruit coactivators (Beekman *et al.*, 1993) (see below). The receptors dimerise and bind to DNA at sites including the oestrogen response element (ERE).

EREs are located upstream of promoter regions in oestrogen responsive genes leading to transactivation of target genes, such as *c-myc*, *tgf- $\alpha$* , *bcl2*, *cyclin D1* (Ferguson *et al.*, 1997), the progesterone receptor (PR) and oxytocin receptors (Young *et al.*, 1998). In some cases, the receptors cause repression of transcription where the ER complex interacts with corepressors and associated histone deacetylases (Xu *et al.*, 1999). Formation of a stable pre-initiation complex, with the assembly of basal transcription factors, increases the rate of initiation by RNA polymerase II (Mitchell *et al.*, 1989). This is followed by the

hormonal effect: either induction of cellular proliferation/division or production of additional hormone receptors and growth factors.

Transcriptional activation is mediated through both AF-1 (domain A/B) and AF-2 (domain E) although only activation of AF-2 requires hormone binding. Serine 118, within the A/B domain of the receptor, is a target for phosphorylation and is phosphorylated in a ligand dependent manner. This phosphorylation is important for the action of AF-1 (Ali *et al.*, 1993). AF-1 can be activated via the mitogen activated protein kinase (MAPK) pathway as MAPK directly phosphorylates serine 118 (Bunone *et al.*, 1996). Ligand independent activation of the ER occurs by growth factors, for example epidermal growth factor (EGF), that activate the ER by signalling through the MAPK pathway (Bunone *et al.*, 1996), as described below. AF-1 and AF-2 can act independently or synergistically to enhance transcription (Tora *et al.*, 1989; Metzger *et al.*, 1995). Studies in human uterine tissue show that activation of AF-2 is necessary for agonist activity (Hunter *et al.*, 1999).

### **1.3.3 Cell surface oestrogen receptor**

Through the classical ER signalling pathway, oestrogen enters the cell and is translocated to the nucleus to the ER where DNA binding and transcription of oestrogen responsive genes occurs. However, the rapid oestrogen effects observed in vasculature, neurones and bone suggest the involvement of non-genomic signalling pathways. Cell surface ER coupled to intracellular signalling pathways have been reported previously (Pietras *et al.*, 1977). There is now

immunological evidence for ER $\alpha$  localised at the plasma membrane in MCF-7 cells, although further studies are required to determine the individual biological role of the membrane receptors (Monje *et al.*, 2001).

Studies, in ER transfected rodent ovarian cells, have also shown that a single cDNA and RNA transcript are capable of producing both the cell surface and the nuclear ER, and that both have very similar affinities for E<sub>2</sub> (Razandi *et al.*, 1999). Recent data suggests a direct link between cell surface ER and the MAP kinase-signalling cascades (Collins and Webb, 1999).

The MAP kinase family includes extracellular-signal related kinases (ERKs). ERKs signal through a pathway involving sequential activation of Ras, Raf and mitogen-activated protein kinase kinase (MEK) (Collins and Webb, 1999). Upon binding oestrogen, the ER activates ERK-related kinases, leading to cell proliferative effects (Razandi *et al.*, 1999). This concept of ER mediated action suggests a role for the receptor in rapid intracellular signalling pathways involved in cell cycle control (Figure 1.3).

#### **1.3.4 Oestrogen receptor subtypes**

Since the discovery of the ER, now termed ER $\alpha$ , it was believed the action of oestrogen was mediated through this alone. However a second ER, ER $\beta$ , was identified in human tissue (Mosselman *et al.*, 1996), following the discovery of the 54.2kDa subtype in rat prostate (Kuiper *et al.*, 1996).

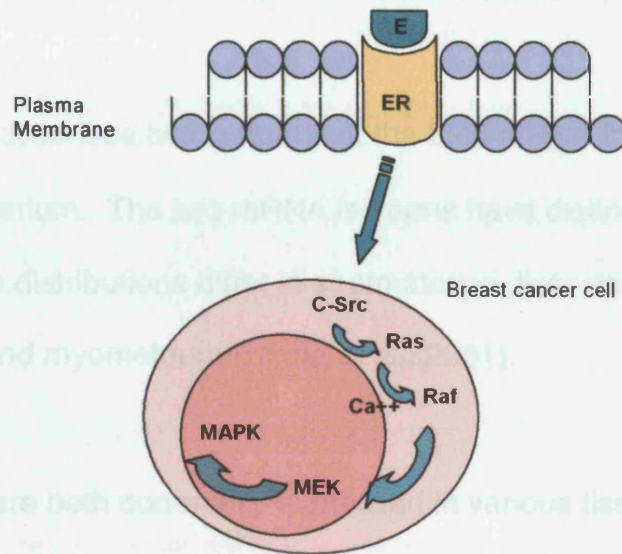


**Figure 1.3** Mechanism of cell surface ER mediated action. In MCF-7 breast cells E<sub>2</sub>-ER interaction results in intracellular Ca<sup>++</sup> dependant activation of the c-src-Ras-Raf-MAPK pathway that may be important in cell cycle control. E<sub>2</sub> binding activates ERKs that signal through sequential activation of Ras, Raf and MEK (adapted from Collins and Webb, 1999).

ER $\alpha$  and ER $\beta$  have a high degree of conservation in the DNA and ligand binding domains (Figure 1.2). There is a 96% level of homology between the DNA binding domains of the two subtypes and a 53% level of homology between the ligand binding domains; suggesting the subtypes would bind to similar response elements. However, the A/B domain, hinge region and F domains show little conservation (Mosselman *et al.*, 1996).

A recent study describes two isoforms of the ER $\beta$  mRNA in normal human uterine endometrium. The two mRNA isoforms have distinct 5' untranslated regions and the distributions differ in spermatozoa, liver and uterine endometrium and myometrium (Hirata *et al.*, 2001).

ER $\alpha$  and ER $\beta$  are both commonly expressed in various tissues, level of expression can differ and, in some cases, may be cell or tissue specific. Mosselman *et al.*, (1996), initially localised human ER $\alpha$  within the ovaries, testis, prostate and skeletal muscle, and ER $\beta$  expression within the thymus, spleen and testis. Thus identifying some overlap in tissue distribution of the two proteins. The specific data on subtype expression will be discussed in Chapter 3. The two receptors also have differing responses to varying ligands including tamoxifen, raloxifene and ICI 164,384, where these ligands have an ER $\alpha$  selective partial agonist/antagonist function and a pure antagonist effect through ER $\beta$  (Barkhem *et al.*, 1998). Novel non-steroidal ligands also show subtype selective differences in ligand binding and transcriptional potency in ER transfected human endometrial and Chinese hamster ovary cell lines (Sun *et al.*, 1999).

### 1.3.5 Oestrogen receptor coactivators and corepressors

Interaction of ER with accessory proteins leads to the modification of the transcription of target genes. In the absence of ligand, ER interacts with corepressors, e.g. N-CoR and SMRT which target histone deacetylases to keep a repressed chromatin structure; in the event of ligand binding the receptors dissociate and interact with coactivators, e.g. steroid receptor coactivator-1 (SRC-1) which amplify ER signal transduction (Ferguson *et al.*, 1997) and enhance the activity of the ER AF-2 (Misiti *et al.*, 1998) (Figure 1.4). The mechanisms by which corepressors repress transcription are thought to be linked to histone deacetylation and to coactivators recruiting histone acetyltransferases. Thus indicating that the whole mechanism is linked to the chromatin structure (Chen *et al.*, 1998).

Nuclear receptor coactivators include the family of p160: SRC-1, N-CoA1 or RAC3 (which potentiate ER activity), TIF2 or GRIP1 (transcriptional intermediary factor) and AIB1. AIB1 is a major ER coactivator in MCF-7 cells that increases with E<sub>2</sub> treatment (Tikkanen *et al.*, 2000). AIB1 can also enhance the functional interaction of the ER with the cyclin D1 promoter that may represent oestrogen-dependent mytogenic stimulation in MCF-7 cells (Planas-Silva *et al.*, 2001). CBP (cAMP response element binding protein) and p300 are also essential coactivators that interact with SRC-1 (Glass *et al.*, 1997). Coactivators CBP, SRC-1 and AIB1 have histone acetyltransferase activity and can modify the chromatin structure (Shang *et al.*, 2000).

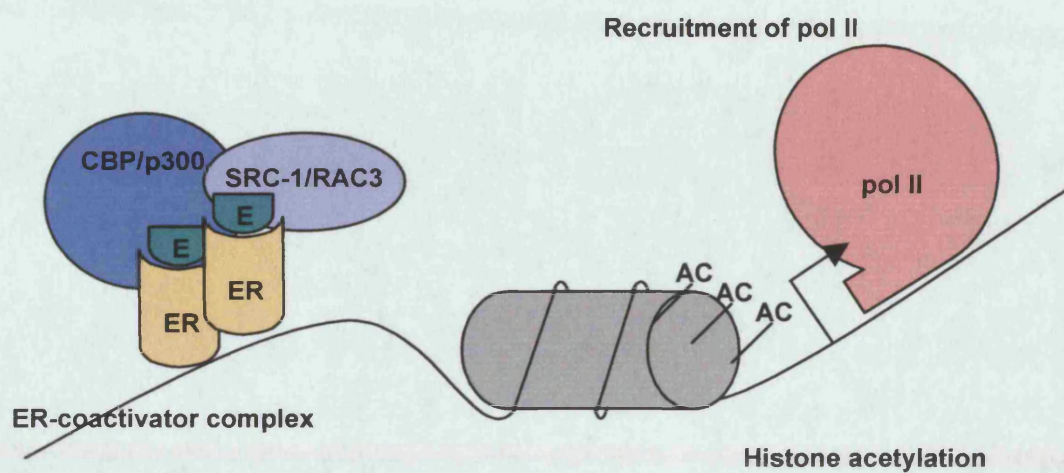


**Figure 1.4** Coactivator interactions with ER in the presence of  $E_2$ . ER recruits coactivators including SRC-1 and CBP leading to histone acetylation, an open chromatin structure and transcriptional activation (adapted from Ferguson *et al.*, 1997).

Ligands regulate ER AF-2 activity by directly affecting the structure of the ligand-binding domain. E<sub>2</sub> and raloxifene bind at the same site within the core of the ligand-binding domain (Brzozowski *et al.*, 1997) but each of the ligands induces a different conformation of helix 12 of the ER. X-ray crystallographic analysis (Brzozowski *et al.*, 1997; Shiau *et al.*, 1998) show that unlike E<sub>2</sub>, the dimethylaminoethoxy side chain of 4-hydroxytamoxifen causes a conformational change in the ligand-binding domain complex, causing helix 12 to occlude the cofactor recognition groove. As described above, several proteins: SRC-1/RAC3 (Onate *et al.*, 1995), TIF2/GRIP1 (Hong *et al.*, 1996) and AIB1 (Anzick *et al.*, 1997) associate in a ligand dependent manner with ER $\alpha$  to enhance transcriptional activation.

Studies of MacGregor and colleagues (1998) showed that in breast cancer cells 4-hydroxytamoxifen acts as an anti-oestrogen silencing AF-2 activity. The crystal structure shows a loose interaction between 4-hydroxytamoxifen and amino acid 351 in the ER. In cell lines in which there is a D351G mutation, 4-hydroxytamoxifen and raloxifene act as pure oestrogen agonists since helix 12 no longer blocks coactivator activation. The amino acid at 351 is an important regulator of the oestrogen-like action of SERMs (Liu *et al.*, 2001). In a study using the D351Y ER $\alpha$  mutant Lui and colleagues describe that to enhance the oestrogen-like properties of the SERM coactivator complexes require AF1 and an intact helix 12.

The corepressor and coactivator proteins have varying levels of expression throughout different tissue and cell types suggesting a role in the tissue specific

activation of oestrogen regulated genes (Misiti *et al.*, 1998). In addition, ligand dependent differences in ER subtype coactivator recruitment have been demonstrated in transiently transfected HeLa cells (Routledge *et al.*, 2000). Therefore expression levels of coactivators and corepressors will determine the effect of a ligand on a particular cell type.

In studies using an ER $\alpha$ -GFP chimera, it has been demonstrated that E<sub>2</sub> and tamoxifen alter the cellular distribution of the ER in MCF-7 cells. It was also shown that ER $\alpha$  and the coactivator SRC-1 co-localise in the nuclear matrix bound fraction in response to E<sub>2</sub> but not tamoxifen, and that the SRC-1 LXXLL motif is required for this intranuclear co-localisation (Stenoien *et al.*, 2000). A further coactivator; PGC-1 has been shown to interact in a ligand dependent manner with the hinge domain of ER $\alpha$ . PGC-1 is functionally and mechanistically distinct from the p160 group of coactivators (Tcherepanova *et al.*, 2000). These findings show that coactivators can bind to the ER $\alpha$  in different ways, this, along with the evidence that the receptor structure changes according to the bound ligand, may provide evidence for the fact that ligands acting through the same receptor can amount to different effects in cell types (Tcherepanova *et al.*, 2000). RAC3 has been identified as a potent ER $\beta$  coactivator interacting with ER $\beta$  via specific LXXLL motifs in the RAC3 receptor-interacting domain (Leo *et al.*, 2000). Recently a new class of ligand-regulated coactivators represented by CIA (coactivator independent of AF-2 function) have been reported (Sauve *et al.*, 2001). Thus adding more diversity to this already complex system.

### 1.3.6 AP-1 pathway

The ER can mediate gene transcription via an AP-1 enhancer element in addition to the classical ERE. The AP-1 element requires ligand and the AP-1 transcription factors fos and jun to enhance transcription via the ER AFs (Webb *et al.*, 1999). *In vitro* studies show that ER $\alpha$  and ER $\beta$  differentially respond to ligands via the AP-1 element (Paech *et al.*, 1997). It appears that SERMs such as tamoxifen and raloxifene can activate ER $\beta$ -mediated transcription (Jones *et al.*, 1999). *In vitro* studies suggest that E<sub>2</sub>-liganded ER enhances AP-1 activity via interactions with p160 coactivators and that anti-oestrogen bound ER enhances AP-1 activity via interactions with corepressors. It was shown that ER $\beta$  only enhances AP-1 dependent transcription in the presence of anti-oestrogens (Webb *et al.*, 1999). These studies suggest subtype specific differential ligand-dependant activation.

### 1.3.7 Oestrogen receptor dimer formation

In addition to homodimers, ER $\alpha$  and ER $\beta$  form heterodimers, suggesting another dimension to oestrogen responsiveness (Pettersson *et al.*, 1997). The heterodimer can also bind to DNA and recruit the coactivator SRC-1 (Cowley *et al.*, 1997, Pace *et al.*, 1997). Heterodimers of ER $\alpha$  and ER $\beta$  have been demonstrated both *in vitro* and *in vivo*, however, the subtypes activate transcription independently. This may be due to the differences in the AF-1, as there is only 30% homology between the sequences of the ER $\alpha$ / $\beta$  A/B domain (Ogawa *et al.*, 1998). Formation of functional heterodimers has been shown in several studies but the consequences of heterodimers on signalling have not

been fully determined. These studies suggest that the formation of heterodimers would add another dimension to the subtype specific activation described so far.

### **1.3.8 Oestrogen receptor variants**

In addition to the classical ER $\alpha$ , variants of the subtype are now being identified, whether or not they play a significant role in these proceedings is yet to be elucidated. Five ER $\alpha$  variants have been reported in the mouse produced by alternative splicing with variation in the 5' untranslated regions (Kos *et al.*, 2000). Human ER $\alpha$  variants have been identified in endometrial adenocarcinoma samples where all specimens contained an exon 5 deletion (Jazaeri *et al.*, 1999).

Variants of the ER $\beta$  gene have also been identified in rodents with expression verified in a range of tissues. A highly expressed ER $\beta$  variant has been isolated from mouse and has a 54-nucleotide insertion between exons 5 and 6. The protein has an 18 amino acid insert in the ligand-binding domain, which a recombinant form of the protein showed reduced the subtype's affinity for oestradiol (Lu *et al.*, 2000). The data from the study of Lu *et al.* suggest that ER $\beta$ 2 may have tissue specific and promoter specific modulatory effects. Rat ER $\beta$ 2 mRNA is expressed at equal levels to ER $\beta$  in rat ovary, prostate and pituitary and encodes a specific functional receptor responsive to oestradiol and oestrogenic agents (Petersen *et al.*, 1998).

Study of human ER variants in breast cancer suggests that their detection by immunohistochemistry may account for some inconsistencies between ER status and response to endocrine therapy (Huang *et al.*, 1999). A recent assessment of ER variants in human breast cancer specimens suggests that the low level occurrence of ER variants in breast cancer did not contribute to its progression (Anandappa *et al.*, 2000). An ER subtype variant, with a significant role in the initiation or progression of malignancy, has not yet been identified.

### **1.3.9 Oestrogen receptor knockout mice**

In order to determine the role of specific ER subtypes knockout animal models have been produced. Lubahn *et al.* first described the ER $\alpha$  knockout mouse (ERKO) in 1993. The mouse was produced by an insertion into exon 2 of the ER gene that inhibited its functional expression (Lubahn *et al.*, 1993). This model allows the determination of the effects of oestrogen through ER $\alpha$  in a variety of tissues, some of which mimic a case of ER $\alpha$  mutation in a male human patient (Korach *et al.*, 1994). Sex determination in the ERKO is not affected and not lethal, however homozygous  $-/-$  mice, both male and female are infertile and there is no uterotrophic response to tamoxifen (Korach *et al.*, 1994). The female ERKO have undeveloped mammary glands, 20-25% lower bone density and the uteri are hypoplastic and half the weight. The male ERKO have reduced testicular weight. Oncogene induced mammary tumours proliferate at a significantly decreased rate suggesting a role for ER $\alpha$  in promotion (Couse *et al.*, 1999). To date, the ERKO suggest that ER $\alpha$  is the major player in oestrogenic response (Cooke *et al.*, 1998).

Krege *et al.* produced the ER $\beta$  knockout mouse (BERKO) by homologous recombination and insertion into exon 3, which prevents functional transcription of ER $\beta$  (Krege *et al.*, 1998). The mice appear to have reduced fertility and older males show bladder and prostate hyperplasia. Results from this early study suggest that ER $\beta$  has essential roles in normal ovulation but not in sexual differentiation or fertility (Krege *et al.*, 1998). There is increased cell proliferation and an exaggerated response to E<sub>2</sub> in the immature BERKO uterus. This suggests that ER $\beta$  has a role in modulating these effects, or that ER $\alpha$  and ER $\beta$  have a combined anti-proliferative role in the immature uterus (Weihua *et al.*, 2000).

### **1.3.10 Oestrogen receptor $\gamma$**

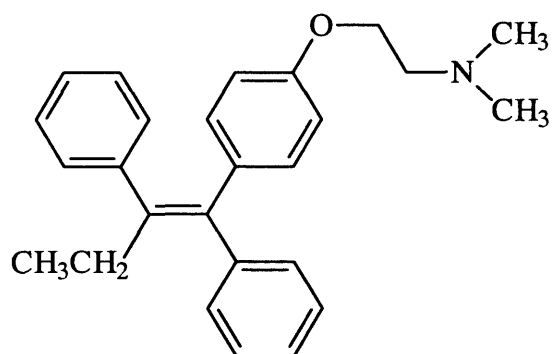
A third functional ER (termed ER $\gamma$ ) has been isolated and studied in the teleost fish. ER $\gamma$  has amino acid differences in the ligand binding domain and receptor activation regions, and is genetically distinct from ER $\alpha$  and ER $\beta$ . The study shows that the three ERs have differential expression in the reproductive tissues and opens up the possibility that the effect attributable to E<sub>2</sub> in ER $\alpha$  and ER $\beta$  knockout mice maybe due to a third ER (Hawkins *et al.*, 2000). Data on ER $\gamma$  is limited and so far has not been identified in other species.

## 1.4 Tamoxifen

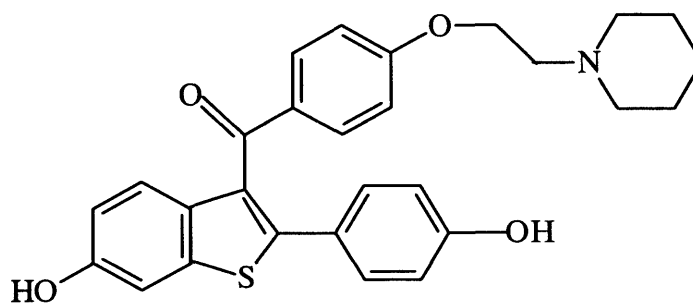
Tamoxifen, (Z)-1-[4-[(dimethylamino)ethoxy]phenyl]-1,1-diphenyl-1-butene (Figure 1.5), has been successfully used for the endocrine treatment of breast cancer since 1971. There is a 60% response rate reported in ER positive tumours and tamoxifen is most beneficial in the treatment of postmenopausal women with breast cancer (Baum, 1998). It is estimated that 400 000 women are alive due to adjuvant tamoxifen treatment (Jordan, 2000). Tamoxifen is under trial for use in the prevention of breast cancer in those individuals who are considered to be at high risk. During the BCPT National Surgical Adjuvant Breast and Bowel Project P-1 Study, over 13 000 healthy women with increased risk of breast cancer, were treated with tamoxifen at 20mg/day. Results from this trial showed that treatment with tamoxifen over 5 years reduced their risk of invasive breast cancer by 49% and non invasive breast cancer by 50% (Henderson *et al.*, 2000) although it is not clear whether this reduction is a delay in the onset of tumour development.

### 1.4.1 Uterotrophic effects

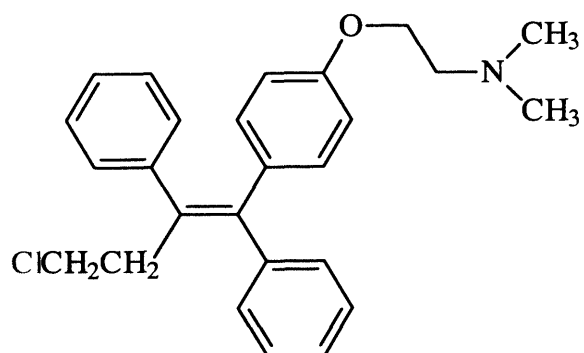
Tamoxifen has a stimulatory effect in the uterus behaving as an oestrogen agonist and can cause an increase in endometrial cancers (Fisher *et al.*, 1994; Rutqvist *et al.*, 1995). During the BCPT study of over 13 000 women at risk for breast cancer it was shown that the cumulative incidence of endometrial cancer, over 66 months, was 13 and 5.4 per 1000 women in the tamoxifen and placebo groups respectively. The cumulative incidence of invasive breast cancer was 22 and 43 per 1000 women in the tamoxifen and placebo groups.



Tamoxifen



Raloxifene



Toremifene

**Figure 1.5** Chemical structures of the SERMs; tamoxifen, raloxifene and toremifene

These data demonstrate that the advantages of treatment with tamoxifen are seen to outweigh the risks (Roe *et al.*, 2000). However, women with a history of oestrogen replacement therapy use and obesity (which are known to be endometrial cancer risk factors) should be under closer surveillance when treated with tamoxifen (Bernstein *et al.*, 1999). Reduction in risk has to be evaluated against the risk of treated women becoming pregnant, as treatment of pregnant mice with tamoxifen increases the female offspring's risk of breast cancer, alterations in the development of the reproductive tract have also been observed (Hilakivi-Clarke *et al.*, 2000).

Tamoxifen's weak oestrogenic effects on the female genital tract can cause an array of endometrial lesions including simple to atypical hyperplasia, polyps and adenocarcinoma. There have also been reports of the relatively rare adenomyosis in postmenopausal women taking tamoxifen (McCluggage *et al.*, 2000). Adenomyosis is characterised by the appearance of endometrial glands and stroma in the myometrial layers of the uterus, although there is some evidence to support variations in the morphological features between cases in tamoxifen treated women and untreated women (McCluggage *et al.*, 2000).

Adenomyosis is discussed further in Chapter 5.

#### **1.4.2 Carcinogenic effects of tamoxifen in rodents**

Tamoxifen was first shown to be a potent liver carcinogen in the rat when administered by gavage over a two-year period (Greaves *et al.*, 1993). This observation was subsequently confirmed in a number of different strains

(Carthew *et al.*, 1995; Hard *et al.*, 1993). However, it was not thought that the induction of liver tumours by tamoxifen in the rat was due to an ER mediated effect. Mice were not susceptible to the carcinogenic effects of tamoxifen in the liver when given in lifetime dosing studies (Martin *et al.*, 1997). Examination of liver tumours from rats given 40mg/kg/day tamoxifen for 3 months showed a reduction in nuclear ER expression (Carthew *et al.*, 1997), although it is not clear whether this reduction in ER is related to the tumour promotion process.

Rats that developed liver tumours following treatment with tamoxifen also showed evidence of DNA damage detected by <sup>32</sup>P-post-labelling (White *et al.*, 1992). The carcinogenic activity of tamoxifen was due to its conversion to reactive metabolites that bind irreversibly to DNA (Phillips *et al.*, 1994). The active metabolite of tamoxifen,  $\alpha$ -hydroxytamoxifen, has a role in liver DNA damage of rats treated with tamoxifen (White, 1999) and this metabolite has been identified in women taking tamoxifen (Poon *et al.*, 1995). In contrast, in the mouse tamoxifen does not act as a liver carcinogen and it has been proposed that this is due to the lack of cumulative DNA damage or cellular proliferation in the liver caused by tamoxifen (Martin *et al.*, 1997).

It has been proposed that there is a causal link between the presence of adducts in tamoxifen treated rats and future development of liver tumours (White, 1999). <sup>32</sup>P-post-labelling studies of DNA damage in the livers of tamoxifen treated women show no significant difference in adduct levels between control and treated women (Martin *et al.*, 1995). Previous <sup>32</sup>P-post-labelling studies, investigating DNA adducts in human endometria, provided no

evidence of adducts in tamoxifen treated women (Carmichael *et al.*, 1996 and 1999). The levels of DNA adducts in the endometrial tissues of tamoxifen treated women prove to be inconclusive. These findings show that tamoxifen has the potential to be genotoxic in women. However, epidemiological studies have found no association between the treatment of women with tamoxifen and liver cancer (IARC, 1996). This may be related to the high levels of activity of glucuronyltransferases in human liver compared with the rat, capable of detoxifying the  $\alpha$ -hydroxytamoxifen active metabolite (Boocock *et al.*, 2000).

### **1.4.3 Tamoxifen resistance**

Drug resistance to tamoxifen may arise through loss of wild-type ER or by other mechanisms such as the induction of *MDR-1* expression. Studies in a MCF-7 derived cell line show that the tamoxifen active metabolite;  $\alpha$ -hydroxytamoxifen can induce stable direct silencing of gene expression and that this inactivation is associated with modification of the chromatin structure. These observations may be involved in the process of acquired tamoxifen resistance (Badia *et al.*, 2000). In the search for genes that may be involved in tamoxifen resistance BCAR3 has been identified in ZR-75-1 breast cancer cells (Van Agthoven *et al.*, 1998). Transfection of this gene into MCF-7 breast cancer cells induces tamoxifen resistance. The gene encodes a protein that contains an SH2 domain found in many cytoplasmic signalling molecules (Van Agthoven *et al.*, 1998).

#### 1.4.4 Tamoxifen's affinity for the oestrogen receptor

Studies show that tamoxifen-ER binds the ERE with a lower affinity than E<sub>2</sub>-ER or 4-hydroxytamoxifen-ER (Klinge *et al.*, 1998). Klinge *et al.*, (1998) also demonstrated that one molecule of both tamoxifen or 4-hydroxytamoxifen dissociate from the ER dimer as it binds to the ERE. It is suggested that tamoxifen agonist activity stems from AF-1 and not AF-2 (Webb *et al.*, 2000). A study tested the ability of 4-hydroxytamoxifen to inhibit AP-1 activity, which is one of the first events following growth factor receptor activation, using MCF-7 cells transiently transfected with an AP-1 responsive gene. ER mediated stimulation of the AP-1 response was inhibited by 4-hydroxytamoxifen and activated by oestrogens (Philips *et al.*, 1993).

#### 1.5 Uterine histology

As discussed earlier, one of the primary targets for oestrogen action is the uterus. The adult rodent uterus consists of three layers the inner most being the mucus membrane endometrium. This is surrounded by a thick muscular myometrium and the perimetrium that is the outer serosal layer (Figure 1.6). The lumen of the uterus is surrounded by the luminal epithelium that is a columnar epithelial cell layer usually one to two cells thick. The endometrium lines the uterus and is made up of a number of different cell types. The endometrial stroma is mainly stromal cells, lymphocytes and fibroblasts set in connective tissue. It also contains the endometrial glands that secrete into the lumen. These secretory glands are tubular and are surrounded by their own single cell layer glandular epithelium. The endometrial stroma also contains

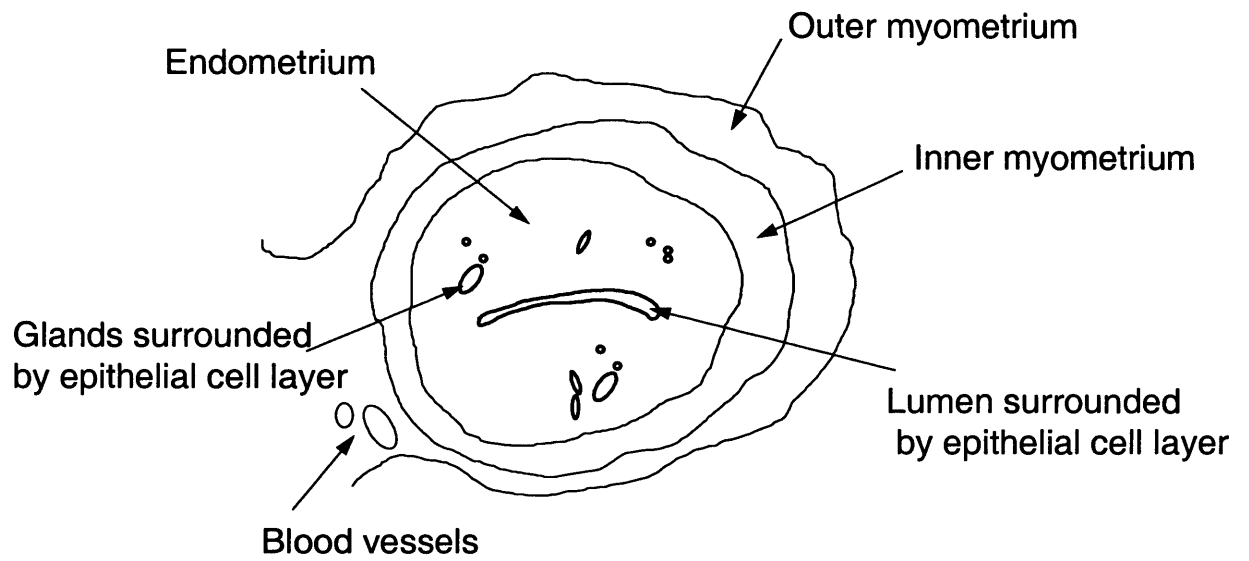


**Figure 1.6** Representative structure of the adult rodent uterus.

some blood vessels but these are mostly located within the muscular myometrium of the uterus.

The myometrium consists of two layers of smooth muscle cells set in connective tissue. The orientation of the smooth muscle cells signifies the difference between the inner and outer layers of the myometrium. The inner myometrial layer is composed of muscle fibres in a circular orientation and in the thicker outer layer the fibres are arranged longitudinally. Blood vessels within the uterus are rapidly changing but the arteries and veins, surrounded by pericytes (smooth muscle cells), are found mainly in the thicker outer layer of the myometrium. The perimetrium surrounds the myometrium and is composed of a single layer of mesothelial cells set in connective tissue.

## **1.6 Endometrial cancer**

Endometrial cancer is the most common female genital tract cancer of which there has been a significant increase in specific death rate over the last few years (Homesley *et al.*, 1996). There are three major stages used for diagnosis according to the International Federation of Gynecology and Obstetrics (1988); stage I (a-c) myometrial invasion, stage II (a-b) tumour grading and stage III (a-c) extrauterine tumour spread. In studies in human tissues with high grade classification there has been a decrease in ER and PR expression, several oncogenes have also been assessed with significant correlation between k-ras and PR expression (Niederacher *et al.*, 1999). However, an in depth study of the genetic alterations in endometrial carcinomas has yet to be completed.

Low-grade endometrial stromal sarcomas are rare and account for only 0.2% of all genital tract malignancies occurring predominantly in postmenopausal women. These malignancies express both ER and PR and are sensitive to sex steroids (Reich *et al.*, 2000).

Risk factors for endometrial tumours in women are increased and unopposed oestrogen exposure, late menopause, sequential oral contraceptives, obesity and oestrogen replacement therapy. Protective factors include decreased oestrogen exposure, pregnancy and the use of combined oral contraceptives (Henderson *et al.*, 2000). In premenopausal women the risk of endometrial cancer is attributed to the increased mitotic activity during the first half of the menstrual cycle when the oestrogen is not opposed by progesterone. Obesity in postmenopausal women increases risk by the conversion of androstenedione to oestrone in adipose tissue. Studies in tamoxifen treated endometrial tissue samples, compared with normal age matched samples, showed a significant decrease in ER expression which was attributed to tamoxifen's weak oestrogenic effects in the endometrium (Cohen *et al.*, 1997a). A recent study assessing 36 human endometrial cancers, using PCR and Western blotting, has identified ER $\beta$  as important in the progression of myometrial invasion. Levels of ER $\beta$  protein were high in comparison to ER $\alpha$  in endometrial cancers with severe myometrial invasion (Takama *et al.*, 2001).

## 1.7 Selective oestrogen receptor modulators

As oestrogens are suggested to have a role in the initiation and progression of some cancers, such as those of the uterus and breast as described above, the most effective way of inhibiting the oestrogenic effects is to block the action of the hormone at the cellular level.

Selective oestrogen receptor modulators (SERMs) are a group of compounds that have mixed oestrogen agonist/antagonist effects on target tissues. They are structurally distinct from oestrogens. Due to the oestrogenic effects that tamoxifen has on the uterus, and the anti-oestrogenic effect the compound has on the breast, it has more commonly become known as a SERM. The ideal SERM should have anti-oestrogen properties on the breast and uterus and an oestrogenic effect on the brain (to prevent hot flushes). It should also have an oestrogenic affect on the liver (to lower cholesterol synthesis) and on bone (to maintain calcium). Also, it should exert no effect on the coagulation system. Other SERMs may also be effective in a breast cancer chemopreventative role and some (e.g. raloxifene) may have lesser oestrogenic effects in the uterus (Black *et al.*, 1983). Currently, tamoxifen is the SERM of choice for use in the prevention of breast cancer and in the adjuvant setting it remains the benchmark for comparison with other agents.

### 1.7.1 Toremifene

Toremifene is a tamoxifen analogue (Figure 1.5) that has been approved as second line treatment of breast cancer patients (Tonetti *et al.*, 1998). The side

effects of toremifene resemble those of tamoxifen and its efficacy also appears to be no less than that of tamoxifen (Holli *et al.*, 2000). Comparative studies on tamoxifen and toremifene concluded that the effects of the compounds on human endometrial tumours implanted into athymic mice were not significantly different (Tonetti *et al.*, 1998). These data suggest that as the two compounds produce identical effects, toremifene may be associated with an increased incidence of endometrial cancer (O'Regan *et al.*, 1998). Unlike tamoxifen, toremifene does not result in liver tumours in rats following long-term dosing (Hard *et al.*, 1993).

### **1.7.2 Raloxifene**

Raloxifene is a benzothiophene compound that was originally designed as a treatment for advanced breast cancer. Raloxifene has potential for breast cancer treatment. Raloxifene reduced the risk of breast cancer diagnosis in an ongoing trial assessing the treatment of 8000 women with osteoporosis. In a 29-month follow up, raloxifene treatment had reduced the risk of breast cancer diagnosis by 74% (Cummings *et al.*, 1999). Raloxifene is currently used for the treatment of osteoporosis in postmenopausal women.

One hypothesis for oestrogenic action of raloxifene involves its competition with  $E_2$  for the ER preventing stimulation by oestrogen; another possibility is a mutation in the ER causing raloxifene to act as either an oestrogen or anti-oestrogen (Levenson *et al.*, 1998). In tissues where raloxifene mimics the effect of oestrogen it is thought that the raloxifene-ER complex forms a different

conformation that binds to a specific raloxifene response element (RRE) recruiting other transcription factors such as TGF $\beta$ 3 (Yang *et al.*, 1996b). Therefore, the oestrogen agonist activity of raloxifene could be due to specific genes containing RREs in the bone and cardiovascular system. Several genes including the neuron-specific growth-associated protein: GAP-43 and the protooncogene c-myc have RRE related sequences (Yang *et al.*, 1996b). A recent study describes raloxifene as an oestrogen antagonist via the ERE in osteoblast cells and the compound shows some antagonistic activity in human breast cells (Nuttall *et al.*, 2000).

In the rat, raloxifene binds with high affinity to the ER, comparable with E<sub>2</sub>, producing an effect similar to that of oestrogen on the bone (Turner *et al.*, 1994). However, raloxifene behaves as an oestrogen antagonist in the rat reproductive tissues (Black *et al.*, 1983) and therefore could potentially limit the risk of endometrial cancer if used in humans.

### **1.7.3 SERM clinical trials**

Many clinical trials are underway to test the various SERMs. Previous trials of tamoxifen as adjuvant breast cancer treatment showed major benefits in post-menopausal women over the age of 50 with ER positive tumours (Baum, 1998). The optimal duration of tamoxifen treatment is still undetermined, however, it is known that 5 years treatment with tamoxifen of women with breast cancer is more effective than two years (Rutqvist *et al.*, 1996). At present individual trials are under way: Adjuvant Tamoxifen Treatment (aTTom) and Adjuvant

Tamoxifen - Longer Against Shorter (ATLAS). These trials involve the treatment of breast cancer patients with tamoxifen and a relapse free two years will lead to treatment for five years plus (Baum, 1997). Raloxifene is at present involved in a trial where its effects will be compared to tamoxifen; the Study of Tamoxifen and Raloxifene (STAR), which involves the treatment of 22 000 postmenopausal women (McNeil, 1998).

#### **1.7.4 Aromatase inhibitors**

Aromatase (CYP19, oestrogen synthase) is an enzyme present in fat, liver, and breast tissue and perhaps breast cancer cells, which converts androstenedione to oestrone. The new aromatase inhibitors cause little or no inhibition of glucocorticoid synthesis and thus there is no risk of hypoadrenalism and potential need for supplementary glucocorticoids.

There are two types of aromatase inhibitors. Type I are steroidal compounds and include 4-hydroxy-androstenedione. Steroidal aromatase inhibitors are non-competitive inhibitors that interfere with the cytochrome P450 site on the enzyme to bring about irreversible inhibition. Type II aromatase inhibitors are non-steroidal competitive inhibitors of the flavoprotein site on the aromatase enzyme. They include the triazole analogues anastrozole (Arimidex) and letrozole. Within several days after administration of these agents to postmenopausal women, serum oestradiol levels are suppressed to extremely low levels. Aromatase inhibitors are not very effective in pre-menopausal women because of the high level of oestradiol synthesis in the ovaries.

## 1.8 Anti-oestrogens

Pure anti-oestrogens such as faslodex (ICI 182,780) might be expected to be more effective than tamoxifen in the treatment of breast cancer. However, the early anti-oestrogens have low oral bioavailability and are administered by intramuscular injection. Faslodex is a pure steroidal oestrogen antagonist, with no oestrogen agonist activity (Wakeling *et al.*, 1992) and although this compound has potential as treatment for breast cancer patients it is not as widely accepted as tamoxifen (White, 1999). Cell proliferation in the uterus of women in treatment with faslodex was not affected (Howell *et al.*, 1996) and there have been decreases in breast tumour proliferation in tamoxifen resistant patients. The drug inhibits growth of human breast cancer cells and down regulates the expression of the ER (Howell *et al.*, 2000).

Faslodex has a high affinity for the ER and completely blocks the trophic effect of E<sub>2</sub> in the adult ovariectomized rat uterus. Treatment of rodents, or stromal cells from rodent uterus, with faslodex can selectively block induction by SERMs of the oestrogen responsive genes such as c-fos and VEGF in a dose dependent manner. These studies suggest that it would be possible to selectively block the effect of oestrogens in target tissues by grading doses of pure anti-oestrogens (Hyder *et al.*, 2000). Faslodex has been shown to block transcriptional activation by progesterone suggesting the therapeutic effects of this drug may include anti-progestin effects in addition to its well-documented anti-oestrogenic effects (Nawaz *et al.*, 1999a).

Various anti-oestrogens induce distinct ER $\alpha$ -ligand conformations and have distinct effects on inhibition of oestrogen agonist mediated activities (Wijayarathne *et al.*, 1999). Anti-oestrogens e.g., RU 58668, may modify the subcellular localisation of the ER on binding and inhibit its normal nuclear localisation by sequestering it in the cytoplasm (Devin-Leclerc *et al.*, 1998). This is one of several theories on the mechanisms of anti-oestrogenic action, which include accelerated/alternative receptor degradation or reduction in receptor half-life (Dauvois *et al.*, 1992), perhaps the inability of anti-oestrogen bound receptor to form dimers (Arbuckle *et al.*, 1992; Parker *et al.*, 1993) and the interaction of varying coactivators and corepressors.

## **1.9 Rodent models for oestrogen receptor regulation**

### **1.9.1 The rat model**

Treatment of neonatal Wistar rats with tamoxifen, 1mg/kg body weight per day for 2-5 days after birth, subsequently gave rise to endometrial and vaginal cancer during the following 25-35 months (Carthew *et al.*, 2000). There was little evidence of any oestrogen agonist action as demonstrated by the absence of endometrial hyperplasia suggesting that the oestrogenic action of tamoxifen is not required in this case for carcinogenic action in the reproductive tract of the rat.

Studies show dramatic down regulation of ER protein levels observed in the ovariectomised Holtzman rat uterus following treatment with 2 $\mu$ g 17 $\beta$ -oestradiol for 3 days. ER protein was down regulated by 65% within 4h of E<sub>2</sub>

administration but ER levels were replenished by 20h. ER processing was thought to involve the loss of ER binding activity although this data suggests that new ER protein is produced to replenish lost ER protein levels (Zhou *et al.*, 1993). Other studies have also shown, in ovariectomised Wistar rats, that treatment with oestradiol benzoate (50µg/kg/day) reduced luminal epithelium expression of nuclear ERα protein at 24, 48 and 72h after dosing (Carthew *et al.*, 1999b). In contrast nuclear ERα expression was not decreased by tamoxifen or toremifene at these time points. These investigations on the effect of E<sub>2</sub>, tamoxifen and toremifene on the ovariectomised rat uterine tissue demonstrated clear differences between E<sub>2</sub> and the other compounds tested. E<sub>2</sub> decreased the expression of ERα in the luminal epithelium of the uterus and induced myometrial hypertrophy, which was not observed with either tamoxifen or toremifene: indicating the difference between a partial and full agonist in the rat uterus (Carthew *et al.*, 1999b).

### **1.9.2 The mouse model**

The ovariectomised adult mouse is used frequently to study the varying effects of oestrogenic compounds on the reproductive tract. In the adult mouse uterus, treatment with 1µg/day E<sub>2</sub> for 4 days caused a compartment specific effect on the regulation of the ERα protein expression between cell types of the uterus. Levels of ERα were decreased in the stromal and glandular epithelial cells and increased in the luminal epithelium and myometrium (Tibbetts *et al.*, 1998).

Ovariectomised CD-1 mice treated with E<sub>2</sub>, tamoxifen, toremifene or raloxifene for 72h were assessed for uterine effects including uterine weight and DNA synthesis. Both E<sub>2</sub> and tamoxifen caused comparative hypertrophic effects (increase in cell size). But it was concluded that uterine weight alone should not be taken as a singular measure of oestrogenic effect on the uterus (Carthew *et al.*, 1999a).

### 1.9.3 The neonatal mouse model

The study of the mechanisms involved in the malignant transformation of target cells, or the progression of hormonally induced tumours, is aided greatly by the use of the *in vivo* model. An *in vivo* model, where tumours can be hormonally induced at a high frequency, is beneficial in the study of the mechanisms involved in the development of reproductive tract cancers.

Adverse effects of hormonally active chemicals can be observed in laboratory animals over their lifetimes. *In utero* and early postnatal periods of developmental exposure are particularly important since altered levels of hormones during this time can result in permanent changes. The neonatal mouse undergoes extensive reproductive tract development postnatally, such that at birth, the reproductive tract is of equivalent development to that of the human foetus in the third trimester. Exposure to oestrogenic compounds at this stage of development leads to the induction of tumours of the reproductive tract (Newbold *et al.*, 1990; 1997; 2000; 2001).

#### 1.9.4 Tumour formation

Newbold and colleagues described a neonate rodent model for hormonal carcinogenesis (1990). CD-1 mice were treated neonatally, on days 1-5, with 0.2-2 $\mu$ g/pup diethylstilbestrol (DES) subcutaneously. There was a dose related increase in uterine neoplasia. Up to 90% developed uterine adenocarcinoma at 18 months at a dose of 2 $\mu$ g/pup whereas no such tumours were observed in control mice or those mice that were ovariectomised at puberty. No tumours were observed in mice treated with 17 $\beta$ -oestradiol at 2 $\mu$ g/pup but DES-induced adenocarcinomas grown in nude mice were enhanced by subcutaneous implantation of oestradiol pellets (0.5 $\mu$ g). These results suggest that in the reproductive tract, neonatal exposure to DES results in oestrogen dependent induced tumours (Newbold *et al.*, 1990). Cell lines were established from these DES-associated tumours. After subcutaneous injection into nude mice, all cell lines formed solid tumours within 4 weeks (Hebert *et al.*, 1992). Tumour formation by developing cell lines from these malignancies may be a useful model for studying molecular changes in hormonal carcinogenesis, although, unlike the developing adenocarcinomas formed in the DES-treated mice, the growth of the transformed cells in nude mice was not enhanced or dependent on the presence of oestrogen (Hebert *et al.*, 1992).

Similar studies have been conducted in CD-1 mice treated neonatally with tamoxifen, up to 50 $\mu$ g/pup subcutaneously, for days 1-5 after birth. Tissues were examined at 14-17 months for reproductive tract changes. Of the tamoxifen treated uteri, 100% displayed uterine hypoplasia; the highest

incidence of uterine adenocarcinoma was 50% at a dose of 10µg/pup/day. Doses of 2µg/pup/day resulted in a 19% incidence of adenocarcinomas but none were seen at the higher dose level (50µg/pup/day). Conclusions from this study were that the developing reproductive tract is highly sensitive to perturbation by compounds with oestrogenic activity. It is a possibility that tamoxifen acts as an oestrogen agonist at low doses but as an oestrogen antagonist at higher doses (Newbold *et al.*, 1997). In a further study Newbold's group examined the effects of neonatal DES exposure on future generations, they found that F1 and F2 generations inherited the susceptibility to adenocarcinoma of the uterus and reproductive tract (Newbold *et al.*, 1998).

A recent study by Newbold's group showed an incidence of uterine adenocarcinoma of 35% in neonatal mice treated on days 1-5 with 50mg/kg/day of the naturally occurring phytoestrogen genestein. Thus demonstrating that genestein is carcinogenic during this critical period of development when given within one order of magnitude of human diet exposure levels (Newbold *et al.*, 2001).

### **1.9.5 The role of oestrogen receptor expression in cell proliferation**

Oestrogen mediates its effects on target tissues via the ER as described above.

The expression and regulation of this receptor is therefore important in the understanding of the effects of oestrogenic compounds on the reproductive tract. By using a model for tumour formation, it may be possible to elucidate the role of the ER in cell proliferation.

In normal mice, ER protein expression in uterine epithelial cells was observed by day 4 and gradually increased, as determined by immunohistochemical staining, until day 22 (Yamashita *et al.*, 1989). Previous studies have shown the ER to be regulated by oestradiol in the uterus of the neonate mouse model. Korach *et al.*, (1988) studied the levels of ER protein in epithelial and stromal fractions of uterine tissue from 5 and 10 day old CD-1 mice. They demonstrated that ER protein is able to bind ligand as evidenced by affinity labelling with tamoxifen azridine, and was higher in the stromal tissue than in the epithelial cells. Treatment with DES increased levels of ER in the epithelial tissue fractions at 18h after dosing as determined by Western blotting. An increase in the level of ER suggests that an increase in cell proliferation and growth factor mediated effects may occur in these cells. In ERKO mice there is no increase in uterine weight in response to oestrogens or tamoxifen (Korach *et al.*, 1994).

At this critical time of 1-5 days after birth, changes in gene expression induced by oestrogen treatment may provide insight into the mechanism of oestrogen induced reproductive tract cancer. In addition, alterations in expression of the ER subtypes will provide insight into how oestrogen mediates its effects on the cells and tissues studied. Changes in expression of certain key genes could play a role in the formation and promotion of the cancer. The neonatal mouse therefore provides, not only a model for the study of the effects of oestrogens on the developing reproductive tract, but also for the study of the mechanisms involved in the development of tumours induced by oestrogenic compounds.

### **1.10 Uterotrophic responses to SERMs in adult rodents**

Ovariectomised rats or mice have also been used as models for the study of the effects of oestrogenic and anti-oestrogenic compounds on the uterus. The effects of oestrogen on the uterus are marked by an increase in uterine weight caused by the uterotrophic effect of fluid retention and an increase in cell proliferation. Faslodex is capable of completely blocking this effect (Kangas 1992) suggesting that these effects are mediated through the ER.

Tamoxifen acts as a partial agonist and antagonist in the rat uterus (Wakeling *et al.*, 1983). Treatment of adult Wistar (Han) rats with tamoxifen for three months caused an increase in uterine weight and amount of myometrium for up to 9 months after treatment. A low incidence of uterine tumours was also found in the tamoxifen treated rats (Carthew *et al.*, 1996). In the same study adult mice treated with tamoxifen for two years showed no incidence of uterine tumours (Carthew *et al.*, 1996). Toremifene also shows oestrogen agonist activity on the developing neonatal rat uterus. An increase in uterine weight and luminal epithelial cell height suggests that this SERM is harmful to the developing rat reproductive system (Medlock *et al.*, 1997).

### **1.11 Degradation pathways of the oestrogen receptor**

ER expression is essential in the tissue specific effects of compounds that bind to the ER as ligands and influence the expression of genes. Therefore investigation of ER receptor degradation is important, as this is one mechanism whereby receptor levels are controlled, and may represent a control point in the

cell's response to oestrogens and SERMs. Receptor levels have been studied in many tissue types, both at the mRNA and protein level, in *in vivo* and *in vitro* models. The levels of the receptor are controlled by receptor turnover induced by ligands. As described previously the receptor is subject to auto-regulation by oestrogen but is also regulated by other oestrogenic and anti-oestrogenic compounds. The effect of various SERMs on receptor levels, in turn affects the reaction of the tissue or cell type to a specific compound.

It appears that oestrogens and anti-oestrogens differentially regulate levels of the ER. Seo *et al.*, (1998) demonstrated breakdown of the ER in MCF-7 cells following 1h incubation with E<sub>2</sub>. This continued when the hormone was removed and cells were incubated in fresh media. The degradation of the ER was inhibited by cyclohexamide suggesting the involvement of protein synthesis. In contrast, the addition of 4-hydroxytamoxifen to the growth media caused an increase of ER at 1h, which also continued for 5h in the absence of the drug thus demonstrating a differential response of ER levels to ligands.

### **1.11.1 Proteasome-mediated degradation**

Many proteins are targeted for degradation by the ubiquitin pathway, including those that are defective ribosomal products, and those targeted for degradation following the normal aging process (Schild *et al.*, 2000). The latter invariably have a short half-life and are involved in many of the cell processes including the down regulation of receptors, cell cycle progression, and transcriptional regulation (Kierszenbaum *et al.*, 2000). The multicatalytic 26S proteasome

(Figure 1.7) is located in the cytosol and the nucleus and functions include the removal of abnormally assembled proteins, the degradation of cyclins which control the cell cycle, and the processing and degradation of transcription factors (Kierszenbaum *et al.*, 2000).

The process of marking proteins for degradation by the ubiquitin pathway involves a cascade of enzymes in the recognition and ligation of ubiquitin to a lysine residue in the target protein. Phosphorylation of the target protein is the most favoured theory of recognition although others such as PEST elements (enriched with Pro, Glu, Ser and Thr residues) are also a possibility.

A protein subunit within the 19S cap of the 26S proteasome acts as a receptor for the polyubiquitin chain. The 20S catalytic core of the proteasome contains several subunits that have specialised proteolytic functions for degradation of the protein (Hershko *et al.*, 1998; Kierszenbaum *et al.*, 2000). The ubiquitin-proteasome pathway leads to the selective degradation of regulatory proteins with a short half-life where ubiquitinated proteins are targeted for proteasome mediated degradation. It is possible that, as ER has a short half-life of 3-4h (Pakdel *et al.*, 1993), it could be targeted for ubiquitin-mediated proteolysis (Nawaz *et al.*, 1999b). In ER transfected HeLa cells, the proteasome inhibitors MG132 or lactacystin can block E<sub>2</sub> dependent ER degradation. In addition proteasome inhibitors promote the accumulation of higher MW forms of the ER protein (Nawaz *et al.*, 1999b).

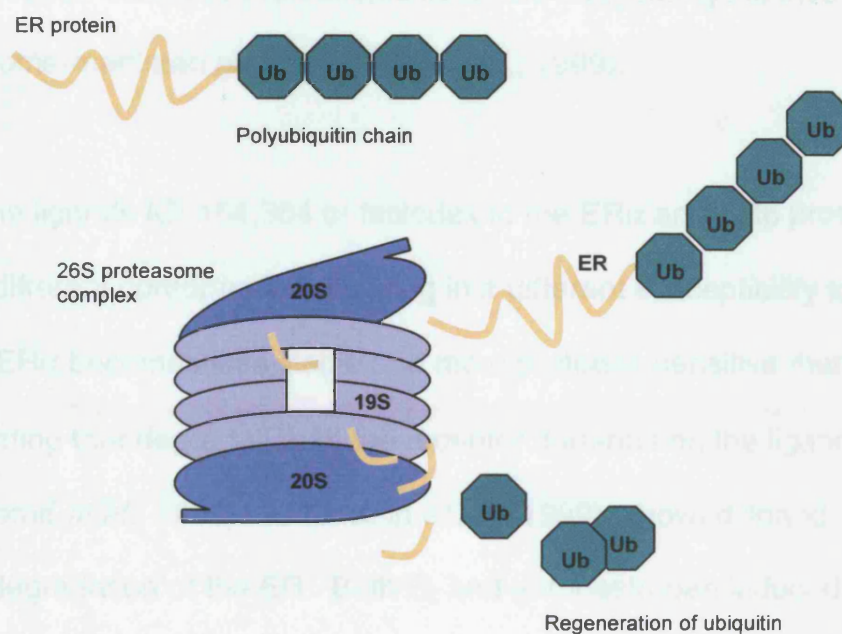


**Figure 1.7** Ubiquitination and 26S proteasome mediated degradation of the ER (adapted from Kierszenbaum *et al.*, 2000).

A second study in the MCF-7 cell line demonstrated that the degradation of ER induced by E<sub>2</sub> or the anti-oestrogen, RU 58668, are mediated through a proteasomal pathway but may involve different targeting mechanisms (El Khissiin *et al.*, 1999). It is therefore possible that the ligand bound to the ER would influence its degradation and consequently the level of ER in the cell. E<sub>2</sub> treatment of a human anterior pituitary cell line caused a reduction in ER half-life from 3 to 1hr. The E<sub>2</sub> induced degradation was again blocked by the addition of peptide aldehyde proteasome inhibitors suggesting the involvement of a proteasome-mediated pathway (Alarid *et al.*, 1999).

Binding of the ligands ICI 164,384 or faslodex to the ER $\alpha$  and ER $\beta$  proteins results in a different conformation resulting in a different susceptibility to proteases. ER $\alpha$  becomes less stable and more protease sensitive than the ER $\beta$ ; suggesting that degradation of the receptor depends on the ligand bound (Van Den Bemd *et al.*, 1999). El Khissiin *et al.*, (1999), showed ligand dependent degradation of the ER. Both E<sub>2</sub> and anti-oestrogen induced degradation involve proteasome pathways, but two differing uptake mechanisms dependent on bound ligand (El Khissiin *et al.*, 1999). Studies in MCF-7 and T47D human breast cancer cells demonstrate the proteasome dependent degradation of ER $\alpha$  following treatment with E<sub>2</sub> and TCDD (Wormke *et al.*, 2000). It appears that the ligand bound to the ER determines receptor stability by subtle differences in receptor conformation altering interaction of the receptor with components of the proteasome complex (Wijayaratne *et al.*, 2001). Thus ER $\alpha$  and ER $\beta$  may be differentially degraded depending on conformational changes caused by ligand bound and interaction with the

proteasome complex. However, no studies to date show subtype independent degradation of ER $\alpha$  and ER $\beta$  or the differing effects of ligands on this degradation.

## 1.12 Aims

The recent discovery of ER $\beta$  has posed many new questions relating to the mechanisms of action of SERMs within the reproductive tissues. Research to date has suggested there may be different roles for the two ER, particularly concerning the regulation of oestrogen responsive tissues (Paech *et al.*, 1997; Ogawa *et al.*, 1998). The variation in expression of the two receptors between tissue and cell types, and the effects of this expression on ER responsive genes, could be related to the oestrogen agonist and antagonist effects of compounds in oestrogen responsive tissues (Mitchner *et al.*, 1998).

The aim of this study was to investigate the mechanisms by which tamoxifen results in an increase in endometrial tumours in women. Rodent models have been used in order to study this problem and to assess the likelihood of other drugs of this class, eg toremifene or raloxifene, having similar long-term effects. It is clear from previous studies that ER $\alpha$  and ER $\beta$  play pivotal roles in controlling the uterine cellular responses to SERMs.

In order to overcome oestrogen related cycling changes that occur in adult rodents, initial studies used adult ovariectomised animals to establish localisation of ER $\alpha$  and ER $\beta$  in the endometrial, glandular and myometrial cells

of the uterus both by *in situ* hybridisation and immunohistochemistry and the response of the receptors to oestrogen and tamoxifen.

During the course of this study it became clear that long term dosing of adult rats or mice would not lead to the development of endometrial tumours seen in women. The mechanism of tumour formation was clearly different from the genotoxic actions of tamoxifen in the rat liver (White, 1999). However, the studies of Newbold *et al.* (1997) showed that the neonate mouse model, where tamoxifen was given on days 1-5 after birth, did give rise 14-17 months later, to endometrial adenocarcinomas. The subsequent aims of this work were therefore to establish the role of ER $\alpha$  and ER $\beta$  and differential gene expression in the development of uterine lesions in the neonate model.

Finally, using cell lines the role of the ER degradation pathway was investigated *in vitro*. Several compounds were assessed to evaluate the mechanism/s of ER degradation within human breast and endometrial cell lines.

## **Chapter 2: Materials and Methods**

## 2.1 Materials and Methods

### 2.1.1 Animals and treatments

All animal studies were carried out under the authority of the United Kingdom Home Office Animals (Scientific Procedures) Act 1986. The staff of the Biomedical Services Division of Leicester University carried out the dosing of the animals.

Female CD-1 mice were ovariectomised at 6 weeks of age by the supplier, Charles River, Margate, Kent, UK. After a recovery period of 3 weeks, groups of 4 ovariectomised mice (weighing approximately 30g) were subcutaneously dosed daily, for 3 days, with 2µg/kg oestradiol benzoate or 0.4mg/kg tamoxifen citrate. These doses were chosen since previous studies had shown them to give the most effective uterotrophic effects in ovariectomised rats (Carthew *et al.*, 2000). Compounds were dissolved in DMSO and administered in a volume of 1ml/kg using Hamilton Syringes. Controls received DMSO vehicle only. Animals were housed, 4 per cage, in negative pressure isolators for the duration of the study and allowed access to food and water *ad libitum*. Groups of 4 animals were sacrificed by cervical dislocation 24h after the last dose. Body and uteri weights were recorded. Representative sections of both uterine horns were fixed in 3.7% neutral buffered formalin or snap frozen in liquid nitrogen.

Groups of ten female neonatal mice were dosed orally via capillary tubing on days 2-5 after birth (day of birth is day 1), for 4 days consecutively. Mice were

dosed with 5.3nmol/kg oestradiol benzoate, 2.7 $\mu$ mol/kg tamoxifen citrate, toremifene citrate or raloxifene hydrochloride in peanut oil/lecithin/condensed milk mixture (2:0.2:3 v/v) at a dose volume of 5 $\mu$ l/g body weight. Controls received vehicle only. On day 6, mice were sacrificed and uteri were removed, weighed and fixed in 3.7% neutral buffered formalin, Carnoys or snap frozen in liquid nitrogen.

Wistar (Han) rats were ovariectomised at 6 weeks of age by the supplier, Charles River, Margate, Kent, UK. After a recovery period of 3 weeks, groups of 4 ovariectomised rats, approximately 225g in weight, were given oestradiol benzoate (5.3nmol/kg) or tamoxifen citrate (2.7 $\mu$ mol/kg) subcutaneously, daily, for 3 days. Controls received tricaprilin vehicle only. Animals were housed, 4 per cage, in negative pressure isolators for the duration of the study and allowed access to food and water *ad libitum*. Groups of 4 animals were sacrificed by pentobarbital overdose at 72h. Body and uteri weights were recorded. Representative sections of both uterine horns were fixed in 10% neutral buffered formalin or were snap frozen in liquid nitrogen.

### **2.1.2 Chemicals and reagents**

The following chemicals and reagents were obtained from the sources listed:

#### **Affinity Bioreagents Inc., Golden, CA, USA**

Polyclonal (rabbit) anti-human oestrogen receptor  $\beta$  antibody: PA1-313. PA1-313 was raised against a synthetic peptide corresponding to the C-terminal residues 467-485 of human oestrogen receptor  $\beta$ .

**Ambion, Austin, TX, USA**

DNA-Free: Kit 1906 (for removal of DNA)

**Amersham International Pic., Little Chalfont, Bucks**

Enhanced Chemiluminescent (ECL) Western blotting detection kit, ECL hyper film, Hybond-ECL nitrocellulose membrane, [ $\alpha^{32}\text{P}$ ] dATP 111TBq/mmol specific activity

**Anachem, Anachem House, Luton, Bedfordshire**

30% Acrylamide/Bis (37.5:1) solution

**Applied Biosystems, Warrington, Cheshire**

*Taq* polymerase

**Astra Zeneca, Alderley Edge, Macclesfield**

Tamoxifen, tamoxifen citrate, raloxifene hydrochloride

**Bachem Biochemica (UK) Ltd, St. Helens, Merseyside**

Suc-LLVY-AMC peptide substrate for proteasome complex

**BDH Laboratory Supplies, Poole, Dorset**

Gurr's Aquamount mountant

**Calbiochem-Novabiochem Co., Beeston, Nottingham**

Oestrogen receptor  $\alpha$  (330655); 66kD human recombinant functionally active protein and oestrogen receptor  $\beta$  (330657); 53kD human recombinant functionally active protein.

**Clontech, Palo Alto, CA 94303, USA**

Choma Spin-10 Columns, Mouse 1.2 cDNA Atlas Arrays and hybridisation kits including Express-Hyb solution, CDS primer mix, 5x Reaction Buffer, 10x dNTP mix, DTT, MMLV Reverse Transcriptase, Termination Mix,  $C_{0T-1}$  DNA and Chroma Spin-200 DEPC- $H_2O$  Columns

**DAKO Ltd, High Wycombe, Bucks**

StreptABComplex/HP Duet kit

**European Collection of Cell Cultures, Salisbury, Wiltshire**

MCF-7: human breast adenocarcinoma epithelial cells and Ishikawa human endometrial cells

**Fisher Scientific UK, Loughborough, Leicestershire**

Histoclear

**Genetic Research Instrumentation, Essex**

Blue Sensitive X-ray film for autoradiography

**Gibco BRL Ltd, Glasgow, Scotland**

Dulbecco's Modified Eagle's medium (DMEM) Cat. No. 11039, trypsin/EDTA solution (10x), trypan blue, and foetal calf serum

**Life Technologies, Paisley, Scotland**

Aqueous phenol, oligo dT, Superscript II RNase H<sup>-</sup> reverse transcriptase

**Novacastra, Balliol Business Park West, Newcastle upon Tyne**

Monoclonal (mouse) anti-human oestrogen receptor  $\alpha$  antibody, Cat. No. NCL-ER-6F11. The antibody was raised against a prokaryotic protein corresponding to the full-length human oestrogen receptor  $\alpha$

**Orion Farnos, Turku, Finland**

Toremifene hydrochloride

**Promega UK, Southampton**

RNase free DNase 1, RNasin

**Protein and Nucleic Acid Chemistry Laboratory, University of Leicester**

Oligonucleotide probes and primers

**Roche Diagnostics Ltd., Lewes, East Sussex**

TdT and TdT buffer, DIG-NHS, Anti-digoxigenin (HRP) antibody, Proteinase K, Klenow enzyme and reaction buffer

**Schleicher and Schuell UK Ltd., London**

Nylon filter: Nytran 0.45 $\mu$ M

**Stratagene Europe, The Netherlands**

NucTrap Push columns, RNA Microisolation kit: 200344-16

**Upstate Biotechnology/TCS Biologicals Ltd., Botolph Claydon,  
Buckingham**

Monoclonal (mouse) anti-bovine oestrogen receptor  $\alpha$  antibody, Cat. No. 05-394, cross reactive with rat, mouse and human. Antibody was raised against purified SDS-denatured calf uterus oestrogen receptor  $\alpha$ .

Rabbit polyclonal anti-rat and mouse oestrogen receptor  $\beta$  antibody, Cat. No. 06-629. Antibody raised against a synthetic peptide representing amino acids 54-71 of rat and mouse oestrogen receptor  $\beta$ .

**Sigma Aldrich Co., Poole, Dorset**

All other chemicals and reagents unless specified otherwise

**2.2 Localisation of ER mRNA by *in situ* hybridisation**

The ER mRNA target of *in situ* hybridisation is unstable and is subject to degradation by RNase. RNase is stable under most conditions and is very difficult to remove from tissue sections. Therefore all glassware used in these procedures was autoclaved and all solutions were treated with 0.1% (v/v)

diethyl pyrocarbonate (DEPC) before autoclaving to inactivate RNases. Where indicated, DEPC H<sub>2</sub>O represents Ultrapure sterile water containing 0.1% DEPC.

### **2.2.1 Oligonucleotide probes for *in situ* hybridisation**

Various oligonucleotide probes specific for either mouse ER $\alpha$  or ER $\beta$  mRNA or rat ER $\alpha$  or ER $\beta$  mRNA sequences were designed using the EMU-TEK molecular biology packages, version V6.09 (Tables 2.1 to 2.4). For ER $\alpha$  or ER $\beta$ , five oligonucleotide probes were made rather than a single one in order to get sufficient sensitivity for immunochemical detection (see below).

Oligonucleotides with high loop factors and areas rich in only one or two bases were avoided when selecting the probes. The probes were 25-30 base pairs (bp) long to enable them to reach the target and for optimal hybridisation conditions, had an approximate 50% guanosine/cytosine (GC) content and a melting temperature ( $T_m$ ) of  $70 \pm 2^\circ\text{C}$ . The probes were checked for homology to other sequences held at Genbank using the Basic Local Alignment Search Tool (BLAST) sequence similarity software (National Institutes of Health, Bethesda, USA. [www.ncbi.nlm.nih.gov/BLAST/](http://www.ncbi.nlm.nih.gov/BLAST/)). Homology to other relevant mRNA sequences, i.e. those expressed within the target organisms, was not found. Probes were synthesised with a 5' amino link required for subsequent digoxigenin labelling.

## 2.2.2 Purification and quantification of oligonucleotide probes

Each oligonucleotide (Tables 2.1-2.4) was purified and quantified individually following synthesis (Protein and Nucleic Chemistry Lab, Leicester University). A volume of 200 $\mu$ l of the oligonucleotide, in dilute ammonium hydroxide, was added to 2M sodium acetate pH 7.0 to give a final concentration of 0.2M. The mixture was vortexed and three times the volume of ice-cold isopropanol was added. The mixture was vortexed, incubated on dry ice for 30min then centrifuged at 10 000g for 30min at 4°C. The supernatant was discarded and the pellet vortexed in 1ml of 80% ethanol before centrifuging at 10 000g for 15min at room temperature (RT). The previous step was repeated before removing the supernatant and resuspending the dried pellet in 40 $\mu$ l sterile Ultra-pure (UP; sterile 18.2 M $\Omega$ , ELGA Maxima) water. For quantification, the oligonucleotide was diluted 1:100 with sterile UP water and the concentration and purity measured by reading absorbance at 260nm and 280nm (DNA/RNA Calculator, Pharmacia Biotech). The purity of the oligonucleotide was calculated using the ratio of the 260 and 280nm readings. The ratio of the purified oligonucleotides was optimally 1.8, however oligonucleotides were re-purified if they had a ratio below 1.5. The following equation was used to calculate the concentration of the oligonucleotide.

$$\text{Equation 2.1: oligonucleotide } (\mu\text{g/ml}) = (A_{260} \times 33)^* \times \text{dilution factor}$$

\* 1 Absorbance unit at 260nm ( $A_{260}$ ) of single stranded (ss) DNA = 33 $\mu$ g/ml  
(Promega Life Sciences, Technical References, 2001)

**Table 2.1 Mouse ER $\alpha$  oligonucleotide probe sequences for *in situ* hybridisation**

Base pair reference	Genbank reference M38651 Anti-sense 5'-3'	T <sub>m</sub> °C	%GC
157	TGAAGGGTCATGGTCATGGTAAGTGG	68.9	50
300	AGTTGAACACAGTGGGCTTGCTGTTG	69.5	50
1722	CGTCCATGCCTTTGTTACTCATGTGC	68.7	50
1889	TAAGGAATGTGCTGAAGTGGAGCTGG	68.5	50
1982	GTTGCAGGGATTCTCAGAACCTTTCG	68.9	50

**Table 2.2 Mouse ER $\beta$  oligonucleotide probe sequences for *in situ* hybridisation**

Base pair reference	Genbank reference U81451 Anti-sense 5'-3'	T <sub>m</sub> °C	%GC
93	TAAAGGAGAGAGGTGTCCAGAAGTTGGC	68.5	50
123	ATAGAGAAGCGATGATTGGCAGTGGG	69.2	50
151	CACACCAAGGACTCTTTTGAGGTTCTGC	69.8	50
1969	AGGAGGAACAAGGTCACATCCAAGCT	68.3	50
1997	AGCCAAGCAGGAAGAAAGAGGATCTAGG	68.6	50

**Table 2.3 Rat ER $\alpha$  oligonucleotide probe sequences for *in situ* hybridisation**

Base pair reference	Genbank reference Y00102 Anti-sense 5'-3'	T <sub>m</sub> °C	%GC
81	GCTGAGACAGTAAGACGGAAGGAAGGAATG	70.3	50
696	GTCGATTGTCAGAATTGGACCTGTAGAAGG	69.3	47
1130	CTTAGTGTGCTTGATCACAAGTGGACTTGG	69.4	47
1649	GATGTGGTCCTTCTCTTCCAGAGACTTCAA	69.4	47
1980	GGGGGGATGTAGTAGGTTTGTAAGGAATGT	68.2	47

**Table 2.4 Rat ER $\beta$  oligonucleotide probe sequences for *in situ* hybridisation**

Base pair reference	Genbank reference U57439 Anti-sense 5'-3'	T <sub>m</sub> °C	%GC
159	TCTCTAAATGCAGACAGGTGCTTTCCTCAG	70.0	47
256	ACTCCTTGTGAGAAGAGGTACAGATGGACA	68.1	47
356	CAGGGGTAGGATGGACTGGCTACAGTTATA	68.4	50
2458	ATAAGCAGGCTCTAAGGATGTAACCCAAGG	68.5	47
2555	CGGGAGAGAGAGAAAGATGACATAGCTTCA	69.3	47

Each oligonucleotide was diluted to a concentration of  $1\mu\text{g}/\mu\text{l}$  in sterile UP water. Oligonucleotide cocktails were made with equal concentrations of each oligonucleotide and stored at  $-20^{\circ}\text{C}$ .

### **2.2.3 Allyl amine labelling of oligonucleotides with digoxigenin at 5' and 3'**

Oligonucleotide cocktails (Tables 2.1-2.4) were labelled with digoxigenin at both the 3' and 5' end. 3' allyl addition reaction mixture ( $5\mu\text{g}$  of the oligonucleotide cocktail containing  $1\mu\text{g}$  of each of the five oligonucleotides probes,  $1\text{mM}$  manganese chloride,  $3\text{mM}$  AA-dUTP,  $25\text{U}$  terminal deoxynucleotide transferase (TdT),  $1\times$  TdT buffer,  $0.5\text{mM}$  cobalt chloride) was incubated in a water bath at  $37^{\circ}\text{C}$  for 2h. The reaction was stopped by the addition of  $5\mu\text{l}$  of  $1\text{M}$  ethylenediaminetetraacetic acid tetrasodium salt (EDTA) pH 8.0. TdT-labelled oligonucleotides were extracted by the addition of  $200\mu\text{l}$  phenol/chloroform:isoamyl alcohol (25:24:1 v/v), followed by inversion and centrifuging for 1min at  $13\ 000g$ . The aqueous phase, containing labelled oligonucleotides, was transferred to a new Eppendorf tube and residual traces of phenol and unincorporated nucleotides were removed using Chroma spin-10 columns (Clontech) according to the manufacturers instructions.

To  $34\mu\text{l}$  of a  $10\text{mg}/\text{ml}$  solution of freshly prepared digoxigenin 3-*O*-methylcarbonyl- $\epsilon$ -aminocaproic acid *N*-hydroxysuccinimide ester (DIG-NHS) (Roche Diagnostics) in dimethyl formamide was added  $156\mu\text{l}$  of  $160\text{mM}$  sodium borate and  $100\mu\text{l}$  of the Chroma spin-10 column purified oligonucleotide

cocktail (above). This was diluted with water to a total volume of 250 $\mu$ l to give a final concentration of 1.4 mg/ml DIG-NHS and 0.1M sodium borate. The DIG-NHS/oligonucleotide cocktail solution was incubated for approximately 18h, overnight, at RT. The labelled oligonucleotide cocktail was purified to remove reaction components using Chroma spin-10 columns, quantified as described above (see 2.2.2) and stored at -20°C. Concentration of oligonucleotide cocktails at this stage ranged from 10 $\mu$ g/ml to 15 $\mu$ g/ml.

#### **2.2.4 Dot blot hybridisation to test labelling efficiency**

Diluent for the oligonucleotide cocktails was prepared by denaturing 400 $\mu$ g of single stranded (ss) salmon sperm DNA (supplied by Sigma as an aqueous solution, 10mg/ml) at 100°C for 5min. The denatured DNA (40 $\mu$ l) was added to 1360 $\mu$ l UP water and 600 $\mu$ l 20x SSC (0.3M sodium chloride, 0.03M sodium citrate, pH 7.0) to give a diluent with a final concentration of 0.2mg/ml salmon sperm DNA and 6x SSC. The oligonucleotides cocktails were diluted using the prepared diluent (0.2mg/ml salmon sperm DNA and 6x SSC) to give a range of concentrations from 1pg/ $\mu$ l to 1ng/ $\mu$ l of oligonucleotide cocktail. The diluted oligonucleotide cocktails, in 1 $\mu$ l volumes, were dotted onto a strip of nitrocellulose membrane with a positively labelled control sample (1 $\mu$ l) and baked, in an envelope of 3MM filter paper, at 80°C for 2h. The membrane was incubated for 20min at 37°C in pre-warmed blocking solution containing 3% bovine serum albumin (BSA) in tris buffered saline (TBS: 0.1M tris, 0.15M NaCl) containing 0.1% v/v triton X-100. The membrane was removed from the blocking solution and baked in a filter paper envelope at 80°C for 20min. The

membrane was washed twice in blocking solution (8ml) for 5min at RT and a horseradish peroxidase conjugated anti-digoxigenin antibody (Roche Diagnostics) was added at a dilution of 1:1000 in 8ml of blocking solution for 30min at RT. 3, 3'-diaminobenzidine tetrahydrochloride (DAB) substrate solution was added for 5min at RT. The membrane was rinsed briefly in water. Brown spots indicated a positive result for the digoxigenin labelling of the oligonucleotide cocktails.

### **2.2.5 Aminopropyl triethoxysilane (APES) coated slides**

To avoid loss of tissue and morphological damage during the process of *in situ* hybridisation, glass slides were coated with APES. Slides were prepared by washing in 10% Teepol detergent overnight and then washing in hot tap water before rinsing in distilled water. Slides were then washed in IMS and dried at RT before immersing in APES (2% v/v in IMS) for 1-2min. The slides were rinsed twice in IMS and finally in acetone before drying for 24h at 37°C.

### **2.2.6 Siliconised coverslips**

Coverslips were siliconised by immersing them in dimethyldichlorosilane solution, allowing them to dry in air for 15min. The coverslips were then washed twice in UP water for 15sec and dried at RT.

### 2.2.7 Histology

Rodent uteri were removed and representative sections from both horns of the rat uterus were fixed in 10% neutral buffered formalin, and the mouse uterus fixed in 3.7% neutral buffered formalin. This fixative is superior to protein precipitating fixatives for the retention of mRNA in tissue samples (Lawrence *et al.*, 1985), as formaldehyde is known to form cross-links between RNA and protein (Chaw *et al.*, 1980). Tissues were paraffin embedded and sectioned onto APES coated slides at 5µm for histology analysis.

### 2.2.8 Preparation of sections

Paraffin sections (5µm) of rodent uterus were prepared by the Histology Department of the MRC Toxicology Unit. Sections were de-paraffinised by immersing in HistoClear<sup>®</sup> (Fisher Scientific) twice for 10min then re-hydrated first by immersion in industrial methylated spirits (IMS) twice for 5min, then 80% IMS (prepared using 0.1% DEPC-H<sub>2</sub>O) for 5min, and finally rinsing in 0.1% DEPC-H<sub>2</sub>O. Following re-hydration, sections were transferred to 2x SSC (0.3M sodium chloride, 30mM sodium citrate, 0.1% DEPC H<sub>2</sub>O), and incubated in this buffer at 70°C for 10min followed by 5min in 0.1% DEPC H<sub>2</sub>O at RT. RNA within the tissue was unmasked by the removal of protein using the proteolytic enzyme proteinase K. Proteinase K concentration was optimised for each set of tissues and was used at a concentration of 2 to 10µg/ml, in 50mM tris/HCl buffer pH 7.5. Sections were partially digested in the proteinase K solution by incubation in a humidifying chamber for 1h at 37°C. Sections were rinsed twice in 0.1% DEPC H<sub>2</sub>O for 5min at 4°C. RNA retention was increased by mild

fixation of the sections in paraformaldehyde 0.4% w/v in PBS buffer for 20min at 4°C followed by rinsing in 0.1% DEPC H<sub>2</sub>O for a minimum of 5min.

### **2.2.9 Hybridisation of sections**

Sections were pre-hybridised in a 55°C humidified chamber for 1h in 50-100µl hybridisation buffer which contained 0.6M NaCl, 10% dextran sulphate, 50% formamide, 150µg/ml ss salmon sperm DNA and 1x PE (50mM tris/HCl pH 7.5 containing: 0.1% sodium pyrophosphate, 0.2% polyvinylpyrrolidone, 0.2% Ficoll, 5mM EDTA). After incubation, the buffer was removed and 50µl hybridisation buffer, containing 0.5-1.5µg/ml of digoxigenin labelled oligonucleotide probe cocktail depending on tissue type (see tables 2.1-2.4 and method 2.2.3) was added to the tissue section. A siliconised coverslip was overlaid to ensure even coverage and to prevent evaporation of the solution. Sections were incubated overnight in a dark humidified chamber at 55°C. Following hybridisation, coverslips were removed and sections were washed to remove probes bound to tissue elements non-specifically or in a mismatched manner. Stringency of the post-hybridisation wash was increased by increasing the concentration of formamide from 30% to 50%, decreasing the salt concentration from 2x SSC to 0.1x SSC and increasing temperature from RT to 55°C.

### **2.2.10 Detection of hybridised probes**

To reduce non-specific binding of antibody, sections were incubated for 5min at RT in blocking solution (3% BSA, 0.1% Triton X-100 in TBS) prior to the addition of 100µl horseradish peroxidase conjugated anti-digoxigenin antibody (Roche Diagnostics) at 1:50 dilution in blocking solution. The sections were incubated in a humidified chamber at RT for 30min. Sections were washed in TBS twice for 5min. Sections probed with the horseradish peroxidase conjugated antibody were detected with DAB substrate solution for 5-10min at RT. Placing sections in running tap water stopped the reaction. Sections were lightly counterstained and mounted with DPX as in Methods 2.3.1. Sections were photographed using a Leitz DIAPLAN microscope with various objectives and Kodak 400 film.

### **2.2.11 *In situ* hybridisation controls**

Several controls were used in the process of optimising the *in situ* hybridisation technique. To test for any endogenous horseradish peroxidase activity in the tissues, a parallel section, with omission of probe in the hybridisation step, was included as a negative control. To verify the specificity of the oligonucleotides by competition, a fifty-fold increase of unlabelled probe was added to the labelled probe and used in hybridisation. Estimation of the retention of RNA was made by hybridising parallel sections with a probe specific to 28S ribosomal RNA. This allowed the estimation of levels of RNA available for hybridisation, as opposed to a stain for RNA that enters the cells at a different level and efficiency to oligonucleotide probes. An oligonucleotide probe was

synthesised specific to a conserved region of 28S ribosomal RNA (Yoshii *et al.*, 1995). The oligonucleotide was labelled with digoxigenin, as described, and used to probe parallel sections at a concentration of 0.2µg/ml. Sense versions of the oligonucleotide cocktails were synthesised and used to probe parallel sections.

### **2.2.12 RT-PCR study to confirm *in situ* hybridisation probe specificity**

RT-PCR was used to produce a template for the verification of *in situ* hybridisation probe specificity. Reverse transcription of RNA followed by the polymerase chain reaction can be used to detect low amounts of RNA.

Reverse transcription transcribes RNA into cDNA that is then used in PCR as a template producing numerous copies of a specific sequence.

#### **2.2.12.1 RNA extraction for RT-PCR**

Rodent uterine tissue (~60mg) was snap frozen with liquid nitrogen in a pre-chilled sterile pestle and mortar and ground to a fine powder. 1ml of solution D (4M guanidine thiocyanate, 25mM sodium citrate pH 7.0, 0.5% N-lauryl sarcosine and 0.1M β-mercaptoethanol) was added to the powdered tissue in the mortar and mixed carefully by pipetting. The solution was transferred to two sterile Eppendorf tubes. Aqueous phenol (Life Technologies) (500µl), 2M sodium acetate (50µl) and 24:1 v/v chloroform:isoamyl alcohol (100µl) were added to each tube, vortexed and incubated on ice for 15min. Samples were

### **2.2.12.2 cDNA synthesis**

Total RNA (1µg in a volume of 11µl of 0.1% DEPC H<sub>2</sub>O) was incubated at 70°C for 10min with 1µl oligo (dT)<sub>12-18</sub> (0.5µg/µl in 0.1%DEPC-H<sub>2</sub>O, Life Technologies) and 1µl RNasin ribonuclease inhibitor (40U/µl, Promega). After chilling on ice, 4µl 5x First Strand buffer, 2µl of 0.1M dithiotheitol (DTT) (5x First Strand buffer and 0.1M DTT supplied by Life Technologies with Superscript II, below) and 1µl 10mM deoxynucleotide triphosphates (dATP, dTTP, dCTP, dGTP, Life technologies) were added. Sample was mixed by vortexing and incubated at 42°C for 2min. Superscript II RNase H<sup>-</sup> reverse transcriptase (200U/µl, Life Technologies) was added. cDNA was synthesised by incubation for a further 50min at 42°C before inactivating the reaction by heating at 70°C for 15min.

### **2.2.12.3 RT-PCR amplification of rat ER $\alpha$ and ER $\beta$ full length transcripts**

PCR primers were designed to be situated at the 5' and 3' ends of the ER $\alpha$  and ER $\beta$  full-length transcripts and checked for homology to other sequences. Primers were synthesised, purified and quantified as before (See 2.2.2; Tables 2.5 and 2.6). A 5µM stock solution was made of each primer, aliquotted and stored at -20°C.

**Table 2.5 Rat ER $\alpha$  oligonucleotide primers for PCR**

Base pair reference	Genbank Y00102	T <sub>m</sub> °C	%GC
Sense and anti-sense 5'-3'			
Sense 50	CAC ATT CCT TCC TTC CGT CT	51.9	50
Anti-sense 2035	GTT TCA GGG ATT CGC AGA AC	51.6	50

**Table 2.6 Rat ER $\beta$  oligonucleotide primers for PCR**

Base pair reference	Genbank U57439	T <sub>m</sub> °C	%GC
Sense and anti-sense 5'-3'			
Sense 53	CAC CCA GGT CTG CAA TAA AG	58.2	50
Anti-sense 2536	CGG GAG AGA GAG AAA GAT GA	51.6	50

PCR amplification was performed using a Hybaid OmniGene Thermal Cycler (Hybaid Ltd, UK). Reaction mixtures were of 50 $\mu$ l volume and contained: 2 $\mu$ l of template cDNA (see 2.2.12.2), 1x PCR Reaction buffer with 15mM MgCl<sub>2</sub> (supplied with *Ampli*Taq by Applied Biosystems), 0.1mM dNTPs, (dATP, dTTP, dCTP and dGTP, Life Technologies) 0.5 $\mu$ M sense and anti-sense primers (see Tables 2.5 and 2.6), 1U *Ampli*Taq DNA polymerase (Applied Biosystems) and 29.8 $\mu$ l sterile UP water. Approximately 20 $\mu$ l of mineral oil was added to prevent evaporation of PCR reagents during PCR cycling. Tubes were briefly centrifuged and subjected to the following PCR conditions: 95°C for 2min, followed by 30 cycles of 95°C for 1min (denaturation), 55°C for 1min

(annealing), 72°C for 2min (elongation) and concluding with 72°C for 10min. PCR products were stored at -20°C until analysis by 1.5% agarose gel electrophoresis. PCR samples were separated by electrophoresis in a 1.5% agarose gel (100ml volume) containing ethidium bromide (5µg/ml) using 1x TBE (90mM Tris, 90mM boric acid, 2mM EDTA) as the running buffer. A 17µl aliquot of the PCR product was mixed with 3µl gel loading buffer (30% glycerol in tris/HCl pH 8.0, 0.25% w/v bromophenol blue) and electrophoresed at 100 volts for 30min. The gel was visualised under a UV transilluminator and photographed using Polaroid film (Type 55, pos/neg).

#### **2.2.12.4 Sequence confirmation by restriction enzyme digestion**

Sequences of the PCR products were confirmed by restriction enzyme digestion. 1µl of PCR product was added to 12µl of sterile dH<sub>2</sub>O, 2µl of 10x buffer (supplied by Promega with the restriction enzymes) and 1µl of restriction enzyme (*Stu1* for ER $\alpha$  and *BamH1* for ER $\beta$ ). Reactions were incubated at 37°C for 1h and products analysed using agarose gel electrophoresis and photographed as described above.

#### **2.2.12.5 Approximate quantification of PCR products using ethidium bromide**

Salmon sperm (ss) DNA (10mg/ml) was used as a DNA standard and diluted from 1ng/µl to 20ng/µl in a volume of 5µl UP water. ER $\alpha$  and ER $\beta$  PCR products (Method 2.2.12.3) were diluted 1:5, 1:25 and 1:125 in a volume of 5µl

UP water. Ethidium bromide was added to all samples and standards to a final concentration of 0.5µg/ml. Samples and standards were dotted onto saran wrap within a grid and photographed under UV light (Method 2.2.12.3). Intensity of samples and standards was then used to approximate the concentration of the PCR products.

### **2.2.12.6 <sup>32</sup>P labelling of oligonucleotide cocktails**

The oligonucleotide cocktails (Tables 2.1-2.4) were labelled with <sup>32</sup>P to enable detection of their hybridisation to the ERα and ERβ PCR products on the dot blot. The 50µl reaction mixture contained: 25ng of each of the five oligonucleotides for ERα or ERβ, a dNTP mix (100µM dATP, dTTP, dGTP and 50µM dCTP, Life Technologies) 5µl Klenow Reaction buffer (10x), 5µl random hexamers (100pmol/µl) and 1µl Klenow enzyme (5U/µl) (all supplied by Promega), 5µl (1.85MBq) dCTP (dCTP (α <sup>32</sup>P) specific activity 250µCi, 9.25MBq) (Amersham). The tubes were incubated at 37°C for 30min and the reaction mixtures were immediately purified as described below.

### **2.2.12.7 Column purification of labelled oligonucleotides**

NucTrap Push columns (Stratagene), used to remove unlabelled oligonucleotides, were pre-wetted with 70µl 20mM tris/HCl pH 7.5 buffer containing 100mM NaCl and 10mM EDTA (STE buffer) by pushing through using a Hamilton syringe over 20-30sec. The oligonucleotides, in a volume of 70µl STE buffer, were pushed through the column resulting in labelled

oligonucleotides in a 100µl volume. Labelled (approximately  $8 \times 10^5$  cpm) oligonucleotide cocktails were stored at  $-20^{\circ}\text{C}$  for up to one week.

### **2.2.12.8 Dot blot hybridisation of PCR products and oligonucleotide cocktails**

Dot blot hybridisation was used to test the specificity of the  $^{32}\text{P}$  labelled ER $\alpha$  and ER $\beta$  oligonucleotide cocktails (Method 2.2.12.6) against the PCR amplified full-length transcripts of ER $\alpha$  and ER $\beta$  (Method 2.2.12.3). The PCR products, approximately 100pg (quantified as in Method 2.2.12.5) in a volume of 4µl of 6x SSC, were denatured by incubating at  $100^{\circ}\text{C}$  in the Hybaid OmniGene Thermal Cycler (Hybaid Ltd, UK) for 10min before snap cooling on ice. A nylon membrane, Nytran 0.45µM (Schleicher and Schuell), was cut to 10x10cm and pre-wetted with 6x SSC before being placed onto Whatman 3MM filter paper. The PCR product DNA was applied in 2µl volumes, allowing each one to dry, to reach a final concentration of 100pg. The membrane was allowed to dry completely and placed onto a stack of 3MM filter paper saturated with denaturing solution consisting of 1.5M NaCl in 0.5M NaOH. After 10min the membrane was transferred to a stack of filter paper saturated in a neutralising solution of 1M NaCl in 0.5M tris/HCl buffer, pH 7.0 for 5min. The filter was allowed to dry and DNA was immobilised by UV crosslinking (automatic program using Stratalinker 2400, Stratagene™).

### **2.2.12.9 Hybridisation and detection**

To help reduce background binding and to provide optimum conditions for hybridisation, pre-hybridisation of the dot blot was performed by incubation at 42°C in hybridisation buffer consisting of 50% de-ionised formamide, 5x Denhardt's solution (Sigma), 5x SSC, 100µg/ml ss salmon sperm DNA, 10% dextran sulphate, for a minimum of 1h. The <sup>32</sup>P labelled oligonucleotide cocktails (40µl) were added to the 20ml hybridisation buffer and the blot was hybridised overnight at 42°C with continuous rotation. To remove any unbound probe and non-specifically bound probe, the blot was subjected to stringent post-hybridisation washes with SSC by lowering salt concentration from 2x SSC to 0.2x SSC and increasing the temperature from 42°C to 50°C until the cpm had been reduced to 5-10cpm. The labelled bound probe was detected by placing the blot into an autoradiography cassette and exposing to X-ray film (Genetic Research Instrumentation) at -80°C for 48h to 72h before developing.

## **2.3 Immunochemical methods of ER protein localisation**

### **2.3.1 Immunohistochemistry**

#### **2.3.1.1 Preparation of sections for ER $\alpha$ and ER $\beta$ detection**

Formalin fixed 5µm paraffin sections of rodent uterus were de-waxed by immersing in HistoClear<sup>®</sup> for 10min (twice). Re-hydration was performed in IMS for 5min (twice) and 80% IMS for 5min before washing in dH<sub>2</sub>O. Sections were transferred to 0.01M citric acid/NaOH buffer, pH 6.0 and microwaved at 700W

for 20min. Following microwaving, the sections were washed briefly in dH<sub>2</sub>O at RT. Endogenous peroxidase activity was blocked by immersing the sections in freshly prepared hydrogen peroxide, 10% v/v in dH<sub>2</sub>O, for 20min at RT. The sections were washed for 10min under running tap water and finally immersed in PBS for 3x 2min.

### **2.3.1.2 Antibody detection of ER $\alpha$**

ER $\alpha$  was detected in rodent tissue sections using a Novacastra mouse monoclonal antibody (NCL-ER-6F11) raised against a recombinant protein corresponding to the full length human ER $\alpha$ . Following the treatments described above, the sections were incubated for 3h with 100 $\mu$ l of mouse monoclonal anti-ER $\alpha$  diluted 1:40 in PBS at RT. Bound primary antibody was detected with DAKO StreptABCComplex/HP Duet kit, following manufacturers instructions, and visualised with DAB solution supplied with the kit. Sections were lightly counterstained with hematoxylin before dehydration through graded alcohol, clearing and mounting with DPX. Omission of primary antibody was used as a negative control on parallel sections.

### **2.3.1.3 Antibody detection of ER $\beta$**

ER $\beta$  was detected in rodent tissue sections using an Upstate Biotechnology rabbit polyclonal antibody (06-629) raised against a synthetic peptide representing amino acids 54-71 of rat and mouse ER $\beta$  and amino acids 46-63 of human ER $\beta$ . Sections were prepared as for ER $\alpha$  detection and the rabbit

polyclonal anti-ER $\beta$  was diluted 1:10 in PBS. 100 $\mu$ l was applied to each section and incubated overnight at RT. Bound primary antibody was detected using the DAKO StreptABComplex/HP Duet kit, following manufacturers instructions, and visualised with DAB solution. The sections were cleared and mounted as above. As a negative control, the primary ER $\beta$  antibody was saturated with a blocking peptide (Upstate Biotechnologies) and used to probe parallel sections.

#### **2.3.1.4 Oil red O staining of fat deposits**

Oil red O staining of fat deposits in neonate mouse uterine sections was performed by the Histology Department of the MRC Toxicology Unit.

### **2.3.2 Western blotting**

#### **2.3.2.1 Protein concentration determination**

Protein concentration of samples for Western blotting was determined using a commercial kit (Sigma procedure number TPRO-562). BSA protein standards, 0.2, 0.4, 0.6, 0.8 and 1mg/ml, were prepared using appropriate diluent. Each sample (1:10 to 1:100 dilution), standard or blank was pipetted into a microtitre plate with 200 $\mu$ l of bicinchoninic acid/copper sulphate solution (50ml of bicinchoninic acid solution was combined with 1ml of a 4% solution of copper (II) sulphate pentahydrate). The plate was mixed for 30sec and incubated at 37°C for 1h. Absorbances were determined at 540nm using a Labsystem Multiskan Plus microtitre plate reader. A standard curve was plotted and used to determine the protein concentration of the samples.

### 2.3.2.2 SDS-polyacrylamide gel electrophoresis and Western

#### blotting

In order to visualise ER proteins by Western blotting the solubilised protein samples were separated by vertical sodium dodecyl sulfate (SDS) polyacrylamide gel electrophoresis (PAGE). Mini-gel apparatus (BioRad) was prepared with a 7.5% polyacrylamide resolving gel of 0.38M tris/HCl buffer pH 8.8 containing 7.5% acrylamide/bis solution (Anachem) and 0.1% SDS. The polymerised resolving gel was overlaid with a 3% polyacrylamide stacking gel containing 0.13M tris/HCl buffer, pH 6.8 with 3% acrylamide/bis solution and 0.1% SDS. Samples were prepared by combining 30µg of protein in a volume of 10µl dH<sub>2</sub>O with 10µl of 2x sample loading buffer (0.125M tris/HCl buffer, pH 6.8 containing 4% SDS, 20% v/v glycerol, 0.2M DTT and 0.02% bromophenol blue) and heating to 100°C for 3min in a Hybaid Omnigene Thermal Cycler (Hybaid Ltd, UK). Protein samples were cooled on ice and loaded into the stacking gel wells. ER $\alpha$  and ER $\beta$  human recombinant proteins, molecular weights 66 and 53kDa (Calbiochem, catalogue numbers 330655 and 330657 respectively) were used as positive controls, prepared as above, and loaded at a concentration of 10ng. In some instances standard curves of these proteins were prepared over a concentration range of 1 to 50ng per lane. Samples were electrophoresed using electrode buffer (0.025M tris, 0.192M glycine, 0.1% SDS) for approximately 1h at RT at a constant current of 40mA. Hybond nitrocellulose membrane (Amershem), 6x9cm, and polyacrylamide resolving gels were equilibrated for 5min at RT in Towbin transfer buffer (25mM tris, 192mM glycine, 20% v/v methanol). Proteins were transferred from the gels

onto nitrocellulose membrane using Towbin transfer buffer at 100 volts over 90min. Membranes were stained with Ponceau S to check for complete transfer and, after washing in dH<sub>2</sub>O, membranes were blocked overnight at 4°C in non-fat milk (Marvel) 5% w/v in tris buffered saline (TBS: 100mM tris/HCl buffer, pH 7.6 containing 0.9% NaCl). The gels were stained in PAGE blue protein stain (10% acetic acid, 20% methanol, 0.25% w/v bromophenol blue) overnight and then de-stained to check for complete protein transfer.

### **2.3.2.3 Detection**

Nitrocellulose membranes were washed for 15min and twice for 5min in PBS with 0.1% Tween 20 (PBS-T20) to remove non-fat milk blocking solution. ER $\alpha$  was detected with a monoclonal (mouse) anti-ER $\alpha$  IgG antibody, (Upstate Biotechnology; 05-394) raised against purified, SDS-denatured, calf uterus ER (cross-reactive with human, bovine, rat and mouse). The antibody was used at a concentration of 1:500 in 10ml of 5% w/v non-fat milk in PBS to help reduce non-specific binding, and was incubated on a rocking platform for 2h. Following incubation the primary antibody solution was removed and the membranes were washed in PBS-T20 for 15min and twice for 5min. Bound ER $\alpha$  primary antibody was detected with a peroxidase-conjugated anti-mouse IgG (Sigma) at 1:1000 in 10ml of 5% w/v non-fat milk in PBS, which was incubated for 1hr at RT on a rocking platform. Following incubation, the secondary antibody solution was removed and the membranes were washed in PBS-T20 for 15min and then twice for 5min in UP water.

ER $\beta$  was detected in Western blots with a polyclonal (rabbit) anti-ER $\beta$  antibody (Affinity Bioreagents; PA1 313), raised against N-terminal amino acid residues 55-70 of rat, mouse and human ER $\beta$ . The antibody was used at a concentration of 1:2500 and detected with a peroxidase-conjugated anti-rabbit IgG (BioRad) at 1:7000. Antibody diluent, incubation times and washing steps were as for ER $\alpha$  detection described above.

The Amersham ECL Chemiluminescent detection kit was used to visualise the ER $\alpha$  and ER $\beta$  proteins on Amersham Hyper film as recommended by the manufacturers. Films were exposed for a minimum of 30sec. The density of the chemiluminescent bands was quantified either using an imager (Image Quant, Molecular Dynamics) or directly on the nitrocellulose filter using a Kodak 440CF Image station (Eastman Kodak Company). Concentrations of ER $\alpha$  and ER $\beta$  proteins were initially quantified relative to the corresponding recombinant human protein run on the gel at the same time.

## **2.4 Cell culture**

### **2.4.1 Cell culture**

Cell culture was carried out aseptically in Class II laminar flow cabinets and cell lines were maintained in a Sanyo CO<sub>2</sub> incubator at 37°C in a humidified 95% air: 5% CO<sub>2</sub> atmosphere. Human breast adenocarcinoma derived MCF-7 cells and human endometrium derived Ishikawa cells were obtained from the European Collection of Cell Cultures. Frozen ampoules were thawed

completely in a 37°C water bath and resuspended in 10ml Dulbecco's modified Eagle's medium (DMEM) (containing 10% foetal bovine serum (FBS) and 2% glutamax) before centrifuging at 200g, for 5min at 4°C. Supernatant was discarded and the pelleted cells resuspended in 15ml of culture media. Viable cells were established as mycoplasma free by Core Tissue Culture Technicians of the Hodgkin building, University of Leicester. Cells were maintained as monolayer cultures in 75cm<sup>2</sup> flasks and passaged when confluent.

#### **2.4.2 Subcultures**

All culture media was removed from confluent flasks by pipetting and cells were washed twice with PBS before the addition of 2ml of trypsin/EDTA.

Trypsin/EDTA solution contained, in 10ml UP water, trypsin (50mg), EDTA (20mg), NaCl (85mg). Flasks were incubated at 37°C for 5min until cells had detached from the surface. 8ml of culture media was added to resuspend the cells and inactivate the trypsin. Cell suspensions were centrifuged at 200g, for 5min at 4°C and the supernatant was removed. The cell pellet was resuspended in 10ml of the culture media. New flasks were seeded with approximately 10<sup>6</sup> cells in culture media and maintained as described.

#### **2.4.3 Preparing cells for storage in liquid nitrogen**

Cell lines were frozen at a low passage number to provide stocks. Cells were prepared as for subculture (Method 2.4.2). However, the cell pellets were resuspended in freezing medium of 40% serum-free DMEM media, 50% serum

and 10% DMSO cryoprotectant, at a concentration of  $1 \times 10^6$  cells/ml. Vials of cells were stored at  $-80^\circ\text{C}$  in a polystyrene container (to slow the freezing rate) for up to 7 days and moved to liquid nitrogen for long-term storage. Cells were revived as method 2.4.1.

#### **2.4.4 Preparation of dextran charcoal stripped serum**

Foetal bovine serum (FBS) was stripped using dextran-coated charcoal to reduce levels of endogenous oestrogenic compounds. A 200mg/ml solution of dextran-coated charcoal was prepared in UP water and 1.25ml of the suspension (DCC) added to 50ml of FBS. FBS was mixed at  $56^\circ\text{C}$  in a shaking water bath for 30min and centrifuged at  $1000g$ , for 20min at  $4^\circ\text{C}$ . This procedure was repeated before filter sterilising the stripped serum using a  $0.22\mu\text{M}$  bottle top filter. Stripped serum was stored at  $-20^\circ\text{C}$ .

#### **2.4.5 Treatment of cells**

All cell culture experiments were carried out in triplicate in 6 well plates. Oestrogenic and anti-oestrogenic compounds were dissolved at various concentrations in DMSO as indicated below and then stored as stock solutions at  $-20^\circ\text{C}$ . Cell lines were plated at  $4 \times 10^5$  cells/well with 2ml DMEM culture media and incubated for 24hr. Culture media was removed and cells washed twice with PBS then media containing 10% dextran-charcoal stripped serum (Method 2.2.4) was added 48h before dosing. Cells were dosed by addition of the following SERMs to the existing culture media:  $17\beta$ -oestradiol  $1 \times 10^{-9}$  M,

tamoxifen  $1 \times 10^{-6}$  M, raloxifene  $1 \times 10^{-6}$  M, faslodex  $1 \times 10^{-6}$  M and incubated under normal culture conditions until cell lysates were prepared at the times indicated in the results. In some instances, the proteasome inhibitors MG132 or MG115 (Sigma) were added 1h prior to treating the cells with the test compounds.

#### **2.4.6 Estimation of cell viability by trypan blue exclusion**

The cytotoxic effect of compounds used in this study was assessed using the trypan blue exclusion assay. Cell membrane permeability allows dye entry and this is a non-specific method for detection of cell death. Cells were maintained for 24h before changing media and dosing as Method 2.4.5. Monolayer cells were removed by the trypsin/EDTA method described in 2.4.2: 1ml of trypsin/EDTA was added to each well and the plates were incubated at 37°C until the cells detached (5min). 20 $\mu$ l of cell suspension was mixed with 20 $\mu$ l of trypan blue solution (GibcoBRL). The numbers of stained and unstained cells were counted in triplicate using a haemocytometer with 4 random fields counted per sample. Viability was expressed as a percentage of total cells.

#### **2.4.7 Preparation of cell lysates for Western blotting**

Culture media was removed from 6 well plates and cells washed twice with 2ml PBS. Cells were treated with trypsin/ EDTA as described in Method 2.4.2 and the cell pellet (approximately  $1 \times 10^7$  cells) resuspended in 1ml PBS and centrifuged at 200g for 5min. Cells pellets were resuspended and lysed in 20 $\mu$ l extraction buffer by incubation on ice for a minimum of 10min with occasional vortexing. A clear cell lysate was obtained by centrifuging at 10 000g for 5 min

at 4°C. The extraction buffer was prepared as described by Nawaz *et al.*, (1999b) and contained 50mM tris/HCl buffer, pH 8.0, 5mM EDTA, 1% (v/v) Nonidet P-40, 0.2% (w/v) sarcosyl, 0.4M NaCl, 100µM sodium vanadate, 10mM sodium molybdate and 20mM sodium fluoride. Supernatants were stored at -20°C until protein concentration determination, Method 2.3.2.1.

#### **2.4.8 Fluorescence based determination of proteasome activity using Suc-LLVY-AMC**

Proteasome activity was assessed following the addition of proteasome inhibitors by a peptide substrate for the proteasome complex that produces fluorescence when degraded. 50µM Suc-LLVY-AMC (dissolved in 10% DMSO) was obtained from Bachem Biochemica. Cells were grown in 6 well culture plates (Ishikawa 1 x10<sup>5</sup> cells/well and MCF-7 3 x10<sup>5</sup>/well) as per Methods 2.4. Cells were treated with oestradiol or tamoxifen as described in Methods 2.4.5 and incubated at 37°C for 3h (the proteasome inhibitors, MG115 or MG132 were added 1h prior to dosing). Cells lysates were prepared as described in Method 2.4.8 in cell extract buffer (100mM HEPES, 10% sucrose and 0.1% CHAPS). 100µM of protein extract was treated with 50µM Suc-LLVY-AMC in a total volume of 200µl with 5mM MgCl<sub>2</sub>, 5mM ATP, 50mM Tris-HCl pH 7.8, 20mM KCl and 5mM magnesium acetate. The protein extract was incubated for 1h at 37°C and the reaction was terminated by the addition of 200µl of 0.1M sodium borate, pH 9.0 in water/ethanol (144:16). The fluorescence of aminomethylcoumarin was measured using excitation and emission wavelengths of 365 and 460nm respectively in a fluorometer. Standard curves

were prepared containing 7-amino-4-methylcoumarin using the same reagents buffers.

## **2.5 Clontech Mouse 1.2 cDNA microarray analysis**

### **2.5.1 Total RNA extraction for cDNA arrays**

Total RNA was extracted from the uteri of each group of treated neonatal mice (control, oestradiol, tamoxifen, toremifene and raloxifene, see 2.1.1) using a Microisolation Kit from Stratagene (cat No 200344) for subsequent analysis by cDNA expression array. In order to obtain sufficient material from the newborn mice, 4 to 6 uteri taken from liquid nitrogen storage were pooled and then ground to a fine powder in a sterile pestle and mortar pre-chilled using liquid nitrogen. The Microisolation Kit (Stratagene) denaturing solution (500 $\mu$ l containing 3.6 $\mu$ l  $\beta$ -mercaptoethanol) was added to the tissue fragments in the mortar. The tissue suspension was then transferred to a sterile Eppendorf tube (RNase and DNase free) on ice, where 50 $\mu$ l of 2M sodium acetate, 500 $\mu$ l water saturated phenol and 150 $\mu$ l chloroform-isoamyl alcohol were added. The mixture was vortexed for 1 min, incubated on wet ice for 15min before centrifuging (13 000g for 30min at 4°C), to separate the aqueous and organic phases. The upper aqueous layer containing RNA was transferred to a new microfuge tube and 500 $\mu$ l of ice-cold isopropanol added. The sample was mixed by inversion and incubated at -80°C for a minimum of 30min. RNA sample was pelleted by centrifuging 13 000g, for 30min at 4°C. The pellet was washed in cold 70% ethanol by vortexing and spinning for 5min at 4°C. The

supernatant was carefully removed and the pellet allowed to air dry on ice before resuspending in 10-50 $\mu$ l of 0.1% DEPC UP water. Pellets were stored at -80°C or treated with DNase immediately as described below.

### **2.5.2 DNase treatment of total RNA**

For elimination of contaminating DNA, the isolated total RNA samples (50 $\mu$ l) in 500 $\mu$ l Eppendorf centrifuge tubes, were mixed with 5 $\mu$ l DNase buffer and 4 Units of DNase 1 (Ambion DNA-free kit cat: 1906) and incubated at 37°C for 50min. Subsequently, in order to destroy DNase activity, 5 $\mu$ l of the DNase inactivation reagent (Ambion) was added to the samples and incubated for 2min at RT with occasional agitation. Samples were centrifuged (13 000g for 1min at RT) to pellet the inactivation reagent. The supernatant containing the RNA was transferred to a fresh Eppendorf tube. Concentration and purity of the RNA sample was calculated as in method 2.2.12.1. Only those samples with a  $A_{260}/A_{280}$  ratio of greater than 1.6 were processed further since the quality of the RNA is the most important factor for generating high sensitivity hybridisation probes.

### **2.5.3 Preparation of cDNA probes**

The protocols for the completion of the cDNA microarray analysis were performed using the Clontech Mouse 1.2 expression array kit according to the manufacturer's instructions, all materials, except DEPC treated water and total RNA, were supplied by Clontech. Total RNA (5 $\mu$ g) was converted into  $^{32}\text{P}$

labelled first strand cDNA probes for hybridisation to the cDNA expression array.

Mouse 1.2 CDS Primer mix (1µl) was added to 5µg of total RNA in a volume of 2µl 0.1% DEPC treated H<sub>2</sub>O in a 500µl Eppendorf tube. RNA samples were mixed well and incubated for 2min at 70°C in a heating block followed by 2min at 48°C. After cooling to RT, 8µl of master mix was added. The master mix contained: 2µl reaction buffer, 1µl dNTP mix (5mM of each dCTP, dGTP, dTTP), 35µCi [ $\alpha$ -<sup>32</sup>P] dATP (specific activity 3,00Ci/mmol, 3.5µl), 6.5mM DTT and 50U Moloney Murine Leukemia Virus Reverse Transcriptase. Samples (11µl) were mixed gently by pipetting and incubated at 48°C for a further 50min. The reaction was stopped by the addition of 1µl Termination mix and the samples were stored briefly on ice.

#### **2.5.4 Purification of labelled cDNA probes**

Labelled cDNA was purified from unincorporated <sup>32</sup>P-labelled nucleotides and <0.1kb cDNA fragments. Choma Spin-200 DEPC-H<sub>2</sub>O columns (Clontech) were allowed to warm to RT for a least 1h before inverting several times to resuspend to gel matrix. The top and bottom caps were removed and the columns placed in 1.5ml microcentrifuge tubes where the water drained through until the surface of the gel was observed. The <sup>32</sup>P-labelled samples (12µl) were applied to gel's surface with extreme care. Fraction 1 was collected when the samples were fully absorbed, 40µl of 0.1% DEPC-H<sub>2</sub>O was added and allowed to drain. Fraction 2 was collected by the addition of 250µl 0.1% DEPC-H<sub>2</sub>O. A

further 6 fractions were collected into fresh microcentrifuge tubes by the repeated addition of 100 $\mu$ l of 0.1% DEPC-H<sub>2</sub>O. The radioactivity of each fraction was measured by taking a 1 $\mu$ l aliquot of each fraction and counting for 1min using a liquid scintillation analyser (1500 Tri-Carb, Packard). The total radioactivity of each fraction was calculated. The purified labelled probe was usually found in fractions 4 and 5.

### **2.5.5 Hybridisation of labelled cDNA to the Atlas Array**

Clontech Atlas cDNA expression arrays include 1176 mouse cDNA spotted onto a nylon membrane. Plasmid and bacteriophage DNAs are included as negative controls to confirm hybridisation specificity along with several housekeeping genes that act as orientation marks and as positive controls. Salmon sperm DNA (10mg/ml) was denatured at 100°C for 5min and cooled quickly on ice. 0.5mg was added to 5ml ExpressHyb solution (to enhance specificity of the hybridisation) that was pre-warmed to 68°C. An Atlas Array was wet in a bath of dH<sub>2</sub>O. It was then placed in a hybridisation tube with 5ml of ExpressHyb/salmon DNA solution and prehybridized for 30min at 68°C with continuous agitation in a pre-heated hybridisation oven. Labelled probe, with a radioactivity of between 2 and 20 x 10<sup>6</sup> cpm (~200 $\mu$ l), was added to 22 $\mu$ l of denaturing solution, containing 10mM NaOH and 10mM EDTA, and was incubated for 20min at 68°C before addition of 5 $\mu$ l C<sub>OT</sub>-1 DNA (for blocking purposes) and 225 $\mu$ l neutralizing solution (1M NaH<sub>2</sub>PO<sub>4</sub>, pH 7 adjusted with NaOH). The probe was incubated for a further 10min at 68°C. Prepared probe

was added carefully to the hybridisation tube containing the Array and hybridised overnight at 68°C with constant agitation.

### **2.5.6 Post hybridisation washes and exposure**

Hybridisation solution was carefully discarded to a drain suitable for disposal of radioactive isotopes and 100ml of wash solution 1 (2x SSC, 1% SDS), pre-warmed to 68°C, was added. The Array was washed for 30min at 68°C with constant agitation; this was repeated 3 more times and twice with 100ml of wash solution 2 (0.1x SSC, 0.5% SDS). The Array was finally wrapped in Saran wrap to prevent drying and exposed to a phosphor imager plate (Molecular Dynamics) at RT for 3h, 24h and 3-5 days. The density of the exposed array spots was determined as described in Method 2.5.8.

### **2.5.7 Stripping cDNA probes from Atlas Array**

In order to re-use the Array after exposure, cDNA probes were immediately stripped from the membranes. The Array was removed from Saran wrap and placed into a beaker containing 500ml of boiling 0.5% (w/v) SDS and boiled for 10min then allowed to cool for 10min. Subsequently the membrane was rinsed in wash solution 1 (Method 2.5.6) and wrapped in Saran wrap. Efficiency of stripping was assessed by exposure overnight to a phosphor imager plate. If radioactivity was detected stripping procedure was repeated and the stripped Array was stored at -20°C.

### 2.5.8 Analysis of Atlas cDNA Expression Array

Following exposure of the phosphor imager plates to the Array for the required period of time (usually 72h), the plates were scanned using a phosphor imager (BioRad). The data was assessed using image analysis software (Image Quant, Molecular Dynamics). Each array was orientated according to the orientation spots and a grid was applied to incorporate the cDNA spots. The densities of the hybridised cDNA spots were corrected against background values taken randomly from the array and normalised against the sum of densities. Density values from the treated sample arrays were plotted against control values in a log-log scatter plot. Expression variations over two fold and densities over 1000 were taken to be significant.

### 2.5.9 Corroboration of Atlas Array results by semi-quantitative RT-PCR

Using the neonatal mouse RNA extracted for the cDNA arrays, semi-quantitative RT-PCR for genes *ngfa*, *pref-1* and *igf-2* were determined and normalised against the housekeeping gene *gapdh*. This was carried out in order to verify the changes in gene expression determined by cDNA array technology described above. For each sample, a template of 1.0µg total RNA (Method 2.5.1) was used in cDNA synthesis using oligo dt<sub>12-18</sub> primer and Superscript II RNase H- reverse transcriptase (both Life Technologies), according to manufacturers instructions. Expression of each gene was amplified in duplicate in a total volume of 20µl using 0.5U *AmpliTaq* DNA polymerase (Applied Biosystems), 0.2mM dNTPs (Life Technologies), 0.2µM

each sense/antisense primer (PNA<sup>CL</sup>, Table 2.7) in thin-walled microfuge tubes (Advanced Biotechnology) and overlaid with mineral oil. The following PCR incubation times were used: 94°C for 5 min followed by 26 cycles of 94°C for 30s, 60°C for 30s, 72°C for 30s and concluded by 72°C for 5 min in a Hybaid OmniGene Thermal Cycler (Hybaid Ltd, UK). The number of cycles for each gene target was previously determined so that amplification was in the linear phase (Personal communication Dr A. Green, MRC Toxicology Unit). A negative control, where water (Sigma) was substituted for cDNA, was included in each PCR experiment. The resulting PCR products for each sample were electrophoresed in parallel through a 2% agarose (Life Technologies) gel in 1x TBE containing 5µg/ml ethidium bromide (Sigma) and visualised under UV (method 2.2.12.3).

**Table 2.7 Mouse primer sequences**

Gene (Genbank ref.)	Primer sequence	Product size (bp)
<i>gapdh</i> (M32599)		
Sense	ACCCAGAAGACTGTGGATGG	
Antisense	GGAGACAACCTGGTCCTCAG	300
<i>Ngf-<math>\alpha</math></i> (M11434)		
Sense	AGCCTCCTGAATGAGCACAC	
Antisense	TCCATCTCTCCTGCACACAG	299
<i>Pref-1</i> (L12721)		
Sense	GAAATAGACGTTTCGGGCTTG	
Antisense	ATCGTTCTCGCATGGGTTAG	297
<i>Igf-2</i> (M14951)		
Sense	GTCGATGTTGGTGCTTCTCA	
Antisense	AAGCAGCACTCTTCCACGAT	195

The densities of the bands were determined using densitometry (Molecular Dynamics/ImageQuant software) and in each instance normalised against the density of the corresponding *gapdh* PCR product. Representative PCR products were verified by DNA sequencing (PNAACL).

**Chapter 3: ER protein degradation: response of the ER to  
oestradiol and related SERMs *in vitro***

### 3.1 Introduction

As described in Chapter 1, the level of the ER within the cells of the uterus and breast is a key factor in the mediation of the tissues response to oestrogenic and anti-oestrogenic compounds. The ER protein is subject to auto-regulation and to specific regulation by its differing ligands. It is widely recognised that oestradiol causes down regulation of the ER in some cell types. Studies in MCF-7 cells have demonstrated the loss of ER protein levels following treatment with oestrogenic compounds (Seo *et al.*, 1998; El Khissiin *et al.*, 1999). These studies illustrate the control of ER protein levels through ligand binding. One of the major aims of this Chapter was to discover how ligand binding affected the stability of ER and if this represented a control mechanism for the action of these compounds at the cellular level.

Several studies have been conducted demonstrating ER response to oestrogenic compounds in MCF-7 cells (El Khissiin *et al.*, 1999; Wormke *et al.*, 2000). Few studies to date describe the response of ER $\beta$  in breast and uterine cell types to oestrogenic compounds. The overall aim of the work presented in this chapter was to compare the response of ER $\alpha$  and ER $\beta$  to oestradiol, tamoxifen and related compounds, in breast and uterine cell lines. These data are required to determine the ligand dependent response of ER $\alpha$  and ER $\beta$  to these compounds in the human cell lines for prediction of what may happen in the human uterus.

The ubiquitin-proteasome mediated degradation pathway is responsible for the breakdown of proteins involved in a number of cellular processes, including cell cycle regulation, signal transduction, differentiation and the degradation of tumour suppressors (Kierszenbaum *et al.*, 2000). Proteins are targeted for degradation by ubiquitin, which binds to the protein forming a chain (Figure 3.1). The proteasome complex acts as a receptor for the polyubiquitin chain and the protein is degraded leaving the ubiquitin to be recycled. The ER is a possible candidate for this degradation pathway as it has a short half-life of 3-4h (Pakdel *et al.*, 1993; Nawaz *et al.*, 1999b). This degradation may be ligand dependent and ER subtype specific (Van Den Bermd, 1999; El Khissiin *et al.*, 1999).

Both the human breast adenocarcinoma cell line; MCF-7 and the Ishikawa human endometrial adenocarcinoma cell line have been tested in this study following treatment with oestrogen, tamoxifen, raloxifene, and the anti-oestrogen faslodex. The peptide aldehyde proteasome inhibitors: MG115 and MG132 can enter mammalian cells and reversibly bind to active sites of the 20S proteasome and inhibit cleavage of substrates (Rock *et al.*, 1994). These inhibitors have been used to investigate proteasome-mediated degradation of the ER. Their time and concentration dependent effects on ER stability, in the presence or absence of the ligands described above, are investigated in this Chapter.

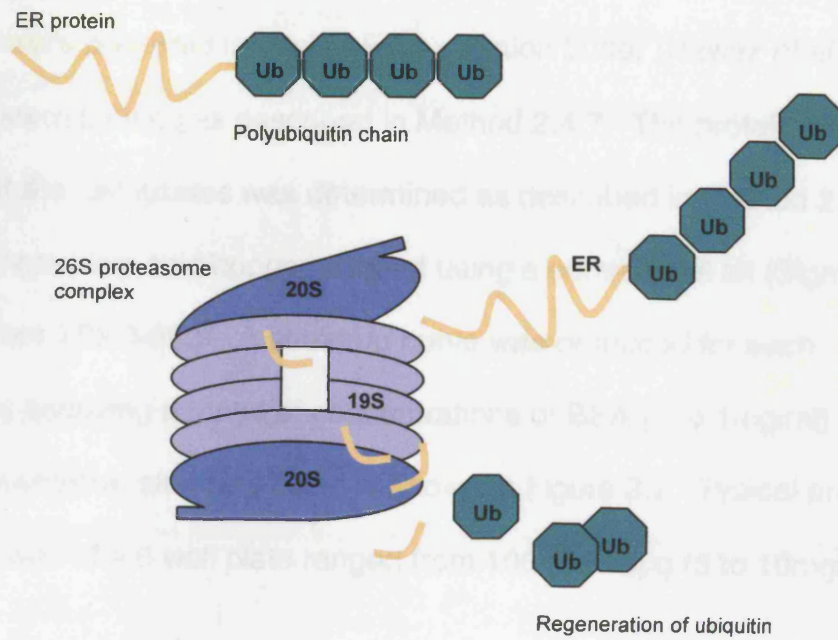


**Figure 3.1** Ubiquitination and 26S proteasome mediated degradation of the ER (adapted from Kierszenbaum *et al.*, 2000).

## **3.2 Methods and Results**

### **3.2.1 Preparation of cell lysates for Western blotting**

MCF-7 and Ishikawa cells were maintained in DMEM (10% FBS and 1% glutamax) as described in Methods 2.4.1 to 2.4.3. Cell lysates from each well of 6 well plates were prepared in 20 $\mu$ l of ER extraction buffer (Nawaz *et al.*, 1999b), for Western blotting as described in Method 2.4.7. The protein concentration of the cell lysates was determined as described in Method 2.3.2.1 based on a bicinchoninic acid/copper reagent using a commercial kit (Sigma procedure number TPR0-562). A standard curve was produced for each protein assay by assaying a range of concentrations of BSA (0 to 1mg/ml) at 540nm; a representative standard curve is shown in Figure 3.2. Typical protein yield from each well of a 6 well plate ranged from 100 to 200 $\mu$ g (5 to 10mg/ml).

### **3.2.2 Western blot controls and recombinant protein concentrations**

ER $\alpha$  and ER $\beta$  have large regions of homology in their protein sequences and due to their similar molecular weights distinguishing between cross reactivity of the antibodies and a specific signal on a Western blot is a concern. Positive controls for antibody specificity were therefore required.

To determine the specificity of the antibodies used for ER $\alpha$  and ER $\beta$  detection by Western blotting, commercially available human recombinant ER $\alpha$  and ER $\beta$

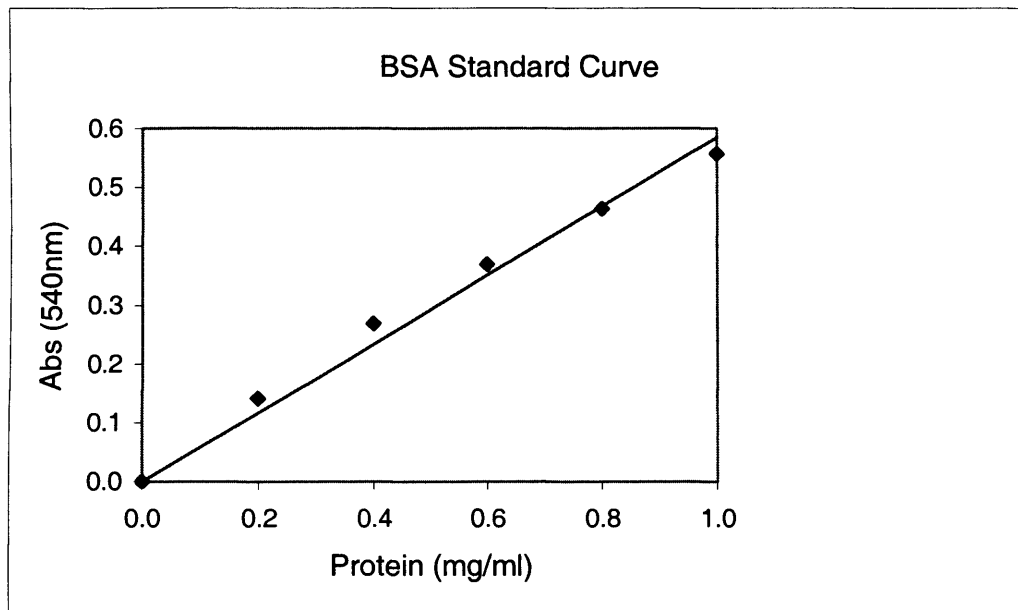


**Figure 3.2** Representative bovine serum albumin (BSA) standard curve for determination of protein concentration. A serial dilution of BSA was prepared (0 to 1mg/ml) and protein concentration was assayed using 96 well plates as per Method 2.3.2.1. Absorbancies were determined at 540nm and the above standard curve plotted.

proteins (Calbiochem) were utilised. Serial dilutions of the recombinant protein (1 to 50ng) formulated in loading buffer were electrophoresed and probed with Upstate anti-ER $\alpha$  (at 1:500) and ABR anti-ER $\beta$  (at 1:2500) (see Figure 4.3) as in Methods 2.3.2.2/3. Figure 3.3 shows a representative Western blot of the ER $\alpha$  and ER $\beta$  recombinant proteins illustrating that the antibodies recognise only their specific target protein. It was determined that 10ng of recombinant ER $\alpha$  or ER $\beta$  protein would be sufficient to use as a positive standard for the Western blotting of this Chapter. However, the recombinant human ER $\alpha$  and ER $\beta$  proteins were remarkably unstable and although a fresh aliquot was taken from storage at -80°C for each blot, occasionally the recombinant bands on Western blots sometimes did not appear uniform as shown in Figure 3.4a,3.

### **3.2.3 MCF-7 and Ishikawa ER expression**

As discussed above ER $\alpha$  and ER $\beta$  protein expression varies greatly between different cell types, it was therefore necessary to confirm ER subtype expression within the MCF-7 and Ishikawa cell lines investigated. Levels of endogenous ER $\alpha$  and ER $\beta$  protein expression were determined in MCF-7 and Ishikawa cells grown in DMEM phenol red free media containing 10% FCS and 1% glutamax (Methods 2.4.1). Cells were lysed using ER lysis buffer as described in Method 2.4.7 and the protein concentration was determined as above.

Figure 3.4 shows a representative Western blot of MCF-7 and Ishikawa cell lysates probed for ER $\alpha$  and ER $\beta$ . MCF-7 cells grown in the conditions

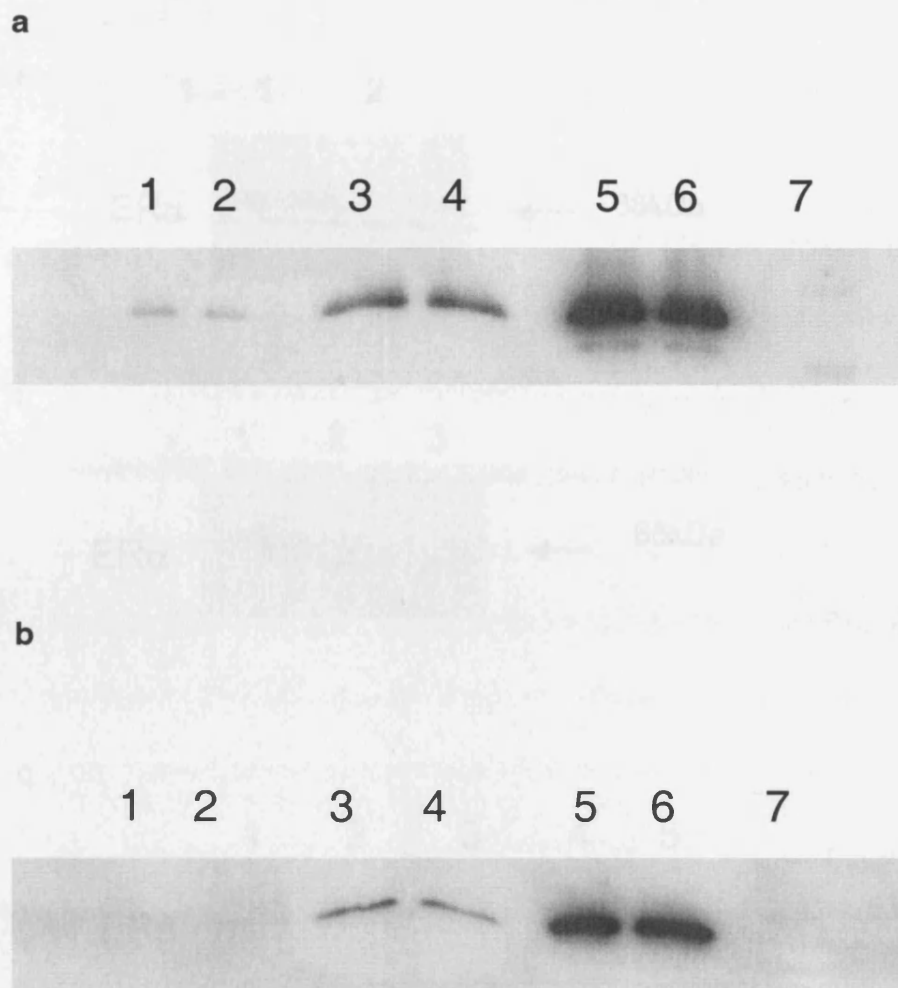


**Figure 3.3** Representative Western blots of recombinant human ER $\alpha$  and ER $\beta$  proteins (Calbiochem) detected with Upstate and ABR antibodies as described in Methods 2.3.2. HRP-conjugated secondary antibodies detected with Amersham ECL chemiluminescence detection kit; exposure time 1 min. **a:** blot probed for ER $\alpha$ . Lane 1 and 2: 1ng ER $\alpha$  protein, lane 3 and 4: 10ng ER $\alpha$  protein, lanes 5 and 6: 50ng ER $\alpha$  protein and lane 7: 10ng ER $\beta$  protein. **b:** blot probed for ER $\beta$ . Lane 1 and 2: 1ng ER $\beta$  protein, lane 3 and 4: 10ng ER $\beta$  protein, lanes 5 and 6: 50ng ER $\beta$  protein and lane 7: 10ng ER $\alpha$  protein.

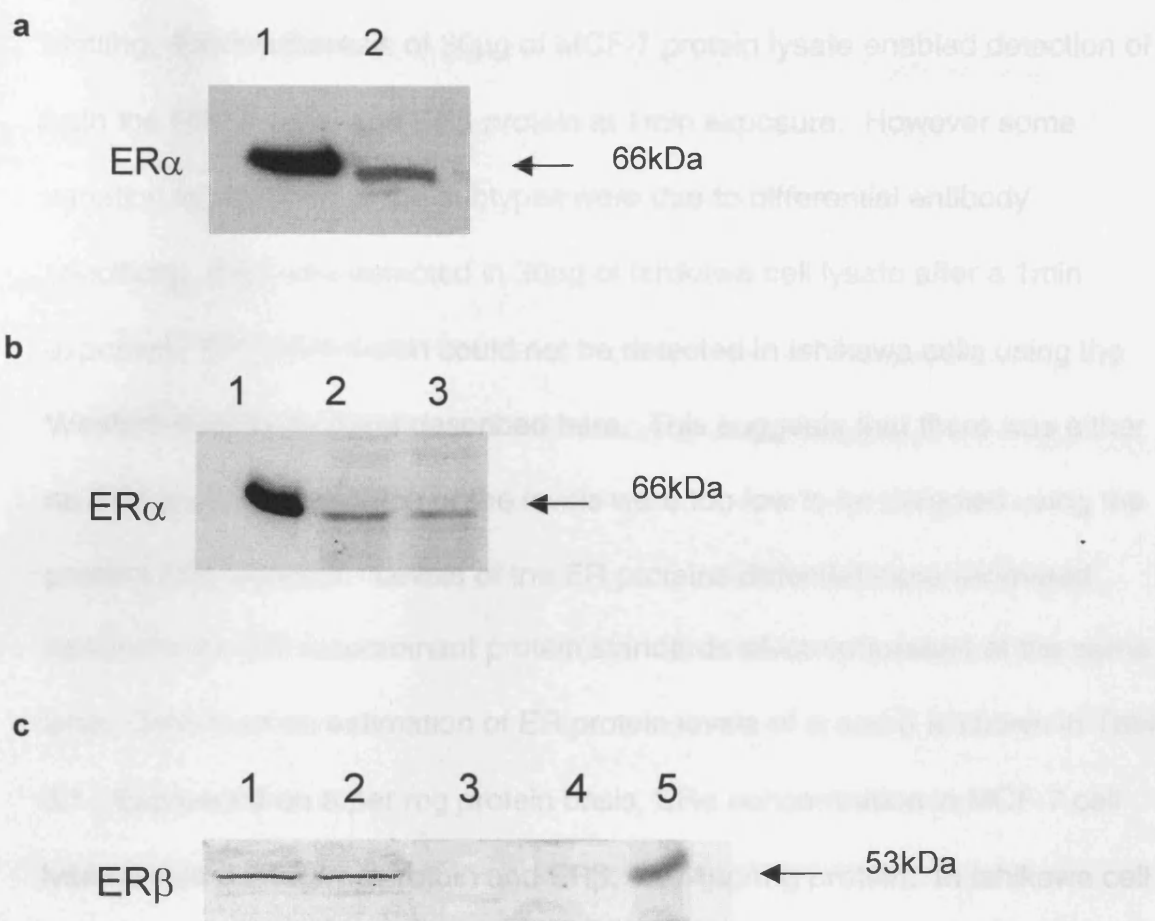


**Figure 3.4** Western blots of MCF-7 and Ishikawa cells, probed for ER $\alpha$

(**a** and **b**) and ER $\beta$  (**c**). **a**: lanes 1: 10 $\mu$ g recombinant ER $\alpha$ , lane 2: 30 $\mu$ g MCF-7 cell lysate. **b**: lane 1: 10ng recombinant ER $\alpha$ , lanes 2 and 3: 30 $\mu$ g Ishikawa cell lysate (Upstate anti-ER $\alpha$  antibody). **c**: lanes 1 and 2: 30 $\mu$ g MCF-7 cell lysate; lanes 3 and 4: 30 $\mu$ g Ishikawa cell lysate, and lane 5: 10ng recombinant ER $\beta$  (ABR anti-ER $\beta$  antibody). Exposure time 1min, ECL detection reagents.

described express ER $\alpha$  and ER $\beta$  protein at levels detectable by Western blotting. Electrophoresis of 30 $\mu$ g of MCF-7 protein lysate enabled detection of both the ER $\alpha$  protein and ER $\beta$  protein at 1min exposure. However some variation in detection of the subtypes were due to differential antibody specificity. ER $\alpha$  was detected in 30 $\mu$ g of Ishikawa cell lysate after a 1min exposure. ER $\beta$  expression could not be detected in Ishikawa cells using the Western blotting protocol described here. This suggests that there was either no ER $\beta$  protein expression or the levels were too low to be detected using the present ECL protocol. Levels of the ER proteins detected were estimated relative to the ER recombinant protein standards electrophoresed at the same time. Data from an estimation of ER protein levels of  $\alpha$  and  $\beta$  is shown in Table 3.1. Expressed on a per mg protein basis, ER $\alpha$  concentration in MCF-7 cell lysates was 0.24 $\mu$ g/mg protein and ER $\beta$ , 0.074 $\mu$ g/mg protein. In Ishikawa cell lysates the corresponding values for ER $\alpha$  were 0.039 $\mu$ g/mg protein, while ER $\beta$  was below the detection limit.

**Table 3.1 ER $\alpha$  and ER $\beta$  protein levels calculated from the density of the recombinant proteins**

Cell type	ER $\alpha$	ER $\beta$
	Protein (ng)	
MCF-7 lysate (30 $\mu$ g)	7.20 $\pm$ 0.39	2.22 $\pm$ 0.01
Ishikawa lysate (30 $\mu$ g)	1.17 $\pm$ 0.19	ND

\*Results represent the mean for 4 determinations  $\pm$ SE. ND = not detectable

### 3.2.4 Growth curves with SERMs

The oestrogenicity of each compound was determined by its effects on cell proliferation. Growth curves for the cells in response to oestradiol, tamoxifen, raloxifene and faslodex treatment were produced. MCF-7 or Ishikawa cells were seeded into 6 well plates at  $4 \times 10^5$  or  $1 \times 10^5$  cells/well (respectively) in 2ml of culture media and 24h after seeding, standard culture media (Method 2.4.1) was replaced with DMEM containing 10% charcoal stripped serum. 48h later cells were treated with the test compounds (Method 2.4.5). These were oestradiol ( $10^{-9}$  M) or tamoxifen, raloxifene and faslodex at  $10^{-6}$  M concentrations. Cells were cultured at  $37^\circ\text{C}$  in 5%  $\text{CO}_2$  in air. At 0, 24, 48 and 72h, viable cell numbers were determined using the trypan blue exclusion method (Method 2.4.6).

#### MCF-7 cells

Oestradiol induced cell proliferation up to 2 fold higher than in vehicle (DMSO) treated MCF-7 cell cultures at the 72h time point whereas the pure anti-oestrogen faslodex inhibited cell proliferation by 2.5 fold (Figure 3.5).

Tamoxifen reduced the number of viable MCF-7 cells by 6.7 fold, showing this compound acted as an oestrogen antagonist having a more dramatic effect than faslodex on cell proliferation. In contrast, raloxifene reduced cell proliferation by almost 1.8 fold, showing a weak oestrogen antagonist effect in this cell type.

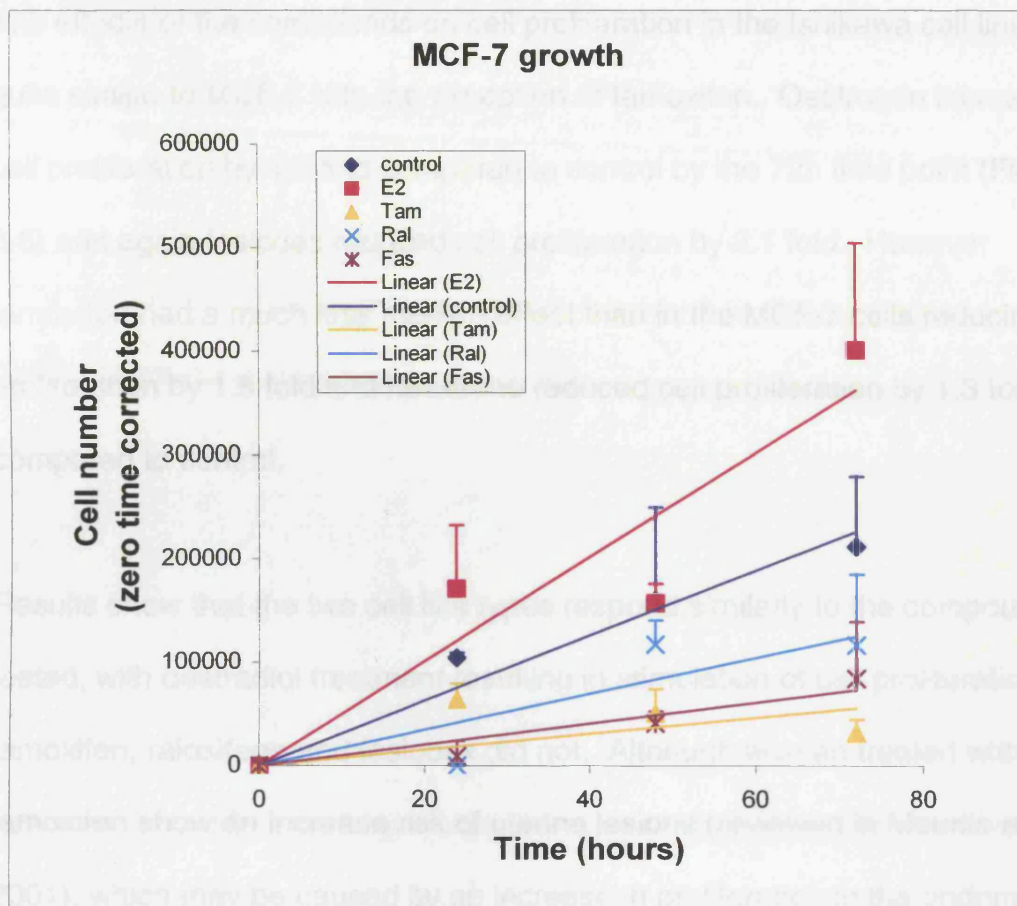


**Figure 3.5** Response of MCF-7 cell proliferation to oestradiol and related SERMs. Cells were treated with oestradiol ( $10^{-9}$ M), tamoxifen, raloxifene and faslodex ( $10^{-6}$ M), and counted over a period of 72h as described in Method 2.4. Results represent the mean  $\pm$ SE of three individual experiments; all treatments were in duplicate.

### **Ishikawa cells**

The effects of the compounds on cell proliferation in the Ishikawa cell line were quite similar to MCF-7 with the exception of tamoxifen. Oestrogen increased cell proliferation by 1.3 fold compared to control by the 72h time point (Figure 3.6) and again faslodex reduced cell proliferation by 2.1 fold. However tamoxifen had a much less marked effect than in the MCF-7 cells reducing cell proliferation by 1.8 fold and raloxifene reduced cell proliferation by 1.3 fold compared to control.

Results show that the two cell line types respond similarly to the compounds tested, with oestradiol treatment resulting in stimulation of cell proliferation while tamoxifen, raloxifene and faslodex did not. Although women treated with tamoxifen show an increase risk of uterine lesions (reviewed in Mourits *et al.*, 2001), which may be caused by an increase in proliferation in the endometrium, an oestrogen agonist effect was not evident in the transformed Ishikawa cell line.

#### **3.2.5 Response of ER $\alpha$ expression to oestradiol and tamoxifen**

The oestrogenic and anti-oestrogenic effects of the compounds were further investigated to see if cell proliferation could be related to levels of ER $\alpha$  and ER $\beta$  protein expression of the MCF-7 and Ishikawa cells and whether any changes could be related to stability of ER and proteasome degradation.

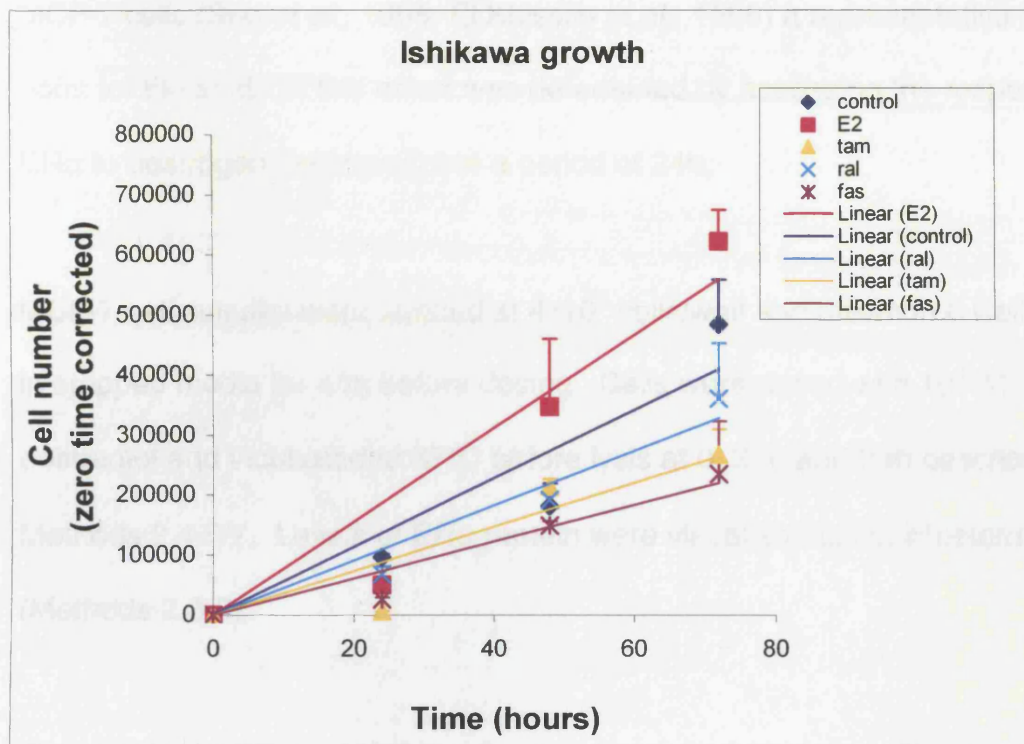


**Figure 3.6** Response of Ishikawa cell proliferation to oestradiol and related SERMs. Cells were treated with oestradiol ( $10^{-9}$ M), tamoxifen, raloxifene and faslodex ( $10^{-6}$  M), and counted over a period of 72h as described in method 2.4. Results represent the mean  $\pm$ SE of three individual experiments; all treatments were in duplicate.

As the ER $\alpha$  protein is known to be reduced following oestrogen treatment in MCF-7 cells (Seo *et al.*, 1998; El Khissiin *et al.*, 1999) a representative time point for the study of this effect was determined by assessing the response of ER $\alpha$  to oestrogen treatment over a period of 24h.

MCF-7 cell cultures were seeded at  $4 \times 10^5$  cells/well and grown in 6 well plates in stripped media for 48h before dosing. Cells were dosed with  $10^{-9}$  M oestradiol and incubated at 37°C before lysis at 0, 3, 6 and 24h described in Methods 2.4.5/7. Levels of ER $\alpha$  protein were visualised using Western blotting (Methods 2.3.2).

The stability of ER $\alpha$  in MCF-7 cells was diminished over time (Figure 3.7). Over a 24h period, relative to controls, treatment with oestradiol resulted in an approximate 50% loss of ER $\alpha$ , this effect being observed after a 3h incubation.

### **3.2.6 Effect of proteasome inhibitors on cell viability**

Proteasome inhibitors used in this study are known to cause apoptosis in cells following treatment (Lopes *et al.*, 1997). In order to study the effects of these compounds on ER expression it was important to establish that the concentrations used would not result in cell death over the time period of the investigation.

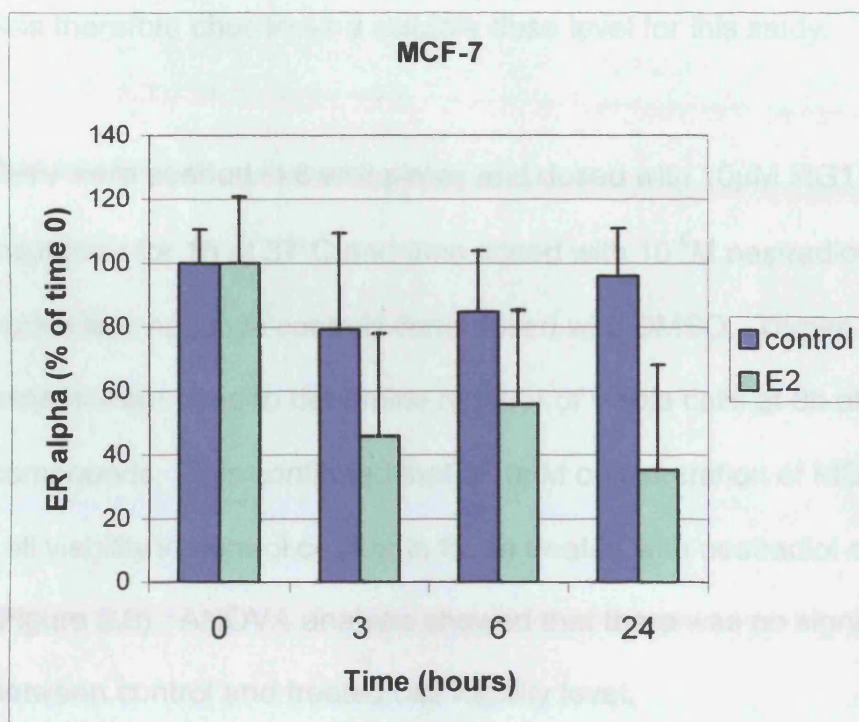


**Figure 3.7** Expression of ER $\alpha$  protein over a period of 24h, following dosing at time zero with  $10^{-9}$  M oestradiol (cells lysed at 0, 3, 6, and 24h). Western blots were probed with Upstate ER $\alpha$  antibody and detected with ECL. Films were then scanned using a PDSI densitometer (Molecular Dynamics) with densities determined using ImageQuant software. Results represent the mean  $\pm$ SE of 3 experiments. Densities are plotted against each time point as a percentage of the control value at zero time.

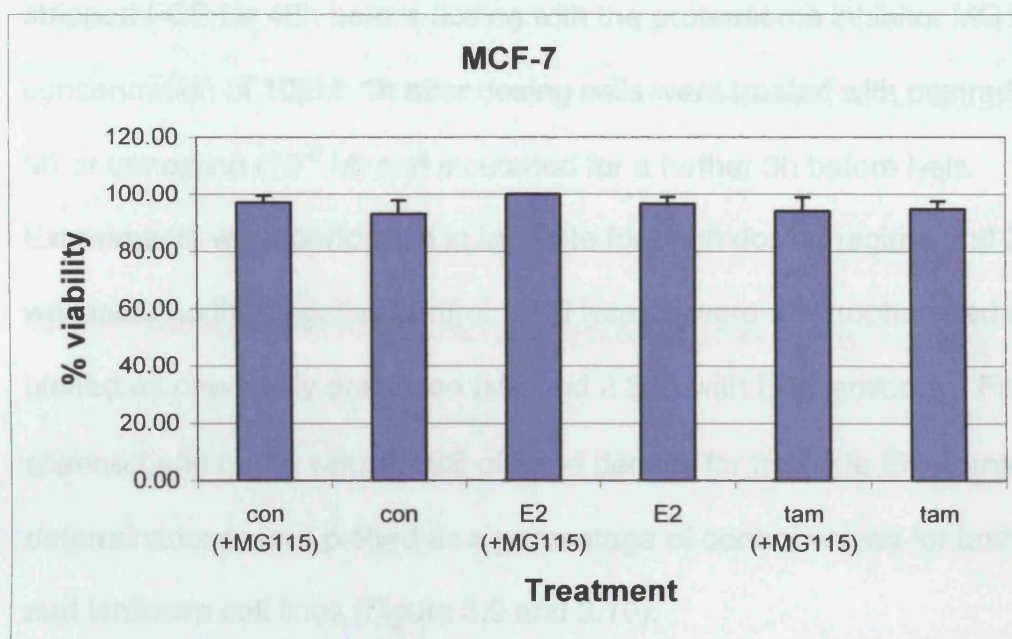
Cell viability assays were therefore carried out on MCF-7 and Ishikawa cells. Peptide aldehyde proteasome inhibitors have previously been shown to inhibit degradation of the ER at 10 $\mu$ M in a breast cell line (Wormke *et al.*, 2000); this was therefore chosen as a suitable dose level for this study.

Cells were seeded in 6 well plates and dosed with 10 $\mu$ M MG115; cells were incubated for 1h at 37°C and then dosed with 10<sup>-9</sup>M oestradiol or 10<sup>-6</sup>M tamoxifen, negative controls were dosed with DMSO. Trypan blue exclusion assays were used to determine number of viable cells at 3h after treatment with compounds. This confirmed that a 10 $\mu$ M concentration of MG115 did not affect cell viability in control cells or in those treated with oestradiol or tamoxifen (Figure 3.8). ANOVA analysis showed that there was no significant difference between control and treated cell viability level.

### **3.2.7 Effect of proteasome inhibitors on ER expression**

In MCF-7 cells over a 24h period ER $\alpha$  protein levels were decreased by oestradiol treatment relative to controls (Figure 3.7). This is in agreement with an earlier observation that showed ER protein is degraded more rapidly in response to oestradiol treatment than in the corresponding controls in the MCF-7 cell line by 3h (Seo *et al.*, 1998; El Khissiin *et al.*, 1999; Wormke *et al.*, 2000). ER levels in the cell lines were assessed following treatment with oestradiol or tamoxifen in combination with MG115.

a



b

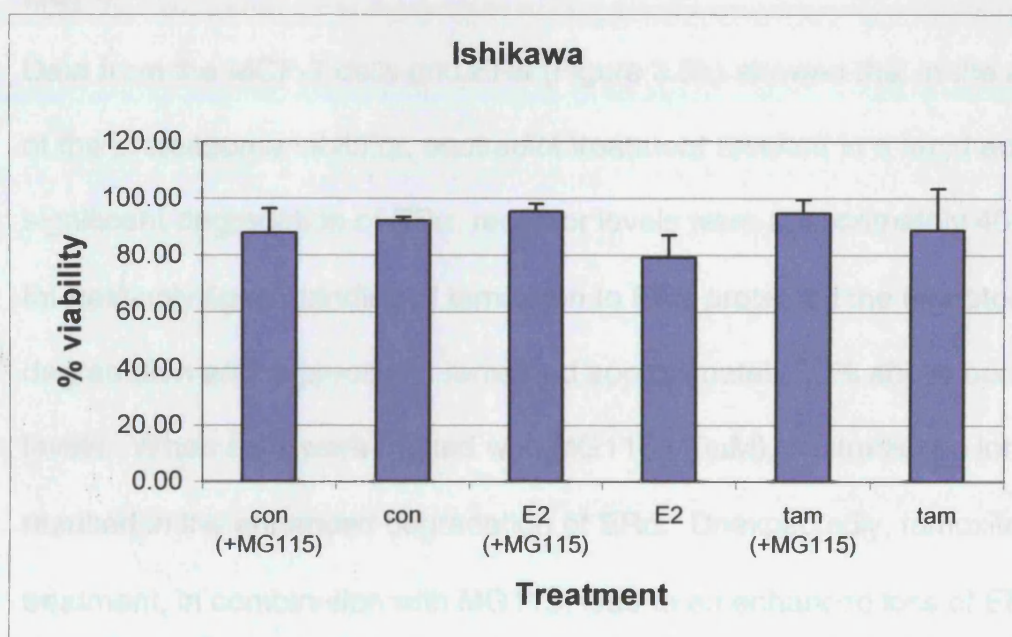


**Figure 3.8** Effect of proteasome inhibitor (MG115 10 $\mu$ M) treatment on cell viability 3h following dosing with oestradiol (10<sup>-9</sup> M) or tamoxifen (10<sup>-6</sup> M). Values expressed as percentage viability formulated from mean value  $\pm$ SE of 3 experiments. **a:** MCF-7 cell viability. **b:** Ishikawa cell viability.

Both MCF-7 and Ishikawa cells were grown in media containing 10% charcoal-stripped FCS for 48h before dosing with the proteasome inhibitor MG115 at a concentration of 10 $\mu$ M: 1h after dosing cells were treated with oestradiol (10<sup>-9</sup> M) or tamoxifen (10<sup>-6</sup> M) and incubated for a further 3h before lysis.

Experiments were performed in triplicate for each dosing regime and DMSO was used as the negative control. Cell lysates were electrophoresed and blotted as previously described (Method 2.3.2) with ER $\alpha$  antibody. Films were scanned and mean values  $\pm$ SE of band density for triplicate ER $\alpha$  protein determinations were plotted as a percentage of control values for both MCF-7 and Ishikawa cell lines (Figure 3.9 and 3.10).

### **MCF-7**

Data from the MCF-7 cells and ER $\alpha$  (Figure 3.9a) showed that in the absence of the proteasome inhibitor, oestradiol treatment resulted in a rapid and significant degradation of ER $\alpha$ , receptor levels were approximately 40% lower. Interestingly ligand binding of tamoxifen to ER $\alpha$  protected the receptor from degradation and expressions remained approximately 50% above control levels. When cells were treated with MG115 (10 $\mu$ M), oestradiol no longer resulted in the enhanced degradation of ER $\alpha$ . Unexpectedly, tamoxifen treatment, in combination with MG115, lead to an enhanced loss of ER $\alpha$  relative to controls although this loss is not significant. Oestradiol bound ER $\alpha$  may have a conformation that exposes those sites recognised for ubiquitination. In the case of ER $\beta$ , oestradiol treatment resulted in protein levels that were below the limit of detection. As with ER $\alpha$  the addition of

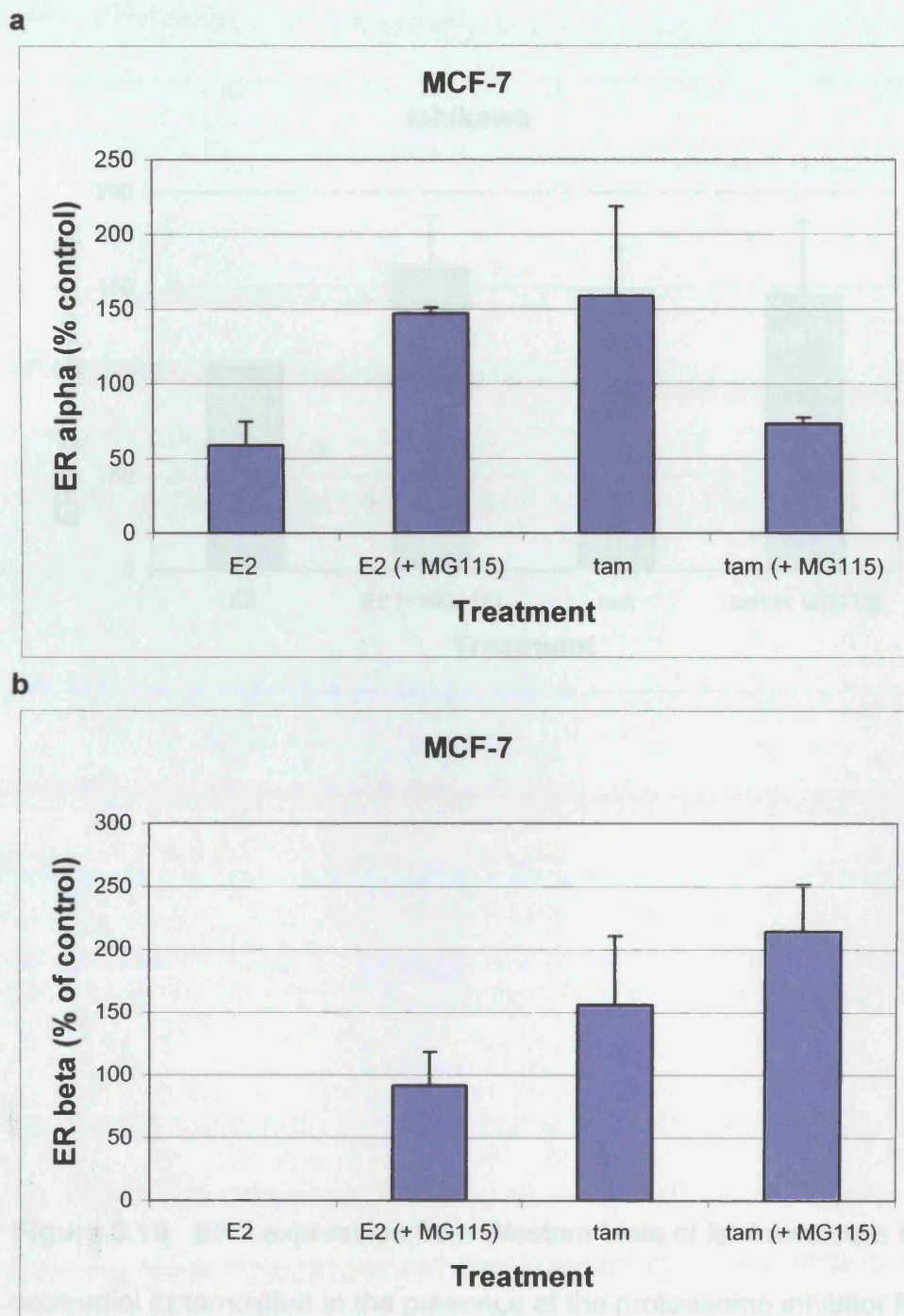
MG115 restored ER $\beta$  levels though not to greater than controls. Tamoxifen treatment resulted in an increase in ER $\beta$  above control level but the addition of MG115 did not significantly affect ER $\beta$  concentrations.

### **Ishikawa**

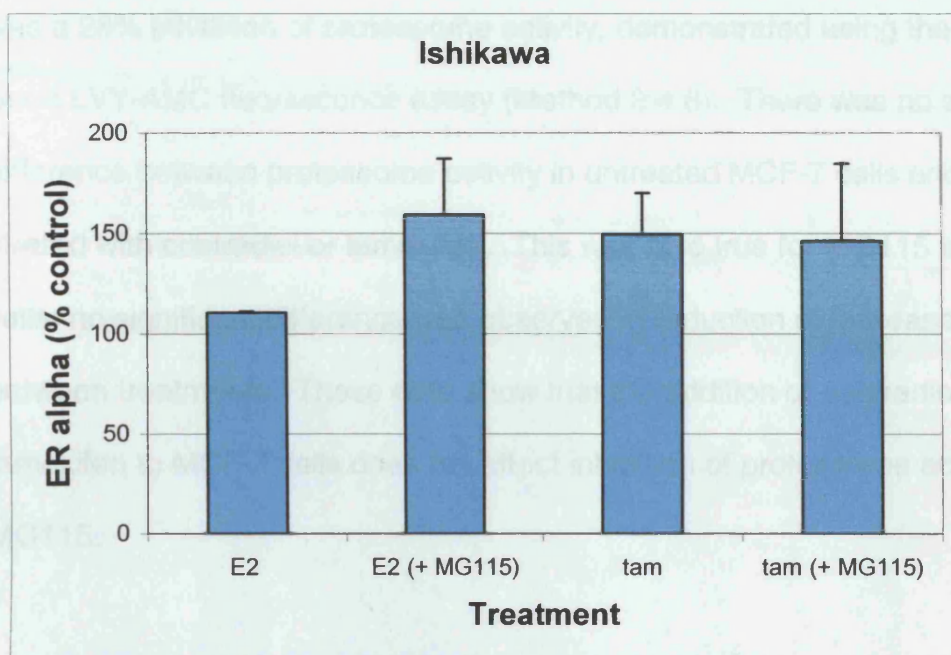
The increased instability of the ER $\alpha$  receptor on oestradiol binding seen in MCF-7 cells may not be a general phenomenon (Figure 3.10). As with the MCF-7 cells tamoxifen treatment enhanced the ER $\alpha$  concentration in the cells. When the proteasome inhibitor MG115 was added, both oestradiol and tamoxifen treated cells had the high level of ER $\alpha$  maintained.

#### **3.2.7.1 Assessment of proteasome activity using Suc-LLVY-AMC**

Degradation of the ER $\alpha$  in MCF-7 cells has been inhibited by the addition of the proteasome inhibitor MG115 (Figure 3.9). As described in Method 2.4.8, the fluoropeptide Suc-LLVY-AMC can be used to determine proteasome activity by measuring the fluorescence produced as the proteasome degrades the fluoropeptide substrate. Therefore the level of proteasome activity in the MCF-7 cells treated with MG115 and oestradiol or tamoxifen was assessed.



**Figure 3.9** ER expression from Western blots of MCF-7 cells treated with oestradiol or tamoxifen in the presence of the proteasome inhibitor MG115 (10 $\mu$ M). **a:** ER $\alpha$  and **b:** ER $\beta$ . Cells lysed 3h following treatment (Methods 2.4). Expression levels are expressed as a percentage of control level. Results represent the mean  $\pm$ SE of 3 experiments.



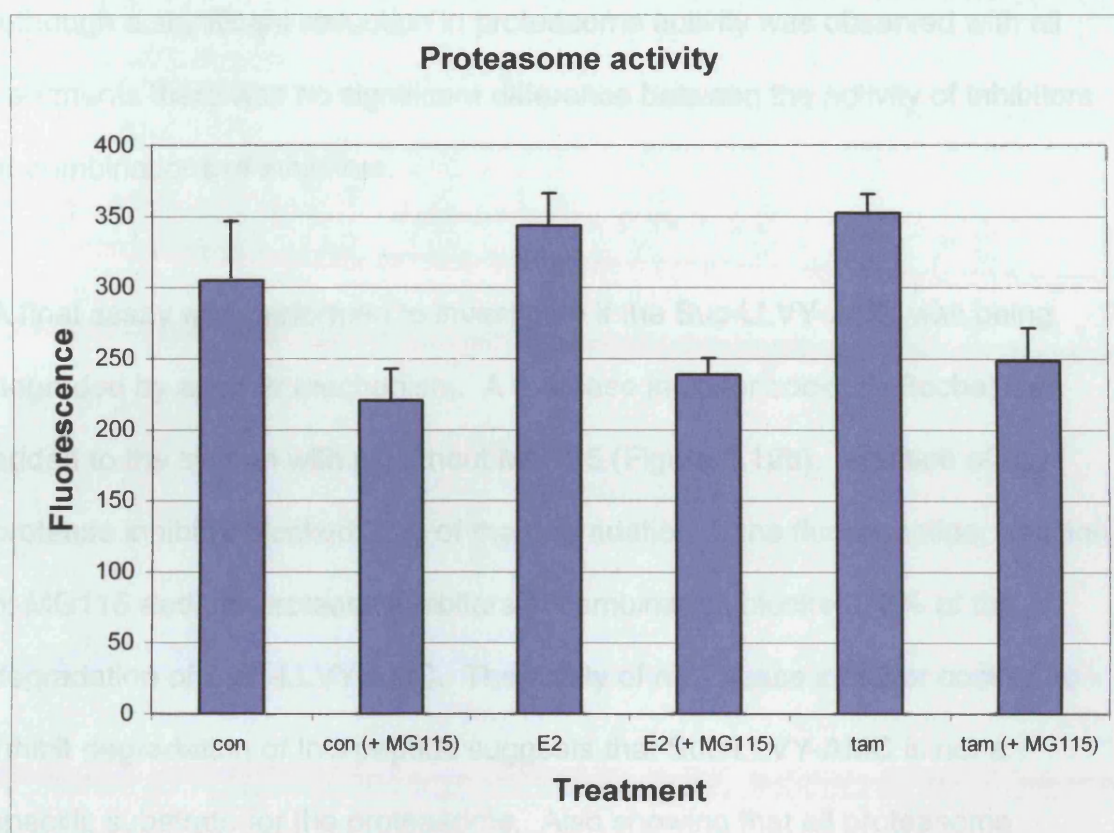
**Figure 3.10** ER $\alpha$  expression from Western blots of Ishikawa cells treated with oestradiol or tamoxifen in the presence of the proteasome inhibitor MG115 (10 $\mu$ M). Cells lysed 3h following treatment (Methods 2.4). Expression levels are expressed as a percentage of control level. Results represent the mean  $\pm$ SE of 3 experiments.

Figure 3.11 shows that when MCF-7 cells are treated with MG115 (10 $\mu$ M) there was a 28% inhibition of proteasome activity, demonstrated using the peptide Suc-LLVY-AMC fluorescence assay (Method 2.4.8). There was no significant difference between proteasome activity in untreated MCF-7 cells and those treated with oestradiol or tamoxifen. This was also true for MG115 treated cells; no significant difference was observed in reduction of proteasome activity between treatments. These data show that the addition of oestradiol or tamoxifen to MCF-7 cells does not affect inhibition of proteasome activity by MG115.

These data show that at this concentration MG115 (10 $\mu$ M) does not appear to fully inhibit activity of the proteasome. This was investigated further by the addition 100 $\mu$ M MG115 to MCF-7 cells in the conditions described above. This increase in concentration of MG115 had absolutely no effect on proteasome activity over the 30% reduction showed in Figure 3.11 (data not shown).

It is known that MG115 inhibits only part of the proteasome activity and this may explain the data described in Figure 3.11. Addition of a cocktail of inhibitors may provide a more successful inhibition of the proteasome and therefore allow complete inhibition of the ER degradation. Other inhibitors were tested for their ability to completely inhibit proteasome activity using the model Suc-LLVY-AMC substrate. Another peptide aldehyde inhibitor MG132 and a more specific inhibitor lactacystin, which modifies the proteasome's active site, were tested in the fluorescence assay.

Figure 3.11 shows data from the fluorescence assay of proteasome activity in MCF-7 cells dosed with various combinations of proteasome inhibitors.



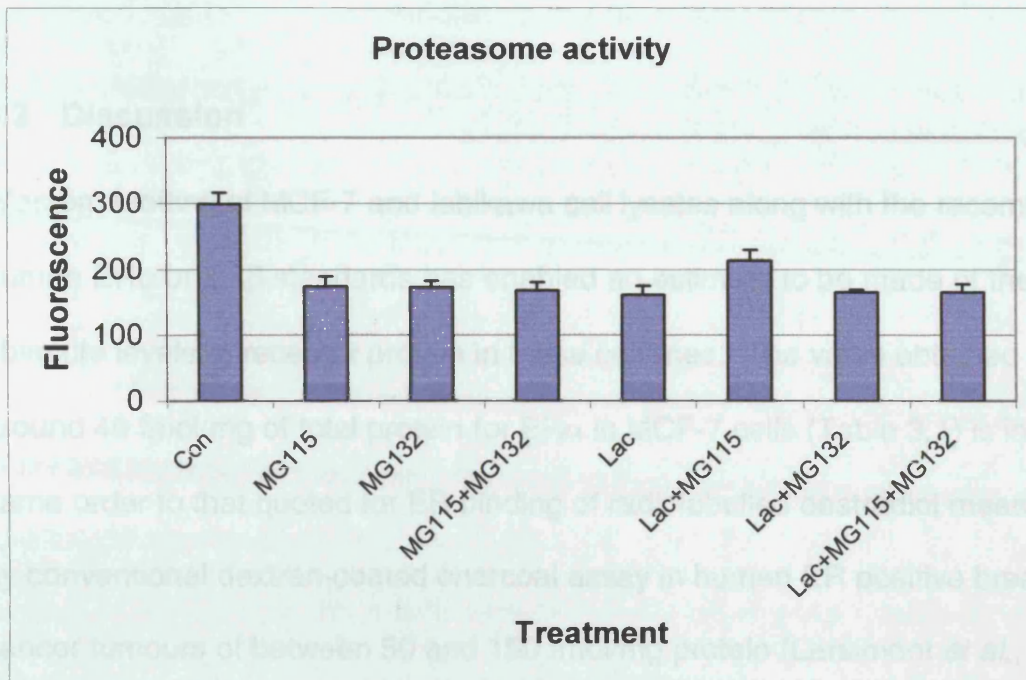
**Figure 3.11** Representative graph of proteasome activity assay, Method 2.4.8.

Data presented is taken from the mean  $\pm$ SE of three independent experiments involving the cell dosing regimes described in Methods 2.4.5. Cells were dosed with MG115 ( $10\mu\text{M}$ ) for 1h and with  $10^{-9}$  M oestradiol or  $10^{-6}$  M tamoxifen, and lysed after a further 3h.

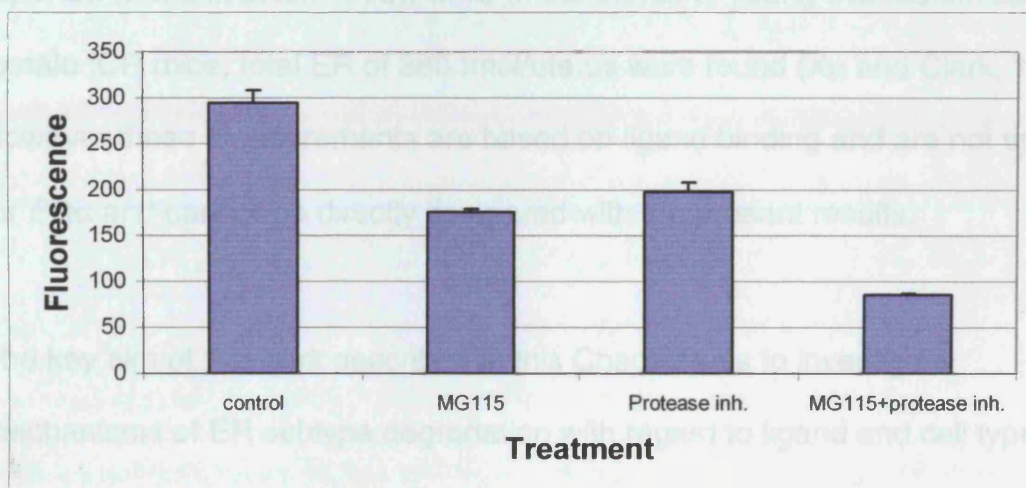
Figure 3.12 shows data from the fluorescence assay of proteasome activity in MCF-7 cells dosed with various combinations of proteasome inhibitors.

Although a significant reduction in proteasome activity was observed with all treatments there was no significant difference between the activity of inhibitors or combinations of inhibitors.

A final assay was performed to investigate if the Suc-LLVY-AMC was being degraded by another mechanism. A protease inhibitor cocktail (Roche) was added to the system with or without MG115 (Figure 3.12b). Addition of the protease inhibitor blocked 33% of the degradation of the fluoropeptide, addition of MG115 and the protease inhibitors in combination blocked 70% of the degradation of Suc -LLVY-AMC. The ability of a protease inhibitor cocktail to inhibit degradation of this peptide suggests that Suc-LLVY-AMC is not a specific substrate for the proteasome. Also showing that all proteasome inhibitors have the same effect on blocking degradation of the peptide, thus suggesting that this is the maximum degradation of this peptide by a proteasome pathway. Time did not permit exploration of the effects of this combined protease inhibitor system on ER expression. Such a potent mixture may well have had profound effects on cell viability over this time period.



a



b

**Figure 3.12** Representative graphs of proteasome activity assay, Method 2.4.8. Data  $\pm$ SE presented is taken from the mean of three independent experiments involving the cell dosing regimes described in Methods 2.4.5.

Cells were dosed with MG115 ( $10\mu\text{M}$ ), MG132 ( $10\mu\text{M}$ ) or lactacystin ( $20\mu\text{M}$ ) and lysed after 4h.

### 3.3 Discussion

Western blotting of MCF-7 and Ishikawa cell lysates along with the recombinant human ER $\alpha$  or ER $\beta$  standards has enabled an estimate to be made of the absolute levels of receptor protein in these cell lines. The value obtained of around 40 fmol/mg of total protein for ER $\alpha$  in MCF-7 cells (Table 3.1) is in the same order to that quoted for ER binding of radiolabelled oestradiol measured by conventional dextran-coated charcoal assay in human ER positive breast cancer tumours of between 50 and 150 fmol/mg protein (Larsimont *et al.*, 1989). In the liver of rats, nuclear ER levels of 60 fmol/mg protein has been reported (Koritnik *et al.*, 1995), while in the uterus of young ovariectomised female ICR mice, total ER of 380 fmol/uterus were found (Xu and Clark, 1990). However these measurements are based on ligand binding and are not specific for ER $\alpha$  and cannot be directly compared with the present results.

The key aim of the work described in this Chapter was to investigate mechanisms of ER subtype degradation with regard to ligand and cell type specific response including cell proliferation. Several studies have shown that ER is a target for proteasome mediated degradation (Nawaz *et al.*, 1999; Wormke *et al.*, 2000), although few studies to date have examined the effect of the proteasome pathway on ER $\beta$ .

The present results showed that MCF-7 cells express over 3 fold more ER $\alpha$  than ER $\beta$ . Previous studies have reported low levels of ER $\beta$  expression in this

cell line compared to ER $\alpha$  (Vladusic *et al.*, 2000). Low expression of the ER in Ishikawa cells has been reported previously (Mueller *et al.*, 2000) however; no data is currently available on the absolute levels of ER $\alpha$  or ER $\beta$  expression in this cell line. Ishikawa cells are known to express ER $\alpha$  (Hata and Kuramoto, 1992) but as far as is known the presence of ER $\beta$  has not been reported. ER $\beta$  expression could not be detected in the Ishikawa cell line. Data from growth curves of the MCF-7 and Ishikawa cells demonstrated a conventional increase and decrease in cell growth by oestradiol and faslodex, respectively. Although tamoxifen did not increase cell proliferation in the uterine cell type, it did have a marginally less marked oestrogen antagonist effect.

Assessment of the effect of oestradiol on ER $\alpha$  over a period of 24h demonstrated that by 3h after treatment levels of ER $\alpha$  were reduced by approximately 50% confirming previous studies in MCF-7 cells showing a reduction in ER at this time point (Seo *et al.*, 1998; Wormke *et al.*, 2000; Wijayaratne *et al.*, 2001). This was partly blocked by actinomycin D cyclohexamide (Seo *et al.*, 1998). Whether this effect was due to a proteasome mediated pathway was investigated further in the present study. A dose of 10 $\mu$ M of the peptide aldehyde proteasome inhibitor MG115 was as effective at blocking the proteasome degradation as a higher dose of the same inhibitor, or a similar compound MG132, or by lactacystin which inhibits proteasome mediated degradation by a different mechanism. MG115 did not affect cell viability at 10 $\mu$ M and was therefore not inducing apoptosis at the 3h time point. These results suggest that in the case of ER $\alpha$  oestradiol enhanced

degradation is indeed mediated via the ATP/ubiquitin-dependant proteolysis. Tightly ordered proteasomal degradation of proteins critical for cell cycle control implies a role of the proteasome in maintaining cell proliferation and cell survival. However, the dose of MG115 used decreased the rate of MCF-7 cell proliferation to almost zero over a period of 24h (data not shown). These findings suggest that the concentration of MG115 used, while not affecting cell viability (Figure 3.8) may, over a longer time period be sufficient to induce apoptosis. This was not investigated further in the present study.

Results from the treatment of MCF-7 cells with oestradiol and tamoxifen, in combination with MG115, show that ligand specific degradation of both ER $\alpha$  and ER $\beta$  occurs. ER $\alpha$  and ER $\beta$  protein levels are reduced when MCF-7 cells are treated with oestradiol; this loss of ER $\alpha$  and ER $\beta$  is not observed when the cells are pre-treated with MG115. Therefore, binding of oestradiol to ER $\alpha$  and ER $\beta$  could induce a change in conformation targeting the protein for ubiquitination and degradation by the proteasome involving the 20S subunit that is specifically inhibited by MG115. It is also possible that binding of tamoxifen to the ER $\alpha$  and ER $\beta$  causes a different conformational change of the ER that is not recognised for proteasome mediated degradation. X-ray crystallographic studies have in fact shown that binding of oestradiol to the ligand binding domain of ER $\alpha$  results in quite a different conformation of helix 12 from that seen with tamoxifen or raloxifene (reviewed by Jordan, 2001). This pathway for ER $\alpha$  degradation appears also to be cell type specific, as ER $\alpha$  is not degraded in response to oestradiol treatment in Ishikawa cells in this system.

It is interesting that ER $\alpha$  and ER $\beta$  appear to respond in a similar manner to these two ligands, as differential effects of oestradiol and tamoxifen on the ER subtypes could partially resolve the cell specific effects of these two compounds. However, the ligand specific effects on ER degradation described here may begin to explain the differing effects oestradiol and tamoxifen have in the MCF-7 cells. With regard to their proliferation in response to oestradiol and not tamoxifen, the altered levels of ER within the cell in response to these compounds may lead to further downstream effects that are mediated through the ER which result in cell proliferation. Further studies are required to determine if, indeed, the ER plays a key role in the mediation of oestradiol, but not tamoxifen, induced cell proliferation in the breast cell, and to determine the differences in the endometrial cell which are not mediated through ER degradation via the proteasome pathway.

**Chapter 4: Localisation of ER $\alpha$  and ER $\beta$  in the ovariectomised rat and mouse uterus: visualised by *in situ* hybridisation and immunohistochemistry**

## 4.1 Introduction

There is considerable evidence to suggest that treatment with tamoxifen has a stimulatory effect in the uterus and can cause endometrial cancers (Rutqvist *et al.*, 1995). It is not clear by which mechanism tamoxifen has this stimulatory effect. Tamoxifen is a potent carcinogen in the rat liver (Greaves *et al.*, 1993) producing measurable levels of DNA adducts (White *et al.*, 1992). The carcinogenic activity of tamoxifen is due to its conversion to active metabolites that bind to DNA (Philips *et al.*, 1994). The active metabolite:  $\alpha$ -hydroxytamoxifen has a role in liver damage of rats (White, 1999) and has been identified in women taking tamoxifen (Poon *et al.*, 1995). However, studies conducted in women treated with tamoxifen show no increase in DNA adducts of the liver (Martin *et al.*, 1995) and the presence of DNA adducts in the endometrium remain inconclusive.

The lack of evidence for the genotoxic effects of tamoxifen in the endometrium of treated women suggests that tamoxifen stimulation of the uterus is mediated by an epigenetic mechanism. It seems that the oestrogenic effects tamoxifen has on the uterus are likely the cause of endometrial cancers and abnormalities in tamoxifen patients. Evidence suggests that the oestrogen agonist effects of tamoxifen are mediated through the oestrogen receptor since in ER $\alpha$  knockout mice, treatment with tamoxifen results in no uterotrophic action (Korach 1994).

As discussed in Chapter 1, ER $\alpha$  and ER $\beta$  are ligand activated transcription factors that mediate tissue response to oestrogenic compounds. There is

substantial evidence to suggest that the ER subtypes produce ligand specific effects depending on cell type, among other factors. The localisation of the ER $\alpha$  and ER $\beta$  within cell types of the uterus is therefore primary to the response of the tissue to oestrogenic and anti-oestrogenic compounds.

Techniques such as RT-PCR and Western blotting are suitable for comparing ER mRNA or protein levels within whole tissue samples, however the specific aims of this study were to assess the localisation and variability of ER $\alpha$  and ER $\beta$  within uterine cell types. Due to the lack of commercial antibodies available for immunohistochemistry at the time of this investigation (which was carried out before the results in Chapter 3 were obtained), an *in situ* hybridisation technique has been optimised for visualisation of ER $\alpha$  and ER $\beta$  mRNA in rat and mouse uterine tissues. *In situ* hybridisation involves the design of 20-30mer oligonucleotide probes complementary to the mRNA target. These probes are labelled non-radioactively with digoxigenin, allowing visualisation of mRNA-bound probe by the addition of horseradish peroxidase conjugated antibody and substrate. This technique is suitable for the localisation of target mRNA *in situ*.

With the recent development of commercial antibodies, specific for ER $\alpha$  and ER $\beta$ , a number of studies have been published detailing ER expression in the adult rat uterus (Saunders *et al.*, 1997; Shughrue *et al.*, 1998; Hiroi *et al.*, 1999; Katsuda *et al.*, 1999; Carthew *et al.*, 1999b; Carthew *et al.*, 2000; Pelletier *et al.*, 2000) and mouse uterus (Bergman *et al.*, 1992; Tibbets *et al.*, 1998; Tan *et*

*al.*, 1999). These studies will be discussed in detail, with reference to the findings of this thesis, in the discussion.

ER $\alpha$  and ER $\beta$  protein and mRNA have been localised in the adult ovariectomised rat and mouse uterus. The effects of oestradiol and tamoxifen on the expression pattern of the subtypes have been compared to control, to determine the involvement of ER in response to each of the compounds in the various tissue compartments. *In situ* hybridisation studies have enabled localisation of ER $\alpha$  and ER $\beta$  within cells of the uterus before commercial antibodies were available. The mRNA pattern of expression determined by *in situ* hybridisation was subsequently compared to that obtained by immunostaining.

The methods of *in situ* hybridisation and immunohistochemistry were employed with these aims:

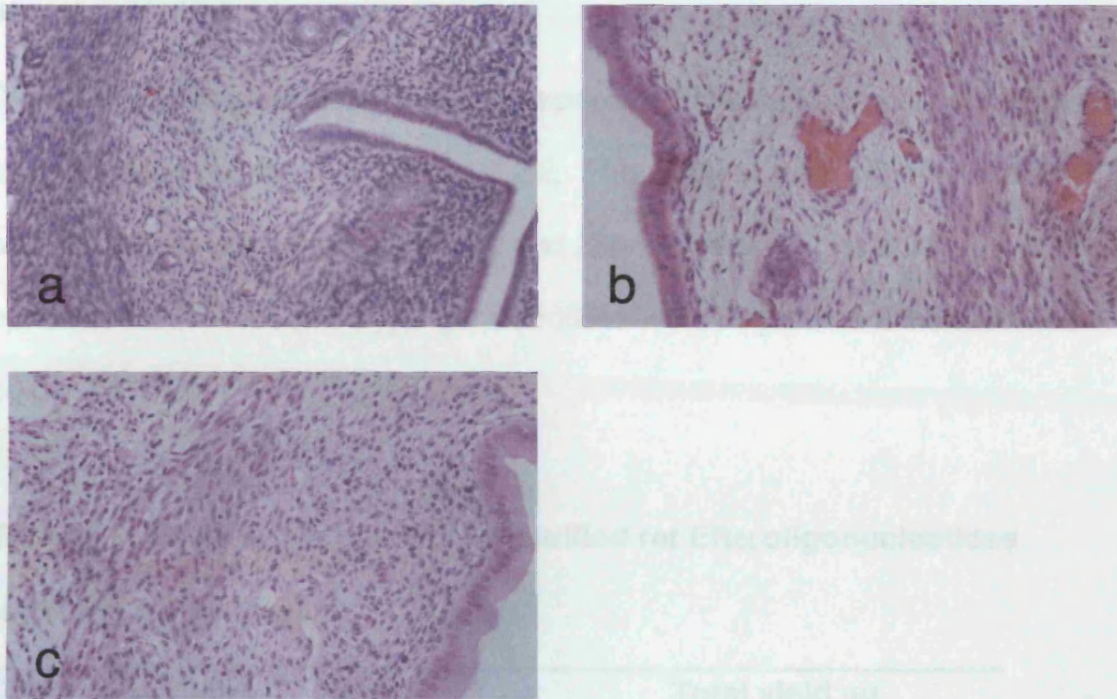
- To develop a suitable technique for investigating ER $\alpha$  and ER $\beta$  expression *in situ*, in the ovariectomised rat and mouse uterus, whilst no commercial antibodies are available.
- Optimise recently available antibodies and use to localise ER $\alpha$  and ER $\beta$  protein within the rat and mouse uterus and compare patterns of expression to mRNA *in situ* hybridisation results.
- Localise ER subtype mRNA and protein expression within the rat and mouse uterus following treatment with oestradiol and tamoxifen and examine changes in treated tissues compared to control animals.

## 4.2 Methods and Results

### 4.2.1 Morphological changes in ovariectomised rat uterus following treatment with oestradiol and tamoxifen

Adult Wistar (Han) rats, ovariectomised at 6 weeks, were dosed subcutaneously at the age of 9 weeks with oestradiol benzoate (5.3nmoles/kg), tamoxifen citrate (2.7 $\mu$ moles/kg) or vehicle only for 3 days (Method 2.1.1). Representative sections of both uterine horns were taken and fixed in 10% neutral buffered formalin, before embedding in paraffin and sectioning at 5 $\mu$ m onto APES coated slides (Method 2.2.7). Localisation of ER $\alpha$  and ER $\beta$  mRNA and protein in parallel sections has been completed by *in situ* hybridisation and by immunohistochemistry with commercial antibodies.

Following 3 days dosing, a similar level of luminal epithelial cell hypertrophy was produced by both oestradiol and tamoxifen in the ovariectomised rat uterus (Figure 4.1). Oestradiol produced hypertrophy in the myometrial layer of the rat uterus whereas tamoxifen did not have this effect in the cells of the myometrial layer. This result suggests there is a difference in the effect of these two compounds in the myometrial compartment of the uterus. Whether levels of the oestrogen receptor were involved in the mediation of this dissimilarity was investigated by the localisation of ER subtypes within tamoxifen and oestradiol treated ovariectomised rat uterus.

4.2.3. ER $\alpha$  and ER $\beta$  mRNA localisation in the ovariectomised rat

Group	Mean length (mm)	Total yield (mg)
Untreated	1.380	284
Oestradiol	1.272	284
Tamoxifen	1.202	303
Control	1.407	79
1990	1.178	273

**Figure 4.1** Representative ovariectomised rat uterine sections stained with hematoxylin and eosin. **a:** untreated tissue section, original magnification x25. **b:** oestradiol treated tissue section, original magnification x25. **c:** tamoxifen treated section, original magnification x25. For treatment regimes and histology methods see Methods 2.1.1 and 2.2.7.

in situ (DAB) (Figure 4.2)

## 4.2.2 ER $\alpha$ and ER $\beta$ mRNA localisation in the ovariectomised rat uterus

Oligonucleotides were designed (synthesised at PNAOL, Leicester) and purified as described in Methods 2.2.1 and 2.2.2. The purity of each oligonucleotide was calculated using the ratio of 260 and 280nm readings, the ratio was optimally 1.8. Subsequently, oligonucleotides were re-purified if the ratio was below 1.5.

**Table 4.1 Representative data for purified rat ER $\alpha$  oligonucleotides following purification**

Oligonucleotide	Ratio	Total yield $\mu$ g
81	1.980	288
696	1.612	284
1130	1.523	353
1649	1.987	79
1980	1.718	273

Oligonucleotide cocktails were labelled with digoxigenin at both the 5' and 3' ends according to the methods of Chu and Orgel, 1985. Dot blot hybridisation was utilised to test the labelling efficiency of Method 2.2.3 following each set of digoxigenin labelling. Oligonucleotide cocktails were dotted onto a nitrocellulose membrane as described in Method 2.2.4, and probed with the HRP conjugated anti-digoxigenin antibody (Roche Diagnostics) and specific substrate (DAB) (Figure 4.2).

#### 4.2.2.1. In situ hybridisation of ER $\alpha$ and ER $\beta$ mRNA in the

##### 4.2.2.1.1. In situ hybridisation of ER $\alpha$ mRNA in the

The in situ hybridisation technique was optimised for each tissue block and set the final choice of reagents and conditions. This was necessary as the technique is extremely

susceptible to a large set of variables particularly tissue fixing and accessibility

of RNA. In this instance, the optimal concentration of digoxigenin was

20  $\mu$ g/ml with a concentration of 1.0  $\mu$ g/ml of labelled cocktail, depending on the

labelling efficiency. Serial dilutions of the cocktail were dotted onto

nitrocellulose membrane (1: 1  $\mu$ g, 2: 100pg, 3: 50pg), with positive controls (A

and B), and probed with a horseradish peroxidase conjugated anti-digoxigenin

antibody (1:1000): as described in Method 2.2.4. Black dots indicate

successful digoxigenin labelling of oligonucleotide cocktails.

The pattern of expression of ER $\alpha$  and ER $\beta$  expression are also

present in the first experimental report. Levels of expression in the different

samples are similar but to lower extent. The pattern of expression of ER $\alpha$  and

ER $\beta$  expression are also

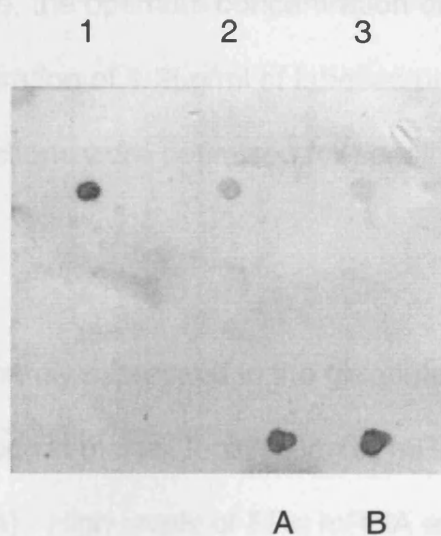


**Figure 4.2** Representative dot blot of digoxigenin labelled rat ER $\alpha$  oligonucleotide cocktail. Serial dilution of labelled cocktail was dotted onto nitrocellulose membrane (1: 1  $\mu$ g, 2: 100pg, 3: 50pg), with positive controls (A and B), and probed with a horseradish peroxidase conjugated anti-digoxigenin antibody (1:1000): as described in Method 2.2.4. Black dots indicate successful digoxigenin labelling of oligonucleotide cocktails.

#### **4.2.2.1 *In situ* hybridisation of ER $\alpha$ and ER $\beta$ mRNA in the ovariectomised adult rat uterus**

The *in situ* hybridisation technique was optimised for each tissue block and set of labelled probes. This was necessary as the technique is extremely susceptible to a large set of variables particularly tissue fixing and accessibility of mRNA target. For the rat uterine sections used for the detection of ER subtypes in this instance, the optimum concentration of proteinase K was 20 $\mu$ g/ml, with a concentration of 1-2 $\mu$ g/ml of labelled probes, depending on the labelling efficiency. Sections were optimised for specific staining compared with controls.

ER $\alpha$  mRNA is predominantly expressed in the glandular epithelial cells of the untreated ovariectomised rat uterus, localisation of mRNA is visualised as a brown stain (Figure 4.3a). High levels of ER $\alpha$  mRNA expression are also prevalent in the inner myometrial layer. Levels of expression in the endometrial stroma are evident but to lesser extent. The pattern of expression of ER $\alpha$  and ER $\beta$  is very similar. Expression of ER $\beta$  is most common in the glandular and luminal epithelium and the myometrium (Figure 4.3b). Localisation of the two ER subtypes within the glandular epithelium and myometrial cell types of the ovariectomised rat uterus appear to be comparable at this stage in the ovariectomised untreated rat uterus. It is important to note that the levels of expression of mRNA of the two subtypes cannot be compared due to the variations in probe-target specificity.

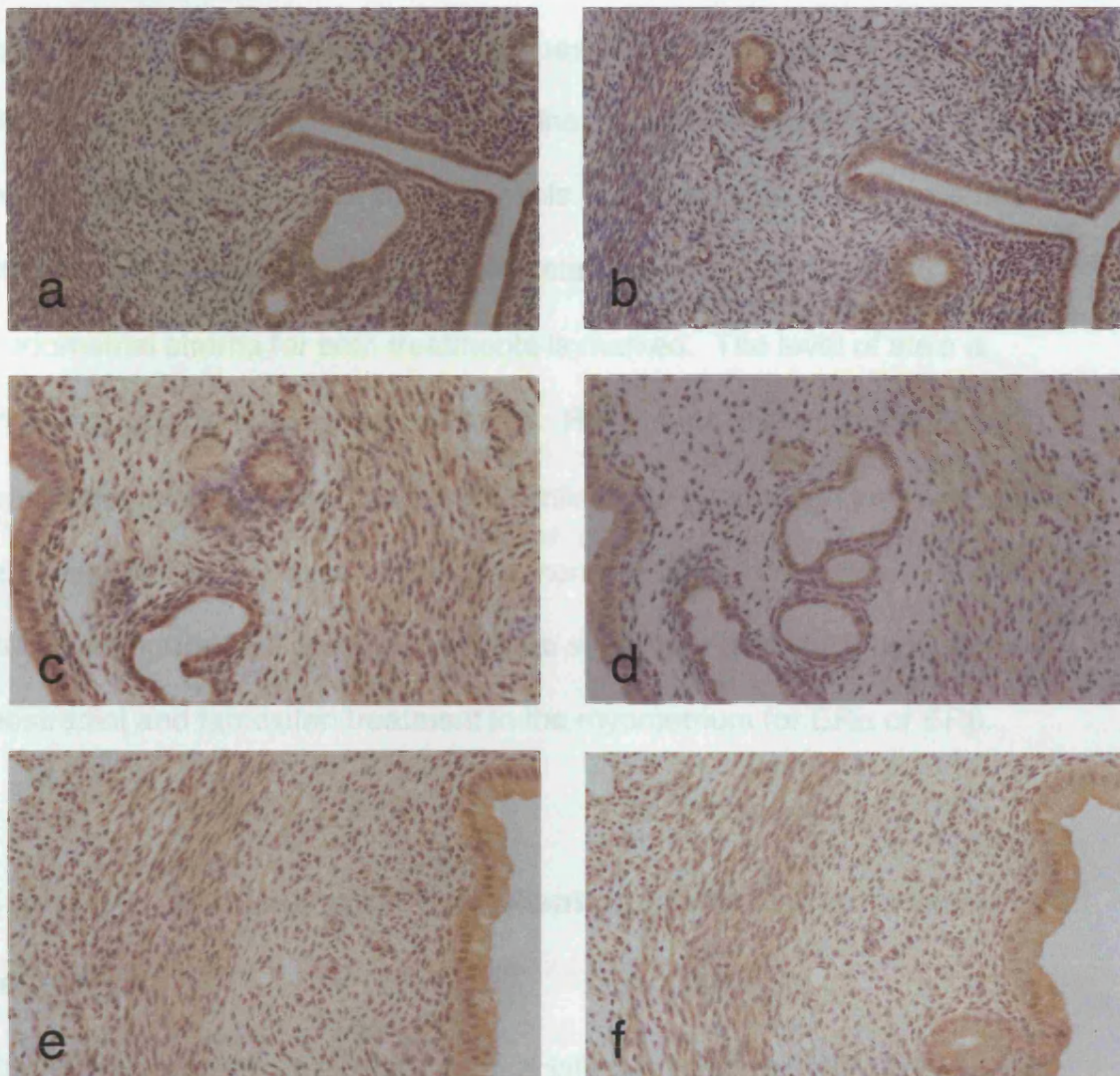


**Figure 4.3** Representative adult ovariectomised rat uterine tissue sections probed for ER $\alpha$  or ER $\beta$  mRNA by *in situ* hybridisation (Methods 2.2). **a**: untreated uterine section probed for ER $\alpha$  and **b**: ER $\beta$ , original magnification x25. **c**: oestradiol treated uterine section probed for ER $\alpha$  and **d**: ER $\beta$ , original magnification x25. **e**: tamoxifen treated uterine section probed for ER $\alpha$  and **f**: ER $\beta$ , original magnification x25. The concentration of Proteinase K was 20 $\mu$ g/ml and ER $\alpha$  and ER $\beta$  oligonucleotide cocktails were hybridised at 1 $\mu$ g/ml. Brown positive staining for ER $\alpha$  and ER $\beta$ . Hematoxylin counterstain.

Following oestradiol and tamoxifen treatment, ER $\alpha$  mRNA expression appears to be increased throughout most cell types of the rat uterus (Figure 4.3c and e). Due to the hypertrophy seen in the luminal epithelium it is difficult to make conclusive comparisons of staining levels in this cell type between treated and control. However, the increase in cells staining for ER $\alpha$  mRNA in the endometrial stroma for both treatments is marked. The level of stain is indistinguishable between all cell types. Results for ER $\beta$  mRNA staining in oestradiol and tamoxifen treated are similar to ER $\alpha$  although levels of staining are less intense, it is possible that the increase is more significant for this subtype (Figure 4.3d and f). There is no significant difference between oestradiol and tamoxifen treatment in the myometrium for ER $\alpha$  or ER $\beta$ .

#### **4.2.3 ER $\alpha$ and ER $\beta$ protein localisation in the ovariectomised adult rat uterus**

Of the several antibodies now commercially available two were chosen that gave optimal results for detection of ER $\alpha$  or ER $\beta$  protein in the rat and mouse uterine sections. The Novacastra mouse monoclonal antibody, NCL-ER-6F11 (Figure 4.4) was used at a concentration of 1:40 for 3h at RT (see Methods 2.3). ER $\beta$  was detected using the Upstate Biotechnology rabbit polyclonal antibody, 06-629 (Figure 4.4) at a concentration of 1:10 in an overnight incubation at RT (see Methods 2.3). HRP-conjugated secondary antibodies and DAB substrate were utilised localising nuclear ER $\alpha$  or ER $\beta$  as a brown stain.

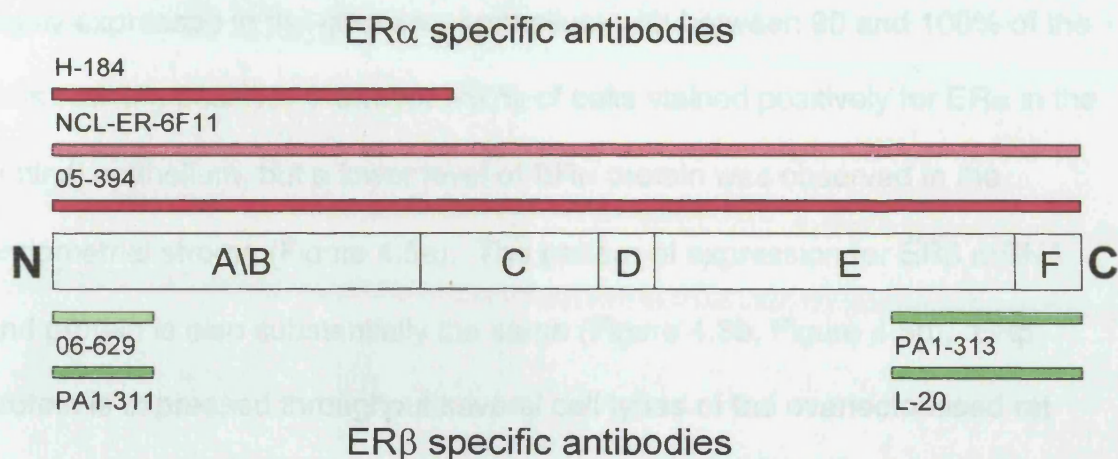


**Figure 4.4** ER functional domains as described in Chapter 1. Diagrammatic map showing epitopes of specific ER $\alpha$  and ER $\beta$  antibodies optimised for immunohistochemistry in rodent tissues (striped bars) see Methods 2.3.1 or Western blotting of human cell lines (solid bars) see Methods 2.3.2. H-184 (Santa Cruz Biotechnologies) rabbit polyclonal specific for mouse, rat and human ER $\alpha$ . NCL-ER-6F11 (Novacastra) mouse monoclonal specific for human ER $\alpha$ . 05-394 (Upstate Biotechnologies) mouse monoclonal specific for rat, mouse and human ER $\alpha$ . 06-629 (Upstate Biotechnologies) rabbit polyclonal specific for rat, human and mouse ER $\beta$ . PA1-311 (Affinity Bioreagents) rabbit polyclonal specific for rat, mouse and human ER $\beta$ . PA1-313 (Affinity Bioreagents) rabbit polyclonal specific for human ER $\beta$ . L-20 (Santa Cruz Biotechnologies) goat polyclonal specific for human ER $\beta$ . Diagram modified from Pavao *et al.*, 2001.

In general the cellular localisation of expression of ER $\alpha$  mRNA and ER $\alpha$  protein is comparable in the untreated ovariectomised rat uterus (Figure 4.3a, Figure 4.5a). Protein staining was most intense in the cell nucleus while as expected the mRNA staining had a more general cytoplasmic location. ER $\alpha$  protein is highly expressed in the glandular epithelium with between 90 and 100% of the cells staining positive. However >50% of cells stained positively for ER $\alpha$  in the luminal epithelium, but a lower level of ER $\alpha$  protein was observed in the endometrial stroma (Figure 4.5a). The pattern of expression for ER $\beta$  mRNA and protein is also substantially the same (Figure 4.3b, Figure 4.5b). ER $\beta$  protein is expressed throughout several cell types of the ovariectomised rat uterus. Approximately all of luminal epithelium and glandular epithelium epithelial cells are positively stained for ER $\beta$  protein. The number of cells staining positively in the endometrial stroma appears to be marginally more than ER $\alpha$  protein as is the case in the myometrial layers (Figure 4.5b).

As described for the ER $\alpha$  and ER $\beta$  mRNA, following oestradiol and tamoxifen treatment there appears to be a general increase of ER subtype protein staining throughout the cells of the uterus compared with controls (Figure 4.5c-f). A small reduction in positive ER $\alpha$  protein staining is seen in the epithelial cells of the lumen and glands, although what appears to be a reduction in stain in the luminal epithelium may be due to a reduction in intensity due to an increase in cell size.

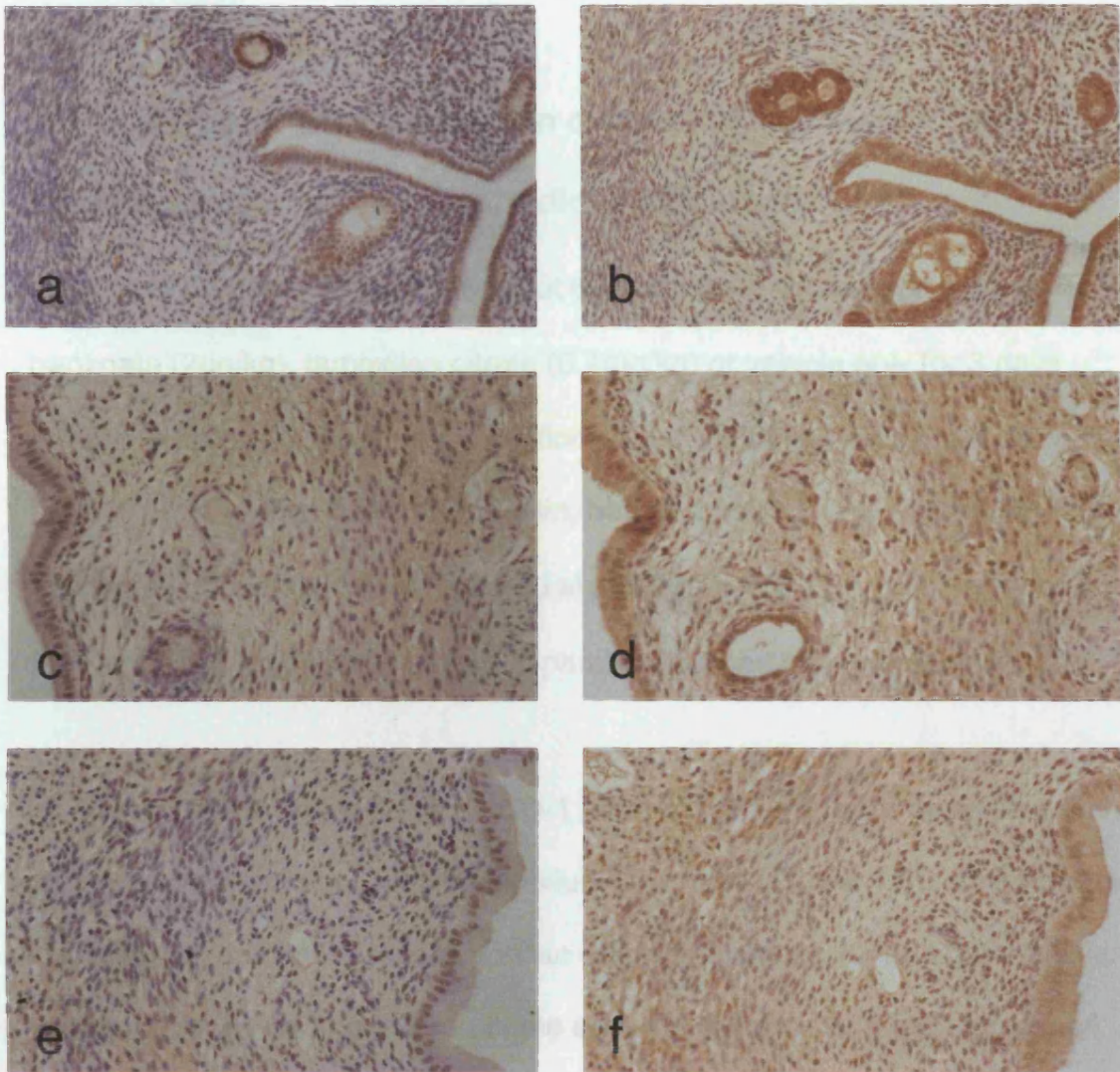


**Figure 4.5** Representative adult ovariectomised rat uterine tissue sections probed for ER $\alpha$  or ER $\beta$  protein by immunohistochemistry (Methods 2.3). **a**: untreated uterine section probed for ER $\alpha$  and **b**: ER $\beta$ , original magnification x25. **c**: oestradiol treated uterine section probed for ER $\alpha$  and **d**: ER $\beta$ , original magnification x25. **e**: tamoxifen treated uterine section probed for ER $\alpha$  and **f**: ER $\beta$ , original magnification x25. ER $\alpha$  was detected using NCL-ER-6F11 and ER $\beta$  using 06-629. Sections were counterstained for 10sec with hematoxylin.

#### **4.2.4 Morphological changes in ovariectomised mouse uterus following treatment with oestradiol and tamoxifen**

Female CD-1 mice, ovariectomised at 6 weeks were treated with oestradiol benzoate (2 $\mu$ g/kg), tamoxifen citrate (0.4mg/kg) or vehicle only for 3 days (Method 2.1.1). Representative sections of both uterine horns were taken and fixed in 3.7% neutral buffered formalin, before embedding in paraffin and sectioning at 5 $\mu$ m onto APES coated slides (Method 2.2.7). Localisation of ER $\alpha$  and ER $\beta$  mRNA and protein in parallel sections has been completed.

Treatment of the ovariectomised CD-1 mice with oestradiol or tamoxifen both caused an increase in luminal epithelium thickness (Figure 4.6). The increase in luminal epithelium thickness was an effect of hypertrophy and hyperplasia. Hypertrophy was also observed in the endometrial stroma in both tamoxifen and oestradiol treated tissues. Oestradiol caused a greater increase in hypertrophy in the endometrial stroma than tamoxifen compared to the untreated animals. The similarities in these two compounds, with respect to their effects on the morphology of the ovariectomised mouse uterus, were investigated further by assessment of ER $\alpha$  and ER $\beta$  mRNA and protein expression.

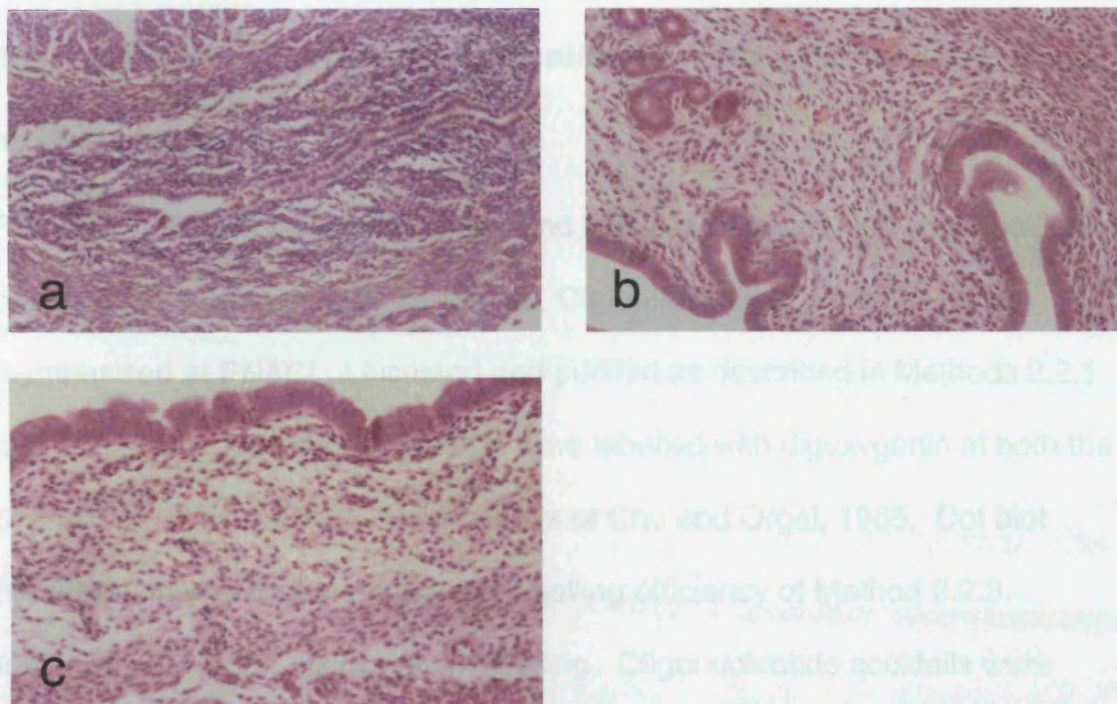


**Figure 4.6** Representative ovariectomised mouse uterine sections stained with hematoxylin and eosin. **a:** untreated tissue section, original magnification x25. **b:** oestradiol treated tissue section, original magnification x25. **c:** tamoxifen treated section, original magnification x25. For treatment regimes and histology methods see Methods 2.1.1 and 2.2.7.

#### **4.2.5 ER $\alpha$ and ER $\beta$ mRNA localisation in the ovariectomised adult mouse uterus**

Procedures for the design, synthesis and labelling of the mouse oligonucleotide cocktails were as described for the rat. Oligonucleotides were designed (synthesised at PNACL, Leicester) and purified as described in Methods 2.2.1 and 2.2.2. Oligonucleotide cocktails were labelled with digoxigenin at both the 5' and 3' ends according to the methods of Chu and Orgel, 1985. Dot blot hybridisation was utilised to test the labelling efficiency of Method 2.2.3 following each set of digoxigenin labelling. Oligonucleotide cocktails were dotted onto a nitrocellulose membrane as described in Method 2.2.4, and probed with the anti-digoxigenin antibody (Roche Diagnostics) and specific substrate (DAB). Dot blots were identical to those obtained from the rat labelling (Figure 4.2) and are therefore not shown.

##### **4.2.5.1 *In situ* hybridisation of ER $\alpha$ and ER $\beta$ mRNA in the ovariectomised adult mouse uterus**

Proteinase K digestion and probe concentration were again optimised for the mouse, as for the rat, for each set of freshly labelled probes and tissue sections. The optimum proteinase K concentration was 2 $\mu$ g/ml, which gave the best signal while preserving the structures of the tissue. Probe and antibody concentrations were optimised at 1-2 $\mu$ g/ml of probe and an antibody concentration of 1:50, to provide the best signal. Expression of the ER subtypes was minimal in the control animals; therefore the procedure was

optimised using sections from oestradiol and tamoxifen treated tissues. Signal was optimised against control sections. Expression of ER $\alpha$  and ER $\beta$  in control untreated animals was minimal; positive staining was observed in glandular and luminal epithelial cells (Figure 4.7a and b). A low number of endometrial stromal cells were also positive for ER $\alpha$  mRNA expression with little or no stain in the myometrium.

Staining for ER $\alpha$  mRNA was greatly increased in the endometrial stroma of the mouse uterus following treatment with oestradiol or tamoxifen (Figure 4.7c and e). Staining for ER $\alpha$  mRNA appeared to be decreased in the epithelial cells of the lumen and glands and unchanged in the myometrium. Expression of ER $\beta$  mRNA mirrored that of ER $\alpha$  mRNA (Figure 4.7d and f). The low level of stain for ER $\beta$  mRNA, observed in the epithelial cells of the uterus, was reduced compared to control and staining levels in the endometrial stroma were increased, with no marked change in the myometrium.

#### **4.2.6 ER $\alpha$ and ER $\beta$ protein localisation in the ovariectomised adult mouse uterus**

The Novocastra anti-ER $\alpha$  (NCL-ER-6F11) and the Upstate Biotechnology anti-ER $\beta$  (06-629) have been optimised for use with mouse uterine tissue sections. ER $\alpha$  and ER $\beta$  protein were detected as for the rat, using the same conditions (Methods 2.3.1).

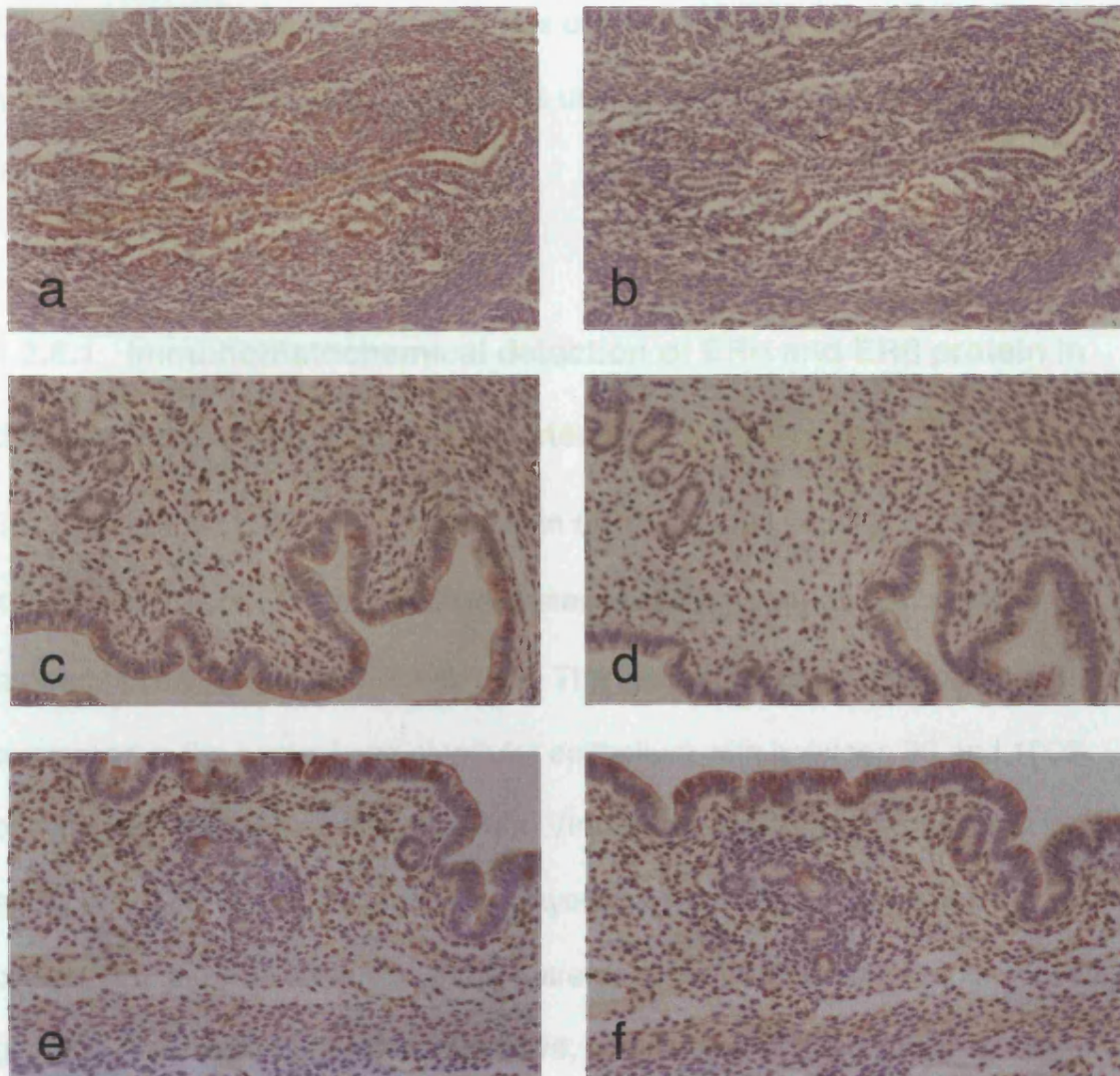


**Figure 4.7** Representative adult ovariectomised mouse uterine tissue sections probed for ER $\alpha$  or ER $\beta$  mRNA by *in situ* hybridisation (Methods 2.2). **a:** untreated uterine section probed for ER $\alpha$  and **b:** ER $\beta$ , original magnification x25. **c:** oestradiol treated uterine section probed for ER $\alpha$  and **d:** ER $\beta$ , original magnification x25. **e:** tamoxifen treated uterine section probed for ER $\alpha$  and **f:** ER $\beta$ , original magnification x25. Proteinase K was used at a concentration of 2 $\mu$ g/ml and ER $\alpha$  and ER $\beta$  oligonucleotide cocktails were hybridised at 1 $\mu$ g/ml giving ER mRNA a positive brown stain with 1:50 anti-digoxigenin antibody. Sections were counterstained for 10sec with hematoxylin.

ER $\alpha$  specific antibody (Novocastra) was used at 1:40 and the ER $\beta$  specific antibody (Upstate Biotechnologies) was used at a concentration of 1:10, giving rise to a positive brown nuclear stain.

#### **4.2.6.1 Immunohistochemical detection of ER $\alpha$ and ER $\beta$ protein in the ovariectomised adult mouse uterus**

Staining for ER $\alpha$  protein was localised in the nucleus of positive cells (Figure 4.8a). A low level of ER $\alpha$  protein is expressed in the untreated mouse uterus as was observed with the ER $\alpha$  mRNA. The highest levels of ER $\alpha$  protein are expressed in the luminal and glandular epithelium with between 90 and 100% of cells staining positive (Figure 4.8a). Virtually no staining was observed in the endometrial stroma and myometrium layers. A much higher level of ER $\beta$  protein staining was observed in the untreated mouse with 100% of luminal and glandular epithelial cells staining positive, a high level of stain was also seen throughout the endometrial stroma and myometrial layers (Figure 4.8b).

Following treatment with oestradiol and tamoxifen a similar picture was seen for both ER $\alpha$  and ER $\beta$  protein (Figure 4.8c-f). An increase was observed for ER $\alpha$  protein in the endometrial stroma and myometrium however no change occurred in either the luminal and glandular epithelium. There was little change in expression of ER $\beta$  in the endometrial stroma of treated tissues, although the same decrease in ER $\beta$  expression in the epithelial cells occurred.

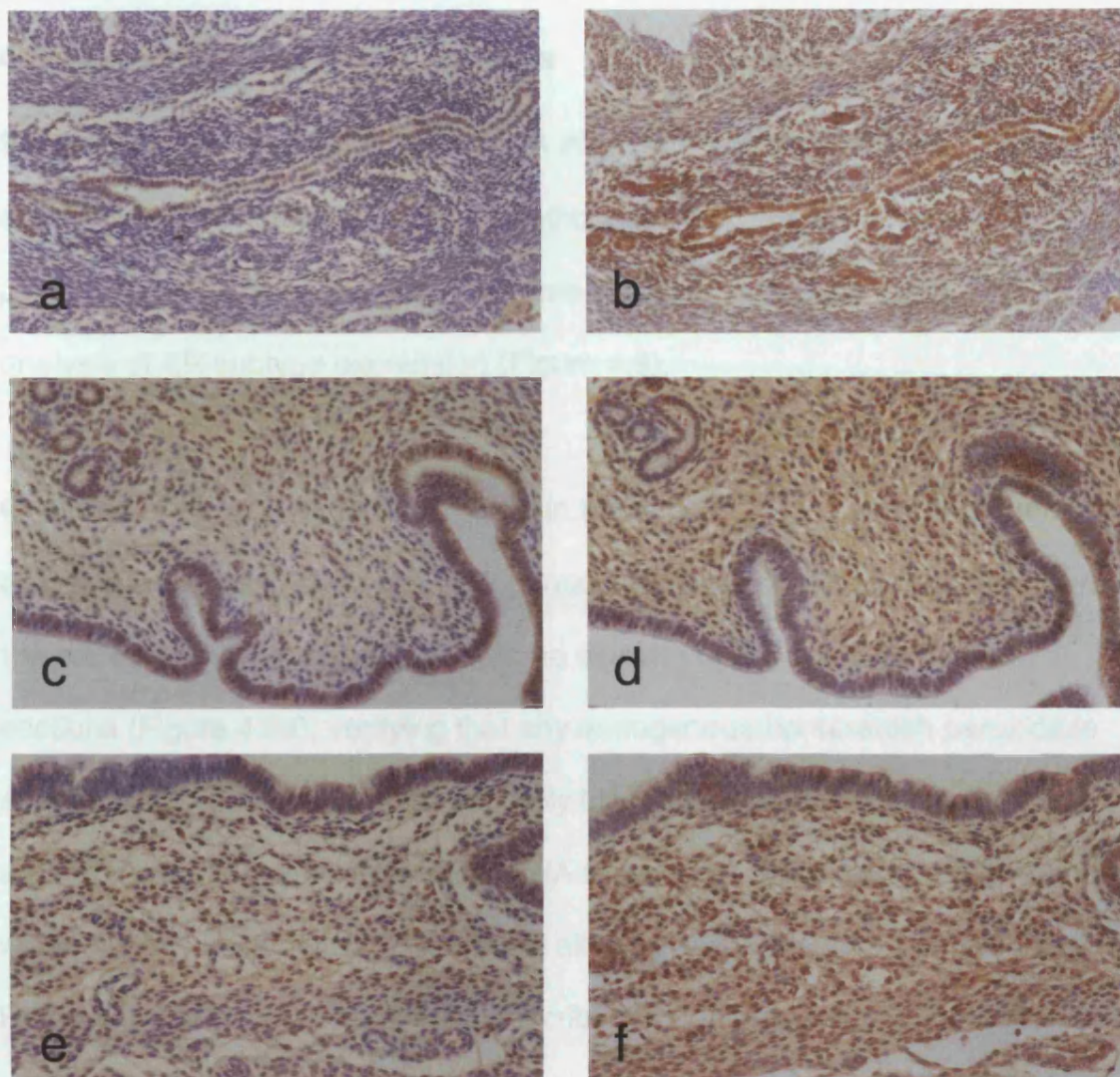


**Figure 4.8** Representative adult ovariectomised mouse uterine tissue sections stained for ER $\alpha$  or ER $\beta$  protein by immunohistochemistry (Methods 2.3). **a**: untreated uterine section probed for ER $\alpha$  and **b**: ER $\beta$ , original magnification x25. **c**: oestradiol treated uterine section probed for ER $\alpha$  and **d**: ER $\beta$ , original magnification x25. **e**: tamoxifen treated uterine section probed for ER $\alpha$  and **f**: ER $\beta$ , original magnification x25. ER $\alpha$  was detected using NCL-ER-6F11 and ER $\beta$  using 06-629 with ER protein staining brown in the nucleus. All sections were counterstained for 10sec with hematoxylin.

#### 4.2.7 *In situ* hybridisation controls

Several controls have been included in the *in situ* hybridisation procedure to ensure specificity of the technique (Methods 2.2.11). The controls were performed on sections cut from the same block as those involved in the analysis of ER subtype expression (Figure 4.9).

Omission of the oligonucleotide probe in the hybridisation step was included as a negative control to check for endogenous horseradish peroxidase activity in the sections. As expected there was no staining within any cells in these sections (Figure 4.9a), verifying that any endogenous horseradish peroxidase activity in the tissue had been effectively blocked. Sections were probed with an oligonucleotide specific for 28S rRNA to estimate the levels of RNA retention within the tissue sections. This control allowed assessment of the levels of RNA available for hybridisation as described in the Methods 2.2.11. The staining in this section demonstrated a high level of hybridisable RNA within the uterine tissues (Figure 4.9b), confirming that significant levels of RNA were not lost throughout the *in situ* hybridisation procedure.

The sense versions of the ER $\alpha$  and ER $\beta$  oligonucleotide cocktails were labelled and used as hybridisation specificity controls (Figure 4.9c). Occasionally some background was observed in sections used in these control procedures although the staining observed in sections probed with the sense versions of the oligonucleotide cocktails was at a uniform level throughout all cells of the uterus.

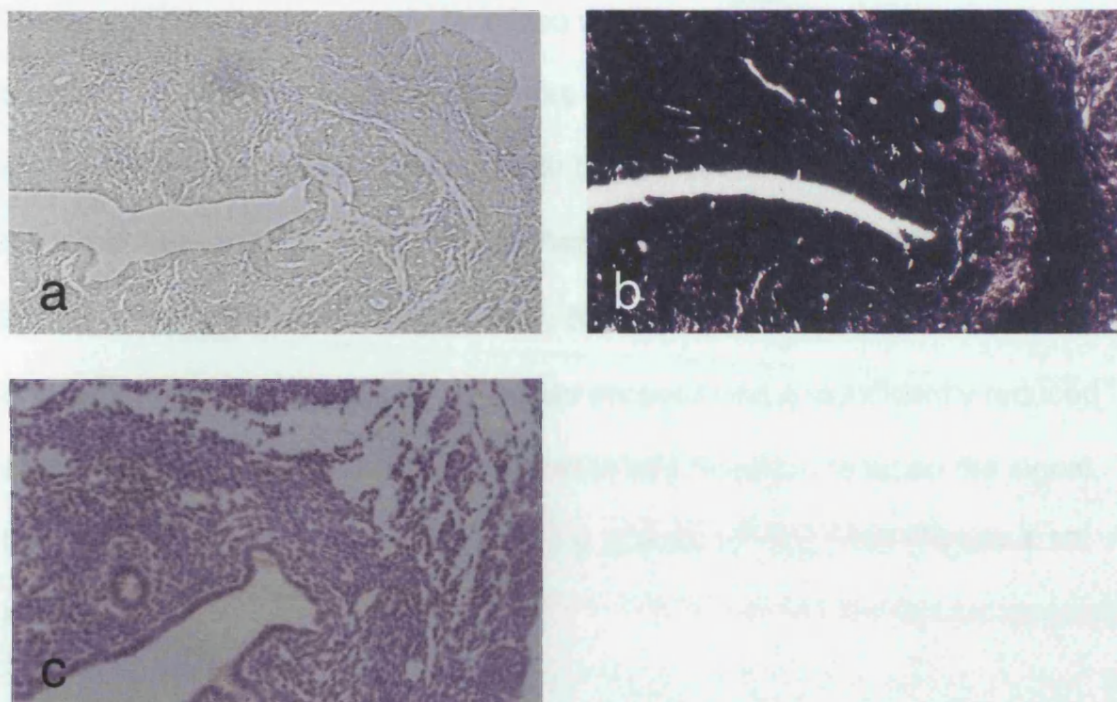


**Figure 4.9** Representative mouse uterine sections used as controls for the *in situ* hybridisation technique. See methods 2.2.11. **a:** omission of digoxigenin labelled oligonucleotide cocktail showing no endogenous peroxidase activity, original magnification x10. **b:** positive control for hybridisable RNA with 28s rRNA specific probes verifying a high level of hybridisable RNA, original magnification x10 (digoxigenin detected with a alkaline phosphatase antibody as no counterstain was required). **c:** hybridisation with sense versions of the ER $\alpha$  oligonucleotide cocktail, original magnification x25.

There was none of the specific localised staining observed with the antisense cocktails. It is of note that specific areas of stain within the luminal epithelium and glandular epithelium, observed with the ER cocktails, were not visible in these control sections. A fifty-fold increase of unlabelled probe (50 $\mu$ g/ml) was added to the hybridisation step to verify the specificity of the oligonucleotide cocktails (1 $\mu$ g/ml) by competition. These sections had a significantly reduced amount of staining. The unlabelled cocktail had therefore reduced the signal from labelled oligonucleotides by blocking specific binding sites (Figure 4.10 and 11).

#### **4.2.7.1 Reverse transcriptase polymerase chain reaction (RT-PCR) confirmation of oligonucleotide probe specificity**

ER $\alpha$  and ER $\beta$  full-length transcripts were amplified using RT-PCR (see methods 2.2.12). Figure 4.12 shows the ER $\alpha$  PCR product visualised using agarose gel electrophoresis. Using the 100bp ladder the PCR product can be estimated at the correct 1985bp. The size of the ER $\beta$  PCR product, 2483bp, was also estimated using gel electrophoresis.

The identity of the ER $\alpha$  and ER $\beta$  PCR products were additionally confirmed using restriction enzyme digests (Method 2.2.12.4). The ER $\alpha$  PCR product was digested with *Stu1* producing fragments of 1096bp and 889bp thus confirming that the PCR product was ER $\alpha$ , illustrated in Figure 4.12c.

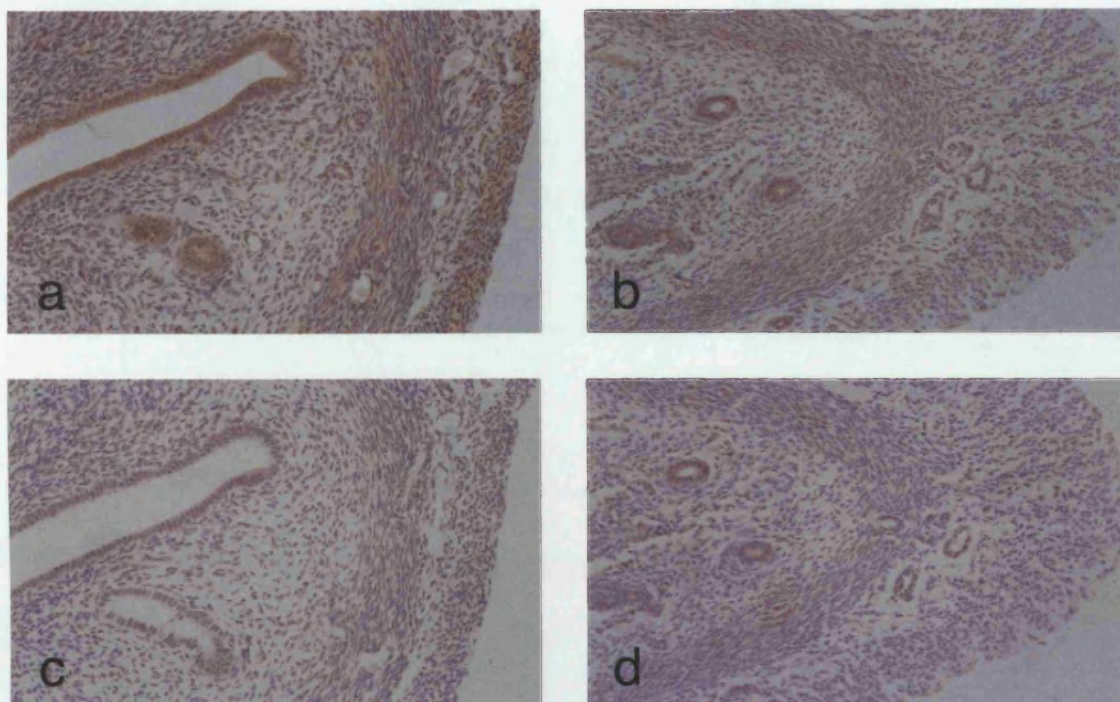


**Figure 4.10** Representative rat uterine sections hybridised with standard oligonucleotide probes for ER $\alpha$  or ER $\beta$  (a and b) or with a fifty-fold increased concentration of unlabelled specific oligonucleotide cocktail (50 $\mu$ g) added to the ER $\alpha$  or ER $\beta$  (1 $\mu$ g) pre-hybridisation mix, demonstrating reduced signal. Sections are prepared from the block of tissue used for the *in situ* hybridisation study. **a:** rat uterine section probed for ER $\alpha$ , original magnification x25. **b:** rat uterine section probed for ER $\beta$ , original magnification x25. **c:** rat uterine section probed with ER $\alpha$  oligonucleotide-block, original magnification x25. **d:** rat uterine tissue section probed with ER $\beta$  oligonucleotide-block, original magnification x25.

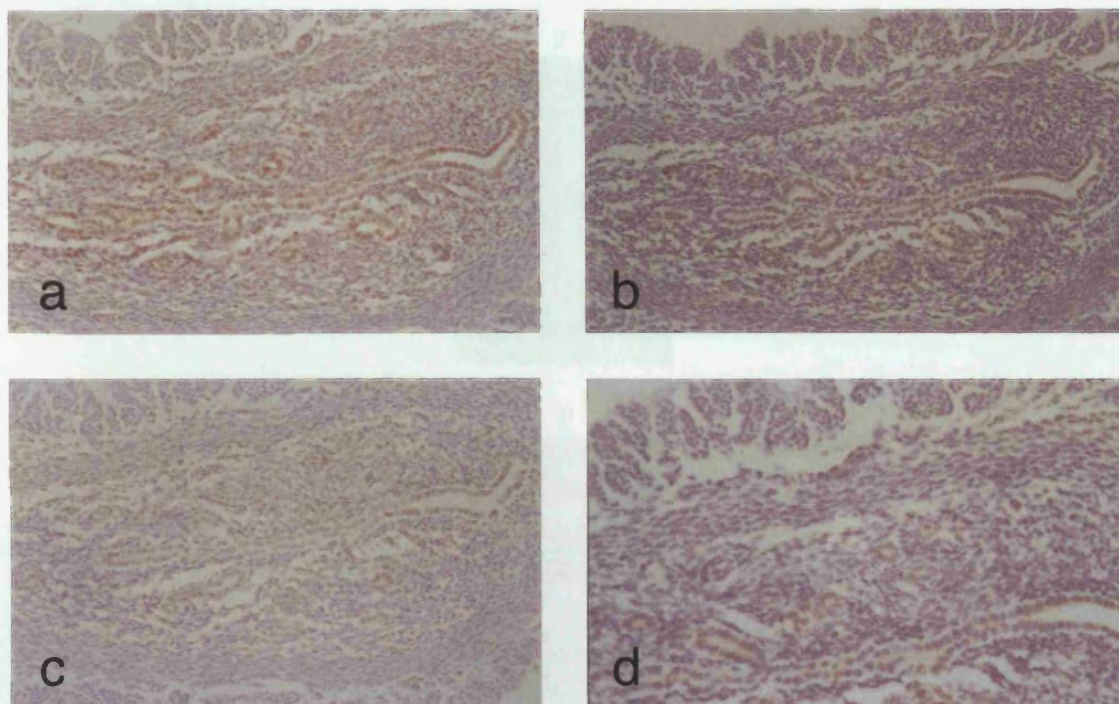


**Figure 4.11** Representative mouse uterine sections hybridised with standard oligonucleotide probes for ER $\alpha$  or ER $\beta$  (a and b) or a fifty-fold increased concentration of unlabelled specific oligonucleotide cocktail (50 $\mu$ g) added to the ER $\alpha$  or ER $\beta$  (1 $\mu$ g) pre-hybridisation mix, demonstrating reduced signal.

Sections are prepared from the block of tissue used for the *in situ* hybridisation study. **a:** mouse uterine section probed for ER $\alpha$ , original magnification x25. **b:** mouse uterine section probed for ER $\beta$ , original magnification x25. **c:** mouse uterine section probed with ER $\alpha$  oligonucleotide-block, original magnification x25. **d:** mouse uterine tissue section probed with ER $\beta$  oligonucleotide-block, original magnification x25.

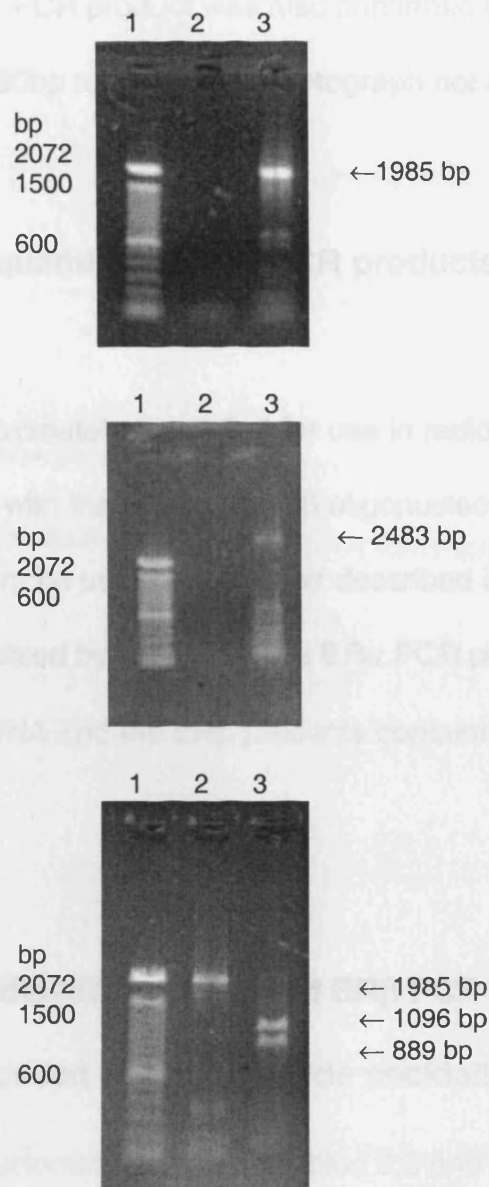


**Figure 4.12** **a:** representative PCR product amplified using ER $\alpha$  primers and ovariectomised rat uterus cDNA. Lane 1: 100bp ladder, lane 2: negative control, lane 3: 1985bp ER $\alpha$  PCR product. **b:** representative PCR product amplified using ER $\beta$  primers and ovariectomised rat uterus cDNA. Lane 1: 100bp ladder, lane 2: negative control, lane 3: 2483bp ER $\beta$  PCR product. **c:** restriction digest of a representative ER $\alpha$  PCR product. Restriction enzyme *Stu1* producing 1096bp and 889bp fragments. Lane 1: 100bp ladder, lane 2: uncut ER $\alpha$  PCR product and lane 3: digested ER $\alpha$  PCR product.

The sequence of the ER $\beta$  PCR product was also confirmed using *Bam* H1 producing fragments of 880bp and 1603bp (photograph not available).

#### **4.2.7.2 Approximate quantification of PCR products using ethidium bromide**

PCR products were approximately quantified for use in radioactive labelling and subsequent hybridisation with the ER $\alpha$  and ER $\beta$  oligonucleotide probe cocktails. This was performed using the method described in 2.2.12.5. Figure 4.13 shows the grid visualised by UV light. The ER $\alpha$  PCR products contained approximately 7ng/ $\mu$ l of DNA and the ER $\beta$  products contained approximately 5ng/ $\mu$ l of DNA.

#### **4.2.7.3 Dot blot hybridisation of ER $\alpha$ and ER $\beta$ PCR products and detection with $\alpha^{32}$ P labelled oligonucleotide cocktails**

Rat ER $\alpha$  and ER $\beta$  oligonucleotide cocktails (Tables 2.3 and 2.4) were labelled with  $\alpha^{32}$ P to enable their detection when bound to the PCR products immobilised onto the nylon membrane. Both ER $\alpha$  and ER $\beta$  cocktails were successfully labelled (Method 2.2.12.6) resulting in approximately  $8 \times 10^5$  cpm. Approximately 100pg of each ER $\alpha$  or ER $\beta$  PCR product was applied to the nylon membrane and immobilised.  $\alpha^{32}$ P labelled oligonucleotide cocktails were hybridised overnight and detected by autoradiography. However, even after an exposure of 72h at -80°C no signal could be detected from the radiolabelled oligonucleotide cocktails.

The results of the *in vitro* hybridisation experiments are shown in Figure 4.12. The results of the *in vitro* hybridisation experiments (Section 2.7) had confirmed the specificity of the probes and the agreement with the dot blot confirmation was not surprising.

## 4.2 Discussion

An *in vitro* hybridisation technique has been developed and optimised for the detection of ER $\alpha$  and ER $\beta$  mRNA in general and oestrogen treated

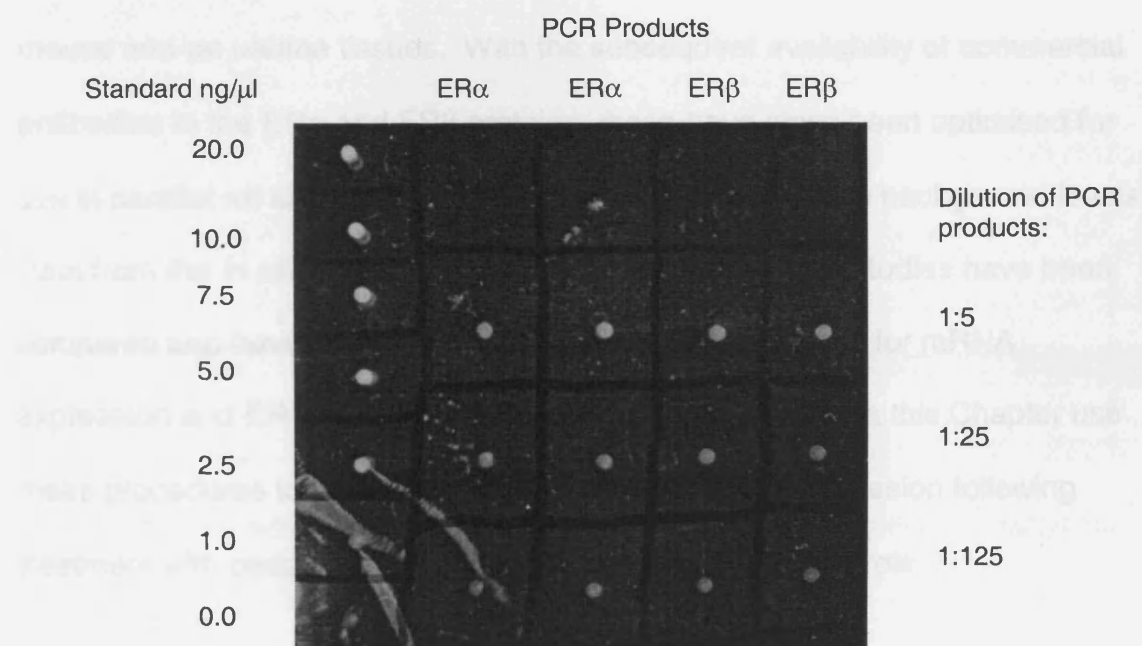


**Figure 4.13** Representative photograph of ethidium bromide stained ER $\alpha$  and ER $\beta$  PCR products visualised by UV light for approximate quantification (Methods 2.2.12).

Three repeats were performed unsuccessfully. Due to the fact that BLAST data and other *in situ* hybridisation controls (Section 4.2.7) had established the specificity of the cocktails, perseverance with the dot blot confirmation was not deemed necessary.

### 4.3 Discussion

An *in situ* hybridisation technique has been developed and optimised for detection of ER $\alpha$  and ER $\beta$  mRNA in control and oestradiol or tamoxifen treated mouse and rat uterine tissues. With the subsequent availability of commercial antibodies to the ER $\alpha$  and ER $\beta$  proteins, these have since been optimised for use in parallel rat and mouse uterine sections with negligible background levels. Data from the *in situ* hybridisation and the immunostaining studies have been compared and have been shown to give comparable results for mRNA expression and ER protein localisation. Results presented in this Chapter use these procedures to assess changes in ER $\alpha$  and ER $\beta$  expression following treatment with oestradiol and tamoxifen compared with controls.

In untreated ovariectomised Wistar (Han) rat uterine tissue sections, ER $\alpha$  and ER $\beta$  mRNA were located in predominantly the same cell types. Positive staining was mainly localised in the glandular epithelial cells and the inner myometrial layer, with a low level of expression in the endometrial stroma. The pattern of expression of ER protein provided evidence that ER $\alpha$  and ER $\beta$  were in the same cell types as the mRNA. In contrast to the mRNA staining, ER $\alpha$  protein staining was not prevalent in the myometrial layers. This could indicate

that the stability of the ER protein differs between cell types and may be more stable in the luminal and glandular epithelium.

Carthew and colleagues (1999b) described strong expression of ER $\alpha$  protein in the luminal and glandular epithelium and approximately 50% of endometrial stromal cells in untreated ovariectomised Wistar (Han) rats. Expression of ER $\beta$  was not described. However, Saunders and colleagues (1997) have previously described expression of both ER $\alpha$  and ER $\beta$  protein in the luminal and glandular epithelial cells in the adult rat uterus by immunohistochemistry. This confirmation of the results presented in this thesis verifies the specificity of the techniques used. A further study of ER subtype expression in Sprague-Dawley rats showed variation localising ER $\beta$  protein expression only in glandular, not luminal epithelium (Hiroi *et al.*, 1999). This variation in expression might be due to strain variation, or to the sensitivity of the different ER $\beta$  antibodies. Following treatment of rats with oestradiol, expression of ER $\alpha$  protein in the myometrium increased and levels in the luminal epithelium cells decreased compared with controls (Carthew *et al.*, 1999b). Tamoxifen treatment had a similar effect on ER $\alpha$  expression in the myometrium, but levels in the luminal epithelium were unchanged. Expression patterns from both the present *in situ* hybridisation and immunostaining studies are in agreement with these results.

Previous *in situ* hybridisation studies using radiolabelled probes have localised ER $\alpha$  mRNA in the Sprague-Dawley rat uterus predominantly in the glandular epithelium and the endometrial stroma, however only a weak signal for ER $\beta$

mRNA could be detected in the same cell types (Shughrue *et al.*, 1998). The low detection of ER $\beta$  by in the Shughrue study is most likely due to the lack of sensitivity of the radioactively labelled *in situ* probes. However, the lower level of ER $\beta$  mRNA in the ovariectomised rats described in this Chapter may not be due to a variation in probe sensitivity. A study conducted in oestrous cycling rats demonstrated a fundamental relationship between ER mRNA expression and oestrogen levels (Katsuda *et al.*, 1999). This study again, localised the expression of ER mRNA in the luminal epithelium and glandular epithelium cells of the rat uterus.

In the ovariectomised mouse uterus detection of both ER $\alpha$  and particularly ER $\beta$  mRNA expression is close to the limit of detection by the present method. Increased expression in the endometrial stroma of ER $\alpha$  and ER $\beta$  at 72h following oestradiol and tamoxifen treatment was observed for both protein and mRNA. Cells staining for ER $\alpha$  and ER $\beta$  mRNA were observed in all compartments of the oestradiol and tamoxifen treated uterus, but predominantly in the endometrial stroma, a decrease in cells staining positive was seen in the epithelial cells with no change in the myometrium. There was also a marked increase in the number of cells staining for ER $\alpha$  protein in the endometrial stroma following either oestradiol or tamoxifen treatment. ER $\beta$  protein staining appeared to be much higher in the untreated uterus, with a decrease of protein occurring in the epithelial cells following both oestradiol and tamoxifen treatment.

Tibbetts and colleagues (1998) studied ER expression in ovariectomised mice. ER protein expression was confirmed in glandular epithelium and some luminal epithelium, 76% of endometrial stroma and weakly in the myometrium compartments (Tibbetts *et al.*, 1998). Those mice treated for 4 consecutive days with 1µg of oestradiol showed an increase in the number of cells staining for ER in the luminal epithelium and the myometrium. This data verifies the pattern of expression obtained for ER $\alpha$  in this study and supports the concept that both oestrogens and SERMs have varying effects on different compartments of the uterus. The increase in number of cells staining in the luminal epithelium described by this group would relate to the findings of this Chapter, as the number of cells of the luminal epithelium increased and therefore the number of cells staining positive for ER $\alpha$ . The intensity of staining however was not changed after treatment.

The morphological effects of oestradiol and tamoxifen on the rodent uteri have provided some helpful insights into the mechanism of action of these two compounds. In both rodent models oestradiol and tamoxifen increased luminal epithelium cell hypertrophy. Specifically, in the rat, oestradiol produced myometrium hypertrophy while tamoxifen treatment did not result in myometrial hypertrophy, there appeared to be no significant difference between these two compounds with regard to their effects on ER mRNA or protein expression in the myometrial layer of the treated uteri. This indicates that in the rats there is no direct relationship between ER expression and hypertrophy. In the mice a similar increase in luminal epithelial cell hypertrophy was produced by both compounds, this effect was also observed in the endometrial stroma. However,

a greater increase in hypertrophy of the endometrial stroma was seen in the oestradiol treated mice. A similar increase in staining for both ER mRNA and protein was an effect produced by both tamoxifen and oestradiol, suggesting that neither ER $\alpha$  nor ER $\beta$  levels are directly related to cell hypertrophy produced by these compounds in the mouse.

Specific stains for proteins rather than mRNA are superior as proteins are at the functional level having a more direct effect on the cell and tissues. There are no major subtype differences in either species of uterus. However it is not possible to compare levels of expression, as neither technique is accurately quantifiable at this stage. Radioactive *in situ* hybridisation can be made quantifiable but no data are available on relative levels of ER $\beta$  expression in uterine samples. As illustrated in the work described in this Chapter, the potential for background levels can be high and this risk would be even greater with radioactive labelled probes.

The technique of *in situ* hybridisation has been optimised for use with ovariectomised rat and mouse uterus sections fixed in neutral buffered formalin and paraffin embedded. ER $\alpha$  and ER $\beta$  oligonucleotide probe cocktails, designed for *in situ* hybridisation studies, are specific for their targets to the limitations of the various controls described. Competition or blocking of the cocktails with unlabelled probe has demonstrated that the probes are binding to specific sites within the mRNA and the 28S rRNA positive control has demonstrated a high level of viable RNA within the tissue sections. The levels of background occasionally observed with sense versions of the oligonucleotide

probes were to be expected as although these probes are the sense versions they are, in fact, a completely different set of probes that may hybridise to other mRNAs in manner not resembling that of the specific probes. The combination of *in situ* hybridisation and immunohistochemistry described in this Chapter have demonstrated that ER $\alpha$  and ER $\beta$  are regulated in response to both oestradiol and tamoxifen in a similar manner, therefore the downstream effects of these two subtypes could play key roles in the oestrogenic effects tamoxifen has on the uterus. There appears to be no obvious species-specific differences in the expression of ER in response to these compounds.

Techniques using laser capture micro-dissection (LCM) which allow RNA extraction from one tissue compartment or cell population, down to one cell and RT-PCR could be combined to study levels of RNA within one particular cell type or tissue compartment. This technique is more specific as it focuses on the highly optimised technique of RT-PCR that has a far narrower margin for error than *in situ* hybridisation. However the advantages of *in situ* hybridisation are that the mRNA can be visualised in the context of its expression which is important when studying the compartmental effects of oestrogenic action in the uterus. LCM, in combination with RT-PCR, will be used in the future to study expression of genes that are downstream candidates for the mediation of oestrogenic compound effects on the uterus through the ER. The combination of LCM, RT-PCR and microarray technology will be used to elucidate the mechanism of oestrogenic action in the uterus of rodent models.

**Chapter 5: The neonatal mouse model: uterine pathological changes and microarray identification of genes altered in response to oestradiol and related SERMs**

## 5.1 Introduction

Epidemiological evidence suggests that tamoxifen has a stimulatory affect in the uterus and can cause endometrial cancers (Rutqvist *et al.*, 1995; Fisher *et al.*, 1998). Treatment of postmenopausal women with tamoxifen has also lead to reports of adenomyosis (Cohen *et al.*, 1997b), a condition characterised by the haphazard localisation of glands and stroma within the myometrium of the uterus. In contrast, raloxifene behaves as an oestrogen antagonist in the rat uterus (Black *et al.*, 1983) and may reduce the risk of reproductive tract lesions when used in humans.

As discussed in Chapter 1, the neonatal mouse model has been used to study the effects of oestrogenic compounds in tumour formation within the reproductive tract. Altered levels of hormones during *in utero* and early post-natal periods of development are particularly important and can result in permanent changes. Exposure to oestrogenic compounds during this period leads to the induction of tumours within the reproductive tract (Newbold *et al.*, 1990; 1997; 2000, 2001). Adenomyosis has been described previously in the neonatal mouse model surgically implanted with a pituitary gland (Koujyo *et al.*, 1998; Zhou *et al.*, 1999) and adenomyosis develops spontaneously in older mice (Faccini *et al.*, 1990). However, this condition has not been described in neonatal mice treated with the SERMs investigated in this thesis.

cDNA arrays are increasingly being used in the determination of changes in mRNA expression levels. It may be of particular value in assessing the effects

of a toxic compound on the cell. In the case of oestrogens, the mechanisms of tamoxifen resistance were examined in MCF-7 cells by Hilsenbeck *et al.*, 1999. This group found outlier genes *ERK-2* and *HSF-1* could be used as markers of altered expression associated with the development of resistance.

The effects of the SERMs tamoxifen, toremifene and raloxifene have been compared to oestradiol in the developing neonatal mouse reproductive tract. Histological findings, ER status and gene expression data have been examined in treated mice. In order to determine the early gene changes involved in the development of reproductive tract lesions, the membrane Clontech Mouse 1.2 cDNA microarray has been employed to begin to elucidate the mechanisms involved. The development of microarray technology permits the quantification of hundreds of genes in one experiment. This array has 1176 cDNAs to allow investigation of the expression changes in cellular mRNA expression in response to drug treatment. In addition there are bacterial DNA spots to act as negative controls, mouse genomic DNA as positive controls, orientation marks and 9 housekeeping genes, see Figure 5.1. A full list of genes has been given in Appendix 1. These factors have been assessed in CD-1 mice treated on days 2-5 with tamoxifen, toremifene and raloxifene. Tissues have been processed at day 6, 42 and 90 to provide an early, intermediate and progressed time point for pathological assessment.

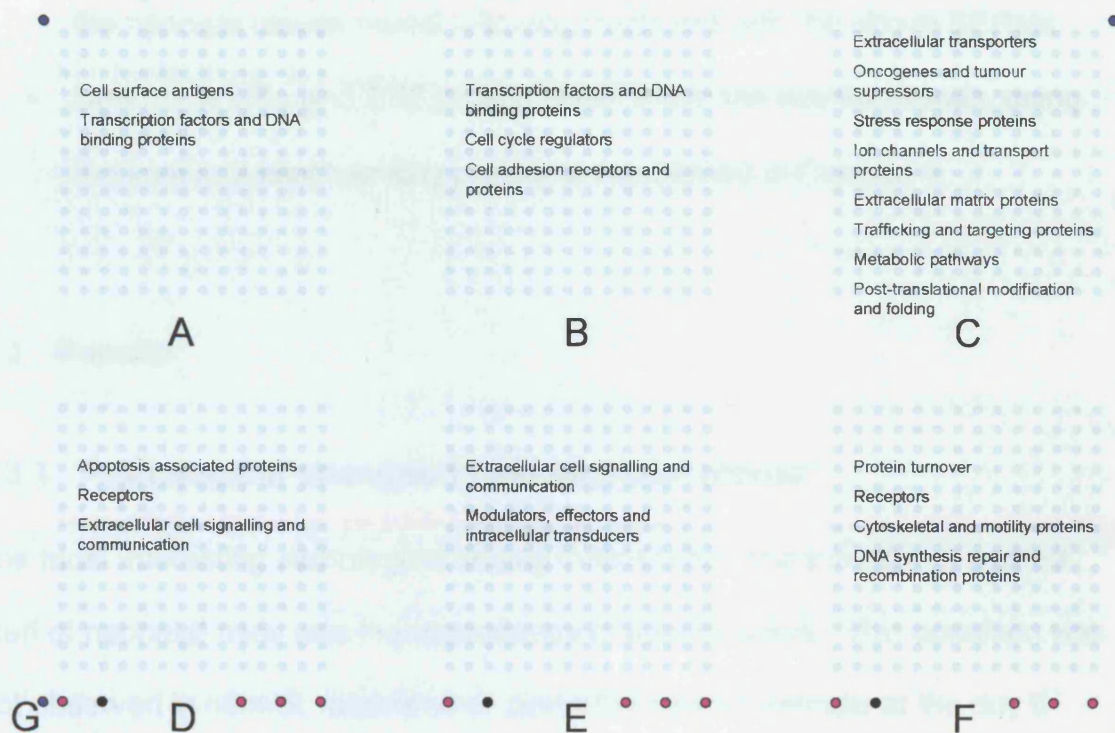


**Figure 5.1** Diagram to show location of genes on the array membrane. Also marked are the orientation points (blue), negative bacterial DNA (black) and positive mouse genomic DNA and house keeping genes (pink).

The established model for the CD-1 neonatal mouse was treated and examined with these aims:

- Assess pathological changes that occur in the uterus in response to tamoxifen, toremifene and raloxifene relative to oestradiol.
- Using cDNA microarray technology establish the gene changes involved in the early stages of lesion development within the reproductive tract of the neonate mouse model following treatment with the above SERMs.
- Determine ER $\alpha$  and ER $\beta$  protein levels within the uterine tissues, using the immunohistochemistry protocols established in Chapter 4.

## **5.3 Results**

### **5.3.1 Pathological changes in the neonatal uterus**

The most interesting pathological finding in tamoxifen and toremifene treated uteri of neonatal mice was the appearance of adenomyosis. This condition was not observed in control, raloxifene or oestradiol treated animals at the day 6 time point and may be central to a tamoxifen/toremifene specific action.

Because of time limitations, changes in gene expression that accompany the development of adenomyosis by three and 12 months have not been determined, although these time points would obviously provide valuable data.

Dr Peter Greaves of the MRC Toxicology Unit provided the detailed pathological assessments used in this study.

### **5.3.1.1 Adult animals**

At the 90 day time point, all 10 mice treated with tamoxifen and 9/10 treated with toremifene in the neonatal period showed adenomyosis. Only one of 10 animals treated with raloxifene and none of the three groups of 10 untreated controls showed adenomyosis. In affected animals adenomyosis was characterised histologically by the presence of simple endometrial glands, associated with variable but small amounts of endometrial stroma which infiltrated all layers of the myometrium, reaching but not penetrating the uterine peritoneal surface (Figure 5.2b and d). Another feature associated with affected animals was the disruption to the concentric and longitudinal smooth muscle bands. Instead of regular concentric layers of smooth muscle cells seen in control mice at 90 days (Figure 5.2a and c), there were interwoven, thickened bands of smooth muscle cells. Ovaries were similar in treated animals and controls. At the 42 day time-point adenomyosis was also observed in all mice treated with tamoxifen, three out of four treated with toremifene but none of controls or mice treated with raloxifene or oestradiol.

### **5.3.1.2 Neonatal animals**

At six days, in mice treated with raloxifene or oestradiol the uterus showed similar histological appearances to controls. The endometrial lumen was a simple slit lined by epithelial cells. A layer of cellular stromal tissue in which occasional mitoses were evident surrounded the lumen. A uniform layer of young concentric smooth muscle fibres also containing mitotic figures

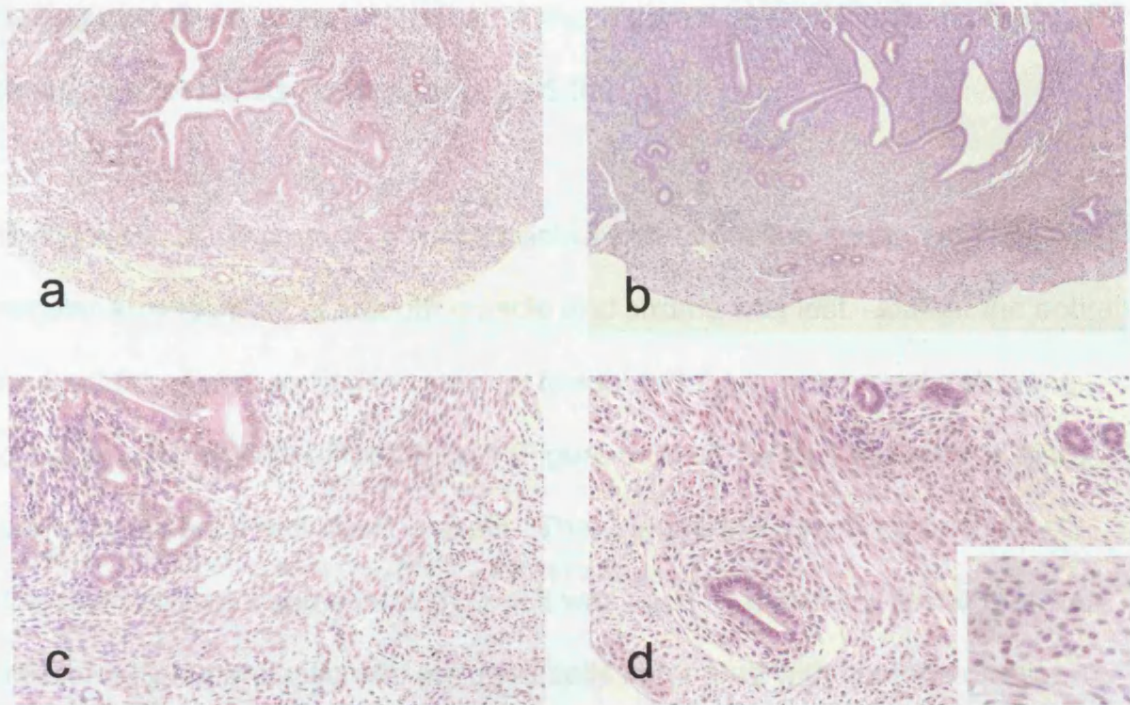


**Figure 5.2** Representative tissue section of the mouse uterus at 90 days. **a:** untreated control showing endometrial glands and stroma surrounded by well-defined layers of smooth muscle cells. H&E original magnification, x10. **b:** uterus from tamoxifen treated mouse showing adenomyosis with endometrial glands penetrating deeply into the myometrium which does not have the uniform bands of smooth muscle seen in the controls. H&E; original magnification x10. **c:** higher power of the section seen in **a**, showing well defined layers of smooth muscle surrounding the endometrium. H&E, original magnification x25. **d:** higher power of section on **b** showing glands penetrating the poorly defined myometrium. H&E, original magnification x25. Inset shows the polymorphonuclear cells within the myometrium, original magnification x40.

surrounded the endometrial tissue. A thin external layer of longitudinal smooth muscle cells was also present (Figure 5.3a).

By contrast, at six days, in all mice treated with tamoxifen and toremifene, this regular arrangement of smooth muscle and stroma was lost. Almost the entire body of the uterus comprised stromal tissue and there was no cells showing overt smooth muscle differentiation (Figure 5.3b-e). Within this stroma there were prominent small blood vessels. The endometrial lumen retained its slit-like character with some infolding but it was lined by glandular tissue that was moderately hyperplastic with enlarged cells compared with controls or mice given raloxifene or oestradiol.

### **5.3.2 Uterine weights**

Uterine weight and its increase in response to oestrogen treatment is a controversial measurement of oestrogenicity. To assess the oestrogenic effect of each of the SERMs on the neonate uterus, the weights of the tissues were compared to control at 6, 42 and 90 days. The results are a mean  $\pm$  SE of 8 representative uteri per treatment.

A comparison of effects on uterine weights of tamoxifen, toremifene and raloxifene at day 6 after dosing and at day 42 and day 90, relative to vehicle dosed controls, is shown in Table 5.1. At day 6, all treatments resulted in a significant increase in uterine weights relative to controls. In contrast, after 42

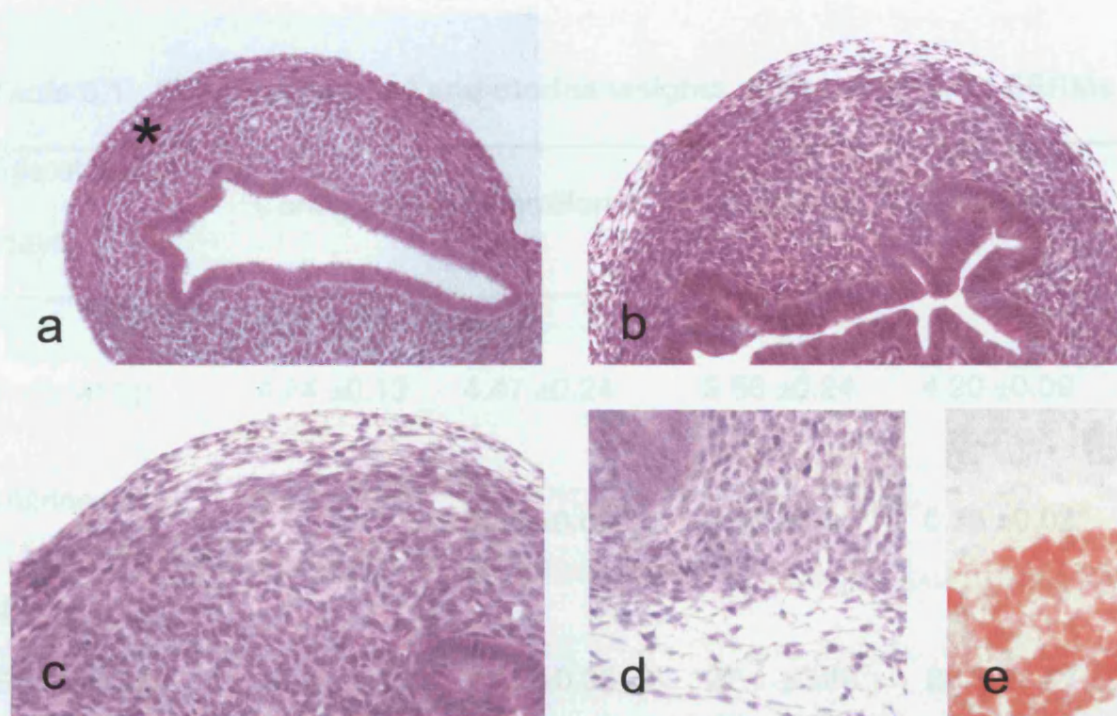


**Figure 5.3** Representative section of the mouse uterus at 6 days. **a:** untreated mouse uterus showing endometrial lumen, with well defined endometrial stroma and smooth muscle layers. H&E, original magnification x25. **b:** toremifene treated mouse showing slightly hyperplastic endometrial lumen surrounded by a completely disrupted endometrial stroma. H&E, original magnification x25. **c:** higher power of section **b** showing a layer of clear cells at the periphery of the uterus. H&E original magnification x40. **d:** shows vacuolated clear cells which Oil red O stains confirmed contained lipid (**e**). H&E, original magnification x40.

**Table 5.1 Effects on animal and uterine weights of treatment with SERMs**

Age of mouse (days)	Controls	Tamoxifen	Toremifene	Raloxifene
<b>6</b>				
Body wt (g)	4.24 ±0.13	4.47 ±0.24	3.56 ±0.24	4.20 ±0.09
Uterine wt <sup>a</sup>	0.24 ±0.03	<b>0.48 ±0.05*</b>	<b>0.45 ±0.04*</b>	<b>0.36 ±0.03*</b>
<b>42</b>				
Body wt (g)	28.4 ±0.80	27.5 ±0.38	27.1 ±0.48	28.3 ±2.47
Uterine wt <sup>a</sup>	0.63 ±0.06	<b>0.39 ±0.04*</b>	<b>0.43 ±0.05*</b>	0.69 ±0.11
<b>90</b>				
Body wt (g)	32.2 ±0.60	29.1 ±0.72	35.3 ±2.14	30.0 ±0.86
Uterine wt <sup>a</sup>	0.62 ±0.05	<b>0.38 ±0.05*</b>	0.50 ±0.03	<b>0.77 ±0.07*</b>

<sup>a</sup> Mean uterine weight expressed as percentage of body weight.

\*Statistically significant at the 5% level by ANOVA

days both tamoxifen and toremifene showed a significant decrease in weight compared to controls. After 90 days, only the uteri of the raloxifene treated animals showed an increase in weight, whereas tamoxifen treatment resulted in a significant decrease.

### **5.3.3 Localisation of ER protein**

To further assess the effects of the SERMs and oestrogen on the neonate uterus, the ER status of the cells was determined by immunohistochemistry (see Method 2.3.1). ER $\alpha$  and ER $\beta$  labelling of control neonatal uterine tissue was most dense in the cells of the endometrial stroma, with little or no staining in smooth muscle or endometrial glandular cells. In tamoxifen treated mice, labelling of the disordered stroma was similar to that of endometrial stroma in controls. Labelling of nuclei from the hyperplastic glandular tissue was also more prominent than in controls (Figure 5.4).

### **5.3.4 Protein staining of fat cells**

Another striking feature of the outer aspect of the altered myometrium was the presence of vacuolated cells. Oil red O staining showed that these cells were lipocytes (Figure 5.3).

### **5.3.5 RNA extraction data**

Total RNA was isolated from 4-6 neonatal mouse uteri per group of treatment: control, oestradiol, tamoxifen, toremifene or raloxifene as described in Method

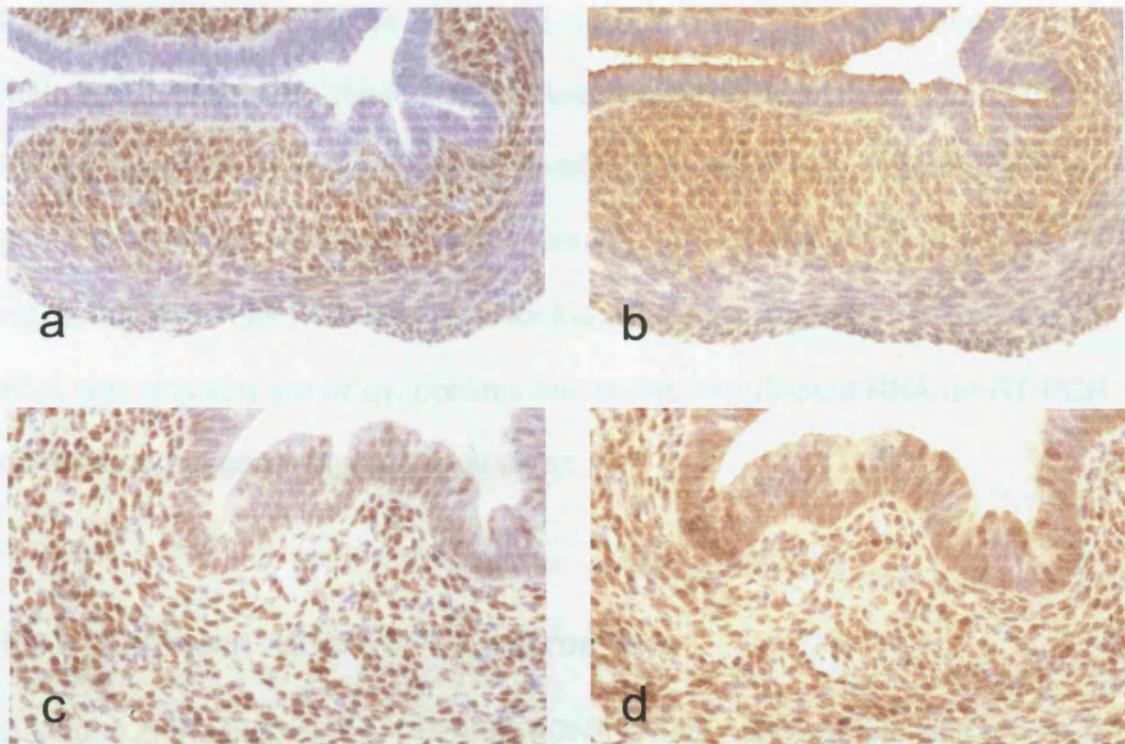


**Figure 5.4** Expression of ER $\alpha$  and ER $\beta$  in the uterus from control and treated mice, immunoperoxidase, hematoxylin counterstained. **a:** control ER $\alpha$ , original magnification x25. **b:** control ER $\beta$ , original magnification x25. **c:** tamoxifen treated ER $\alpha$ , original magnification x40. **d:** tamoxifen treated ER $\beta$ , original magnification x40.

2.5.1. The RNA was DNase treated as in Section 2.5.2 and quantified as per Method 2.2.12.1. Only those samples with a ratio of  $A_{260}/A_{280}$  of greater than 1.6 were processed further since the quality of the RNA was important in the generation of high sensitivity hybridisation probes. Absorbances are representative of all RNA isolations for the microarray analysis. As only 5 $\mu$ g of RNA was required per array, pooling uteri provided sufficient RNA for RT-PCR confirmation of gene expression analysis.

### **5.3.6 Clontech Atlas™ cDNA microarrays**

Because of the high cost of the Atlas cDNA arrays each sample was run on two membranes. Total RNA isolated from the uteri of pooled treated groups shown in Table 5.2 was converted into  $^{32}\text{P}$  labelled cDNA probes for hybridisation to the cDNA array (Method 2.5.3). The total radioactivity of each set of cDNA probes was calculated, as described in Method 2.5.4, to ensure an adequate level of radioactivity incorporation. For each 100 $\mu$ l fraction, 1 $\mu$ l was measured; therefore actual counts were 100 fold. Radioactivity in column fractions (Methods 2.5.5) is shown in Table 5.3. Fractions 3-5 were pooled and used to probe the Atlas arrays.

### **5.3.7 Microarray data and gene analysis**

Following hybridisation and post hybridisation washes (Section 2.5.6); the arrays were exposed in the dark to phosphor imager plates for 3-5 days.

**Table 5.2 Total RNA yield from pooled neonatal mouse uterine tissues following DNase treatment**

Sample	Absorbance	Absorbance	Ratio	Total RNA
	260nm	280nm	(A <sub>260/280</sub> )	µg
Control	1.036	0.546	1.90	165.6
Oestradiol	0.280	0.152	1.84	44.8
Tamoxifen	0.450	0.247	1.82	72.0
Toremifene	0.964	0.563	1.71	154.4
Raloxifene	1.195	0.741	1.61	191.2

**Table 5.3 Total radioactivity of <sup>32</sup>P labelled cDNA probes for microarray analysis**

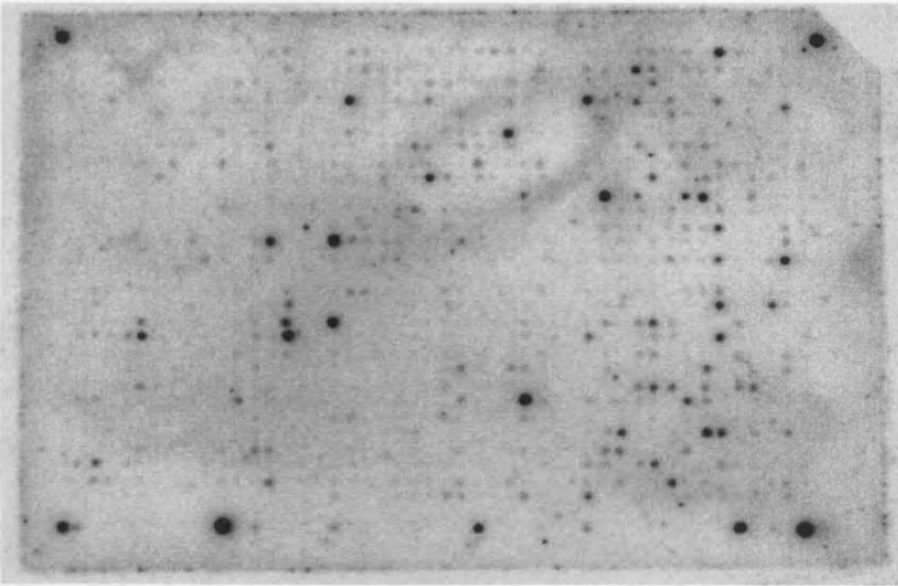
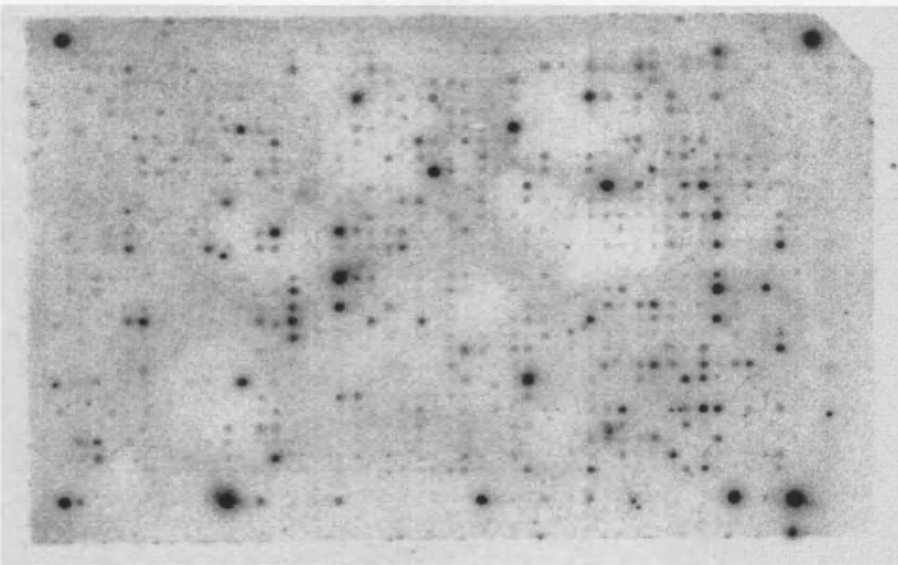
Fraction	cpm/µl				
	Control	Oestradiol	Tamoxifen	Toremifene	Raloxifene
1	2796	235	1182	9153	747
2	76447	55938	22193	183311	147041
3	30477	101724	68289	37606	41429
4	13007	42456	31646	12583	9940
5	18680	9649	7560	10480	5573
6	32638	7126	19697	10143	24274
Total	6.21 x10 <sup>6</sup>	1.53 x10 <sup>7</sup>	1.07 x10 <sup>7</sup>	6.07 x10 <sup>6</sup>	5.69 x10 <sup>6</sup>

radioactivity  
used (cpm)

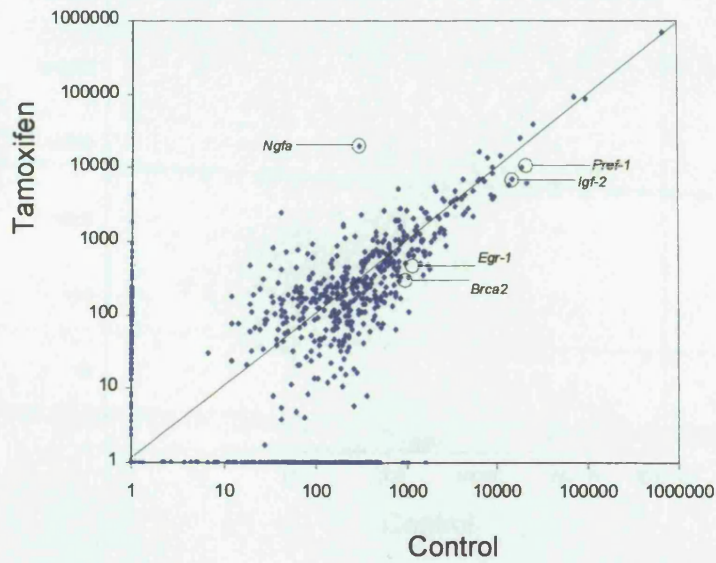
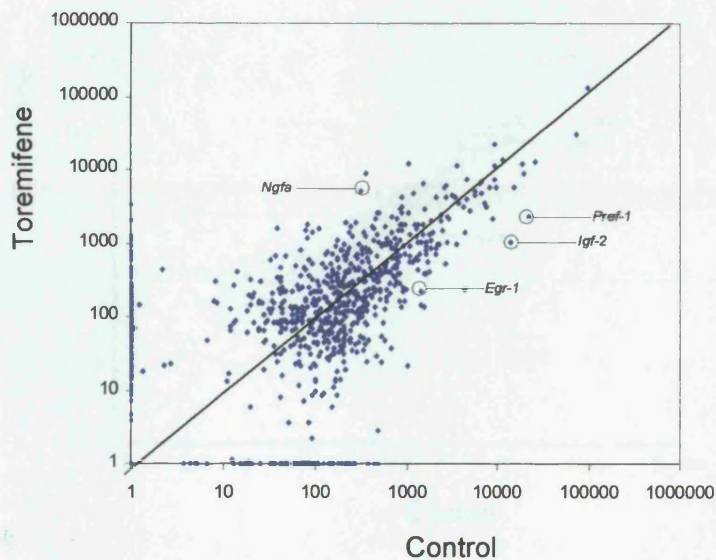
Phosphor imager plates were scanned on a Molecular Dynamic imager as described in Method 2.5.8. A representative scan of control and tamoxifen treated arrays is shown in Figure 5.5.

Densities of all within the grids of the array were combined, using Excel spreadsheets, with the gene list and array coordinates obtained from the Clontech website ([www.clontech.com](http://www.clontech.com)). Density values were normalised against background values taken from the array and against the sum of all densities. Normalised densities from treatment groups were plotted individually against control values in log-log scatter plots. Results of plotting control against control from separate analysis show a narrow spread of data except at the lower expression levels, suggesting a good inter-experimental reproducibility (Appendix 2). Because of the lower reproducibility of spot densities <1000, results of changes in gene expression when the density was less than this, and gene expression altered less than 2 fold against control, were not considered significant.

Results showed that when neonatal mice were treated with tamoxifen on days 2-5, there was marked up and down regulation in the expression of a number of genes (Figure 5.6). Changes in gene expression with tamoxifen and toremifene were broadly similar (Table 5.4). In contrast these results differed greatly from the effects observed with oestradiol (Figure 5.7).

**a****b**

**Figure 5.5** Representative scans of Mouse 1.2 Atlas cDNA microarray images probed with  $^{32}\text{P}$  labelled cDNA synthesised from neonate mouse uterine total RNA extracts, **a**: control and **b**: tamoxifen treated. Arrays were orientated according to orientation marks and grids were applied to incorporate cDNA spots and housekeeping genes

**a****b**

**Figure 5.6** Log-log scatter plot of normalised tamoxifen **a** or toremifene **b** treatment group gene array data plotted against control group data. Each point on the plot represents the expression level of one of the 1176 genes. Selected genes are labelled whose expression was changed by two fold and density values were greater than 1000.

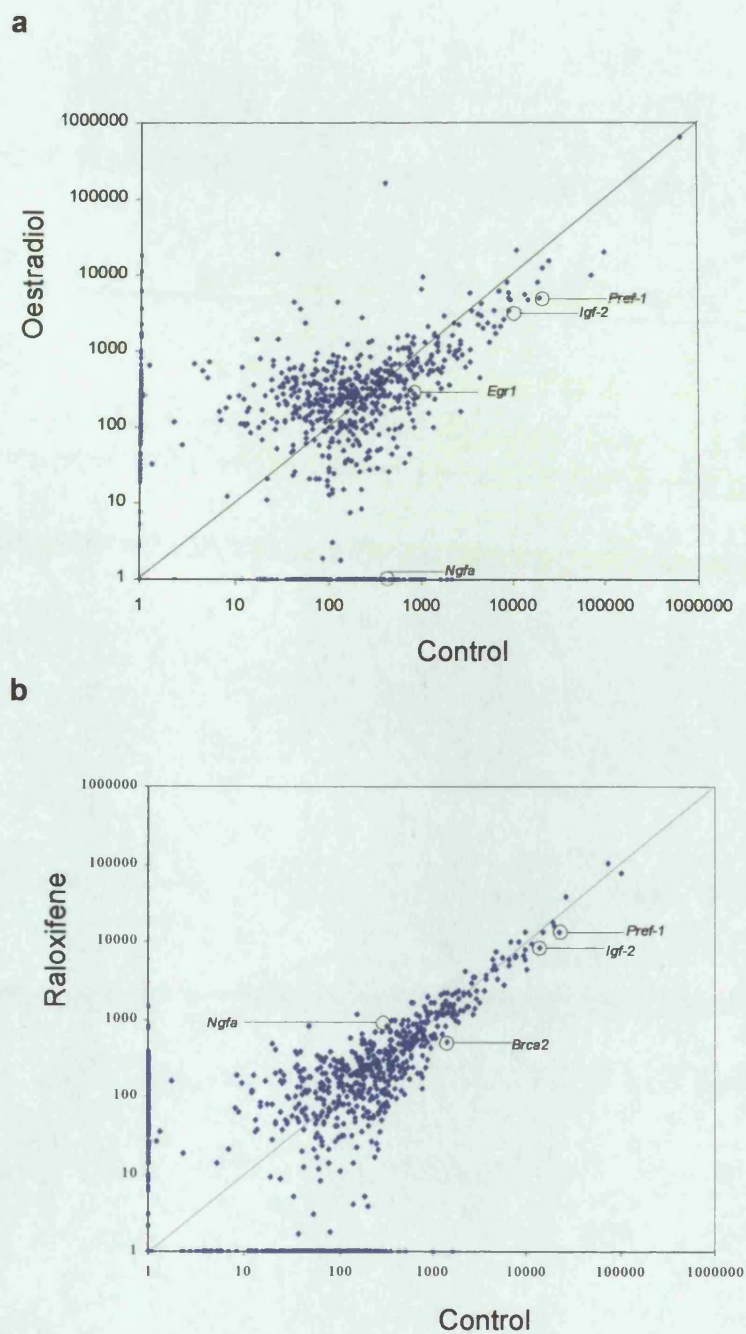


**Figure 5.7** Log-log scatter plot of normalised oestradiol **a** or raloxifene **b** treatment group gene array data plotted against control group data. Each point on the plot represents the expression level of one of the 1176 genes. Selected genes are labelled whose expression was changed by two fold and density values were greater than 1000.

**Table 5.4 Major changes in gene expression that occurred in common following either tamoxifen or toremifene treatment, compared with controls**

Gene name	Fold change tamoxifen	Fold change toremifene
7S nerve growth factor ( <i>ngfa</i> )	+64.7	+16.7
Cytoskeletal epidermal keratin (14 human)	+4.3	+6.8
Proenkephalin A precursor	+2.7	+2.0
CD14 monocyte differentiation precursor	+2.6	+2.8
Cytoplasmic dynein light chain 1	+2.4	+2.2
40S ribosomal protein SA	-2.1	-4.2
<i>Igf-2</i> precursor	-2.3	-12.9
Preadipocyte factor 1 ( <i>pref-1</i> )	-3.6	-9.5
Secreted apoptosis protein 1 ( <i>Sarp1</i> )	-4.3	-11.6
Integrin beta 7	-1015.6	-48.6

Raloxifene had a much weaker effect on altering uterine gene expression than other SERMs investigated (Figure 5.8). These results suggest a fundamental difference in the action of tamoxifen or toremifene and oestradiol in this neonatal uterine model.

A total of 22 genes were up regulated by tamoxifen treatment and 22 were down regulated. In contrast, 45 genes were up regulated by toremifene treatment and 31 were down regulated, see Appendix 1 for complete listings. Genes that showed a common up or down regulation by tamoxifen and toremifene are listed in Table 5.4.

The majority of gene up regulation with tamoxifen and toremifene treatment occurred within the transcription factors and DNA binding proteins, extracellular signalling and communication genes. The most marked up regulation following tamoxifen treatment, mirrored by the toremifene treated uteri, was the 7S nerve growth factor alpha (*ngfa*). The *ngfa* protein is involved in myogenic differentiation and will be discussed in detail later along with the *igf-2* precursor and preadipocyte factor 1 (*pref-1*).

Cytoplasmic dynein light chain or PIN was also upregulated by tamoxifen and toremifene treatment, the PIN protein is expressed in various skeletal muscle fibres in mouse, rat and human and its expression is regulated during skeletal muscle development (Guo *et al.*, 1999). The most marked down regulation was seen in integrin  $\beta 7$ . The beta subunit of integrins are important for regulation of stimulated cell adhesion and adhesion-dependant signal transduction, it has

been shown that gut mucosal TGF $\beta$ 1 increases expression of integrin  $\beta$ 7 (Lim *et al.*, 1998). It is interesting to note that *tgfb1* was up regulated by tamoxifen treatment by 2.1 fold and in contrast was down regulated by oestradiol treatment by over 6 fold. TGF $\beta$ 1 has previously been shown to be up regulated in the uterus of tamoxifen treated patients (Carmichael *et al.*, 2000).

Although it is difficult to make generalisations, the extremes of both up regulation 7S nerve growth factor and down regulation integrin  $\beta$ 7 was seen after tamoxifen treatment while toremifene gave less pronounced changes Table 5.4 and Figure 5.6.

Tamoxifen and toremifene have an oestrogen agonist effect on the mouse uterus from a pathological perspective, in respect to changes in the expression of many genes, oestradiol had quite a different action. A total of 19 genes were up regulated by oestradiol treatment and 47 were down regulated, see Table 5.5 and Figure 5.7a and Appendix 1. Many groups of genes were involved in up regulation by oestradiol although more so in the transcription factors and DNA binding proteins as with tamoxifen and toremifene. The pattern of gene groups down regulated included again, transcription factors and DNA binding proteins, oncogenes and tumour suppressors (i.e. *c-jun* proto-oncogene, *p53*) extracellular cell signalling and communication (i.e. insulin-like growth factors).

Treatment of neonate mice with raloxifene did not result in many large changes in gene expression (Figure 5.7B and Appendix 1). A total of only 5 genes, with an expression intensity of >1000 were up regulated >2 fold by raloxifene treatment and 7 were down regulated. These are shown in Table 5.6.

Regulation of the genes occurred within several groups. Values for *igf-2* and *pref-1* are included as they are of interest as discussed later. Growth factor 1A and paired mesoderm homeobox were up regulated as with tamoxifen and toremifene. Interestingly, *brca2* was down regulated with all treatments. It is important to note at this time, the significant change of uterine weight in the raloxifene treated animals (Table 5.1), confirming that raloxifene produced an effect at the cellular level.

Density values for any of the treatments were not greater than 1000 for the *er $\alpha$*  gene so the data has not been included with the significant findings described above, *er $\beta$*  is not included on the array. However, although *er $\alpha$*  data cannot be taken as significant, it is interesting to note that treatment with oestradiol increased *er $\alpha$*  mRNA expression by 4 fold whereas the three SERMs did not alter *er $\alpha$*  expression by more than 2 fold. Staining for ER $\alpha$  and ER $\beta$  protein was generally more intense after treatment with tamoxifen (Figure 5.4), suggesting gene expression changes do not necessarily accurately reflect those of protein expression.

### 5.3.8 PCR verification of altered gene expression

Three genes were selected that were considered to be of relevance to the pathological changes seen in the newborn mice following treatment with the SERMs. These were *igf-2*, *pref-1* and *ngfa*, the RT-PCR primers are shown in Table 2.7. The results of the cDNA microarray analysis were compared with results from semi-quantitative RT-PCR using cDNA synthesised from the total

**Table 5.5 Gene changes found only following oestradiol treatment when compared with control**

Gene name	Fold change
Meiotic recombination protein DMC1/LIM15 homolog	+17493.2
TNF-related inducing ligand ( <i>trail</i> )	+1717.9
Cyclin T1	+1629.2
E2F-5 transcription factor	+10981.0
5-hydroxytryptamine 1A receptor; serotonin receptor	+656.1
RalGDSB;GTP/GDP dissociation stimulator for ras-related GTPase	+377.7
Nicotinic acetylcholine receptor	+87.6
Leptin precursor ( <i>lep</i> ); obese factor	+49.4
Interleukin-1 receptor type II precursor	+35.3
Tight junction protein ZO1	+8.8
CD 30L receptor;lymphocyte activating agent	+7.5
Homeobox protein 3.1 ( <i>Hox-3.1</i> )	+4.7
Proliferation associated protein 1 ( <i>plfap</i> )	+2.4
Matrix metalloproteinase 14 precursor ( <i>mmp14</i> )	+2.2
Preadipocyte factor 1 ( <i>pref-1</i> )	-1.8
Adenylate cyclase 6	-2.1
14-3-3 protein eta; protein kinase C inhibitor protein 1 ( <i>kcip1</i> )	-2.2
Granulocyte-macrophage colony-stimulating factor receptor low affinity subunit precursor	-2.3
Apolipoprotein E precursor ( <i>apo-E</i> )	-2.4
Ski proto-oncogene	-2.4
Recombination activating protein	-2.3
<i>Igf-2</i> precursor	-2.5
Frizzled homolog 6 ( <i>fzd6</i> )	-2.5
Rac alpha serine-theonine kinase ( <i>rac-pk-alpha</i> )	-2.6

---

Eyes absent homolog 2 ( <i>eya2</i> )	-2.7
Nucleoside diphosphate kinase B ( <i>ndp kinase B</i> )	-2.8
YB1 DNA binding protein	-3.1
Calpactin I light chain	-3.1
Basigin precursor (basic immunoglobulin family)	-3.2
Insulin-like growth factor binding protein2 precursor ( <i>igfbp2</i> )	-3.3
Retinoid X receptor alpha ( <i>rxr-alpha</i> )	-3.3
Related to drosophila groucho gene	-3.9
Tyrosine-protein kinase ryk precursor; kinase vik	-4.1
Glutathione S-transferase Pi 1 ( <i>gstp1b</i> )	-5.1
Early growth response protein 1	-6.0
Split hand/foot gene	-8.0
7S nerve growth factor ( <i>ngfa</i> )	-307.8
<i>Ear-2</i> ; <i>v-erbA</i> related proto-oncogene	-1085.6
Cyclin D2 (G1/S-specific)	-1873.6

---

**Table 5.6 Gene changes occurring only following raloxifene treatment when compared with control**

Gene	Fold change
Huntingtin-associated protein-1	+1492.0
Paired mesoderm homeobox protein2	+2.9
58-kDa inhibitor of RNA-activated protein kinase	+2.8
7S nerve growth factor ( <i>ngfa</i> )	+2.6
Insulin-like growth factor-1A	+2.3
<i>Igf-2</i> precursor	-1.6
Preadipocyte factor 1 ( <i>pref-1</i> )	-1.7
Glutathione S-transferase Pi 1	-2.0
Non-muscle cofilin 1	-2.0
Thyroid hormone receptor alpha 1	-2.0
Butyrate response factor 1	-2.2
Integrin-linked kinase	-2.3
Breast cancer type 2 suseptibility protein ( <i>brca2</i> )	-2.7
Survival of motor neuron	-1600.6

RNA samples used with the microarray. Products were identified by DNA sequencing and corresponded to expected gene sequences (Appendix 3). Changes in expression of *ngfa*, *pref-1* and *igf-2* were comparable to those observed in the cDNA microarray analysis although quantitatively, RT-PCR results were of a different magnitude to those produced by the array (Table 5.7).

#### **5.4 Discussion**

Pathological changes within the reproductive tissues have been assessed to determine the morphological effects of SERMs on the developing uterus, and oestrogenic effects have been related to changes in uterine weight. In addition, other genes that may be important in the regulation of development and mediation of tamoxifen, toremifene and raloxifene on the target tissues have been determined by comparing gene expression patterns between control and treated tissue using the cDNA microarray. As discussed in Chapter 1, it is assumed that the main pathway for the compounds oestrogenic effects on responsive tissues occurs via the ER $\alpha$  and ER $\beta$ , so subsequent changes in the expression of these proteins within the tissue between control and tamoxifen treated animals have been investigated.

The data from this study clearly shows that short-term treatment of neonatal mice with the SERMs tamoxifen and toremifene, but not raloxifene, leads to adenomyosis in a high proportion of animals by three months of age.

**Table 5.7 Differential expression of *ngfa*, *pref-1* and *igf-2* as identified by cDNA microarray and semi-quantitative RT-PCR.**

Gene	Fold Change				Putative function
	Tamoxifen	Toremifene	Raloxifene	Oestradiol	
<i>Igf-2</i> precursor	-2.3 (-1.1)	-13 (ND)	-1.6 (-1.2)	-2.5 (-1.2)	Insulin-like growth factors stimulate mitogenic activity in human endometrial stromal. <i>IGF-2</i> is involved in the growth of uterine smooth muscle tumours. IGF mediate and modulate steroid hormone actions in the endometrium. IGF-2 is an embryonic growth promoter and cell survival factor.
<i>Pref-1</i>	-3.6 (-1.3)	-9.5 (ND)	-1.7 (-1.4)	-1.8 (-1.4)	<i>Pref-1</i> inhibits the differentiation of preadipocytes into adipocytes and is down regulated during their differentiation.
<i>Ngfa</i>	+65 (+4.3)	+16.7 (ND)	+2.6 (+1.1)	-307 (-7.4)	The receptor p75 <sup>NTR</sup> is highly expressed in the smooth muscle cells of the mouse uterus. Further studies in a mouse muscle derived cell line (C2C12) demonstrate down regulation of nerve growth factor and p75 <sup>NTR</sup> during myogenic differentiation.

\*Fold induction (positive numbers) and reduction (negative numbers) compared with expression in controls. Values in parentheses represent fold change determined by RT-PCR. ND, not determined.

Although several strains of mice develop adenomyosis spontaneously in adulthood, adenomyosis is uncommon in this strain at three months of age usually making its appearance after 6 months of age. Why tamoxifen and toremifene but not raloxifene should have this effect remains unclear, although different SERMs are known to possess diverse effects in various tissues and organs.

The histological features of the adenomyosis produced using this four-day treatment regimen of SERMs showed the histological features previously described in both animal models and in humans (Ferenczy, 1998; Ota *et al.*, 1998; Zhou *et al.*, 1999). Endometrial glands and stroma were present deep within the myometrium. In controls smooth muscle fibres were arranged in uniform layers around the endometrium, in contrast in tamoxifen and toremifene treated mice, this zone comprised irregular smooth muscle bundles interspersed with collagen and often by prominent blood vessels. The smooth muscle changes were more extensive than the appearance of abnormal glands. This suggests that the penetration of endometrial glands might follow the changes to myometrium. These areas of altered smooth muscle organisation were associated with a scattering of polymorphonuclear leukocytes, notably eosinophils. The presence of eosinophils has been reported in both human endometriosis and carcinoma where it has been suggested that they are involved in general tissue remodelling (Blumenthal *et al.*, 2000).

The histological alterations and key genetic changes, which occurred in the neonatal uterus immediately after treatment with tamoxifen and toremifene,

provide additional support for the concept that the basis for the development of adenomyosis is due to the primary derangement of the uterine myometrial tissue differentiation. At 6 days the uterine body in mice treated with tamoxifen and toremifene, but not raloxifene or oestradiol, had none of the normal layers of developing smooth muscle but retained histological appearances and ER status of endometrial stroma. In addition, some unusual patterns of differentiation were observed, particularly the presence of lipocytes in the outer regions of the uterus.

In contrast to the major changes in myometrial differentiation, only modest alterations to histological and ER status in endometrial glandular tissue, were produced. The endometrium continued to show regular cyclical alterations in treated groups similar to those in controls. These data suggest that the functional status of the endometrial glandular tissue is not greatly altered in adenomyosis. In the present study, no cystic ovaries were observed and corpora lutea were seen in all of the treatment groups. This is in contrast to previous findings at 14 -17 months after dosing where corpora lutea were absent when tamoxifen was given subcutaneously on days 1-5 to new born CD-1 mice (Newbold *et al.*, 1997).

The conventional view is that adenomyosis represents down-growth of endometrial glands and stroma into the myometrium with secondary local tissue response (Ferenczy, 1998), however recent evidence underlines the importance of mesenchymal tissue in the development of adenomyosis. Based on histopathological and immunocytochemical analysis of the human uterus, it

has been suggested, that the abnormal smooth muscle in adenomyosis results from a similar metaplastic process to that for endometriosis where smooth muscle has been found associated with endometrium in extrauterine locations. It has been suggested that aberrant endometrial stroma may be produced by metaplasia from primitive pericytes. It is suggested that this is capable of inducing the formation of endometrial glands through local autocrine or paracrine mechanisms controlled by genetic, hormonal and immunological factors (Mai *et al.*, 1997; Anaf *et al.*, 2000). It is also possible that excessive myocyte proliferation may be the cause of adenomyosis rather than its consequence based on T2-weighted magnetic resonance imaging and vaginal sonography in women with adenomyosis. These techniques show more extensive derangement of the myometrium compared with the patchy and focal nature of adenomyosis (Brosens *et al.*, 1998; Kunz *et al.*, 2000).

The pathological changes in mice were mirrored by alterations seen at six days in genes that are believed to be important in the developmental regulation of mesenchymal cells. The up regulation of *ngfa* by tamoxifen and toremifene (Figure 5.6, Table 5.4) is in marked contrast to its down regulation by oestradiol treatment. Nerve growth factor and its low affinity receptor p75<sup>NTR</sup> are believed to have not only a role in synchronising the developing visceral nervous system but also on myogenic differentiation. The receptor p75<sup>NTR</sup> is highly expressed in the smooth muscle cells of the mouse uterus (Seidl *et al.*, 1998). Further studies in a mouse muscle derived cell line (C2C12) demonstrate down regulation of nerve growth factor and p75<sup>NTR</sup> during myogenic differentiation (Lommatzsch *et al.*, 1999). These studies suggest that the up regulation of

*ngfa* observed in the tamoxifen and toremifene treated uteri may contribute to the repression of myometrial differentiation in these tissues. Nerve growth factor has also been shown to act as a growth factor for MCF-7 cells in a manner similar to EGF (Chiarenza *et al.*, 2001) but unlike EGF, the action was inhibited by tamoxifen. The precise action of *ngfa* on uterine cells remains to be established but results suggests it could play a key role in the development of this organ. Further investigation into NGF receptor expression may provide insight into possible action of this factor in the uterus.

*Pref-1* gene product is abundant in preadipocytes and is down regulated during adipocyte differentiation; it is also known that the expression of *Pref-1* inhibits differentiation of mouse 3T3-L1 preadipocytes (Garces *et al.*, 1999). The microarray data presented here demonstrate the down regulation of *Pref-1* in tamoxifen and toremifene treated neonate uteri. This suggests that the down regulation of *Pref-1* contributes to the appearance of adipocytes observed in the abnormally differentiated neonate tissue.

The paternally imprinted *igf-2* precursor gene is repressed by all the SERMs tested, although the effect was most marked with tamoxifen treatment. In contrast, the maternally imprinted gene for the mannose 6-phosphate/insulin-like growth factor-2 receptor showed little treatment related change in expression. Insulin-like growth factors are believed to mediate and modulate steroid hormone actions in the endometrium (Rutanen *et al.*, 1997); *IGF-2* gene expression is also involved in endometrial differentiation (Rutanen *et al.*, 1998). A previous study of patients with endometriosis showed a reduced level of

staining for IGF-2 protein in the eutopic endometria of affected women (Sbracia *et al.*, 1997). Elevated expression of *IGF-2* is often found in tumours, and loss of imprinting is one mechanism by which its expression is deregulated (De Souza *et al.*, 1997). However, the observed reduction in *igf-2* expression may contribute to the altered growth and differentiation of the uterus.

Early growth response protein 1 (*egr-1*) is an inducible transcription factor that has been identified in the array data to be strongly down regulated by tamoxifen, toremifene and oestradiol (-2.9, -6.5, and -6.0 fold respectively). Coactivators can directly interact with *egr-1* and mechanisms dependant on both coactivators and corepressors alters gene transcription. This factor is an example of an immediate early response protein that is rapidly and transiently induced by a large number of growth factor and cytokines (Gashler *et al.*, 1995). The fact that these compounds down regulate the *egr-1* suggests a possible role for this key gene in early response in the treated neonate uterus. Further investigations into the role of this gene are necessary.

Using cDNA microarray technology, changes in gene expression could only be examined taking RNA from the whole uterus. Clearly, the response of the different endometrial, stromal and myometrial components will differ and a small amount of change identified by these methods could refer to a change of a different magnitude when identified in an individual cell types. Techniques such as laser capture microdissection and immunohistochemistry will be needed to examine cell specific responses to these drugs.

In summary, these experimental data from this study support the hypothesis that adenomyosis represents a condition of the uterine body in which the stromal cells have a primary pathogenetic role although some contribution of accelerated epithelial downgrowth cannot be entirely excluded. Disruption of the mesenchymal layers surrounding the endometrium in the neonatal period can give rise to disordered development of uterine stroma, smooth muscle, blood vessels and possibly its innervation. This alteration to the normal functional fibromuscular anatomy of the uterine body provides the framework for the abnormal and aberrant growth of endometrial tissue. Most importantly, these data suggest that discrete hormonal derangements, that produce defects in the formation of the myometrium early in neonatal life in humans, may explain the predisposition to adenomyosis in adulthood.

## **Chapter 6: General discussion**

## 6.1 General discussion

Tamoxifen is known to cause an increase in endometrial tumours in women undergoing long-term treatment (Fisher *et al.*, 1994; Rutqvist *et al.*, 1995). The oestrogenic effects that tamoxifen has on the uterus are thought to be mediated via an epigenetic mechanism, as data from DNA adduct studies provide no strong evidence for genetic damage caused by tamoxifen or its metabolites in the human uterus (Carmichael *et al.*, 1998). The discovery of a second ER subtype, ER $\beta$  (Kuiper *et al.*, 1996) has led to many new questions arising with regard to role ER $\alpha$  and ER $\beta$  play in the mediation of oestrogen agonist and antagonist effects on the uterus. The aim of this thesis was to investigate the mechanisms by which tamoxifen causes an increase in endometrial tumours and to determine if cell proliferation mediated via the ER $\alpha$  or ER $\beta$  is a key factor. Human cell line and rodent models have been used in this investigation of the role ER subtypes play in mediation of oestrogen, tamoxifen and related SERMs.

### 6.1.1 *In vitro* cell line model for ER degradation

The level of ER $\alpha$  and ER $\beta$  in the cells of the tissue is important in the response of the tissue to oestrogenic or anti-oestrogenic compounds. The human MCF-7 breast adenocarcinoma and Ishikawa endometrial carcinoma cell lines have been studied for their expression levels of ER $\alpha$  and ER $\beta$  in response to oestradiol, tamoxifen and related SERMs. These cell lines have been utilised in previous studies to assess the oestrogenicity of compounds (Nuttall *et al.*,

2001), by analysis of a cell proliferation response. The results described in the present study show a typical increase and decrease by oestradiol and faslodex respectively, although tamoxifen did not cause an increase in cell proliferation in the Ishikawa cell line as might have been expected. Previous studies have shown that the ER may be subject to the proteasome mediated degradation pathway (Nawaz *et al.*, 1999; Wormke *et al.*, 2000), this phenomenon has been confirmed in the present study and it has also been shown that both ER $\alpha$  and ER $\beta$  are degraded in a ligand dependant manner and cell type specific manner. The fact that oestradiol binding leads to proteasome mediated degradation of ER $\alpha$  and ER $\beta$  and tamoxifen does not, suggests that alternate ER conformations produced by binding of the ligand will alter levels of receptor proteins in the cell and ultimately the downstream effects of the ER. These are human cell lines and therefore may be of greater significance than rat or mouse cell lines. However, the response of individual cell types of the uterus to these compounds may involve paracrine and cell-cell interactions between different cell types within the uterus. Although *in vitro* studies can provide a mass of information about one individual cell type against another there is a limit to how much information can be gained.

### **6.1.2 Use of animal models for studying human endometrial cancers**

There is some question as to the use of animal models to study the development of human uterine cancers that develop after tamoxifen treatment. The current theory is that in women tamoxifen acts as an oestrogen agonist in

the uterus, leading to hyperplasia of the endometrium and thus promotes endogenous initiated cells to neoplasias. This is reinforced by studies that have demonstrated thickening of the endometrium by ultrasonography during tamoxifen treatment, prior to the development of polyps and adenocarcinomas of the endometrium (Paganini-Hill *et al.*, 1989, Silva *et al.*, 1994). Adult rats (Greaves *et al.*, 1993) or mice (Martin *et al.*, 1997) given tamoxifen do not show such endometrial lesions. In the case of rats this may be because of their susceptibility to hepatocarcinogenesis while in mice tamoxifen undergoes rapid detoxication in the liver and animals do not even get liver cancers following long-term exposure (Martin *et al.*, 1997). A few animal models have been described to mimic the development of endometrial tumours. This occurs in adult rats given a single intravaginal administration of *N*-ethyl- *N'*-nitro-*N*-nitrosoguanidine (AndoLu *et al.*, 1994) while in mice, pten +/- knockout animals exhibit neoplasms in multiple organs including the endometrium (Podsypanina *et al.*, 1999). However, neither of these latter models is particularly amenable to the study of the effects of SERMs. The subcutaneous administration of diethylstilbestrol on days 1 to 5 after birth to CD-1 mouse model by Newbold *et al.*, (1990) and subsequent development of the uterine adenocarcinomas offered an attractive animal system to study the effects of tamoxifen. In the neonate mouse model both tamoxifen and the phytoestrogen genestein have similar effects (Newbold *et al.*, 1997; 2001). It has also been demonstrated that tamoxifen given orally to Wistar rats on days 2 to 5 after birth caused similar uterine lesions 24 to 36 months later (Carthew *et al.*, 2000).

The oestrogenic response of the widely used outbred CD-1 mouse line, which has been selected for large litter size, may make it not a particularly sensitive model for the study of the effects of oestrogen agonists. It has been reported that more than a 16-fold difference in susceptibility to disruption of juvenile male reproductive development by oestradiol was detected between strains of mice and that CD-1 were more variable and less sensitive than the inbred C57 BL6/J strain (Spearow *et al.*, 1999). Because of all of the historical evidence for the susceptibility of CD-1 animals to SERMs, it was decided that for this study, this strain of mice would be used. However, as an initial model, uterine tissues from the adult ovariectomised rat were employed to develop the technologies required for the localisation of ER $\alpha$  and ER $\beta$  mRNA and protein expression.

### **6.1.3 Adult ovariectomised rodent models**

The discovery of ER $\beta$  (Kuiper *et al.*, 1996) meant that the localisation and response of ER $\alpha$  and ER $\beta$  within the uterus had not been described and could be a key factor in the response of the uterus to tamoxifen. A major part of the work involved in this thesis was the development of the *in situ* hybridisation technique for the localisation of ER $\alpha$  and ER $\beta$  mRNA in the uterus whilst no commercial antibodies were available for specific detection of the two proteins. Although this technique required much optimisation it will be useful for future studies where localisation of novel mRNA is required, for example those identified by the microarray.

Key findings from this study demonstrate that ER $\alpha$  and ER $\beta$  protein are involved in the response of the uterus to oestrogen and tamoxifen, as a general increase in both mRNA and protein occurred for both subtypes in tissues following treatment. However, the present results do not show any clear relationship between ER $\alpha$  and ER $\beta$  expression and the ability of sub-populations of target cells in the uterus to respond to stimulation by oestradiol or tamoxifen. The presence of ER $\alpha$  is clearly essential for this to occur since in the ERKO mouse lacking this receptor there is no increase in uterine weight in response to tamoxifen treatment (Korach *et al.*, 1994). Previous studies have shown the increase in uterine weight as a response to tamoxifen is due to both an increase in hypertrophy and cell proliferation (Carthew *et al.*, 1999a). Thus implicating ER $\alpha$  in this proliferative response to tamoxifen. Although it seems as though the ER $\alpha$  and ER $\beta$  do have a role in the mediation of the response of the uterus to tamoxifen, it is clear that other factors must be involved in either the downstream effects of these proteins or by a different pathway.

#### **6.1.4 The neonatal mouse model**

A major development in the technology available during the course of this thesis was of the cDNA Microarray. This technique allows the analysis of hundreds of genes in one experiment, providing a method for identifying candidate genes that may be regulated in response to treatment. The Clontech cDNA Microarrays were employed to identify genes that may be involved in the response of the uterus to oestradiol in comparison with the SERMs.

The treatment of the neonate mouse with tamoxifen and toremifene orally on days 2-5 after birth gave rise to adenomyosis by 3 months of age, this was not seen in oestradiol, raloxifene treated or control animals. This condition has been reported in women undergoing treatment with tamoxifen (Cohen *et al.*, 1997b). This condition has not been previously reported in the neonate mouse model following treatment with tamoxifen, and clearly showed that by this dosing regime tamoxifen and torimifene were having a similar effect on the uterus. Assessment of the gene changes occurring at 6 days, also confirmed that these two compounds were having a remarkably similar effect. Three genes, which may have a role in the development of adenomyosis particularly the disarrangement of the compartments of the uterus; *pref-1*, *igf-2* and *ngfa*, have been identified and their expression changes confirmed by RT-PCR. Whether or not these genes do play a key role in the development of this condition will be determined as future work involving laser capture micro-dissection and protein analysis.

### **6.1.5 Conclusions**

It is clear from the results of this thesis that the ER $\alpha$  and ER $\beta$  do play a major role in the response of the uterus to oestradiol, tamoxifen and related SERMs, although there are potentially many other factors involved. Whether or not the two subtypes have different roles in the mediation of the effects of the compounds have on the uterus remains to be determined, however, the fact that both ER appear to be expressed in the same cell types of the rodent uterus suggests that they have individual roles. The increase in expression of both

ER $\alpha$  and ER $\beta$  in combination with an increase in uterine weight suggests that the ER do have a role in the increase of cell proliferation in this model. The lack of tumours produced by the adult rodent studies makes it difficult to conclude whether changes seen in ER expression in these models would be involved in tumour formation, it can be concluded from this study that oestradiol and tamoxifen have a markedly similar effect at the level of ER expression.

The use of the neonate model enabled an assessment of gene changes occurring during the early stages of adenomyosis development, a condition found in women treated with tamoxifen. Candidate genes identified in the tamoxifen and toremifene treated animals will be analysed as future work and in the longer term comparisons could be made with the development of human endometrial cancers.

## Appendix 1

Clontech gene array data for all treatments: mean of two sets of spot densities

(arbitrary units) (Chapter 5)

Gene Name	control	E2	tam	Tor	ral
BRAIN SPECIFIC POLYPEPTIDE PEP-19 (BRAIN SPECIFIC ANTIGEN PCP-4).	1.0	345.8	1.0	67.1	198.6
myelin-oligodendrocyte glycoprotein precursor (MOG)	201.6	1.0	1.0	31.8	1.0
PERIPHERAL MYELIN PROTEIN 22 (PMP-22) (CD25 PROTEIN) (SR13 MYELIN PROTEIN).	83.8	287.0	1.0	88.8	1.0
gap junction alpha 1 protein (GJA1); connexin 43 (CXN43; CX43); gap junction 43-kDa heart protein	134.9	378.7	1.0	166.6	133.9
gap junction beta 1 protein (GJB1); connexin 32 (CXN32; CX32)	156.8	243.5	1.0	36.5	1.0
gap junction beta 2 protein (GJB2); connexin 26 (CXN26; CX26)	59.6	292.2	460.2	488.4	1.0
gap junction beta 4 protein (GJB4); connexin 31.1 (CXN31.1; CX31.1)	179.6	604.7	113.0	135.5	91.9
gap junction alpha 8 protein (GJA8); connexin 50 (CX50); lens fiber protein MP70	36.4	403.9	46.8	30.5	51.2
gap junction alpha 3 protein (GJA3); connexin 46 (CX46)	1.0	1.0	43.7	3.7	59.2
gap junction alpha 4 protein (GJA4); connexin 37 (CXN37; CX37)	57.5	135.9	215.7	135.4	32.8
gap junction alpha 5 protein (GJA5); connexin 40 (CXN40; CX40)	114.5	266.6	277.7	75.7	1.0
gap junction beta 3 protein (GJB3); connexin 31 (CXN31; CX31)	1.0	152.4	126.1	70.6	1.0
gap junction alpha 6 protein (GJA6); connexin 45 (CXN45; CX45)	1.0	19.7	1.0	83.4	81.3
osteoblast-specific factor 2 precursor (OSF2)	232.3	199.2	125.9	1362.2	1.0
m-numb (m-NB)	120.6	649.2	191.4	182.8	260.2
numbl-like (numbl; m-nbl)	120.3	705.9	118.8	9.2	145.1
rhodopsin (RHO); opsin (mOPS)	40.1	438.8	1.0	83.8	105.3
CD2 antigen	123.2	208.4	1.0	1.0	77.6
CD3 antigen delta polypeptide	1.0	1.0	1.0	1.0	1.0
CD7 antigen	32.4	380.0	1.0	1.0	1.0
CTLA-4 (immunoglobulin superfamily member)	1.0	193.2	1.0	14.9	87.3
glutamate receptor channel subunit gamma	44.7	357.2	113.8	88.9	48.5
CD 4 receptor (T cell activation antigen)	1.0	164.9	1.0	1.0	3.0
chondroitin sulfate proteoglycan 3	1.0	1.0	1.0	1.0	1.0
thymus cell antigen 1, theta	28.8	199.1	84.3	84.1	1.0
TRANSCRIPTION INITIATION FACTOR TFIID 70 KD SUBUNIT (TAFII-70) (TAFII-80) (TAFII80) (P80).	1.0	240.0	33.0	37.8	1.0
transcription factor NFAT 1 isoform alpha	1.0	190.3	1.0	81.3	1.0
transcription initiation factor TF II D; TATA-box factor; TATA sequence-binding protein (TBP)	41.2	48.9	1.0	1.0	114.4
tristetraproline (TTP); tissue plasminogen activator-induced sequence 11 (TPA-induced sequence 11; TIS11); growth factor-inducible nuclear protein 475 (NUP475); ZFP36	422.6	665.9	84.9	239.1	208.2
ENDOTHELIAL TRANSCRIPTION FACTOR GATA-2	367.4	569.4	1.0	118.8	260.5
paired box protein 4 (PAX4)	72.0	231.0	1.0	115.0	1.0
transcription factor 21 (TCF21); basic helix-loop-helix factor COR1; POD1	519.7	245.6	178.8	916.4	497.8
(ALX4) HOMEODOMAIN TRANSCRIPTION FACTOR	150.7	798.5	578.1	72.7	190.9
retinal homeobox protein (RX); retina & anterior neural fold homeobox protein (RAX)	138.8	530.4	1.0	26.6	4.1
myelin transcription factor 1 (MYT1)	1.0	1.0	1.0	19.6	56.8
pituitary homeobox 3 protein (PITX3)	149.3	35.0	251.7	146.9	1190.8
friend of GATA 1 (FOG); ZFPM1	128.7	824.2	232.3	182.3	1.0
EOMESODERMIN - T-BOX GENE	1.0	258.8	28.4	1.0	1.0
T-box protein 15 (TBX15); TBX14; TBX8	1.0	1.0	1.0	5.5	1.0
T-box protein 13 (TBX13); MMTBX7	1.0	367.0	1.0	1.0	1.0
pre-B-cell leukemia transcription factor 2 (PBX2)	360.6	51.5	329.4	141.6	227.3
Drosophila NK2 transcription factor-related locus 6 (NKX-2.6)	1.0	445.0	343.8	1.0	1.0

small unique nuclear receptor co-repressor (SUN-COR)	203.1	1.0	25.3	336.6	1.0
distal-less homeobox protein 5 (DLX5)	505.2	69.6	663.6	172.0	602.1
msx-interacting zinc finger protein 1 (MIZ1)	1.0	41.5	1.0	74.2	100.9
HMG-box transcription factor SOX13	42.9	25.8	159.3	150.3	120.6
helix-loop-helix factor hairy & enhancer of split 1 (HES1)	1.0	287.1	84.1	205.7	69.7
helix-loop-helix atonal protein homolog 1 (mATH1; ATOH1; ATH1)	59.6	229.3	1.0	68.8	11.3
LIM-homeodomain protein L3; LHX8	18.0	1.0	1.0	60.6	1.0
myocyte enhancer factor 2B (MEF2B)	1.0	1.0	1.0	1.0	2.2
sine oculis-related homeobox protein 4 homolog (SIX4); skeletal muscle-specific are-binding protein AREC3	121.3	231.0	1.0	83.1	1.0
aryl hydrocarbon receptor nuclear translocator 2 (ARNT2)	194.7	116.4	1.0	86.2	1.0
zinc finger protein of the cerebellum 1 (ZIC1) + ZIC2	131.9	102.7	167.2	27.0	120.2
zinc finger protein of the cerebellum 3 (ZIC3)	1.0	1.0	1.0	1.0	1.0
transcription factor 8 (TCF8); transcription repressor deltaEF1; meb1	169.9	125.9	192.8	172.3	192.5
zinc finger protein of the cerebellum 4 (ZIC4)	42.1	4371.7	2441.4	31.2	1.0
basic helix-loop-helix mesoderm posterior protein 1 (MESP1)	1.0	26.8	1.0	1.0	242.2
ATONAL HOMOLOG 3 (MAMMALIAN ATONAL HOMOLOG-3)	169.0	359.5	1.0	1.0	1.0
btb & cnc homolog 1 (BACH1)	448.0	520.7	95.9	221.0	119.5
btb & cnc homolog 2 (BACH2)	20.8	264.0	1.0	1.0	1.0
TRANSCRIPTIONAL ENHANCER FACTOR TEF-3 (ETF-RELATED FACTOR-2) (ETFR-2) (TEF-1-RELATED FACTOR 1) (TEF-1-RELATED FACTOR FR-19); TEF3; TEFR1; TCF13R1.	82.1	322.2	8.5	1134.6	1.0
myogenin (MYOG); myoD1-related protein	1.0	100.8	1.0	1.0	1.0
homeobox protein GTX	1.0	1.0	1.0	30.6	1.0
myocyte-specific enhancer factor 2C (MEF2C)	435.1	422.5	759.8	1088.2	602.6
HEPATOCTE NUCLEAR FACTOR 3 FORKHEAD HOMOLOG 4 (HFH-4); HNF-4	18.7	806.4	481.5	1.0	9.3
octamer-binding transcription factor 11 (OCT11; OTF11); pou2F3; EPOC-1	159.3	38.7	46.1	10.5	107.7
neural retina-specific leucine zipper protein (NRL)	24.2	126.9	228.2	64.8	160.5
homeobox protein 10 (HOX10); CHX10	68.0	91.4	1.0	21.6	46.0
Kreisler (maf-related) leucine zipper protein (KRML); basic domain/leucine zipper transcription factor	255.4	107.3	1.0	143.6	1.0
LIM homeobox protein 3 (LHX3; LIM3)	1.0	1.0	1.0	79.6	45.1
renal transcription factor kid1; transcription factor 17 (TCF17)	201.9	1.0	1.0	39.0	114.4
homeobox protein A9 (HOXA9); HOX-1.7	1.0	198.5	1.0	1.0	151.3
MYOGENIC FACTOR MYF-6 (HERCULIN)	34.5	195.7	153.1	213.6	372.6
HOMEBOX PROTEIN HOX-A5; HOX-1.3; M2; HOXA5; HOXA-5	23.4	1.0	1.0	1.0	63.0
DNA-BINDING PROTEIN ID-3 (ID-LIKE PROTEIN INHIBITOR HLH 462)	636.2	398.7	650.1	941.1	657.2
homeobox protein 11L1 (HOX11L1); T-cell leukemia homeobox 2 (TLX2); TLX1L1	1.0	23.0	12.4	1.0	71.6
neccdin (NDN)	153.9	325.8	465.7	728.0	74.0
distal-less homeobox protein 2 (DLX2); tes1	3.2	1.0	1.0	1.0	1.0
BRAIN-SPECIFIC HOMEBOX/POU DOMAINPROTEIN 1; BRN-1; POU3F3; OTF8; BRN1	747.2	835.6	530.1	259.8	345.3
homeobox protein A2 (HOXA2); HOX-1.11	69.2	483.0	50.6	1.0	280.6
ACHAETE-SCUTE HOMOLOG 1	137.6	395.2	1.0	26.3	63.9
snail protein homolog (SNAI1)	142.6	1.0	22.0	63.4	46.5
HELIX-LOOP-HELIX PROTEIN 1 (HEN1) (NSCL); NHLH1; HEN1.	13.0	111.0	1.0	84.7	49.7
BRAIN-SPECIFIC HOMEBOX/POU DOMAINPROTEIN 3C (BRN-3C)	5.7	39.5	1.0	1.0	1.0
homeobox protein 11 (HOX11); T-cell leukemia homeobox 1 (TLX1)	225.8	123.3	37.8	408.8	53.9
LIM homeobox protein 4 (LHX4); GSH4	1.0	1.0	308.9	1.0	762.6
homeobox protein DBX	1.0	173.1	1.0	64.3	1.0
homeobox protein GSH2	1.0	411.7	1.0	1.0	1.0
Drosophila NK5 transcription factor-related locus 2 (NKX-5.2); HMX2	1.0	226.3	170.6	55.2	146.1
distal-less homeobox protein 3 (DLX3)	1.0	73.0	1.0	130.2	139.3
HOMEBOX PROTEIN HOX-D10 (HOX-4.5) (HOX-5.3)	37.1	237.5	1.0	1.0	1.7
TBX2 PROTEIN - T-BOX PROTEIN 2	841.3	273.6	763.8	392.1	900.0
transcription factor 15 (TCF15); paraxis	159.2	266.0	14.5	30.7	118.9
homeobox protein A11 (HOXA11); HOX1.9	24.5	410.8	62.4	155.7	152.9
paired box protein 7 (PAX7)	3.7	665.6	1.0	1.0	1.0
homeobox protein GSH1	22.6	1.0	1.0	2.0	1.0

neurogenic differentiation factor 1 (NEUROD1)	170.5	1.0	1.0	54.1	1.0
myocyte-specific enhancer factor 2A (MEF2A)	1.0	70.4	149.9	66.2	366.2
Drosophila NK2 transcription factor-related locus 2 (NKX-2.2)	85.6	1.8	1.0	61.2	1.0
DERMIS EXPRESSED 1 (TWIST-RELATED BHLH PROTEIN DERMO-1)	188.2	220.2	18.4	791.0	489.6
single-minded homolog 1 (mSIM1; SIM1)	1.0	1.0	1.0	1.0	1.0
transcription factor-like protein 4 (TCFL4) + TCFL4-beta	26.3	9.9	1.0	1.0	194.7
CUT-RELATED HOMEBOXCUX-2 (CUTL2)	101.7	719.5	151.4	146.5	180.2
CUT-RELATED HOMEBOX CUX-1 (CUTL1)	62.7	210.8	165.6	95.4	57.4
TRANSCRIPTIONAL REPRESSOR (NAB1)	341.9	563.2	719.3	307.0	273.4
NGFI-A BINDING PROTEIN 2 (NAB2)	1.0	21.3	139.7	16.0	233.0
T-BRAIN-1 (TBR-1); TES-56 - T-BOX GENE	1.0	121.7	119.1	1.0	142.7
placenta & embryonic expression homeobox protein (PEM)	75.1	1.0	1.0	1.0	115.0
distal-less homeobox protein 1 (DLX1)	1.0	1.0	1.0	1.0	148.9
TBX1	49.9	3493.7	190.8	1.0	174.9
TBX3	454.1	1.0	171.0	381.6	856.8
TBX4	1.0	1.0	1.0	47.3	1.0
TBX5	26.4	92.3	35.1	154.7	48.4
TBX6	1.0	150.0	95.0	134.5	46.4
homeobox protein myeloid ecotropic viral integration site-related 2 (MEIS1-related protein 2; MRG2); MEIS3	81.2	228.3	1.0	1.0	1.0
inhibitor of MyoD family-a (I-MF; MDFI) + inhibitor of MyoD family-b	149.5	396.9	329.1	1.0	22.5
homeobox protein A13 (HOXA13); HOX1.10	402.0	285.2	270.7	401.2	632.2
eyes absent homolog 1 (EYA1)	19.3	168.8	139.3	201.5	79.6
eyes absent homolog 3 (EYA3)	0.1	162.3	358.9	124.8	8.7
LIM homeobox protein 2 (LIM2); LHX5	57.9	1.0	1.0	1.0	16.5
msh-like homeobox protein 3 (MSX3)	89.0	225.2	154.7	30.0	1.0
short stature homeobox protein 2 (SHOX2); SHOT; OG12X; paired-related homeobox protein 3 (PRX3)	158.3	1.0	1.0	245.9	1.0
distal-less homeobox protein 6 (DLX6)	140.3	1.0	1.0	66.4	113.6
basic helix-loop-helix mesoderm posterior 2 (MESP2)	1.0	1.0	1.0	1.0	1.0
transcription factor coe2; early B-cell factor 2 (EBF2); olf-1/EBF-like 3 (OE3); metencephalon-mesencephalon-olfactory transcription factor 1 (met-mesencephalon-olfactory TF1; MMOT1)	1.0	72.4	1.0	193.3	1.0
eyes absent homolog 2 (EYA2); eab1	1587.6	588.5	2493.7	934.5	1556.0
distal-less homeobox protein 7 (DLX7)	1.0	1.0	1.0	18.2	1.0
NEUROGENIN 3 (NGN3); MATH4B (mammalian atonal homolog 4B).	19.6	1.0	33.1	140.8	1.0
CONE-ROD HOMEBOX PROTEIN (CRX) - OTX-LIKE HOMEODOMAIN PROTEIN	186.2	209.3	1.0	14.2	1.0
homolog of chicken slug zinc finger protein (SLUGH)	27.0	116.5	306.4	155.7	1.0
orthodenticle-like homeobox protein 2 (OTLX2) + pituitary homeobox protein 2 isoform a (PITX2; PTX2) + pituitary homeobox protein 2 isoform b + bicoid-related homeodomain protein solurshin; Rieger syndrome homolog (RGS; RIEG)	27.1	244.2	1.0	19.2	1.0
ENDOTHELIAL PAS DOMAIN PROTEIN1 (EPAS1)	519.8	1.0	390.0	394.9	497.2
Drosophila NK3 transcription factor-related locus 2 (NKX-3.2; NKX3B); bagpipe homeobox protein homolog 1 (BAPX1)	24.5	1.0	1.0	1.0	150.2
transcriptional coactivator of AML-1 & LEF-1 (ALY)	1018.6	619.1	1185.7	2579.4	1653.4
EARLY GROWTH RESPONSE PROTEIN 2 (EGR-2) (KROX-20 PROTEIN).	1.0	1.0	1.0	1.0	138.5
BRACHIURY PROTEIN (T PROTEIN) - T-BOX GENE	1.0	12.4	1.0	1.0	1.0
paired mesoderm homeobox protein 2 (PMX2; PRX2); S8	564.9	1.0	2626.6	1692.1	1626.7
even-skipped homeobox protein homolog1 (EVX1)	96.6	416.3	1.0	1.0	131.5
paired box protein 2 (PAX2)	35.6	1.0	1.0	1.0	1.0
octamer-binding transcription factor 1 (OCT1; OTF1); pou2F1; NF-A1	318.5	261.7	2349.4	97.3	157.4
lymphoid enhancer-binding factor 1 (LEF1)	184.8	80.9	31.9	80.6	223.0
homeobox protein D12 (HOXD12); HOX4.7; HOX5.6	42.4	337.4	1.0	1.0	36.9
paired mesoderm homeobox protein 1 (PMX1; mHOX); K2	359.0	339.2	7.8	644.4	272.5
HOMEBOX PROTEIN HOX-C10 (HOX-3.6)	337.1	165.9	458.5	188.9	334.6
transcription factor 12 (TCF12); basic helix-loop-helix ALF1 protein; E-box-binding protein; HTF4; ME1	1.0	201.0	1.0	130.3	254.6
insulin promoter factor 1 (IPF1); islet/duodenum homeobox protein 1 (IDX1); somatostatin transactivating factor 1 (STF1); pancreas/duodenum homeobox protein 1 (PDX1)	1.0	6156.0	4380.1	1.0	189.7
hepatocyte nuclear factor 3 alpha (HNF3A); transcription factor 3A	242.2	1.0	1.0	66.9	238.3

(TCF3A)					
hepatocyte nuclear factor 3 beta (HNF3B); transcription factor 3B (TCF3B)	77.7	199.7	1.0	1.0	131.8
hepatocyte nuclear factor 3 gamma (HNF3G); transcription factor 3G (TCF3G)	62.9	1.0	1.0	91.9	130.7
paired mesoderm homeobox protein 2A (PMX2A; PHOX2A)	53.2	5.5	1.0	52.4	20.3
DNA-BINDING PROTEIN INHIBITOR ID-4	1.0	186.3	1.0	81.0	1.0
Drosophila NK5 transcription factor-related locus 1 (NKX-5.1); H6 homeobox protein 3 (HMX3)	40.6	527.3	1.0	64.7	62.5
Drosophila NK1 transcription factor-related locus 1 (NKX-1.1); spinal cord axial homeobox protein 1 (SAX1) + NKX-1.2	1.0	1.0	1.0	4.5	16.7
ANTERIOR-RESTRICTED HOMEBOX PROTEIN (RATHKE POUCH HOMEBOX);RPX; HESX; HEX-1	1.0	958.2	1.0	1.0	1.0
sine oculis-related homeobox protein 2 homolog (SIX2)	184.6	104.9	1.0	40.2	1.0
sine oculis-related homeobox protein 1 homolog (SIX1)	110.3	184.0	1.0	125.2	31.8
myotonic dystrophy locus-associated homeodomain protein homolog (DMAHP) + sine oculis-related homeobox protein 5 homolog (SIX5)	291.9	402.8	57.6	322.7	80.6
forkhead-related transcription factor 5 (FREAC5); FKHL9; forkhead homolog 2 (FKH2)	68.3	377.9	1.0	1.0	79.3
zinc finger protein 37 (ZFP37)	1.0	200.7	48.9	1.0	118.3
TNF receptor-associated factor 4 (TRAF4); cysteine-rich motif associated to ring & TRAF domains 1 (mCART1; CART1)	199.4	99.0	343.3	109.0	322.6
forkhead-related transcription factor 7 (FREAC7); FKHL11; forkhead homolog 6 (FKH6)	72.8	1.0	1.0	81.8	1.0
TRANSCRIPTION FACTOR FKH-5; MF3 + Winged-helix protein	1.0	1.6	1.0	1.0	1.0
zinc finger protein GLI3	91.0	1.0	965.5	1.0	1.0
zinc finger protein GLI2	64.6	213.0	1.0	89.0	1.0
goosecoid homeobox protein (GSC)	12.0	615.5	77.6	72.7	1.0
homeobox protein D13 (HOXD13); HOX-4.8	1.0	446.8	1.0	14.0	105.0
max-binding protein mnt; basic helix-loop-helix leucine zipper protein rox	383.0	1.0	268.5	1.0	395.0
STRA14 - BASIC-HELIX-LOOP-HELIX PROTEIN.	173.9	36.0	648.8	331.4	221.0
homeobox protein A3 (HOXA3); HOX-1.5; MO-10	358.8	255.3	1.0	78.5	180.1
iroquois-related homeobox protein 3 (IRX3)	1.0	1.0	1.0	17.5	1.0
mesenchyme homeobox protein 2 (MOX2; MEOX2); GAX	1.0	196.8	1.0	110.2	1.0
hematopoietically expressed homeobox protein (HHEX); proline-rich homeodomain-containing transcription factor (PRHX)	367.8	152.5	172.6	739.6	378.3
microphthalmia-associated transcription factor (MITF; MI); microphthalmia-related protein	29.7	331.7	1.0	86.8	1.0
POU DOMAIN, CLASS 6, TRANSCRIPTION FACTOR 1; OCTAMER-BINDING TRANSCRIPTION FACTOR EMB; TRANSCRIPTION REGULATORY PROTEIN MCP-1; POU6F1	39.8	261.2	174.5	234.9	1.0
LIM domain-binding protein 1 (LDB1); nuclear LIM interactor (NLI) + LIM homeobox protein cofactor 2 (CLIM2)	1217.6	2103.4	2144.8	1790.7	1133.6
LIM HOMEBOX PROTEIN COFACTOR CLIM-1A + LIM HOMEBOX PROTEIN COFACTOR CLIM-1B	287.7	108.7	249.9	616.8	177.4
LIM homeobox protein cofactor 1A (CLIM1A); LIM domain-binding protein 3 (LDB3) + LIM homeobox protein cofactor 1B (CLIM1B)					
transducin-like enhancer of split protein 3 (TLE3; ESG)	218.4	183.3	376.6	736.4	1.0
MSG-related protein 1 (MRG1); melanocyte-specific gene 2 (MSG2); Cbp/p300-interacting transactivator with Glu/Asp-rich carboxy-terminal domain 2 (CITED2)	447.3	26.1	355.7	134.3	235.8
hairless protein (HR)	287.0	1.0	1.0	193.8	1.0
melanocyte-specific gene 1 (MSG1); Cbp/p300-interacting transactivator with Glu/Asp-rich carboxy-terminal domain 1 (CITED1)	1.0	111.3	1.0	1.0	1.0
related to Drosophila groucho gene (GRG); amino enhancer of split protein (AES); enhancer of split protein 1 (ESP1)	6609.6	1692.6	7282.4	4913.6	10107.3
BAP-135 homolog; DIWS1T; general transcription factor II-I (GTF2I)	686.5	422.8	632.1	2260.4	764.9
transcription factor maf1; segmentation protein KR; kreisler; KRML	564.5	390.5	146.4	502.9	562.1
CACCC Box- binding protein BKLF	554.1	464.6	990.9	973.7	395.5
DNA-binding protein SMBP2	1.0	317.2	1.0	1.0	34.7
GA-binding protein beta 2 subunit (GABP-beta 2 subunit; GABBP2; GABPB)	103.5	158.2	121.9	299.8	1.0
paired box protein PAX5; B-cell-specific transcription factor; BSAP	84.3	185.5	1.0	609.7	1.0
cAMP responsive element binding protein 1	61.7	184.9	1.0	83.3	232.9
ret finger protein	1.0	39.8	27.0	1.0	335.0

TRANSCRIPTION FACTOR HES-5 (HAIRY AND ENHANCER OF SPLIT 5)	1.0	1.0	1.0	1.0	1.0
zinc finger protein 46	1.0	39.1	1.0	122.4	1.0
zinc finger protein 60	1.0	25.6	1.0	99.6	1.0
neuronal PAS domain protein 1	1.0	1.0	1.0	62.2	1.0
neuronal PAS domain protein 2	1.0	60.9	1.0	6.3	187.1
RETINOBLASTOMA BINDING PROTEIN 6 (PACT)	1.0	182.0	1.0	1.0	1.0
JUMONJI PROTEIN	68.2	199.6	1.0	48.1	141.1
HYPOXIA-INDUCIBLE FACTOR 1 ALPHA (HIF-1 ALPHA) (ARNT INTERACTING PROTEIN).	1.0	36.6	1.0	237.2	1.0
tumor necrosis factor alpha-induced protein 3 (TNFAIP3; TNFIP3); A20 zinc finger protein	109.6	3.0	1.0	1.0	1.0
EARLY GROWTH RESPONSE PROTEIN 3 (EGR-3) (FRAGMENT)	1.0	23.7	1.0	173.5	1.0
HEPATOCYTE NUCLEAR FACTOR 4-ALPHA (HNF-4-ALPHA) (TRANSCRIPTION FACTOR HNF-4) (TRANSCRIPTION FACTOR 14)	1.0	1.0	1.0	426.0	1.0
INTERFERON REGULATORY FACTOR 7 (IRF-7)	69.9	1.0	1.0	40.6	1.0
SA2 NUCLEAR PROTEIN	1.0	71.8	1.0	1.0	1.0
CREB-BINDING PROTEIN	55.3	374.1	33.2	64.3	43.1
YL-1 PROTEIN.	163.2	214.4	98.3	129.4	269.9
ORPHAN NUCLEAR RECEPTOR PXR (PREGNANE X RECEPTOR)	177.4	1.0	1.0	80.0	124.9
TRANS-ACTING TRANSCRIPTION FACTOR 3 (TRANSCRIPTION FACTOR SP3)	191.2	230.8	1.0	111.0	1.0
ablphillin-1 (abi-1); similar to HOXD3	1.0	370.7	31.9	85.8	1.0
activating transcription factor 4 (mATF4)	1.0	1.0	1.0	1.0	1.0
delta-like protein precursor (DLK); preadipocyte factor 1 (PREF1); adipocyte differentiation inhibitor protein; SCP-1	21962.6	12403.6	6116.5	2313.3	13008.8
AT motif-binding factor (ATBF1)	461.5	279.5	1.0	336.4	736.9
brain factor 1 (Hfxbf1)	593.7	265.6	245.6	189.3	626.2
brain specific transcription factor NURR-1	328.8	376.6	77.0	160.8	114.3
Brm-3.2 POU transcription factor	1.0	155.7	1.0	1.0	1.0
butyrate response factor 1	9783.6	4685.5	4042.6	5641.4	4493.5
CCAAT- binding transcription factor (C/ EBP)	25.7	122.6	1.0	1.0	1.0
caudal-type homeobox protein 1 (CDX1)	794.1	541.4	353.5	543.1	740.8
caudal type homeobox 2 (Cdx2)	131.8	319.3	174.1	283.4	375.7
Sim transcription factor	39.2	1.0	1.0	85.2	181.5
transcription factor COE1; early B-cell factor (EBF)	402.8	306.0	1.0	180.9	92.9
engrailed homeobox protein (EN1; MOEN1)	109.3	318.9	1.0	29.6	44.0
engrailed protein (En-2) homolog	209.7	1.0	96.0	59.0	129.1
erythroid transcription factor NF-E2	1.0	142.7	1.0	1.0	1.0
early growth response protein 1 (EGR1); KROX-24 protein; ZIF/268	1441.6	237.7	493.3	220.8	1505.4
ets-related transcription factor; E74-like factor 1 (ELF1)	182.7	1.0	1.0	207.6	1.0
epidermal growth factor receptor kinase substrate EPS8	332.1	49.8	42.0	348.5	453.3
Erf; Ets-related transcription factor	796.0	301.6	389.8	374.3	899.6
erythroid Kruppel-like transcription factor (EKLF)	167.4	242.4	1.0	49.1	1.0
Ets-related protein PEA 3	1.0	1.0	1.0	1.0	1.0
c-ets2	1.0	1.0	1.0	271.6	1.0
serum response factor accessory protein 1A (SAP-1A); ets-domain protein ELK4	223.0	247.6	78.3	201.0	460.2
GATA binding transcription factor (GATA-4)	1.0	36.1	1.0	52.5	76.8
Gbx 2	65.6	1.0	1.0	30.6	1.0
glial cells missing gene homolog (mGCM1)	191.8	159.8	1.0	35.8	1.0
gut-enriched Kruppel-like factor (GKLF); epithelial zinc finger protein (EZP); ZIE	269.6	27.3	254.0	660.3	245.5
heat shock transcription factor 2 (HSF 2)	1.0	247.0	1.0	96.3	59.2
forkhead-related transcription factor 1 (FREAC1); hepatocyte nuclear factor 3; forkhead homolog 8 (HFH8)	332.1	165.8	283.1	294.8	684.5
HMG-box transcription factor from testis (MusSox17)	523.0	497.6	66.6	55.2	242.9
non-histone chromosomal protein HMG-14	1.0	403.5	56.0	3374.6	43.9
homeobox protein 1.1 (Hox-1.1)	63.5	114.6	1.0	111.7	308.1
homeobox protein B5 (HOXB5); HOX-2.1; MU-1; H24.1	493.5	492.7	77.0	342.0	231.1
homeobox protein 2.4 (Hox-2.4)	239.7	167.0	73.4	523.8	268.9
homeobox protein 2.5 (Hox-2.5)	177.5	108.6	1.0	139.2	54.3
homeobox protein 3.1 (Hox-3.1)	269.1	1278.2	169.5	221.7	173.1

homeobox protein D4 (HOXD4); HOX-4.2; HOX-5.1	226.6	221.8	1.0	122.6	277.8
homeobox protein 7.1 (Hox-7.1)	200.3	68.8	48.2	44.6	259.3
homeobox protein 8 (Hox-8)	375.3	455.0	624.2	817.8	966.1
homeobox protein HOXD-3	910.7	1.0	1.0	256.3	425.5
ikaros DNA binding protein	103.6	187.1	93.0	168.2	153.7
Sp4 zinc finger transcription factor	34.9	453.6	1.0	81.9	101.0
interferon inducible protein 1	35.0	1.0	106.0	1.0	133.3
interferon regulatory factor 2 (IRF 2)	457.6	1.0	150.2	28.5	367.7
lung Kruppel-like factor (LKLF)	356.8	252.1	228.2	154.5	551.7
Lbx 1 transcription factor	1.0	168.8	1.0	51.6	216.2
Mph-1 nuclear transcriptional repressor for hox genes	99.6	29.1	1.0	13.5	164.6
MRE-binding transcription factor	35.5	204.9	1.0	38.7	254.2
myocyte nuclear factor (MNF)	252.2	231.8	284.0	227.8	177.1
myogenic factor 5	1.0	260.2	1.0	66.1	1.0
atonal protein homolog 2 (ATOH2; ATH2); helix-loop-helix protein MATH2; NEX1	12.2	228.6	24.8	66.7	121.0
NF-1B protein (transcription factor)	295.2	161.9	107.0	454.7	60.2
nuclear factor kappaB p105 subunit (NF-kappaB p105; NFKB1); KBF1; EBP-1	135.0	88.2	1.0	54.7	1.0
nuclear factor erythroid 2-related factor 2 (NF-E2-related factor 2; NFE2L2; NRF2)	64.0	114.2	1.0	208.3	1.0
nuclear hormone receptor ROR-alpha-1	37.6	191.5	1.0	1.0	1.0
nucleobindin	1615.6	559.0	740.6	801.9	1140.5
octamer binding transcription factor 3 (OCT3; OTF3); OCT4; NF-A3; POU5F1	1.0	362.1	57.4	132.7	138.6
PAX-8 (paired box protein PAX 8)	576.9	216.5	527.2	412.7	480.5
split hand/foot gene	1241.6	155.6	1186.8	1555.8	1360.0
SRY-box containing gene 3 (Sox3)	1.0	1.0	1.0	1.0	54.0
paired box protein 6 (PAX6); SEY	40.3	23.3	5.5	8.1	64.8
POU domain (class 2) associated factor 1	53.3	1.0	39.2	27.4	1.0
PSD-95/SAP90A	105.0	34.1	1.0	1.0	30.3
cellular retinoic acid-binding protein II (CRABP-II; CRABP2)	1.0	192.5	18.2	95.1	2.1
retinoic acid receptor gamma (RXR gamma; RXRG)	1.0	1.0	1.0	20.6	99.3
retinoid X receptor interacting protein (RIP 15)	1705.6	315.5	2477.8	565.5	955.8
T-lymphocyte activated protein; immediate early response 2 (IER2); cycloheximide-induced protein 1 (CHX1)	392.0	186.3	164.9	355.3	315.9
transcription factor 1 for heat shock gene	139.0	117.2	1.0	99.8	1.0
transcription factor BARX1; homeodomain transcription factor	1.0	124.1	1.0	1.0	1.0
transcription factor C 1	2052.6	364.9	1311.8	704.7	2184.1
transcription factor CTCF (11 zinc fingers )	482.7	44.2	132.4	385.9	507.7
transcription factor LIM-1	1.0	28.9	1.0	106.9	1.0
cAMP-dependent transcription factor 3 (ATF3); activating factor 3; transcription factor LRG - 21	14.9	1.0	1.0	5.4	85.1
SRY-box containing gene 4	70.0	67.7	147.7	1.0	320.1
transcription factor relB	161.6	66.7	1.0	14.0	142.6
transcription factor S -II; transcription elongation factor	600.4	689.8	538.5	233.9	467.7
transcription factor SEF2	1462.6	1620.8	1045.2	1287.6	1228.5
octamer-binding transcription factor 6 (OCT6; OTF6); POU domain transcription factor SCIP; POU3F1	1.0	238.9	2.4	1.0	1.0
U2 small nuclear ribonucleoprotein auxiliary factor 35-kDa subunit-related protein 1 (U2AF1-RS1); SP2	43.2	187.0	1.0	125.6	1.0
transcription factor UBF	712.5	659.9	359.6	465.5	203.7
transcriptional enhancer factor 1 (TEF1); protein GT-IIc;	91.5	139.5	1.0	1.0	42.9
transcription factor 13 (TCF13); TEAD1					
YB1 DNA binding protein	8031.6	2610.0	13647.3	5621.8	9789.9
YY1 (UCRBP) transcriptional factor	1.0	1.0	1.0	61.1	1.0
zinc finger Kruppel type Zfp 92	1.0	1.0	1.0	338.4	1.0
zinc finger transcription factor RU49	1.0	59.6	1.0	50.1	1.0
zinc finger X-chromosomal protein (ZFX)	266.2	471.6	1.0	42.8	35.8
MEL18 DNA-binding protein; zinc finger protein 144 (ZFP144)	329.6	28.6	142.2	132.4	74.8
brahma-related protein 1 (BRG1); swi/snf-related matrix-associated actin-dependent regulator of chromatin subfamily a member 4 (SMARCA4)	0.1	544.2	3.5	82.2	1.0
enhancer of zeste homolog 2 (EZH2; ENX1H)	131.9	1.0	1.0	84.0	1.0
chromobox homolog 4 (CBX4); homolog of Drosophila polycomb protein 2 (mPC2)	370.3	400.4	595.2	548.2	291.5

embryonic ectoderm development protein (EED)	1.0	79.7	1.0	97.9	1.0
ring finger protein 2 (RNF2); polycomb-M33-interacting protein ring 1B (RING1B)	184.2	189.6	167.6	266.8	177.7
D-BINDING PROTEIN (DBP) (ALBUMIN D BOX-BINDING PROTEIN)	756.9	44.7	208.0	303.2	129.8
TRANSCRIPTION FACTOR E2F1 (E2F-1)	52.7	1.0	11.3	136.2	1.0
TRANSCRIPTION FACTOR E2F3 (E2F-3)	1.0	1.0	1.0	27.8	1.0
transcription factor E2F dimerization partner 1 (TFDP1); DRTF1 polypeptide 1	351.4	1.0	584.0	830.2	971.7
E2F-5 transcription factor	1.0	10981.0	1.0	163.5	1.0
VITAMIN D3 RECEPTOR (VDR) (1,25-DIHYDROXYVITAMIN D3 RECEPTOR)	379.5	1.0	1.0	46.8	128.7
interferon regulatory factor 1 (IRF1)	739.9	156.0	453.8	627.6	940.9
activating transcription factor 2 (ATF2); cAMP response element DNA-binding protein 1 (CREBP1)	1.0	174.5	1.0	216.8	50.3
Pml; murine homolog of the leukemia-associated PML gene	1.0	165.4	7.8	50.7	76.6
signal transducer and activator of transcription 1 (STAT1)	14.5	85.3	75.6	422.3	74.3
signal transducer & activator of transcription 3 (STAT3); acute phase response factor (APRF)	8.5	250.3	1.0	157.9	186.2
Stat5a; mammary gland factor	1.0	164.7	112.0	142.9	1.0
TRAF family member-associated NF-kappaB activator (TANK)	1.0	57.2	1.0	64.9	105.4
D-3-phosphoglycerate dehydrogenase (PGDH); transcription factor A10	716.6	182.4	346.7	849.0	772.5
Stat6; signal transducer and activator of transcription 6; IL-4 Stat; STA6	292.5	98.2	305.0	423.9	311.1
NF-kappa-B transcription factor p65 subunit (NF-kB p65); relA; NFKB3	635.2	1.0	909.3	204.1	846.6
protein kinase inhibitor beta, cAMP dependent, testis specific	1.0	1.0	1.0	1.0	66.0
protein kinase, cAMP dependent, catalytic, beta	1.0	152.0	1.0	1128.8	1.0
cyclin T1	1.0	1629.2	353.0	3.7	1.0
Cyclin K	86.4	1.0	1.0	37.3	1.0
G1/S-specific cyclin E2 (CCNE2)	4.4	550.4	1.0	1.0	1.0
G2/mitotic-specific cyclin A1 (CCNA1)	1177.6	671.0	778.1	551.5	2068.1
cyclin C (G1-specific)	1.0	1.0	1.0	54.7	122.5
cyclin F (S/G2/M-specific)	106.7	184.3	28.1	263.4	135.3
G2/M-specific cyclin G (CCNG)	1.0	1.0	1.0	205.1	268.5
cyclin G2 (G2/M-specific)	1.0	128.8	1.0	238.2	1.0
G2/M-specific cyclin A2 (CCNA2)	192.5	1.0	39.2	282.6	252.6
G2/mitotic-specific cyclin B1 (CCNB1; CYCB1); CCN2	19.5	1.0	113.6	322.2	472.4
G2/M-specific cyclin B2 (CCNB2; CYCB2)	287.8	318.1	1.0	715.8	196.5
G1/S-specific cyclin D1 (CCND1; CYL-1)	166.6	1.0	250.8	902.7	98.1
cyclin D2 (G1/S-specific)	1873.6	1.0	1000.4	1409.4	1329.3
G1/S-specific cyclin D3 (CCND3; CYL3)	197.1	509.3	341.4	139.8	41.6
G1/S-specific cyclin E1 (CCNE1)	1.0	1.0	107.6	146.9	212.7
cell division protein kinase 4 (CDK4); cyclin-dependent kinase 4; PSK-J3; CRK3	210.1	477.2	446.6	1884.2	1.0
Cdk5; cyclin-dependent kinase 5	158.4	1.0	118.9	213.7	1.0
Cdk7; MO15; cyclin-dependent kinase 7 (homolog of Xenopus MO15 cdk-activating kinase)	1.0	1.0	1.0	195.7	1.0
Bub1 mitotic checkpoint kinase	1.0	167.6	1.0	86.7	1.0
extracellular signal-regulated kinase 1 (ERK1); p44-MAPK; ERT2; microtubule-associated protein 2 kinase; insulin-stimulated MAP2 kinase; MAP kinase 1; MNK1; PRKM3	478.1	646.9	735.1	2646.8	401.9
SERINE/THREONINE-PROTEIN KINASE NEK2 (NIMA-RELATED PROTEIN KINASE 2)	1.0	1.0	1.0	1.0	1.0
BUB1B mitotic checkpoint protein kinase	226.9	174.9	99.0	118.1	471.0
p58/GTA; galactosyltransferase associated protein kinase (cdc2-related protein kinase)	73.1	577.0	1.0	89.5	173.8
NIMA-related protein kinase 3 (NEK3)	1.0	1.0	1.0	1.0	39.2
Cyclin-dependent kinases regulatory subunit 2 (CKS-2)	110.7	895.1	1.0	228.0	1.0
special AT-rich sequence-binding protein 1 (SATB1)	91.2	1.0	1.0	151.7	1.0
ERA-1 protein (ERA-1-993)	1.0	273.2	1.0	76.1	1.0
trans-acting T-cell-specific transcription factor GATA3	133.2	230.4	242.6	165.6	67.9
wee1-like protein kinase	1.0	1.0	1.0	117.2	1.0
cyclin-dependent kinase 6 inhibitor (p18-INK6); cyclin-dependent kinase 4 inhibitor C (p18-INK4C); CDKN2C	76.2	1.0	1.0	118.4	1.0
p19ink4; cdk4 and cdk6 inhibitor	1.0	1.0	4.3	224.4	1.0
cyclin-dependent kinase inhibitor 1 (CDKN1A); melanoma	1.0	1.0	38.5	140.9	58.4

differentiation-associated protein; CDK-interacting protein 1 (CIP1); WAF1					
p27kip1; G1 cyclin-Cdk protein kinase inhibitor; p21-related	249.2	83.4	83.2	310.1	305.9
p57kip2; cdk-inhibitor kip2 (cyclin-dependent kinase inhibitor 1B); member of the p21CIP1 Cdk inhibitor family; candidate tumor suppressor gene	42.7	617.7	145.8	306.8	172.2
myeloblastin; trypsin-chymotrypsin related serine protease	1.0	203.7	1.0	1.0	1.0
proliferation-associated protein 1 (PLFAP); p38-2G4	457.9	1091.9	1347.1	2564.1	970.4
p55CDC	718.1	214.8	518.8	485.0	908.6
Cyclin-D binding Myb-like protein (hDMP1)	1.0	1.0	1.0	1.0	1.0
prothymosin alpha (PTMA)	9296.6	5783.1	9967.7	11230.4	13359.5
Tob antiproliferative factor; interacts with p185erbB2	92.9	1.0	1.0	83.3	76.1
Cdc25a; cdc25M1; MPI1 (M-phase inducer phosphatase 1)	218.0	635.7	1.0	261.8	26.5
Cdc25b; cdc25M2; MPI2 (M-phase inducer phosphatase 2)	8.5	1.0	1.0	1.0	1.0
Geminin	1.0	120.2	1.0	1.0	1.0
neural cell adhesion molecule 2 precursor (NCAM2); olfactory axon cell adhesion molecule (OCAM)	76.4	1.0	1.0	1.0	1.0
galectin 7; galactose-binding soluble lectin 7 (LGALS7)	1.0	126.0	103.8	184.3	125.1
cell surface antigen MS2 precursor; macrophage cysteine-rich glycoprotein; a disintegrin & metalloprotease domain 8 (ADAM8); CD156 antigen	1.0	1.0	1.0	4.7	1.0
cadherin 4 (CDH4); retinal cadherin (R-cadherin; R-CAD)	13.6	1.0	1.0	13.2	37.6
cadherin 6 precursor (CDH6); kidney cadherin (K-cadherin)	1.0	539.0	149.9	133.5	58.5
osteopontin precursor (OP); bone sialoprotein 1; minopontin; early T-lymphocyte activation 1 protein (ETA1); secreted phosphoprotein 1 (SPP1); calcium oxalate crystal growth inhibitor protein	1.0	227.0	1.0	19.8	158.1
cadherin 15 (CDH15); CDH14; muscle cadherin precursor (M-cadherin)	1.0	43.0	5.1	1.0	84.8
ephrin type A receptor 4 (ephr receptor A4; EPHA4); segmentation receptor tyrosine kinase (SEK)	41.0	57.1	1.0	475.1	161.1
occludin (OCLN; OCL)	1.0	1.0	1.0	1.0	348.1
ephrin type A receptor 6 (ephr receptor A6; EPHA6); eph homology kinase 2 (EHK2)	1.0	1.0	53.8	1.0	1.0
desmoglein 3 (DSG3)	1.0	1.0	1.0	1.0	1.0
neural plakophilin-related arm-repeat protein (NPRAP)	117.8	536.2	1.0	512.2	1.0
EPHRIN-A3 (EPH-RELATED RECEPTOR TYROSINE KINASE LIGAND 3) (LERK-3) (EHK1 LIGAND) (EHK1-L); EFNA3; EPLG3; LERK3; EPL3.	261.8	434.6	310.7	1.0	1.0
integrin-linked kinase (ILK); integrin-binding protein kinase	2658.6	1051.8	1467.5	4176.3	1158.9
cadherin 1 (CDH1); epithelial cadherin precursor (E-cadherin; E-CAD); uvomorulin (UM)	816.2	1268.7	286.6	159.9	243.9
neural cell adhesion molecule L1 precursor (N-CAM L1; L1CAM; CAML1)	76.2	123.9	4.0	1.0	71.9
alpha-1 catenin (CTNNA1; CATNA1); alpha E-catenin; 102-kDa cadherin-associated protein (CAP102)	79.5	1.0	172.7	1450.7	260.6
ephrin type A receptor 2 (ephr receptor A2; EPHA2); segmentation receptor tyrosine kinase 2 (SEK2); epithelial cell kinase (ECK)	1.0	85.1	28.1	118.2	32.8
ephrin type A receptor 7 (ephr receptor A7; EPHA7); eph homology kinase 3 (EHK3); embryonic brain receptor tyrosine kinase (EBK); developmental kinase1 (mDK1)	57.1	69.5	1.0	227.3	48.8
cadherin 5 (CDH5); vascular epithelial cadherin precursor (VE-cadherin)	846.1	1.0	1068.7	662.7	1212.3
semaphorin IIIB (SEMA3B); semaphorin A precursor (SEMAA)	275.7	1.0	1.0	201.5	119.8
collapsin 1 precursor; semaphorin IIIA (SEMA3A); semaphorin D (SEMAD; SEMD)	1.0	135.7	1.0	1.0	41.9
semaphorin IIIC (SEMA3C); semaphorin E precursor (SEMAE; SEME)	1.0	1.0	1.0	1977.7	111.5
cadherin 8 precursor (CDH8)	71.3	1.0	1.0	1.0	1.0
desmocollin 1A/1B precursor (DSC1)	106.5	14.9	1.0	1.0	1.0
semaphorin B	776.3	1.0	1058.3	796.8	456.6
semaphorin C	1.0	86.8	606.0	425.1	110.8
semaphorin F	387.4	1.0	1.0	200.1	176.6
semaphorin H	1.0	1.0	1.0	1.0	361.7
semaphorin I	43.5	288.2	78.9	114.1	72.2
semaphorin J	1.0	123.3	243.4	457.6	102.6
semaphorin N	1.0	84.8	1.0	72.6	1.0
CD44 antigen precursor; phagocytic glycoprotein I (PGP1); HUTCH I; extracellular matrix receptor III (ECMR III); gp90 lymphocyte	1.0	123.4	39.4	57.5	1.0

homing/adhesion receptor; hermes antigen; hyaluronate receptor; LY-24					
dystroglycan 1	921.3	485.0	1038.7	1802.3	607.7
vascular cell adhesion protein 1	34.9	1.0	1.0	153.9	1.0
SEMAPHORIN G PRECURSOR (SAMAPHORIN G).	7433.6	2117.5	6531.3	3078.1	6223.0
P-selectin glycoprotein ligand 1 precursor (PSGL1; SELPLG; SELP1)	1.0	1.0	1.0	80.2	1.0
alpha 2 catenin (CTNNA2; CATNA2); alpha catenin-related protein; alphan catenin	32.7	267.7	1.0	110.6	1.0
cell surface adhesion glycoproteins LFA-1/CR3/p150,95 beta subunit precursor; integrin beta 2 (ITGB2); CD18 antigen; complement receptor C3 beta subunit	46.6	1.0	94.3	227.3	180.5
CD31; platelet endothelial cell adhesion molecule 1	494.7	1.0	756.0	448.0	680.9
CD14 monocyte differentiation antigen precursor; LPS receptor (LPSR); myeloid cell-specific leucine-rich glycoprotein	470.4	1.0	1223.2	1329.6	266.9
CD22 antigen	1.0	137.2	1.0	33.9	1.0
cell surface glycoprotein MAC-1 alpha subunit precursor; CR-3 alpha subunit; CD11B antigen; leukocyte adhesion receptor MO1; integrin alpha-M (ITGAM)	1.0	58.6	221.0	582.2	141.0
desmocollin 2	1.0	144.8	191.1	140.2	1.0
platelet membrane glycoprotein IA precursor (GPIA); integrin alpha 2 (ITGA); collagen receptor; VLA2 alpha subunit; CD49B antigen	1.0	1.0	38.5	108.2	141.7
integrin alpha 4	52.8	644.0	1.0	40.2	58.4
integrin alpha 5 (CD51)	175.0	297.4	1.0	601.3	1.0
integrin alpha 6	219.0	1.0	304.6	709.4	193.7
integrin alpha 7	1.0	1.0	1.0	1.0	1.0
fibronectin receptor beta subunit precursor; integrin beta 1 (ITGB1)	47.9	139.4	757.9	669.8	834.0
integrin beta 7	1015.6	1.0	1.0	20.9	1.0
neural cadherin precursor (N-cadherin; CDH2)	342.7	208.5	264.0	218.3	250.1
neuronal cell surface protein F3	220.4	218.9	1.0	1.0	98.9
integrin alpha 3 precursor (ITGA3); galactoprotein B3 (GAPB3); VLA-3 alpha subunit	225.9	1.0	52.1	880.2	348.3
intercellular adhesion molecule 1 precursor (ICAM1); MALA2	1.0	431.2	1.0	268.9	1.0
apolipoprotein E precursor (apo-E)	18864.6	8020.4	25672.5	11914.7	18177.1
lecithin-cholesterol acyltransferase (LCAT); phosphatidylcholine-sterol acyltransferase precursor; phospholipid-cholesterol acyltransferase	1.0	1.0	1.0	40.3	288.1
phospholipid transfer protein precursor (PTLP); lipid transfer protein II; vesicular acetylcholine transporter (VAcHT)	498.4	1.0	431.7	226.8	291.0
TRANSTHYRETIN PRECURSOR (PREALBUMIN) (TBPA) (TTR) (ATTR)	177.4	110.9	1.0	113.7	1.0
transcription termination factor 1 (TTF1)	250.9	1.0	224.0	285.4	277.0
G-protein coupled receptor 25	1.0	1.0	1.0	1.0	192.5
G-protein coupled receptor 27	1.0	209.0	1.0	277.2	1.0
purinergic receptor P2Y, G-protein coupled 1	1.0	1.0	1.0	1.0	1.0
RAB17, member RAS oncogene family	495.8	1.0	1.0	241.5	1.0
RAB19, member RAS oncogene family	1.0	366.3	1.0	116.1	41.4
RAB20, member RAS oncogene family	1.0	1.0	1.0	169.8	1.0
RAB23, member RAS oncogene family	85.7	42.3	312.2	248.1	1.0
RAB24, member RAS oncogene family	163.1	420.5	1.0	13.1	311.7
neurofibromatosis 1	1.0	154.3	1.0	72.8	1.0
von Hippel-Lindau syndrome homolog (VHLH)	1.0	1.0	1.0	1.0	1.0
WT1; Wilms tumor protein; tumor suppressor	5.1	447.7	1.0	1.0	13.6
tumor susceptibility protein 101 (TSG101)	215.1	1.0	198.3	577.1	265.4
integrase interactor 1A protein (INI1A)	321.3	1.0	169.9	324.0	311.4
Gli oncogene; zinc finger transcription factor	256.6	420.0	5.9	148.8	284.3
ets-domain protein elk3; ets-related protein net; ERP	240.4	392.1	81.3	1676.1	100.5
thyroid hormone receptor alpha 1 (THRA); MR1A1; c-erbA alpha	5697.6	1270.4	2269.8	5012.9	2826.8
c-fos proto-oncogene; p55	1.0	18.5	1.0	250.5	1.0
transcription factor AP-1; c-jun proto-oncogene; AH119	2786.6	1372.2	862.6	1018.6	2384.1
c-myc proto-oncogene protein	106.3	69.7	276.9	224.0	277.9
c-rel proto-oncogene	55.0	455.6	1.0	126.1	1.0
Max protein. MAX PROTEIN (MYN PROTEIN)	913.9	781.6	1023.5	930.9	1602.7
fos-B	158.6	159.8	65.0	1.0	280.3
junB	1.0	1.0	1.0	1.0	1.0
junD	2204.6	1636.3	2232.3	960.6	1488.0
Elk-1 ets-related proto-oncogene	94.2	1.0	170.9	22.2	53.2

Fli-1 ets-related proto-oncogene	371.1	314.8	1.0	236.9	281.5
A-myb proto-oncogene; myb-related protein A	10.9	261.8	1.0	13.0	1.0
myb-related protein B; B-myb; mybL2	87.4	579.1	32.9	213.6	1.0
fos-related antigen 2 (FRA2); fos-L2	748.1	580.2	181.3	502.1	183.5
Ear-2; v-erbA related proto-oncogene	1085.6	1.0	677.7	573.5	810.8
c-myc proto-oncogene	1811.6	773.7	697.9	846.8	933.6
L-myc proto-oncogene protein	1.0	378.7	1.0	255.1	1.0
N-myc proto-oncogene protein	228.9	126.7	50.3	261.8	93.8
retinoblastoma-like protein 1 (RBL1); 107-kDa retinoblastoma-associated protein; PRB1	57.9	86.1	1.0	41.2	94.6
retinoblastoma-like protein 2 (RBL2); retinoblastoma-related protein PRB2/p130	1.0	195.5	1.0	1.0	1.0
retinoblastoma-associated protein 1 (RB1); pp105	1.0	1.0	1.0	1.0	1.0
insulin-like growth factor binding protein 2 precursor (IGF-binding protein 2; IGFBP2; IBP2)	2829.6	868.0	2321.0	2165.4	1864.0
c-Mpl; thrombopoietin receptor; hematopoietic growth factor receptor superfamily member	1.0	159.5	1.0	39.2	1.0
DCC; netrin receptor; immunoglobulin gene superfamily member; former tumor suppressor protein candidate	43.7	152.6	1.0	15.3	1.0
Int-3 proto-oncogene; NOTCH family member; NOTCH4	1.0	27.7	1.0	54.7	1.0
Mas proto-oncogene (G-protein coupled receptor)	140.0	625.1	1.0	44.7	1.0
macrophage colony stimulating factor 1 precursor (CSF1; MCSF; CSFM)	201.3	315.8	125.8	255.7	3.8
adenomatous polyposis coli protein (APC)	250.3	378.9	1.0	1226.0	197.3
NF2; merlin (moesin-ezrin-radixin-like protein); shwannomin; murine neurofibromatosis type 2 susceptibility protein	1.0	408.0	1.0	1.0	1.0
EB1 APC-binding protein	1.0	81.5	43.4	340.9	1.0
ezrin; villin 2; NF-2 (merlin) related filament/plasma membrane associated protein	1277.6	766.1	1486.8	1214.4	2246.7
cellular tumor antigen p53 (TRP53; TP53)	1245.6	483.1	1181.2	639.9	643.7
MDM2; p53-associated protein	99.5	39.0	1.0	9.4	141.9
tyro3 precursor; rse; dtk; TK19-2	447.8	555.6	211.1	2211.1	388.7
c-Fms proto-oncogene; macrophage colony stimulating factor 1 (CSF-1) receptor	33.7	219.7	859.2	1.0	237.1
mast/stem cell growth factor receptor (SCFR); c-kit proto-oncogene	1.0	195.3	206.7	1.0	44.8
Met proto-oncogene	126.5	1.0	64.1	61.3	1.0
platelet-derived growth factor receptor alpha precursor (PDGFR-alpha; PDGFRA)	677.7	1082.2	735.4	843.2	548.2
vascular endothelial growth factor receptor 1 (VEGFR1); fms-related tyrosine kinase 1 (Flt1)	92.3	261.5	230.3	69.8	42.3
ret proto-oncogene precursor; c-ret	38.3	592.9	274.8	1596.4	209.7
mothers against dpp protein 1 (msMAD1; mSMAD1; MADH1); TGF-beta signaling protein 1 (BSP1)	775.5	952.4	683.4	620.7	619.7
abl proto-oncogene	408.2	711.9	1.0	1670.3	258.2
c-Src proto-oncogene	660.8	327.8	516.6	1412.3	699.0
proto-oncogene tyrosine-protein kinase fes/fps	1.0	1.0	1.0	154.0	20.0
c-Fgr proto-oncogene	1.0	1.0	1.0	1.0	1.0
SHC-transforming protein	93.5	328.9	387.4	518.9	283.3
c-Cbl proto-oncogene (adaptor protein)	3.3	1.0	1.0	1.0	1.0
A-Raf proto-oncogene	607.7	102.7	688.3	1009.2	621.4
B-raf proto-oncogene	1463.6	1727.7	988.2	1746.4	1456.0
Cot proto-oncogene	1.0	971.4	239.1	20.5	1.0
ski proto-oncogene	4874.6	1992.3	2823.2	2701.1	3321.5
snoN; ski-related oncogene	1.0	76.9	87.7	1.0	1.0
pim1 proto-oncogene	851.1	233.1	1544.8	1797.9	946.8
H-ras proto-oncogene; transforming protein p21	214.9	56.8	52.0	1.0	1.0
N-ras proto-oncogene; transforming G-protein	36.4	782.0	39.0	661.1	46.8
Vav; GDP-GTP exchange factor; proto-oncogene	1.0	1.0	1.0	1.0	1.0
R-ras protein (closely related to ras proto-oncogenes)	398.9	1.0	61.3	455.1	171.1
Lfc proto-oncogene	127.7	1.0	1.0	466.7	120.1
Tiam-1 invasion inducing protein; GDP-GTP exchanger-related	5.8	66.8	1.6	1.0	1.0
maspin precursor; protease inhibitor 5 (PI5)	1.0	81.5	175.3	1.0	58.1
stromelysin 3; matrix metalloproteinase 11 (MMP11)	211.6	1.0	138.5	417.3	1.0
tight junction protein ZO1; tight junction protein 1 (TJP1)	1074.6	9450.0	670.8	929.5	1076.8
BRCA1; breast/ovarian cancer susceptibility locus 1 product	1.0	1.0	1.0	0.6	1.0
breast cancer type 2 susceptibility protein (BRCA2)	1402.6	100.5	522.4	145.9	516.6

nucleoside diphosphate kinase B (NDP kinase B; NDK B); NM23-M2; NME2	9354.6	3393.8	8284.7	22198.2	8063.1
105-kDa heat shock protein (HSP105); HSP110; heat shock-related 100-kDa protein E71 (HSP-E71); 42 degrees C-HSP	1.0	180.8	1.0	1.0	48.4
heat shock 27-kDa protein (HSP27); growth-related 25-kDa protein; HSP25; HSPB1	210.0	1.0	327.1	1.0	250.1
mitochondrial matrix protein P1 precursor; p60 lymphocyte protein; 60-kDa chaperonin; heat shock 60-kDa protein (HSP60); GroEL protein; HSP65; HSPD1	13.3	158.9	1.0	273.7	35.4
MTJ1; DNAJ-like heat-shock protein from mouse tumor	108.4	721.6	46.2	1.0	77.8
84-kDa heat shock protein (HSP84); HSP 90-beta; tumor-specific transplantation 84-kDa antigen (TSTA); HSPCB	9326.6	4824.8	3752.8	7133.2	6057.7
HSP86; heat shock 86-kDa protein	837.5	1255.2	457.1	2985.3	1070.8
Osp94 osmotic stress protein; APG-1; hsp70-related	1.0	149.7	1.0	1213.6	1.0
78-kDa glucose regulated protein (GRP78)	2302.6	2380.6	1322.1	2029.9	2166.7
C3H cytochrome P450; Cyp1b1	1.0	1.0	1.0	1.0	1.0
cytochrome P450 1A1 (CYPIA1; P450-P1)	1.0	1.0	1.0	168.5	130.9
HEME OXYGENASE 2 (HO-2)	1.0	1.0	1.0	51.5	1.0
plasma glutathione peroxidase precursor (GSHPX-P); GPX3	1046.6	1.0	339.1	1326.7	1004.1
glutathione reductase	90.4	227.7	604.1	1430.4	239.7
glutathione S-transferase A	1.0	1.0	1.0	1.0	1.0
microsomal glutathione S-transferase (MGST1; GST12)	857.8	630.6	952.1	4141.5	1144.8
glutathione S-transferase 5 (GST5-5); GST mu (GSTM2)	4404.6	437.8	7004.0	1392.0	5077.6
glutathione S-transferase theta 1 (GST theta 1; GSTT1)	1.0	1.0	1.0	1.0	1.0
glutathione S-transferase Pi 1 (GSTPIB); GST YF-YF	3102.6	604.0	3377.8	4392.4	1602.7
etoposide induced p53 responsive (EI24) mRNA	1.0	173.6	1.0	287.2	96.5
oxidative stress-induced protein mRNA	225.5	390.3	1.0	1.0	193.8
ELECTROCARDIOGRAPHIC QT SYNDROME 2 POTASSIUM CHANNEL SUBUNIT	85.5	283.6	1.0	1.0	1.0
POTASSIUM CHANNEL	1.0	219.3	1.0	52.4	1.0
potassium channel, subfamily K, member 2	1.0	28.5	2.8	257.1	70.6
potassium inwardly-rectifying channel, subfamily J, member 12	1.0	1.0	1.0	130.6	1.0
potassium large conductance calcium-activated channel, subfamily M, alpha member 1	1.0	19.1	49.3	11.3	22.3
potassium voltage gated channel, Shab-related subf	472.8	481.9	185.2	297.4	270.6
potassium voltage-gated channel, Isk-related subfamily, member 1	1.0	7.4	1.0	103.9	1.0
voltage-gated potassium channel protein KQT-like 1 (KVLQT1); potassium voltage-gated channel subfamily Q member 1 (KCNQ1); KCNA9; KV1.9	16.8	46.8	0.7	43.8	163.3
acetylcholine receptor delta submit	1.0	1.0	1.0	229.4	1.0
glutamate receptor; ionotropic NMDA2A (epsilon 1)	1.0	1.0	1.0	14.2	1.0
glutamate receptor; ionotropic NMDA2B (epsilon 2)	15.6	350.0	1.0	1.0	1.0
nicotinic acetylcholine receptor	16.7	1462.9	1.0	1.0	1.0
calcium-activated potassium channel beta subunit; maxi K channel beta subunit; BK channel beta subunit; SLO-beta; K(VCA)beta	45.1	1.0	1.0	36.2	1.0
voltage-gated sodium channel	1.0	1.0	1.0	42.1	1.0
CCHB3; calcium channel (voltage-gated; dihydropyridine-sensitive; L-type) beta-3 subunit)	294.8	553.2	201.7	981.7	127.4
sodium-dependent serotonin transporter; 5HT transporter (5HTT)	13.2	1.0	1.0	79.5	1.0
sodium-dependent noradrenaline transporter; norepinephrine transporter (NET)	238.5	1.0	152.2	1.0	1.0
SYNAPTIC VESICLE MEMBRANE PROTEIN VAT-1 HOMOLOG (FRAGMENT)	265.9	1.0	287.2	1.0	67.2
SYNAPTOTAGMIN III (SYTIII)	1.0	1.0	22.7	1.0	1.0
SYNAPTOTAGMIN VIII (FRAGMENT)	31.5	521.4	480.7	130.5	55.3
SODIUM- AND CHLORIDE-DEPENDENT GLYCINE TRANSPORTER 1 (GLYT-1).	343.9	1.0	107.7	221.0	532.1
SODIUM/HYDROGEN EXCHANGER 1 (NA(+)/H(+)) EXCHANGER 1 (NHE-1) (NA+/H+ ANTIporter, AMILORIDE-SENSITIVE)	1322.6	535.2	1392.5	438.9	811.6
High affinity glutamate transporter; EAAC1 EXCITATORY AMINO ACID TRANSPORTER 3 (SODIUM-DEPENDENT GLUTAMATE/ASPARTATE TRANSPORTER 3) (EXCITATORY AMINO-ACID CARRIER 1).	194.9	1.0	175.6	298.7	60.1
sodium- & chloride-dependent GABA transporter 1 (GABT1; GAT1); SLC6A1	55.0	132.1	166.6	81.9	113.5
GABA-A transporter 3	148.8	1.0	1.0	61.7	1.0
sodium- & chloride-dependent GABA transporter 3 (GABT3; GAT3); GAT4	1.0	319.3	1.0	89.5	1.0
Monocarboxylate transporter MCT1	1.0	203.4	8.5	203.6	113.6

PMCA; ATP2B2; calcium-transporting ATPase plasma membrane (brain isoform 2)	298.0	204.6	286.1	116.9	158.1
ATP-binding cassette 8; ABC8; homolog of Drosophila white solute carrier family 1, member 2	1.0	137.3	1.0	88.2	1.0
solute carrier family 1, member 2	1.0	115.4	1.0	1.0	1.0
solute carrier family 1, member 6	1.0	179.8	13.3	1.0	1.0
solute carrier family 1, member 7	72.9	1.0	82.2	1.0	167.4
solute carrier family 2 (facilitated glucose trans	1.0	2228.7	108.9	1.0	1.0
VESICULAR ACETYLCHOLINE TRANSPORTER (SOLUTE CARRIER FAMILY 18, MEMBER DE 3)	1.0	1.0	129.3	1.0	1.0
Golgi 4-transmembrane spanning transporter (MTRP; MTP)	343.8	355.2	307.1	8909.2	191.7
ZINC TRANSPORTER 4.=	1.0	1.0	246.5	1.0	131.0
myelin protein zero	1.0	73.6	1.0	1.0	301.0
myelin-associated oligodendrocytic basic protein	1.0	1.0	1.0	1.0	108.8
multidrug resistance protein 1 (MDR1); P-glycoprotein 1 (PGY1)	1.0	1.0	1.0	28.5	32.3
prostaglandin D2 synthase (21 kDa, brain)	177.8	245.2	1.0	193.3	165.1
prostaglandin I2 (prostacyclin) synthase	108.9	466.7	165.0	1579.7	226.9
fatty acid amide hydrolase (FAAH); oleamide hydrolase	1.0	1.0	1.0	5.1	1.0
acetylcholinesterase precursor (ACHE)	54.5	120.7	61.2	0.3	54.8
neuroendocrine convertase 1 precursor (NEC 1); prohormone convertase 1 (PC1); proprotein convertase 1	1.0	1.0	1.0	384.6	9.3
neuroendocrine convertase 2 precursor (NEC 2); prohormone convertase 2 (PC2); proprotein convertase 2; KEX2-like endoprotease 2	1.0	1.0	10.9	13.5	1.0
tryptophan 5-hydroxylase (TRPH); tryptophan 5-monoxygenase	19.1	30.5	1.0	41.1	1.0
histidine decarboxylase (HDC)	318.4	197.9	1.0	115.3	221.9
phenylalanine-4-hydroxylase (PAH); phe-4-monoxygenase	1.0	503.8	106.4	4.7	1.0
tyrosine 3-hydroxylase (TYH); tyrosine 3-monoxygenase isozymes	1.0	120.5	1.0	1.0	1.0
dopamine beta-hydroxylase (DBH); dopamine-beta-monoxygenase precursor	61.7	1.0	242.7	23.5	8.3
phenylethanolamine N-methyltransferase (PNMTase); noradrenaline N-methyltransferase	1.0	166.6	1.0	1.0	142.7
ERp72 endoplasmic reticulum stress protein; protein disulfide isomerase-related protein	468.8	810.6	776.0	665.2	586.9
major prion protein precursor (PRP); PRP27-30; PRP33-35C; ASCR	748.5	1125.1	62.2	471.0	663.0
40S ribosomal protein SA; p40-8; lamimin receptor 1 (LAMR1); 34/67-kDa laminin receptor	8995.6	8100.6	4300.5	2139.3	6604.4
SURVIVAL OF MOTOR NEURON (hSMN)	1600.6	1.0	1.0	374.9	1.0
growth arrest and DNA-damage-inducible protein 45 (GADD45); DNA-damage-inducible transcript 1 (DDIT1)	127.6	64.4	150.7	728.4	137.7
CD40L; CD40 ligand	64.1	1.0	1.0	3.6	1.0
fas antigen ligand (FASL); generalized lymphoproliferation disease protein (GLD); TNFSF6; APT1LG1	1.0	1.0	1.0	1.0	14.8
TNF-related apoptosis inducing ligand (TRAIL); TNFSF10	1.0	1717.9	1.0	132.8	47.7
retinoic acid receptor beta-2 (beta2-RAR)	74.2	212.7	78.2	105.0	117.5
RXR-beta cis-11-retinoic acid receptor	128.0	88.7	215.1	93.2	1.0
insulin-like growth factor I receptor alpha subunit (IGF-I-R alpha)	732.3	1085.2	261.7	333.7	453.1
Fas I receptor; Fas antigen (Apo-1 antigen)	170.0	112.3	102.4	616.0	119.4
CD27L receptor precursor; T-cell activation antigen CD27; TNFRSF7	199.7	149.5	280.7	141.6	51.8
CD 30L receptor; lymphocyte activation antigen CD 30; Ki-1 antigen	160.4	1201.3	110.7	76.6	1.0
tumor necrosis factor receptor 1 precursor (TNFR1); TNFRSF1A	70.9	1.0	112.8	100.2	1.0
tumor necrosis factor receptor 2 precursor (TNFR2); TNFRSF1B2	87.4	1.0	1.0	73.5	1.0
adenosine A2A receptor (ADORA2A)	190.9	105.7	1.0	110.2	229.0
adenosine A3 receptor	1.0	305.0	1.0	1.0	1.0
adenosine A1M receptor	40.8	340.5	1.0	1.0	1.0
TNF receptor-associated factor 3 (TRAF3); CD40 receptor-associated factor 1 (CRAF1); TRAFAMN	96.2	226.1	86.6	58.4	29.1
fas-associated factor 1 (FAF1)	174.5	615.7	260.5	308.6	180.7
STAM; signal transducing adaptor molecule	298.5	1.0	1.0	179.2	105.5
receptor interacting protein (RIP; RINP)	42.8	162.5	1.0	257.6	56.7
RIP-associated protein with a death domain (RAIDD); caspase & RIP adaptor with death domain (CRADD)	63.9	194.8	1.0	47.0	94.9
Protein FAN (factor associated with N-smase activation).	447.9	266.6	124.5	104.5	177.5
caspase-2 precursor (CASP2); NEDD2 protein; ICH-1 protease	24.1	302.7	1.0	69.3	1.0
caspase-7; Lice2; ICE-LAP3 cysteine protease	62.3	375.4	1.0	54.3	150.2

caspace-11; ICH-3 cysteine protease; upstream regulator of ICE	1.0	636.7	1.0	1.0	145.1
interleukin-converting enzyme (ICE)	418.7	261.0	1087.2	253.0	479.8
activator of apoptosis harakiri (HRK); neuronal death protein 5 (DP5); BID3	1.0	153.4	140.9	11.6	1.0
BAD protein; BCL2 binding component 6 (BBC6)	45.4	439.5	58.2	166.7	1.0
BCL2 binding athanogene 1 (BAG1)	491.7	403.6	441.9	1033.1	104.8
BAX membrane isoform alpha	347.1	80.9	111.9	386.9	440.9
B-cell lymphoma protein W (BCLW); BCL2L2	50.2	572.6	1.0	3.6	1.0
bcl-x; BCL2L1	349.6	536.5	1.0	42.8	1.0
Mcl-1; induced myeloid leukemia cell differentiation protein	94.0	158.3	1.0	1.0	1.0
BH3 interacting domain death agonist (BID)	80.9	131.8	1.0	132.9	1.8
NIP3; Bcl-2 and adenoviral E1B-interacting protein	13.7	180.0	1.0	89.4	1.0
bcl-2 homologous antagonist/killer (BAK1)	398.6	377.0	660.9	772.9	309.9
B-cell lymphoma protein 2 (BCL2)	204.8	453.7	1.0	66.7	88.6
Granzyme A (EC 3.4.21.78) (T cell-specific serine protease 1) (TSP-1) (CTLA-3) (fragmentin 1) (autocrine thymic lymphoma granzyme-like serine protease).	255.9	177.0	1.0	80.9	20.2
granzyme B(G,H) precursor (GZMB); cytotoxic cell protease 1 (CCP1); CTLA1; fragmentin 2	139.8	204.1	1.0	1.0	13.6
rac alpha serine/threonine kinase (RAC-PK-alpha); C-akt proto-oncogene; protein kinase B (PKB)	2308.6	876.7	2024.4	2473.5	1482.7
T-cell death-associated protein (TDAG51)	950.8	1.0	1330.0	161.5	561.7
interleukin 1 receptor antagonist	1.0	102.1	1.0	40.0	3.0
programmed cell death 2	220.2	15.6	32.3	148.6	1.0
Apaf-1; apoptotic protease activating factor 1	0.3	1.0	1.0	80.6	1.0
programmed cell death 1 protein precursor (PDCD-1; PD-1)	48.1	180.3	1.0	70.6	1.0
FLICE-like inhibitory protein long form (FLIP-L)	118.5	204.7	1.0	8.7	98.4
defender against cell death 1 (DAD1)	170.2	289.4	1.0	162.6	276.5
miAP3; inhibitor of apoptosis protein 3 (X-linked inhibitor of apoptosis protein) (X-linked IAP) (IAP homolog A) (MIAP-3).	104.9	125.2	1.0	45.3	77.3
interleukin-1 receptor	1.0	395.6	1.0	160.9	109.3
nur77 early response protein; nuclear hormone receptor (HMR); N10 nuclear protein; GFRP; NR4A1	1.0	1.0	1.0	1.0	1.0
clusterin precursor (CLU); clustrin; apolipoprotein J (APOJ); sulfated glycoprotein 2 (SGP2; MSGP2)	66.4	502.3	205.0	24.3	128.1
NADPH-cytochrome P450 reductase (CPR); POR	348.9	1.0	244.6	126.1	102.9
fms-related tyrosine kinase 3 Flt3/Flk2 ligand	199.0	1.0	1.0	71.3	1.0
probable calcium-binding protein ALG2; PMP41; ALG-257	2.2	115.6	1.0	441.5	1.0
angiotensin-converting enzyme (ACE) (clone ACE.5.)	349.7	402.1	1.0	83.7	1.0
Sentrin; ubiquitin-like protein SMT3C; ubiquitin-homology domain protein PIC1; UBL1; SUMO-1; GAP modifying protein 1; GMP1 growth arrest & DNA-damage-inducible protein 153 (GADD153); DNA-damage-inducible transcript 3 (DDIT3); C/EBP-homologous protein (CHOP)	98.6	136.0	1.0	82.5	87.9
inducible nitric oxide synthase (INOS); type II NOS; macrophage NOS; NOS2	36.5	1.0	1.0	1.0	1.0
presenilin 2 (PSEN2; PSNL2; PS2); ALG3; Alzheimer disease 4 homolog (AD4H)	11.9	1.0	178.2	131.3	112.4
cytoplasmic dynein light chain 1; protein inhibitor of neuronal nitric oxide synthase (mPIN)	823.9	1.0	1945.9	1784.9	1291.1
T-cell-specific surface glycoprotein CD28 precursor	85.3	1.0	1.0	1.0	1.0
ERBB-2 receptor; c-neu; HER2 protein tyrosine kinase	250.7	1.0	251.8	296.9	388.1
ERBB-3 receptor	150.9	1.0	63.1	444.1	317.1
pre-platelet-derived growth factor receptor	1.0	359.9	1.0	438.3	1.0
C-C chemokine receptor; monocyte chemoattractant protein 1 receptor (MCP-1RA)	100.3	25.7	1.0	21.2	1.0
C5A receptor	97.8	1.0	13.5	1.0	99.0
corticotropin releasing factor receptor	87.0	1.0	1.0	1.0	85.6
endothelin b receptor (Ednrb)	208.8	1.0	329.3	395.6	522.8
CD 40L receptor (TNF receptor family)	1.0	1.0	1.0	157.2	1.0
granulocyte colony - stimulating factor receptor precursor (GCSF receptor; GCSFR; CSFGR); CSF3R	71.3	223.8	8.5	1.0	1.0
erythropoietin receptor precursor (EPOR)	202.3	1.0	234.0	59.3	224.3
fibroblast growth factor receptor 4	25.0	229.4	1.0	5.7	1.0
basic fibroblast growth factor receptor 1 precursor (BFGF-R; FGFR1); MFR; FLG	1749.6	597.1	472.2	401.7	1155.2
granulocyte-macrophage colony-stimulating factor receptor low-affinity subunit precursor (GM-CSF-R)	5511.6	2348.3	4931.2	4359.0	6195.0

activin type I receptor	175.2	1.0	1.0	1.0	69.2
bone morphogenetic protein receptor IA (BMPRI1A); BMP2/BMP4 receptor; serine/threonine-protein kinase receptor R5 (SKR5); activin receptor-like kinase 3 (ACVRLK3; ALK3)	53.5	363.7	1.0	46.0	3.0
tyrosine-protein kinase ryk precursor; kinase vik; nyk-R	1562.6	379.4	759.3	2933.8	2052.1
transforming growth factor beta receptor 1 (TGF-beta receptor 1; TGFR1); ESK2	240.4	1.0	120.2	1.0	24.1
G-protein-coupled receptor	1.0	100.8	1.0	79.0	1.0
TGF-beta receptor type III (betaglycan); candidate tumor suppressor gene	1.0	245.6	235.3	124.5	245.8
insulin-like growth factor receptor II (IGFR II); cation-independent mannose-6-P receptor; elevated in Wilms's tumor cells	573.2	441.5	332.6	449.2	439.4
interferon alpha-beta receptor	1.0	1.0	71.9	40.7	36.3
interleukin-6 receptor alpha subunit precursor (IL-6R alpha; IL6RA)	150.4	106.2	205.8	5.8	149.3
interferon-gamma receptor	64.4	360.4	218.0	98.9	22.7
interleukin-1 receptor type II precursor (IL-1R-2; IL1RB)	126.0	4443.5	1.0	47.1	1.0
interleukin-10 receptor precursor ( IL10R)	122.9	1.0	1.0	45.9	1.0
cytokine receptor common gamma subunit precursor (gamma-C); interleukin-2 receptor gamma subunit (IL-2R gamma; IL2RG)	2.7	58.4	1.0	22.9	1.0
interleukin-3 receptor	1.0	1.0	1.0	1.0	99.5
interleukin-4 receptor alpha subunit precursor (IL-4R-alpha; IL4RA)	1.0	1.0	1.0	1.0	1.0
interleukin-5 receptor alpha subunit precursor (IL-5R alpha; IL5RA)	50.0	1.0	58.8	1.0	1.0
interleukin-7 receptor alpha (IL-7 receptor alpha; IL-7R alpha)	239.8	1.0	1.0	50.9	1.0
interleukin-8 receptor	1.0	1.0	14.1	1.0	83.8
interleukin-9 receptor (IL9R)	1.0	1.0	5.5	1.0	1.0
cholecystokinin	2.3	1.0	1.0	21.4	18.7
cholecystokinin A receptor	154.6	1.0	109.9	33.7	192.3
corticotropin releasing hormone receptor 2	1.0	351.7	18.5	29.6	1.0
galanin receptor 1	1.0	105.4	1.0	11.3	1.0
growth hormone releasing hormone receptor	1.0	89.3	1.0	1.0	1.0
leptin receptor	103.8	1.0	13.5	43.4	1.0
melanocortin 3 receptor	1.0	1.0	108.3	50.9	1.0
melanocortin 5 receptor	1.0	1.0	1.0	39.3	1.0
prostaglandin F receptor	1.0	1.0	1.0	30.0	1.0
prostaglandin I receptor (IP)	74.4	536.5	171.6	49.9	1.0
insulin receptor	143.1	266.2	171.4	124.6	52.9
CALCITONIN GENE-RELATED PEPTIDE-RECEPTOR COMPONENT PROTEIN (CGRP-RECEPTOR COMPONENT PROTEIN).	168.7	1.0	68.1	227.6	303.8
calcitonin receptor 1b	329.0	1.0	1.0	50.1	107.7
adrenergic receptor, beta 2	1.0	1.0	1.0	0.8	1.0
somatostatin receptor 5	1.0	1.0	1.0	1.0	1.0
thromboxane A2 receptor	210.8	64.2	1.0	18.6	1.0
vasoactive intestinal peptide receptor 2	43.4	444.4	1.0	86.2	1.0
androgen receptor	1.0	1.0	64.3	1.0	164.7
STEROID HORMONE RECEPTOR ERR1 (ESTROGEN-RELATED RECEPTOR, ALPHA) (ERR-ALPHA) (ESTROGEN RECEPTOR-LIKE 1)	1.0	1.0	67.7	1.0	153.5
STEROID HORMONE RECEPTOR ERR2 (ESTROGEN-RELATED RECEPTOR, BETA) (ERR-BETA) (ESTROGEN RECEPTOR-LIKE 2)	1.0	1.0	21.1	1.0	85.4
estrogen receptor	118.9	510.2	195.2	63.2	210.6
glucocorticoid receptor form A	62.9	1.0	137.0	125.6	28.9
growth hormone receptor	79.2	1.0	1.0	161.5	1.0
prolactin receptor PRLR2	1.0	1.0	1.0	39.3	1.0
somatostatin receptor 2	205.8	780.6	1.0	67.5	235.3
orphan receptor	40.8	1.0	4.0	62.6	19.7
gamma-aminobutyric acid (GABA-A) receptor, subunit	202.0	1.0	154.9	51.1	258.5
gamma-aminobutyric acid (GABA-A) receptor, subunit beta 2	1.0	28.7	1.0	12.5	1.0
gastrin releasing peptide receptor	8.9	276.9	1.0	56.1	61.4
glutamate receptor, ionotropic, delta 1	84.9	186.1	43.1	1.0	205.7
oxytocin receptor	45.0	169.0	1.0	217.3	110.3
glutamate receptor; ionotropic AMPA 1	198.6	250.7	139.2	24.4	63.4
GLUTAMATE (NMDA) RECEPTOR SUBUNIT ZETA 1 PRECURSOR (NR1) (NMD-R1) (N-METHYL-D-ASPARTATE RECEPTOR).	1.0	1.0	81.1	28.1	70.3

5-hydroxytryptamine (serotonin) receptor 3	1.0	1.0	150.6	88.4	167.7
5-hydroxytryptamine 1A receptor (5-HT-1A); serotonin receptor	28.1	18437.4	75.5	43.9	45.5
mu-type opioid receptor (MOR-1)	1.0	160.7	41.1	11.8	98.7
nociceptin receptor; orphanin FQ receptor; kappa-type 3 opioid receptor (KOR-3)	281.9	1.0	1.0	32.5	109.5
neuropeptide Y receptor type 1 (NPY1-R)	167.1	1.0	90.7	50.7	107.3
melanocortin-4 receptor (MC4-R)	88.0	1.0	1.0	1.0	1.0
melatonin receptor type 1A (MEL-1A-R)	61.9	21.0	4.9	1.0	1.0
Gastrin/cholecystokinin type B receptor (CCK-B receptor) (CCK-BR).	147.0	34.0	169.9	29.8	105.1
acetylcholine receptor alpha	97.2	224.4	0.5	44.3	86.3
acetylcholine receptor alpha 7 neural	101.6	226.6	1.0	56.7	1.0
glutamate receptor 5 precursor (GLUR-5); ionotropic glutamate receptor kainate1	1.0	258.3	1.0	138.3	1.0
gamma-aminobutyric-acid receptor alpha-1 subunit precursor (GABA-A receptor alpha-1 subunit; GABA(A) receptor; GABRA1)	66.1	162.6	68.9	11.9	203.5
5-hydroxytryptamine receptor; serotonin receptor type 2 (5HT2)	57.2	1.0	1.0	1.0	335.5
5-hydroxytryptamine receptor 1B receptor (5HT1B; HTR1B); serotonin receptor	1.0	100.2	6.5	1.0	1.0
5-hydroxytryptamine (serotonin) receptor 1c	62.7	1.0	21.2	1.0	128.2
5-hydroxytryptamine (serotonin) receptor 1e beta	122.1	1.0	1.0	1.0	63.7
5-hydroxytryptamine (serotonin) receptor 2c	1.0	1.0	1.0	59.3	1.0
5-hydroxytryptamine (serotonin) receptor 7	1.0	188.7	1.0	26.0	1.0
adrenergic receptor beta 1	12.3	111.1	1.0	1.2	195.0
cannabinoid receptor 1 (brain)	1.0	105.5	1.0	1.0	1.0
macrophage cannabinoid receptor 2 (CB2)	1.0	409.1	1.0	54.1	1.0
dopamine receptor 4	52.7	1.0	1.0	1.0	1.0
G-protein coupled receptor	1.0	311.2	1.0	15.9	1.0
proteinase-activated receptor 3 precursor (PAR3); thrombin receptor 2	1.0	1.0	1.0	35.9	68.2
presynaptic density protein 95 (PSD-95)	169.8	90.2	282.7	327.4	660.9
D-factor/LIF receptor	21.0	1.0	189.2	180.6	197.4
lymphotoxin receptor (TNFR family)	163.5	284.3	239.8	110.0	229.1
C type 1 mannose receptor precursor (MRC1); macrophage mannose receptor	1.0	1.0	1.0	664.7	0.8
low-density lipoprotein receptor precursor (LDL receptor; LDLR)	448.8	1.0	188.6	1.0	479.6
delta-like protein 1 precursor (delta1; DLL1)	75.4	1.0	1.0	1.0	20.3
epimorphin (EPIM); syntaxin 2	200.4	33.0	289.7	59.3	390.2
myelin proteolipid protein (PLP); lipophilin; DM20	57.6	59.7	1.0	1.0	1.0
neuroblastoma suppression of tumorigenicity protein1 (NBL1); differential screening selected gene aberrative in neuroblastoma (DAN)	265.1	257.7	158.5	463.4	389.4
pro-opiomelanocortin-alpha (POMC)	19.5	344.7	1.0	1.0	27.2
beta-protachykinin a	1.0	167.7	1.0	1.0	58.3
proenkephalin A precursor	2069.6	1132.7	5629.0	4179.2	2061.4
beta-neoendorphin-dynorphin precursor; proenkephalin B precursor; prodynorphin	37.0	1.0	1.0	1.0	219.5
Galanin precursor	1.0	1.0	1.0	1.0	26.7
Secretogranin II precursor (SGII); chromogranin C	1.0	1.0	1.0	9.6	22.3
7B2 neuroendocrine protein , NEUROENDOCRINE PROTEIN 7B2 PRECURSOR (SECRETAGRANIN V)	1.0	73.3	1.0	85.4	83.7
Nociceptin precursor; ORL1 receptor agonist precursor (endogenous agonist of opioid receptor-like ORL1 receptor; orphanin FQ; PPNO)	1.0	175.1	32.5	1.0	244.5
prepro-orexin	1.0	297.5	1.0	1.0	34.6
CILIARY NEUROTROPHIC FACTOR (CNTF).	84.0	1.0	1.0	3.6	1.0
monotype chemoattractant protein 3	67.9	1.0	248.8	1.0	43.6
PLEIOTROPHIN PRECURSOR (PTN) (HEPARIN-BINDING GROWTH-ASSOCIATED MOLECULE) (HB-GAM) (HEPARIN-BINDING GROWTH FACTOR 8) (HBGF-8) (OSTEOBLAST SPECIFIC FACTOR 1) (OSF-1) (HEPARIN-BINDING NEUTROPHIC FACTOR) (HBNF).	524.2	180.7	157.8	24.8	808.8
THYMOSIN BETA-4.	866.1	1487.0	1677.8	3149.1	1199.6
androgen-induced growth factor precursor (AIGF); fibroblast growth factor 8 (FGF8); HBGF8	1.0	83.8	1.0	1.0	1.0
bone morphogenetic protein 1 precursor (BMP1)	399.0	253.6	239.8	372.1	680.9
bone morphogenetic protein 2 (BMP-2) (TGF-beta family)	236.6	92.5	1.0	46.2	142.9
bone morphogenetic protein 4 precursor (BMP4); BMP2B; DVR4	93.8	1.0	1.0	2.2	225.1

bone morphogenetic protein 7 (BMP-7); osteogenic protein 1	328.0	382.1	209.4	35.7	352.1
bone morphogenetic protein 8a (BMP-8a) (TGF-beta family)	296.0	1.0	1.0	98.0	73.3
Cek 5 receptor protein tyrosine kinase ligand	1216.6	255.3	670.8	582.5	1586.7
ephrin A2 precursor (EFNA2); eph-related receptor tyrosine kinase ligand 6 (EPLG6; LERK6); ELF1; CEK7 ligand (CEK7-L)	1.0	31.5	29.1	1.0	312.3
endothelial ligand for L-selectin (GLYCAM 1)	1.0	0.6	1.0	1.0	1.0
epidermal growth factor (EGF)	1.0	1.0	33.1	1.0	1.0
fibroblast growth factor 9	1.0	194.5	13.2	25.2	1.0
folliculin precursor (FST); activin-binding protein	169.9	277.8	173.4	8.8	494.1
gamma interferon-induced monokine precursor (MIG); M119	1.0	1.0	1.0	1.0	1.0
glial cell line-derived neurotrophic factor	1.0	1.0	412.4	1.0	1.0
granulocyte colony-stimulating factor (GCSF; CSFG); colony stimulating factor 3 (CSF3)	4.1	1.0	1.0	1.0	1.0
growth/ differentiation factor 1 (GDF-1) (TGF- beta family)	96.3	1.0	1.0	2.0	1.0
growth differentiation factor 9 (GDF9)	281.0	1.0	16.8	83.7	48.7
heparin-binding EGF-like growth factor (HBEGF; HEGFL); diphtheria toxin receptor (DTR)	144.5	15.5	266.7	83.4	146.3
hepatocyte growth factor (HGF)	82.9	1.0	1.0	133.7	1.0
hepatoma transmembrane kinase ligand	123.3	1.0	320.9	307.1	223.9
inhibin alpha subunit precursor (INHA)	993.3	1.0	500.2	242.1	638.1
inhibin beta A subunit precursor (INHBA); activin beta A subunit	65.0	1.0	1.0	127.0	64.2
insulin-like growth factor binding protein -6 (IGFBP 6)	2171.6	1.0	4817.6	993.3	4125.5
insulin-like growth factor binding protein-1 (IGFBP-1)	1.0	1.0	1.0	18.3	1.0
insulin-like growth factor binding protein 3 (IGF-binding protein 3; IGFBP3; IBP3)	586.5	180.6	497.3	160.8	854.2
insulin-like growth factor binding protein 4 precursor (IGF-binding protein 4; IGFBP4; IBP4)	2645.6	2269.5	3526.7	6153.9	3464.1
insulin-like growth factor binding protein 5 precursor (IGF-binding protein 5; IGFBP5; IBP5)	4275.6	2985.7	2303.9	237.8	5968.3
insulin-like growth factor II precursor (IGF-II; IGF2); multiplication-stimulating polypeptide	13669.6	5459.4	5906.2	1057.1	8365.8
insulin-like growth factor-1A	860.7	100.7	2839.1	2563.4	1985.4
keratinocyte growth factor FGF-7	23.5	1.0	1.0	1.0	1.0
fibroblast growth factor 4 precursor (FGF4); KFGF; HBGF4	1.0	1.0	25.3	70.5	1.0
leukemia inhibitory factor (LIF); cholinergic differentiation factor	41.5	48.6	1.0	79.2	1.0
small inducible cytokine A3 precursor (SCYA3); macrophage inflammatory protein 1 alpha (MIP1A); TY-5; SIS-alpha; heparin-binding chemotaxis protein; L2G25B	90.1	87.5	1.0	87.8	26.1
macrophage inflammatory protein 1 beta (Act 2)	156.0	1.0	1.0	52.3	1.0
macrophage inflammatory protein 2 alpha (MIP2-alpha)	180.3	1.0	1.0	32.7	1.0
Mad related protein 2 (MADR2)	24.0	1.0	1.0	158.2	217.8
mast cell factor	1.0	1.0	1.0	1.0	202.1
MAX dimerization protein (MAD)	18.5	1.0	1.0	120.9	1.0
7S nerve growth factor alpha subunit (alpha-NGF; NGFA); KLK4	307.8	1.0	19932.6	5137.6	800.2
nerve growth factor beta precursor (beta-NGF; NGFB)	1.0	1.0	1.0	1.0	1.0
glucose-6-phosphate isomerase (GPI); phosphoglucose isomerase (PGI); phosphohexoseisomerase (PHI); neuroleukin (NLK)	14849.6	4613.8	6893.8	5732.7	13295.5
oncostatin M (OSM)	1.0	2.8	1.0	1.0	1.0
platelet- derived growth factor (A chain) (PDGF- A)	224.9	8.5	109.8	48.6	54.9
prepro-endothelin-3	349.5	1.0	141.8	186.2	217.1
thrombomodulin	284.0	257.3	1.0	209.5	1.0
thrombopoietin precursor (THPO); megakaryocyte colony stimulating factor (MCSF); c-mpl ligand (ML); megakaryocyte growth & development factor (MGDF)	1.0	194.1	5.5	1.0	1.0
transforming growth factor beta 1 (TGF-beta 1; TGFB1)	591.6	96.8	1285.7	544.4	542.5
transforming growth factor beta 2 precursor (TGF-beta 2; TGFB2)	1.0	107.1	1.0	198.3	1.0
tumor necrosis factor beta (TNF-beta); lymphotoxin-alpha	171.1	119.3	1.0	17.5	1.0
uromodulin	123.8	83.3	50.9	53.0	1.0
vascular endothelial growth factor precursor (VEGF); vascular permeability factor (VPF)	207.3	277.0	197.4	673.4	227.4
fibroblast growth factor 15 (FGF15)	293.4	525.2	201.6	129.6	1.0
secreted apoptosis-related protein 1 (SARP1)	1533.6	1313.6	360.0	131.7	1250.3
fibroblast growth factor 12-related protein (FGF12A); FGF homologous factor 1 (FHF1)	1.0	360.9	1.0	1.0	1.0
dickkopf homolog 1 (mDKK1)	1.0	88.5	20.9	1.0	1.0
cerberus-related protein1 (CERR1)	1.0	152.2	1.0	23.4	1.0
bone morphogenetic protein 5 precursor (BMP5)	1.0	199.3	1.0	21.8	1.0

heparin-binding growth factor 5 precursor (HBGF5); fibroblast growth factor 5 (FGF5)	112.5	428.7	46.4	33.9	1.0
heparin-binding growth factor 2 precursor (HBGF2); basic fibroblast growth factor (BFGF); prostatropin; fibroblast growth factor 2 (FGF2)	183.8	59.0	1.0	202.3	1.0
wingless-related MMTV integration site 3 protein precursor (WNT3); mammary tumor integration site 4 protein (INT4)	207.8	294.3	15.6	1.0	54.0
wingless-related MMTV integration site 4 protein precursor (WNT4)	930.6	251.7	1177.7	714.0	1218.3
wingless-related MMTV integration site 5b protein precursor (WNT5B)	1.0	284.7	1.0	136.0	171.5
wingless-related MMTV integration site 6 protein precursor (WNT6)	310.5	285.9	1.0	53.7	1.0
wingless-related MMTV integration site 7A protein precursor (WNT7A)	234.0	323.1	145.1	203.4	157.7
wingless-related MMTV integration site 7B protein precursor (WNT7B)	90.8	132.9	174.7	311.1	71.8
fibroblast growth factor 6 precursor (FGF6); heparin-binding growth factor 6 (HBGF6)	1.0	95.9	1.0	7.5	1.0
bone morphogenetic protein 3B precursor (BMP3B); growth differentiation factor (GDF10)	1048.6	537.3	113.1	689.4	577.7
wingless-related MMTV integration site 10b protein precursor (WNT10B); WNT12	1.0	576.0	1.0	1.0	9.9
wingless-related MMTV integration site 10a protein precursor (WNT10A)	1.0	145.2	1.0	25.1	86.3
fibroblast growth factor 13 (FGF13); FGF homologous factor 2 (FHF2)	1.0	3586.6	1803.9	29.1	1.0
fibroblast growth factor 11 (FGF11); FGF homologous factor 3 (FHF3)	1.0	273.9	60.3	48.8	124.7
fibroblast growth factor 14 (FGF14); FGF homologous factor 4 (FHF4)	88.3	231.7	23.4	19.9	1.0
secreted frizzled-related sequence protein 3 (SFRP3; mFIZ); frizzled	7.9	180.0	1.0	167.5	70.4
Indian hedgehog homolog (IHH); HHG2	23.5	55.9	72.7	1.0	8.7
inhibin beta-C precursor (INHBC); activin beta-C subunit	6.7	162.6	1.0	1.0	20.8
inhibin beta-E precursor (INHBE); activin beta-E subunit	6.8	123.1	30.1	49.3	1.0
wingless-related MMTV integration site 3A protein precursor (WNT3A)	1.0	247.7	1.0	77.6	1.0
nodal precursor	1.0	97.0	22.3	153.9	1.0
wingless-related MMTV integration site 11 protein precursor (WNT11)	106.7	101.5	1.0	119.0	1.0
sonic hedgehog homolog (SHH); HHG1	1.0	1.0	1.0	27.9	1.0
desert hedgehog homolog precursor (DHH); HHG3	20.1	1.0	1.0	1.0	45.1
bone morphogenetic protein 6 precursor (BMP6); vg-1-related protein 1 (VGR1)	35.0	186.7	1.0	1.0	350.5
inhibin beta-B precursor (INHBB); activin beta-B subunit	81.1	361.4	702.7	1804.4	375.4
stimulated by retinoic acid protein 11 (STRA11); wingless-related MMTV integration site 8D protein precursor (WNT8D)	1.0	115.7	1.0	10.5	186.3
placental ribonuclease inhibitor; angiogenin	340.9	402.5	274.3	165.1	189.4
relaxin	99.7	55.0	1.0	92.4	10.3
preproglucagon	135.0	1.8	176.4	89.3	1.0
corticotropin releasing hormone binding protein	1.0	62.8	1.0	1.0	22.1
INTERFERON BETA PRECURSOR (IFN-BETA)	99.7	97.0	1.0	13.6	1.0
interleukin-1 beta precursor (IL-1 beta; IL1B)	77.1	20.2	1.0	40.2	13.6
interleukin 10	266.6	47.3	1.0	1.0	1.0
interleukin 11 (IL-11)	47.0	90.7	1.0	1.0	117.9
interleukin 12 (p40) beta chain	1.0	48.0	99.3	20.1	1.0
interleukin 15	41.4	127.8	426.6	334.2	12.6
interleukin 4	1.0	99.2	54.0	1.0	96.2
INTERLEUKIN-6 PRECURSOR (IL-6) (INTERLEUKIN HP-1) (B-CELL HYBRIDOMA GROWTH FACTOR)	1.0	1.0	1.0	108.2	0.3
interleukin-7 precursor (IL-7)	86.1	1.0	1.0	1.0	1.0
chromogranin A	1.3	32.3	1.0	18.4	34.9
chromogranin B	1.0	277.3	1.0	13.3	25.4
NEUROMODULIN (AXONAL MEMBRANE PROTEIN GAP-43) (PP46) (B-50) (PROTEIN F1) (CALMODULIN-BINDING PROTEIN P-57)	1.0	1.0	1.0	458.6	228.6
TGF-beta-activated kinase 1 (TAK1); mitogen-activated protein kinase kinase kinase 7 (MAP3K7)	65.7	109.2	86.3	229.6	147.3
zipper (leucine) protein kinase (ZPK); serine/threonine protein kinase dlk	247.2	203.5	62.3	119.0	129.1
tolloid-like protein (TLL)	1.0	1.0	1.0	25.4	1.0

manic fringe homolog precursor (MFNG)	1.0	1.0	73.0	157.3	213.9
radical fringe homolog precursor (RFNG)	1.0	154.8	90.2	226.5	87.2
lunatic fringe homolog precursor (LFNG)	34.4	212.3	1.0	109.0	1.0
maternal embryonic leucine zipper kinase (MELK)	131.5	118.7	1.0	162.9	184.5
axin	178.1	197.8	38.2	271.4	142.5
MAD homolog 7 (MADH7; SMAD7); MADH8	75.9	369.6	123.3	464.1	63.7
SMAD3	206.9	1.0	131.0	120.3	483.8
S-arrestin; retinal S-antigen (SAG); 48-kDa protein; rod photoreceptor arrestin	188.8	288.1	1.0	65.3	5.0
segment polarity protein dishevelled homolog 1 (DVL1); DSH homolog 1	202.6	1.0	1698.2	659.8	356.7
MAD homolog 5 (MADH5); SMAD5	231.6	1.0	1.0	164.6	180.6
recoverin (RCV1; RCVRN); cancer-associated retinopathy protein (CAR protein); 23-kDa photoreceptor cell-specific protein	1.0	1.0	1.0	26.4	5.9
suppressor of cytokines signaling protein 5 (SOCS5)	51.5	1.0	1.0	1.3	1.0
aplysia ras-related homolog D (RHOD; ARHD)	1.0	1.0	1.0	47.1	1.0
rho GDP dissociation inhibitor beta (GDI-beta; ARHGDI3); GDP dissociation inhibitor D4 (GDID4)	1.0	273.1	91.1	136.1	1.0
segment polarity protein dishevelled homolog 3 (DVL3); DSH homolog 3	324.4	256.6	556.0	139.5	308.3
cytokine inducible SH2-containing protein 7 (CISH7); suppressor of cytokines signaling protein 1 (SOCS1); STAT-induced STAT inhibitor 1 (SSI1)	142.9	49.8	514.3	244.9	360.5
cytokine inducible SH2-containing protein 2 (CISH2); suppressor of cytokines signaling protein 2 (SOCS2)	154.3	245.9	199.4	384.6	209.5
cytokine inducible SH2-containing protein 3 (CISH3); suppressor of cytokines signaling protein 3 (SOCS3)	177.9	1.0	45.3	449.6	212.6
DNA fragmentation factor alpha subunit (DFFA); inhibitor of caspase-activated DNase (ICAD-S)	90.4	1.0	1.0	48.3	205.7
DNase inhibited by DNA fragmentation factor (DIDFF); caspase-activated DNase (CAD)	1.0	968.5	1.0	1.0	21.5
prostaglandin E2 receptor EP4 subtype (PGE receptor EP4 subtype; PTGER4); prostanoid EP4 receptor	1.0	1.0	1.0	30.3	1.0
LFA1-alpha; integrin alpha L; leukocyte adhesion glycoprotein LFA-1 alpha chain; antigen CD11A (p180)	95.1	1.0	1.0	30.4	1.0
B7-2; T-lymphocyte activation antigen CD86; CD28 antigen ligand 2; alternative CTLA4 counter-receptor	49.4	1.0	1.0	84.8	1.0
Tie-1 tyrosine-protein kinase receptor	57.5	2299.0	1.0	1.0	231.3
C-C chemokine receptor type 1 (C-C CKR-1; CCR-1); macrophage inflammatory protein-1 alpha receptor (MIP-1alpha-R); RANTES-R	1.0	274.7	1.0	1.0	31.9
Eph3 (Nuk) tyrosine-protein kinase receptor	164.9	1.0	73.1	90.2	187.1
Etk1 (Mek4; HEK) tyrosine-protein kinase receptor HEK	1.0	82.9	1.0	1.0	15.0
Hek2 murine homolog; Mdk5 mouse developmental kinase; Eph-related tyrosine-protein kinase receptor	24.7	112.2	1.0	1.0	36.4
VEGFR2; KDR/flk1 vascular endothelial growth factor tyrosine kinase receptor	1.0	87.0	1.0	16.4	1.0
Tie-2 proto-oncogene	1.0	109.2	1.0	87.5	34.0
TRK-B; bdnf / nt-3 growth factors tyrosine kinase receptor	1.0	1.0	15.7	117.8	1.0
TRK-C; NT-3 growth factor receptor precursor (TRKC tyrosine kinase) (GP145-TRKC)	21.4	10.8	69.8	208.3	48.0
TGF beta RII; TGF-beta receptor type II precursor	1.0	70.4	222.0	149.8	78.6
ephrin type B receptor 4 precursor (EPHB4); developmental kinase 2 (MDK2); tyrosine kinase myk1; HTK	531.3	93.4	281.4	394.3	418.6
Cf2r; coagulation factor II (thrombin) receptor	325.0	310.9	409.9	542.0	263.9
LCR-1; CXCR-4; CXC (SDF-1) chemokine receptor 4; HIV coreceptor (fusin); G protein-coupled receptor LCR1 homolog	27.9	1.0	89.0	107.4	48.0
PAR4; protease-activated receptor 4 G protein-coupled receptor; thrombin receptor	78.1	157.3	128.3	438.6	65.1
Frizzled-3; Drosophila tissue polarity gene frizzled homolog 3; dishevelled receptor	195.5	328.4	245.3	807.7	395.3
IFNgR2; interferon-gamma receptor second (beta) chain; interferon gamma receptor accessory factor-1 (AF-1)	85.4	164.6	336.8	354.2	300.2
interleukin-6 receptor beta chain; membrane glycoprotein gp130	515.8	675.6	468.8	950.5	964.7
uPAR1; urokinase plasminogen activator surface receptor (CD87)	1.0	256.3	1.0	1.0	1.0
cornichon-like protein (CNIL)	861.7	195.4	165.7	135.6	297.9
patched homolog 2 (PTC2; PTCH2)	1.0	60.8	1.0	152.5	1.0
bone morphogenetic protein receptor type II (BMPR2)	1.0	102.2	42.2	47.4	1.0
guanylate kinase membrane-associated inverted protein 1 (GUKMI1; MAGI-1)	34.2	114.5	8.0	130.0	69.2
frizzled homolog 9 (FZD9)	1.0	88.3	1.0	45.4	79.9

neurogenic locus notch homolog 2 (notch2)	570.4	1027.0	431.9	954.1	332.9
retinoic acid receptor gamma-A (RAR-gamma-A; RARG)	138.4	99.9	157.4	149.8	204.3
retinoic acid receptor alpha (RAR-alpha; RARA)	109.3	13.9	125.1	66.4	254.1
activin receptor IIA precursor (ACVR2A)	12.8	103.3	1.0	1.0	1.0
fibroblast growth factor 3 precursor (FGF3; mFR3); heparin-binding growth factor receptor; SAM3	1.0	1.0	1.0	1.0	1.0
activin receptor IIB precursor (ACVR2B)	168.8	132.5	1.0	1.0	115.5
retinoid X receptor alpha (RXR-alpha; RXRA)	1716.6	526.8	2074.4	1301.4	2245.4
frizzled homolog 4 (FZD4)	1.0	203.5	1.0	1.0	1.0
frizzled homolog 6 (FZD6)	1364.6	543.2	776.3	706.9	2188.1
frizzled homolog 7 (FZD7)	176.0	349.7	84.5	160.0	247.7
frizzled homolog 8 (FZD8)	0.2	264.2	139.0	15.3	260.5
patched homolog 1 (PTC1; PTCH)	298.7	153.5	194.2	93.5	397.4
neurogenic locus notch homolog 3 precursor (notch3)	27.7	53.4	1.8	63.0	97.2
neurogenic locus notch homolog 1 precursor (notch1); notch protein	679.2	368.5	615.5	628.7	761.8
syndecan 1 (SYND1)	418.6	553.5	667.4	1589.1	481.7
bone morphogenic protein receptor type 1B (BMPRI1B); serine/threonine-protein kinase receptor 6 (SKR6); activin receptor-like kinase 6 (ACVRLK6; ALK6)	1.0	83.9	1.0	88.7	1.0
Protein-tyrosine kinase transmembrane receptor ror1	1.0	1.0	1.0	108.9	1.0
transferrin receptor protein (p90; CD71)	8.2	12.3	1.0	308.6	1.0
43-kDa postsynaptic protein; acetylcholine receptor-associated 43-kDa protein; RAPSIN	91.8	114.3	1.0	1.0	1.0
insulin receptor substrate-1 (IRS-1)	40.2	154.7	1.0	138.0	1.0
Crk adaptor protein	135.7	397.0	165.1	778.0	188.9
Csk; c-Src-kinase and negative regulator	232.7	120.0	1.0	433.8	16.8
non-receptor type 11 protein tyrosine phosphatase (PTPN11); phosphotyrosine phosphatase (PTPase)	47.3	1.0	1.0	79.4	1.0
hemopoietic cell kinase (HCK); p56-HCK & p60-HCK; B-cell/myeloid kinase (BMK)	19.6	114.6	1.0	6.1	1.0
SLAP; src-like adapter protein; Eck receptor tyrosine kinase-associated	56.3	123.6	1.0	90.2	1.0
CDC25MM; guanine nucleotide releasing protein (GNRP; RASGRF1)	1.0	34.5	1.0	81.3	88.6
proto-oncogene tyrosine-protein kinase fyn	1.0	191.6	1.0	28.9	22.8
Syk tyrosine-protein kinase (activated p21cdc42Hs kinase (ack))	143.9	341.0	38.9	1.0	1.0
serine proteinase inhibitor 3 (SPI3)	146.5	369.4	22.7	517.3	1.0
Sik; Src-related intestinal kinase	1.0	1.0	1.0	1.0	1.0
Blk; B lymphocyte kinase; Src family member	1.0	1.0	1.0	1.0	44.2
ShcC adaptor; Shc-related; brain-specific	152.6	325.7	113.3	296.3	1.0
proto-oncogene tyrosine-protein kinase lck; Isk	359.0	314.4	1.0	23.9	967.2
Grb2; adaptor protein; growth factor receptor-bound protein 2 (SH2/SH3 adaptor (Ash protein); sos-ras pathway member	1.0	210.2	1.0	8.5	1.0
Ack tyrosine-protein kinase; activated p21cdc42Hs kinase	1.0	95.2	1.0	1.0	1.0
LIM domain kinase 1 (LIMK1); KIZ-1	106.8	64.9	1.0	173.8	294.1
PKC-alpha; protein kinase C alpha type	1.0	1.0	250.3	129.9	1.0
protein kinase C beta II type (PKC-beta 2; PKCB)	46.9	250.1	1.0	217.8	1.0
PKC-delta; protein kinase C delta type	61.5	141.5	237.7	138.5	1.0
PKC-theta; protein kinase C theta type	1.0	193.6	1.0	1.0	1.0
CamK II; Ca2+/calmodulin-dependent protein kinase II (beta subunit)	24.6	213.0	1.0	20.3	1.0
calcium/calmodulin-dependent protein kinase IV catalytic subunit (CAM kinase-GR; CAMKIV; CAMK4)	131.6	203.9	1.0	47.0	1.0
cAMP-dependent protein kinase type I-beta regulatory chain	55.0	199.9	91.4	103.3	28.9
Jak3 tyrosine-protein kinase; Janus kinase 3	193.7	1.0	143.8	64.9	1.0
NF-KB essential modulator; Ikb kinase gamma subunit (IKK-gamma) essential regulatory subunit	42.4	1.0	100.8	203.0	1.0
NIMA-related expressed kinase 4 (NEK4)	71.2	20.9	1.0	133.7	203.8
ribosomal protein S6 kinase II alpha 1 (S6KII-alpha; RPS6KA1); ribosomal S6 kinase 1 (RSK1)	220.9	911.6	82.6	140.2	211.1
mitogen- & stress-activated protein kinase 2 (mMSK2)	68.5	395.5	204.3	786.7	1.0
mitogen-activated protein kinase p38 (MAP kinase p38); CRK1; CSBP1; CSBP2	638.0	1131.4	920.6	1004.1	1142.4
MAPKAPK-2; MAP kinase-activated protein kinase; MAPKAP kinase 2	9.5	176.1	1.0	1.0	151.9
dual-specificity mitogen-activated protein kinase kinase 1 (MAP kinase kinase 1; MAPK kinase 1; MAPKK1); erk activator kinase 1	1.0	95.3	1.0	141.2	253.4

(MEK1); PRKMK1					
MAPKK4; MAP kinase kinase 4; Jnk activating kinase 1; (JNKK1; SEK1; MKK4)	1.0	44.1	1.0	1.0	1.0
MAPKK6; MAP kinase kinase 6 (dual specificity) (MKK6)	0.4	40.2	1.0	19.9	1.0
MAP kinase kinase 3 (dual specificity; MAPKK3; MKK3; MEK3)	258.9	328.6	207.4	282.8	84.5
MEKK5 (MAP/ERK kinase kinase 5 (ASK1, MAPKKK5, mitogen activated protein kinase kinase kinase 5))	1.0	164.9	1.0	160.7	1.0
casein kinase II alpha 1 related sequence 4 (CSNK2A1-RS4)	339.3	295.8	292.4	1423.9	718.5
Ksr1; kinase suppressor of Ras-1	1.0	126.2	1.0	1.0	1.0
stress-activated c-jun N-terminal kinase 3 (JNK3); MAP kinase p49 3F12; PRKM10; SERK2	48.1	1.0	84.0	86.1	1.0
WBP6; pSK-SRPK1; WW domain binding protein 6 serine kinase for SR splicing factors	1.0	1.0	120.5	742.6	1.0
protein-tyrosine phosphatase gamma precursor (R-PTP- gamma; PTPRG)	214.2	469.2	408.6	98.5	406.7
protein phosphatase 2C alpha isoform (PP2C-alpha)	323.7	1.0	513.1	880.2	249.4
protein tyrosine phosphatase	1.0	1.0	11.8	8.7	39.6
guanine nucleotide binding protein, alpha inhibiti	537.1	1.0	735.0	518.4	688.4
guanine nucleotide binding protein, alpha o	1.0	321.6	1.0	1.0	1.0
guanine nucleotide binding protein, alpha stimulat	19535.6	4848.7	10009.7	8586.7	15962.3
transducin beta-2 subunit	655.1	318.2	555.0	402.3	562.6
Gem induced immediate early protein; Ras family member	21.4	21.3	1.0	80.6	412.7
Rac1 murine homolog	323.6	491.0	113.5	729.3	334.7
G13; G-alpha-13 guanine nucleotide regulatory protein	1.0	80.1	1.0	164.7	1.0
Transducin beta-5 subunit; GTP-binding protein G(i)/G(s)/G(t) beta subunit 3	1.0	165.6	1.0	0.8	1.0
adenylate cyclase 6	1398.6	674.8	1280.0	1054.2	1232.0
rab2 ras-related protein	350.2	473.7	499.7	1269.5	228.6
Rab-3b ras-related protein	1.0	1.0	85.1	1.0	118.5
ran GTPase activating protein 1 (RANGAP1)	172.3	7.7	201.5	390.1	34.6
Rab GDI alpha; Rab GDP-dissociation inhibitor alpha; GDI-1; XAP4	1.0	1.0	321.9	71.1	95.7
RaiGDSB; GTP/GDP dissociation stimulator for a ras-related GTPase (RALGEF)	435.8	164619.5	681.8	321.9	641.0
CDC42 GTP-binding protein; G25K	1.0	1.0	34.2	436.9	9.9
GapIII; GTPase-activating protein	1.0	262.5	1.0	84.2	38.7
INOSITOL 1,4,5-TRISPHOSPHATE RECEPTOR TYPE 2	1.0	207.0	1.0	220.1	1.0
PI3-K p110; phosphatidylinositol 3-kinase catalytic subunit	1.0	102.5	1.0	1.0	9.7
phosphatidylinositol 3-kinase regulatory alpha subunit (PI3-kinase P85-alpha; PTDINS-3-kinase P85-alpha; PI3K)	157.1	99.0	80.5	382.6	288.6
PLC beta; phospholipase C beta 3	164.8	1.0	1.0	94.7	253.9
PLC gamma; phospholipase C gamma	39.0	322.7	1.0	333.3	371.3
phosphodiesterase 1C	1.0	180.5	1.0	128.8	43.6
guanylate cyclase soluble beta-1 subunit; guanylate cyclase 70-kDa subunit	146.1	232.5	96.1	340.1	96.0
ADENYLATE CYCLASE, TYPE VII (ATP PYROPHOSPHATE-LYASE) (ADENYLYL CYCLASE) (KIAA0037)	130.8	1.0	1.0	117.9	581.7
BST-1; lymphocyte differentiation antigen CD38	1.0	1.0	7.6	1.0	375.3
S100 calcium-binding protein A1; S-100 protein alpha chain	42.7	1.0	119.8	85.8	220.2
calpactin I light chain; p10 protein; cellular ligand of annexin II	2535.6	813.0	3853.9	5834.9	2905.4
calbindin 2	1.7	1.0	1.0	1.0	163.3
calbindin-28K	1.0	1.0	1.0	59.5	1.0
calcyclin binding protein	65.4	1.0	21.7	1.0	25.8
Calmodulin	595.8	247.3	246.8	1131.0	449.9
Cas; Crk-associated substrate; focal adhesion kinase substrate	101.4	13.2	224.7	1.0	231.1
Marcks-related protein (Mac-Marcks) (brain protein F52).	1.0	1.0	231.5	59.8	236.6
linker for activation of T cells (LAT) ZAP-70 tyrosine kinase substrate that links T cell receptor to cellular activation;	43.4	156.6	1.0	1.0	1.0
58-kDa inhibitor of RNA-activated protein kinase	599.4	472.9	574.6	983.8	1666.7
cortactin; protein tyrosine kinase substrate	179.3	251.4	1.0	279.5	548.2
14-3-3 protein eta; protein kinase C inhibitor protein 1 (KCIP1); YWHAH	2772.6	1242.3	2343.7	2249.5	3568.2
nitric oxide synthase 3, endothelial cell	133.2	242.5	12.1	366.2	1.0
phosphoprotein enriched in astrocytes 15	315.8	275.2	298.0	783.0	84.0
disabled homolog 2 (Drosophila)	914.8	700.3	1014.5	221.5	1198.7
period homolog (Drosophila)	1.0	256.7	1.0	1.0	184.7
I-kappa B alpha subunit (IKB alpha)	103.9	62.9	1.0	1.0	261.8

nuclear factor of kappa light chain protein enhancer in B-cells inhibitor alpha (IKB-beta; NFKBIA)	1.0	26.7	241.7	54.0	347.5
Rgs4; regulator of G-protein signaling 4 (RGP4).	1.0	1.0	915.2	1.0	1.0
Tuberin; TSC2 (tuberous sclerosis 2 protein)	32.1	101.1	86.0	25.5	1.0
Leucine-rich repeat protein SHOC-2; Ras-binding protein SUR-8	2.3	1.0	1.0	1.0	1.0
Dvl2; dishevelled-2 tissue polarity protein	617.3	409.5	494.0	401.5	602.8
zyxin (ZYG)	1588.6	1535.0	2476.6	1052.7	1307.6
LYSOSOMAL PROTECTIVE PROTEIN PRECURSOR (EC 3.4.16.5) (CATHEPSIN A) (CARBOXYPEPTIDASE C) (MO54).	828.0	719.0	554.3	275.8	890.6
METHIONINE AMINOPEPTIDASE 2 (EC 3.4.11.18) (METAP 2) (PEPTIDASE M 2) (INITIATION FACTOR 2 ASSOCIATED 67 KD GLYCOPROTEIN) (P67)	137.7	240.8	1.0	57.5	1.0
PLASMINOGEN PRECURSOR (EC 3.4.21.7) [CONTAINS: ANGIOSTATIN]	1.0	230.6	1.0	1.0	1.0
PROTHROMBIN PRECURSOR	176.7	1.0	80.2	1.0	1.0
EPITHIN	212.8	25.5	1122.1	643.0	396.3
SERINE PROTEASE HEP SIN	39.1	46.6	63.4	24.6	1.0
PLASMA KALLIKREIN PRECURSOR (PLASMA PREKALLIKREIN) (KININOGENIN) (FLETCHER FACTOR)	1.0	275.0	45.5	1.0	183.5
granzyme C precursor (GZMC); cytotoxic cell protease 2 (CCP2); B10; CTLA5	1.0	1.0	1.0	1.0	796.4
mast cell protease (MMCP) - 4	1.0	78.8	30.9	1.0	1.0
tissue plasminogen activator precursor (T-plasminogen activator; PLAT; TPA)	1.0	818.2	1.0	138.5	262.3
urokinase type plasminogen activator	490.2	167.2	168.8	301.8	500.9
alpha-1-antitrypsin 1-2 precursor (AAT2); serine protease inhibitor 1-2 (SPI1-2); alpha 1 protease inhibitor 2; alpha-1- antiproteinase	193.1	268.6	10.6	1.0	1.0
cathepsin D (CTSD)	4271.6	2186.5	3833.5	3067.9	4362.9
72-kDa type IV collagenase type; 72-kDa gelatinase; gelatinase A; matrix metalloproteinase 2 (MMP2)	1859.6	2897.1	431.6	2074.8	1846.7
gelatinase B	1.0	1.0	1.0	1.0	1.0
matrix metalloproteinase 14 precursor (MMP14); membrane-type matrix metalloproteinase 1 (MTMMP1)	732.5	1580.0	553.3	1164.3	729.8
membrane metallo endopeptidase	1.0	7.4	1.0	10.5	65.4
DIPEPTIDYL-PEPTIDASE I PRECURSOR (DPP-I) (CATHEPSIN C) (CATHEPSIN J) (DIPEPTIDYL TRANSFERASE)	25.4	767.7	1.0	300.3	155.4
CATHEPSIN W PRECURSOR (LYMPHOPAIN)	1.0	276.6	1.0	1.0	51.6
cathepsin B1 (CTSB)	1136.6	1283.2	1040.2	4682.3	1248.1
cathepsin H	72.1	753.0	93.5	258.1	54.6
cathepsin L precursor (CTSL); major excreted protein (MEP)	437.7	94.0	1.0	240.2	1.0
PROTEASOME COMPONENT C8 (MACROPAIN SUBUNIT C8) (PROTEASOME SUBUNIT K) (MULTICATALYTIC ENDOPEPTIDASE COMPLEX SUBUNIT C8)	1.0	238.6	1.0	1.0	1.0
Alzheimer's disease amyloid A4 protein precursor homolog; protease nexin-II (PN-II); (amyloidogenic glycoprotein) (AG)	1581.6	1144.1	651.0	692.3	1498.7
CYSTATIN C PRECURSOR (CYSTATIN 3)	230.4	2759.2	452.5	276.3	682.6
ANTILEUKOPROTEINASE 1 PRECURSOR (ALP) (SECRETORY LEUKOCYTE PROTEASE INHIBITOR).	5.3	732.1	1.0	1.0	1.0
ANTITHROMBIN-III PRECURSOR (ATIII).	1.0	3.4	1.0	1.0	1.0
NEUROSERPIN PRECURSOR (PROTEASE INHIBITOR 17)	1.0	1.0	1.0	1.0	6.7
protease nexin 1 (PN-1)	689.4	266.4	132.7	368.5	1120.1
plasminogen activator inhibitor	131.7	267.4	1.0	37.3	31.3
macrophage plasminogen activator inhibitor 2 (PAI2; PLANH2)	248.7	36.9	80.8	34.4	1.0
serine protease inhibitor 2-2 (SPI2-2); SPI2 proteinase inhibitor; SPI2/EB4	1.1	259.7	1.0	67.9	1.0
serine protease inhibitor 2.4 (SPI2.4)	1.0	1.0	1.0	1.0	35.9
47-kDa heat shock protein precursor (HSP47); collagen-binding protein 1 (CBP1); serine protease inhibitor J6	3554.6	5708.5	3078.9	11001.3	3328.1
metalloproteinase inhibitor 2 precursor; tissue inhibitor of metalloproteinases 2 (TIMP2)	481.9	554.9	994.7	1.0	450.6
tissue inhibitor of metalloproteinases 3 (TIMP3 ); SUN	865.3	503.8	329.1	1456.5	521.8
dipeptidyl peptidase IV (DPPIV; DPP4); thymocyte-activating molecule (THAM)	1.0	84.3	1.0	1.0	1.0
BASIGIN PRECURSOR (BASIC IMMUNOGLOBULIN SUPERFAMILY) (MEMBRANE GLYCOPROTEIN GP42). (COLLAGENASE STIMULATORY FACTOR) (EXTRACELLULAR MATRIX METALLOPROTEINASE INDUCER) (EMMPRIN) (5F7) (CD147 ANTIGEN).	3441.6	1068.8	3576.7	4214.0	2372.1
receptor-type protein tyrosine phosphatase (PTPRCAP); C polypeptide-associated protein; CD45-associated protein (CD45-	1.0	1.0	26.9	1.0	53.0

AP); LSM					
adenosine A2b receptor	1.0	1.0	12.1	98.8	1.0
bradykinin receptor, beta 2	66.8	20.3	1.0	110.2	88.0
kinesin motor protein 3C (KIF3C)	52.6	1.0	1.0	31.6	1.0
non-muscle cofilin 1 (CFL1)	2691.6	159.6	1251.6	516.7	1344.0
microtubule plus end-directed kinesin motor 3A (KIF3A)	33.8	120.0	1.0	164.0	1.0
acidic keratin complex 1 gene 15; type I cytoskeletal keratin 15 (CK15; KRT1-15; KRT15); cytokeratin 15	1.0	418.4	1.0	279.3	1.0
kinesin heavy chain member 1B (KIF1B)	107.8	323.9	38.4	168.8	115.9
alpha internexin neuronal intermediate filament protein (alpha-INX; INA)	1.0	647.9	199.4	7.2	58.7
tubulin beta 4 (TUBB4)	571.7	422.1	205.6	48.0	315.1
microtubule-associated protein 4 (MAP4; MTAP4)	267.2	324.8	303.5	426.2	210.6
syndecan 2 (SYND2; SDC2); cell surface-associated heparan sulfate proteoglycan core protein 1 (HSPG1); fibroglycan	89.4	90.8	53.9	1.0	206.2
acidic keratin complex 1 gene 13; type I cytoskeletal keratin 13 (CK13; KRT1-13; KRT13); cytokeratin 13; 47-kDa cytokeratin	1.0	1495.6	756.5	110.5	1.0
syndecan 3 (SYND3)	2062.6	990.3	1135.7	858.4	1291.9
mena protein; enabled homolog (ENAH)	1.0	72.7	54.8	79.4	1.0
kinesin motor protein C2 (KIFC2)	1.0	1.0	84.7	1.0	1.0
neurofilament triplet L protein (NEFL; NFL); 68-kDa neurofilament protein; neurofilament light polypeptide	62.3	265.3	808.3	268.7	318.1
basic keratin complex 2 gene 4; type II cytoskeletal keratin 4 (CK4; KRT2-4; KRT4); cytokeratin 4; 57-kDa cytokeratin	1.0	1.0	6.1	885.3	1.0
neurofilament triplet M protein (NEFM; NFM); 160-kDa neurofilament protein; neurofilament medium polypeptide	1.0	1.0	1.0	17.1	1.0
nidogen precursor (NID); entactin (ENT)	4605.6	2963.2	2506.2	3997.3	4485.5
peripherin (PRPH)	1.0	170.4	1.0	183.3	130.9
talin (TLN)	255.0	1.0	18.4	212.8	63.7
vitronectin precursor (VTN); serum-spreading factor; S-protein	1.0	1.0	73.4	20.4	1.0
skelemin	37.5	165.2	1.0	39.3	78.3
thrombospondin 3 precursor (THBS3; TSP3)	1.0	1.0	65.9	65.4	1.0
aggrecan core protein 1 precursor (AGC1); cartilage-specific proteoglycan core protein (CSPCP)	1.0	235.1	1.0	1.0	1.0
thrombospondin 2 precursor (THBS2; TSP2)	32.7	340.7	178.1	586.1	5.2
collagen 9 alpha 1 subunit precursor (COL9A1)	1.0	130.8	1.0	1.0	1.0
bone/cartilage proteoglycan I precursor (PGI); biglycan (BGN)	3653.6	3331.9	3939.2	3476.8	3660.2
laminin beta 1 subunit 1 precursor (LAMB1-1)	112.3	24.7	197.4	87.5	1.0
thrombospondin 1 precursor (THBS1; TSP1)	201.3	441.8	1613.0	986.7	113.8
endoglin precursor (EDG; ENG); cell surface MJ7/18 antigen	1332.6	868.0	1593.7	1801.5	1564.0
laminin alpha 2 subunit precursor (LAMA2); dystrophin muscularis protein (DY); merosin heavy chain; laminin M subunit	1.0	118.2	1.0	70.0	79.3
reelin (RELN; RL); reeler	48.3	309.2	1.0	1.0	1.0
laminin alpha 5 subunit precursor (LAMA5)	171.7	423.2	861.4	1099.8	558.2
laminin beta 2 subunit precursor (LAMB2); laminin synapses polypeptide (S-LAM; LAMS)	296.1	1343.7	115.9	45.8	364.9
laminin beta 3 subunit precursor (LAMB3); kalinin B1 subunit	1.0	441.8	1.0	1.0	41.6
laminin gamma 2 subunit precursor (LAMC2); kalinin/nicein/epiligrin 100-kDa subunit	1.0	253.5	128.0	71.6	1.0
dentin sialophosphoprotein precursor (DSPP)	1.0	1.0	1.0	1.0	1.0
otogelin (OTOG)	1.0	137.5	1.0	1.0	1.0
laminin gamma 1 subunit precursor (LAMC1); laminin B2 subunit	2400.6	1002.2	1543.7	1504.3	2113.4
BONE PROTEOGLYCAN II PRECURSOR (PG-S2) (DECORIN) (PG40).(DCN)	1504.6	1211.2	2772.1	6563.4	1569.4
collagen 6 alpha 1 subunit precursor (COL6A1)	1034.6	6316.4	2736.9	12304.7	1208.4
collagen 10 alpha 1 subunit precursor (COL10A1)	1.0	57.8	1.0	1.0	1.0
fibronectin 1 precursor (FN1)	7309.6	6087.0	7001.7	3592.8	6716.4
laminin alpha 3 subunit precursor (LAMA3)	1.0	26.6	140.2	8.5	207.4
filensin precursor; beaded filament structural protein in lens 1 (BFSP1)	1.0	262.6	1.0	67.2	1.0
collagen 9 alpha 2 subunit precursor (COL9A2)	285.3	836.9	1.0	178.8	178.5
cytoskeletal epidermal keratin (14 human)	271.5	40.3	1174.3	1847.2	670.8
type I cytoskeletal keratin 18 (KRT1-18; KRT18); cytokeratin 18; cytokeratin endo B; keratin D (KERD)	776.9	665.5	2020.9	736.8	1450.7
type I cytoskeletal keratin 19 (CK19; KRT19; K19); cytokeratin 19	6471.6	2041.5	16929.2	7112.9	4982.9
type II cytoskeletal keratin1 (KRT2-1); cytokeratin 1 (KRT1); 67-kDa cytokeratin	1.0	1.0	1.0	1.0	1.0

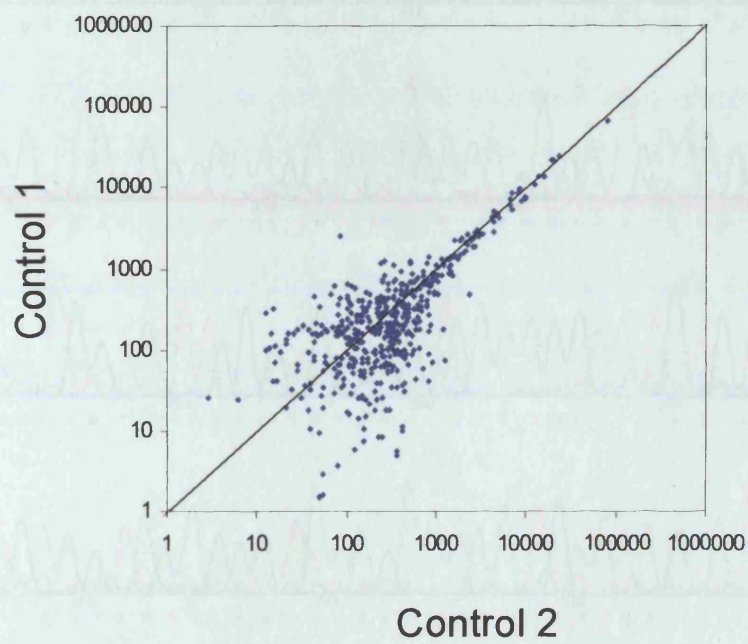
vimentin (VIM)	6333.6	3392.4	6671.0	6688.9	6049.7
kinesin family protein KIF1A	1.0	1.0	1.0	1.0	1.0
neuronal kinesin heavy chain (NKHC); KIF5C	1.0	1.0	1.0	5.8	1.0
kinesin like protein KIF 3B	1.0	1.0	1.0	1.0	43.8
cardiac myosin heavy subunit alpha isoform (MYH6; MYHCA)	1.0	1.0	1.0	261.0	1.0
myosin light subunit 1 atrial/fetal isoform (MLC1A; MLC1EMB)	1.0	64.4	1.0	1.0	1.0
non-muscle myosin light chain 3 (MLC3NM; MYLN): MYL6	4609.6	4270.4	4435.8	7431.2	7355.1
unconventional myosin VI	1.0	1.0	1.0	1.0	1.0
recombination activating protein 1 (RAG1); RGA; novel stromal cell protein	1292.6	558.8	1416.4	604.9	1128.1
DNA polymerase gamma (EC 2.7.7.7) (mitochondrial DNA polymerase catalytic subunit)	1.0	136.9	1.0	84.6	225.9
DNA polymerase delta catalytic subunit (POLD1)	322.8	119.5	1.0	173.9	145.8
DNA topoisomerase I (Top I)	1.0	1.0	1.0	194.9	227.1
DNA topoisomerase II alpha (TOP2A)	1.0	1.0	1.0	33.5	1.0
proliferating cell nuclear antigen (PCNA); cyclin	410.7	388.4	309.9	193.9	488.9
activator 1 140-kDa subunit (A1 140-kDa subunit); replication factor C large subunit (RF-C 140-kDa subunit; RFC1); differentiation-specific element-binding protein; ISRE-binding protein (IBF-1); RECC1	1.0	131.8	46.4	105.6	1.0
MCM2 DNA replication licensing factor.	665.6	33.3	199.1	38.3	201.0
MCM4 DNA replication licensing factor (CDC21 homolog) (P1-CDC21).	1.0	1.0	1.0	174.3	1.0
MCM5 DNA replication licensing factor (CDC46 homolog) (P1-CDC46).	1565.6	983.5	1092.5	394.3	1083.2
MCM6 DNA replication licensing factor (P105MCM).	1.0	1.0	1.0	99.8	1.0
DNA polymerase epsilon subunit B (DNA polymerase II subunit B).	25.0	655.9	1.0	1.0	1.0
Nibrin (NBS1); cell cycle regulatory protein p95	1.0	1.0	1.0	1.0	1.0
Atm; ataxia telangiectasia murine homolog	1.0	160.2	1.0	18.9	1.0
PMS2 DNA mismatch repair protein; yeast PMS1 homolog 2	1.0	1.0	1.0	73.6	1.0
DNA-(apurinic/aprimidinic) lyase; AP endonuclease 1 (APEX nuclease; APEN; APEX)	1.0	93.1	1.0	1.0	1.0
DNA excision repair protein ERCC1	275.5	48.3	1.0	115.2	74.9
DNA-repair protein complementing XP-B cells homolog; xeroderma pigmentosum group B complementing protein homolog (XPBC); DNA excision repair protein ERCC3; basal transcription factor 2 89-kDa subunit (BTF2-p89); TFIIH 89-kDa subunit	18.8	67.4	59.3	1.1	1.0
xeroderma pigmentosum group G complementing protein (XPG); DNA excision repair protein ERCC5	1.0	1.0	1.0	1.0	1.0
Fanconi anemia group C protein (FACC protein).	17.5	1.0	1.0	1.0	1.0
MLH1 DNA mismatch repair protein; MutL homolog	1.0	310.1	1.0	1.0	1.0
MSH2 DNA mismatch repair protein; MutS homolog 2	485.5	1.0	1.0	2.9	206.2
GTBP; G/T-mismatch binding protein; MSH6	1835.6	751.3	2061.9	1062.1	2392.1
RAD23 UV excision repair protein homolog B (MHR23B; RAD23B); xeroderma pigmentosum group C repair complementing 58-kDa protein (XP-C repair complementing 58-kDa protein)	173.0	195.7	244.0	635.2	276.9
RAD23 UV excision repair protein homolog A (MHR23A; RAD23A)	43.9	404.3	44.7	69.8	1.0
photolyase/blue-light receptor homolog	649.4	1.0	817.1	287.1	497.7
purine-rich element binding protein A (PURA); purine-rich single-stranded DNA-binding protein alpha	1.0	5.2	1.0	234.4	163.8
Rad50; DNA repair protein	93.9	422.6	1.0	8.4	180.6
XPAC; xeroderma pigmentosum group A correcting protein	76.5	272.5	1.0	171.9	156.1
Ung1; uracil-DNA glycosylase	555.4	54.3	76.1	79.9	173.9
DNA-repair protein XRCC1	182.3	353.4	87.7	49.1	1.0
ubiquitin-conjugating enzyme E2 17-kDa (UBE2B); ubiquitin-protein ligase; ubiquitin carrier protein; HR6B	3552.6	712.5	4827.8	995.4	3776.2
HR23A; protein involved in DNA double-strand break repair; PW29; calcium-binding protein	1.0	121.9	1.0	148.8	1.0
DNA polymerase alpha catalytic subunit (POLA)	1.0	254.5	96.7	240.5	1.0
ATP-dependent DNA helicase II 70-kDa subunit; 70-kDa thyroid autoantigen; lupus Ku autoantigen protein p70; CTC box-binding factor 75-kDa subunit (CTCBF; CTC75)	1.0	205.4	154.8	341.4	18.2
ATP-dependent DNA helicase II 86-kDa subunit; thyroid Ku (p70/p80) autoantigen p86 homolog; CTC box-binding factor 85-kDa subunit (CTCBF; CTC85); XRCC5; nuclear factor IV; G22P2	1.0	1.0	1.0	1.0	1.0
DNA ligase I; polydeoxyribonucleotide synthase (ATP) (DNL1) (LIG1)	1.0	1.0	73.4	161.4	1.0
DNA ligase III; polydeoxyribonucleotide synthase (ATP) (DNL3)					

MmRad52; yeast DNA repair protein Rad52 homolog	182.3	1.0	1.0	59.9	249.5
structure-specific recognition protein 1 (SSRP1); recombination signal sequence recognition protein; T160	596.9	417.7	195.2	232.6	234.5
meiotic recombination protein DMC1/LIM15 homolog	1.0	17493.2	1.0	1.0	1.0
RAG-1; V(D)J recombination activating protein	1.0	1.0	1.0	105.2	1.0
V(D)J recombination activating protein (RAG2)	78.2	58.6	27.3	1.0	1.0
translin (TSN)	327.7	189.5	174.4	418.3	380.2
DNA repair protein RAD51 homolog 1; recA	1.0	1.0	1.0	1.0	1.0
MmMre11a putative endo/exonuclease	11.5	110.1	1.0	17.2	1.0
methyl-CpG-binding protein 2 (MECP2)	17.4	96.8	20.8	1.0	80.5
DNase I	4.5	1.0	45.9	1.0	1.0
protein phosphatase with EF-hands 2 (PPEF2)	1.0	121.0	1.0	76.2	41.9
involucrin (IVL)	562.9	1479.8	1091.4	131.2	449.8
retinoic acid-inducible E3 protein; stimulated by retinoic acid 13 (STRA13); hematopoietic-specific protein E3; orfB	835.1	433.3	5310.8	1075.2	1178.4
formin (FMN); limb deformity protein (LD)	1.0	58.7	1.0	12.4	1.0
formin 4 (FMN4); limb deformity protein (LD)	97.1	19.8	1.0	143.2	1.0
klotho protein (KL)	1.0	241.4	1.0	117.7	6.6
DiGeorge syndrome chromosome region 6 protein (DGCR6)	1323.6	825.8	787.1	1007.0	1725.4
WSB1 protein	1.0	121.5	1.0	49.4	1.0
WSB2 protein	1.2	641.3	1.0	142.8	25.5
fibrillin 1 precursor (FBN1)	748.3	1053.2	414.9	952.7	551.8
anti-proliferative B-cell translocation gene 2 (BTG2); NGF-inducible protein TIS21	754.4	1.0	195.0	2125.6	588.9
brain lipid-binding protein (BLBP)	99.2	42.6	199.4	109.8	1.0
leptin precursor (LEP); obese factor (OB)	29.2	1443.5	110.2	47.8	93.8
cordons-bleu protein (COBL)	1.0	242.5	111.6	112.1	13.9
four and a half LIM domains 1 (FLH1); skeletal muscle LIM protein 1 (SLIM1)	69.1	1.0	183.0	354.6	120.5
ajuba protein	96.9	16.7	235.1	223.9	1.0
petaxin-related C-reactive protein (CRP); pentaxin 1 (PTX1)	1.0	1.0	1.0	4.0	1.0
PRESENILIN-1; PS1; (S182 PROTEIN).	1.0	975.3	1.0	74.8	1.0
huntingtin-associated protein 1 (HAP1)	1.0	1.0	1.0	1.0	1492.0
fragile X mental retardation syndrome 2 homolog (FMR2)	1.0	241.3	1.0	198.9	8.1
fragile X mental retardation syndrome 1 homolog (FMR1; FMRP)	1.0	1.0	111.5	207.7	177.7
huntingtin; Huntington disease homolog (HDH)	96.0	141.0	1.0	169.2	293.4
frataxin; Friedreich ataxia protein (FRDA)	202.3	328.9	45.0	157.6	113.1
PUTATIVE PROTEIN-TYROSINE PHOSPHATASE PTEN (EC 3.1.3.48) (MUTATED IN MULTIPLE ADVANCED CANCERS 1). PTEN; MMAC1.	251.0	1.0	1.0	75.9	58.0
tubby	105.7	261.1	1.0	101.0	193.5
ubiquitin; UBA52; UBB; UBC; UBCEP1	73033.6	10001.6	94127.2	29918.5	104760.1
phospholipase A2; 14-3-3 protein zeta/delta; protein kinase C inhibitor protein 1 (KCIP1); mitochondrial import stimulation factor S1 subunit; YWHAZ	808.4	125.8	1903.9	1503.6	533.3
hypoxanthine-guanine phosphoribosyltransferase (HGPRTase; HPRT)	74.1	948.6	1.0	7.1	1.0
glyceraldehyde-3-phosphate dehydrogenase (G3PDH; GADPH)	11332.6	21276.9	14997.3	13175.3	9667.2
myosin I alpha (MMI-alpha)	1.0	437.0	170.0	52.9	50.2
ornithine decarboxylase (ODC)	1.0	290.5	486.3	1070.1	1.0
cytoplasmic beta-actin (ACTB)	25692.6	14936.4	39612.6	13106.4	37166.4
45-kDa calcium-binding protein precursor (CAB45); stromal cell-derived factor 4 (SDF4)	1.0	1599.7	1.0	53.5	1.0
40S ribosomal protein S29 (RPS29)	99412.6	19969.7	87930.5	132352.0	79127.8
	680333.2				

## Appendix 2

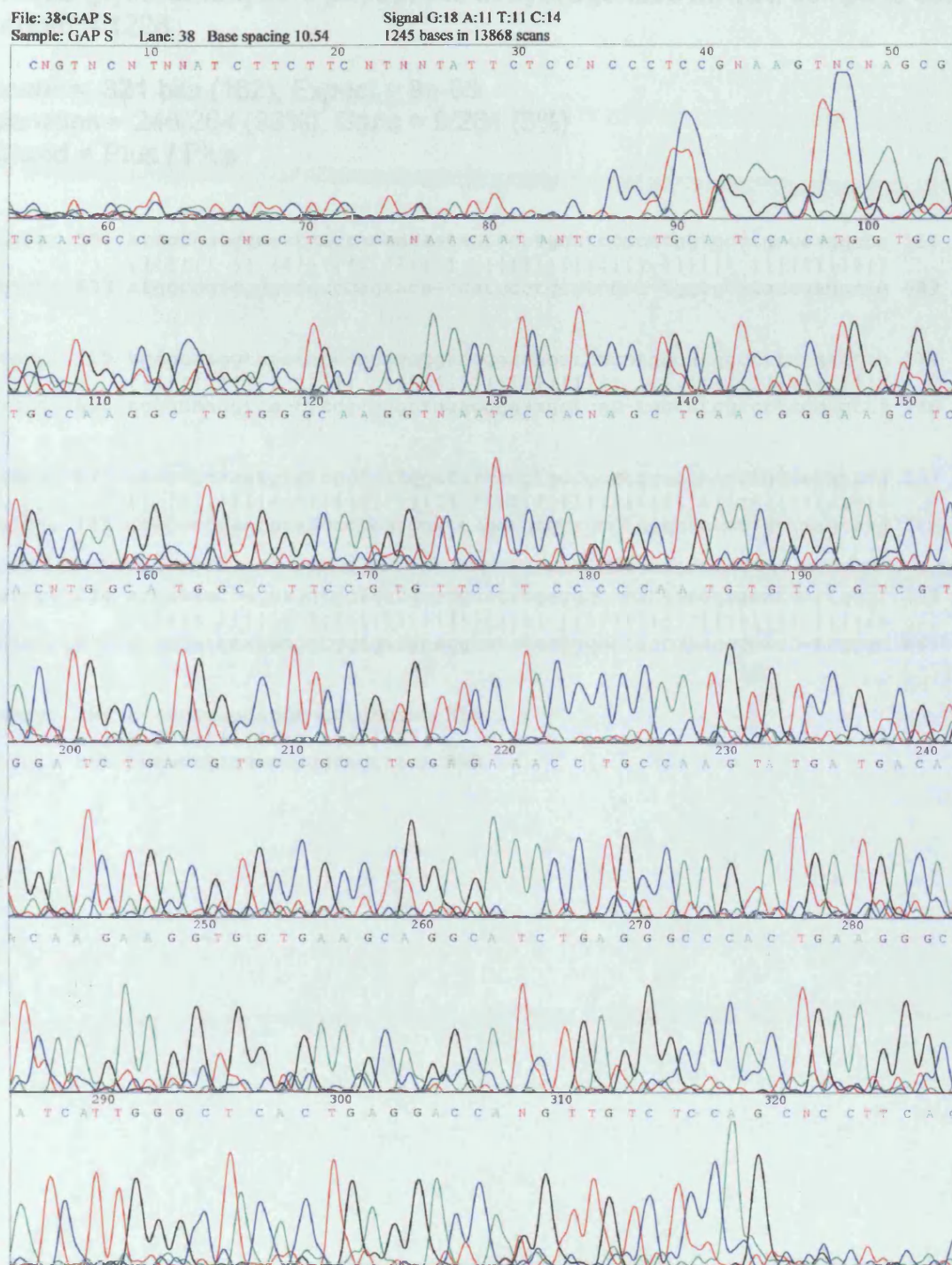
Supplementing data for *control\_1.pdf*, *control\_2.pdf* and *control\_3.pdf* RT-PCR products

Representative log-log scatter plot of two independent groups of normalised control data, each point on the plot represents the expression level of one of the 1176 genes (Chapter 5).



**Appendix 3**Sequencing data for *gapdh*, *ngfa*, *pref-1* and *igf-2* RT-PCR products

(Chapter 5)

**a: *gapdh***

BLAST query comparison of PCR sequencing data to published complete coding sequence.

gi|193423|gb|M32599.1|MUSGAPDH  
**Mouse glyceraldehyde-3-phosphate dehydrogenase mRNA, complete cds**  
Length = 1228

Score = 321 bits (162), Expect = 8e-85  
Identities = 246/264 (93%), Gaps = 9/264 (3%)  
Strand = Plus / Plus

Query: 55 atggccgcgngctgccanaacaatantccctgcatccacatggtgcctgccaaggctg 114  
||||||| || ||||||||| |||| | ||||||||||||| ||||| |||||||||  
Sbjct: 633 atggccgtggggctgccagaaca-tcatccctgcatccac-tggtgc-tgccaaggctg 689

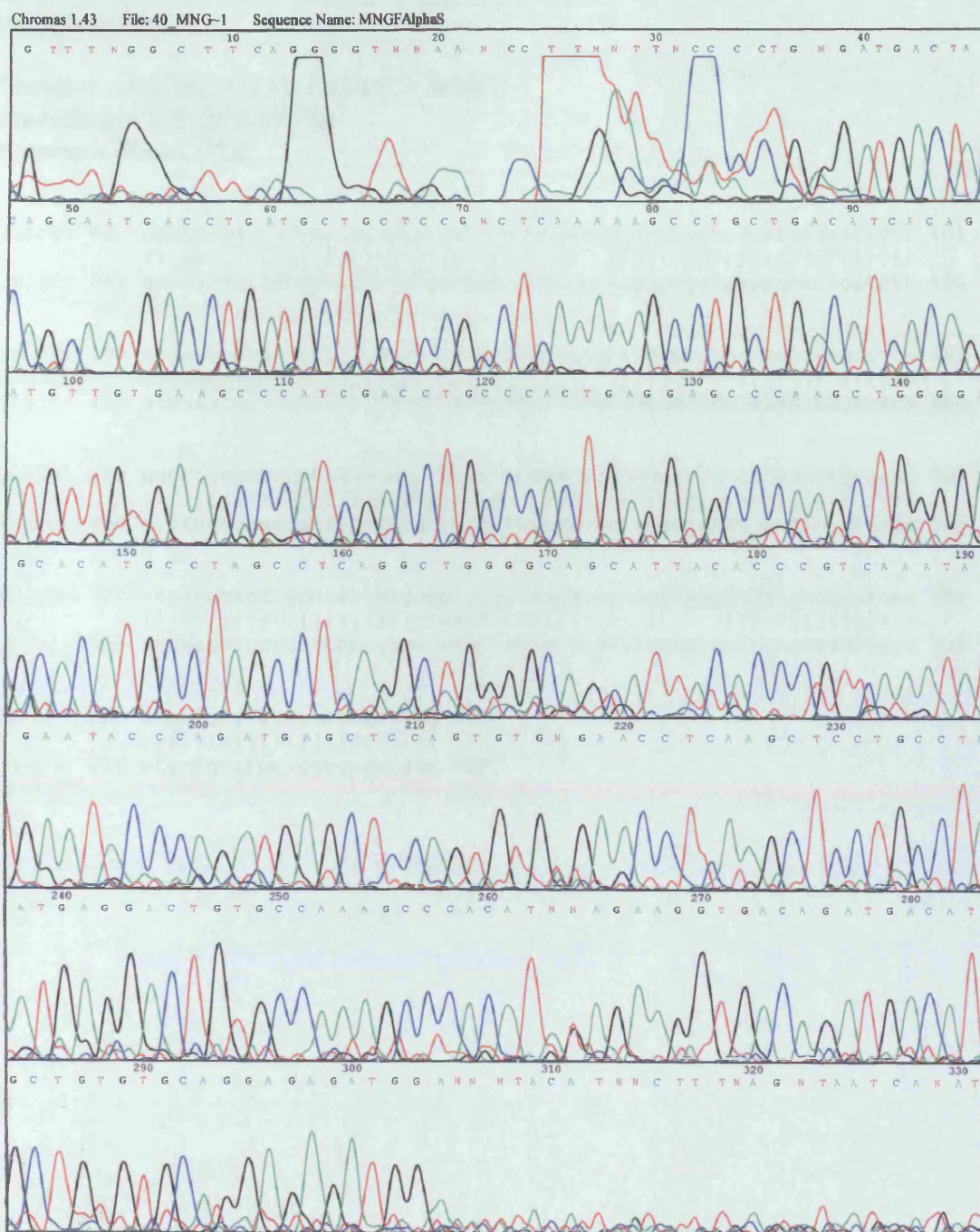
Query: 115 tgggcaaggtnaatcccacnagctgaacgggaagctcacntggcatggccttccgtgttc 174  
||||||| | ||||| ||||||||||||||||||| |||||||||||||||||||  
Sbjct: 690 tgggcaagggtca-tcca-gagctgaacgggaagctcac-tggcatggccttccgtgttc 746

Query: 175 ct-cccccaatgtgtccgtcgtggatctgacgtgccgcctggagaaacctgccaagtatg 233  
|| |||||||||||||||||||||||||||||||||||||||||||||||||||||||  
Sbjct: 747 ctaccccccaatgtgtccgtcgtggatctgacgtgccgcctggagaaacctgccaagtatg 806

Query: 234 atgacaacaagaagggtggtgaagcaggcatctgagggccactgaaggcatcattgggc 293  
||||||| ||||||||||||||||||||||||||||||||||||||||||||||| |||||  
Sbjct: 807 atgacatcaagaagggtggtgaagcaggcatctgagggccactgaaggcatc-ttgggc 865

Query: 294 t-actgaggaccangttgtctcc 316  
| ||||||||||||| |||||||||  
Sbjct: 866 tacactgaggaccaggttgtctcc 889

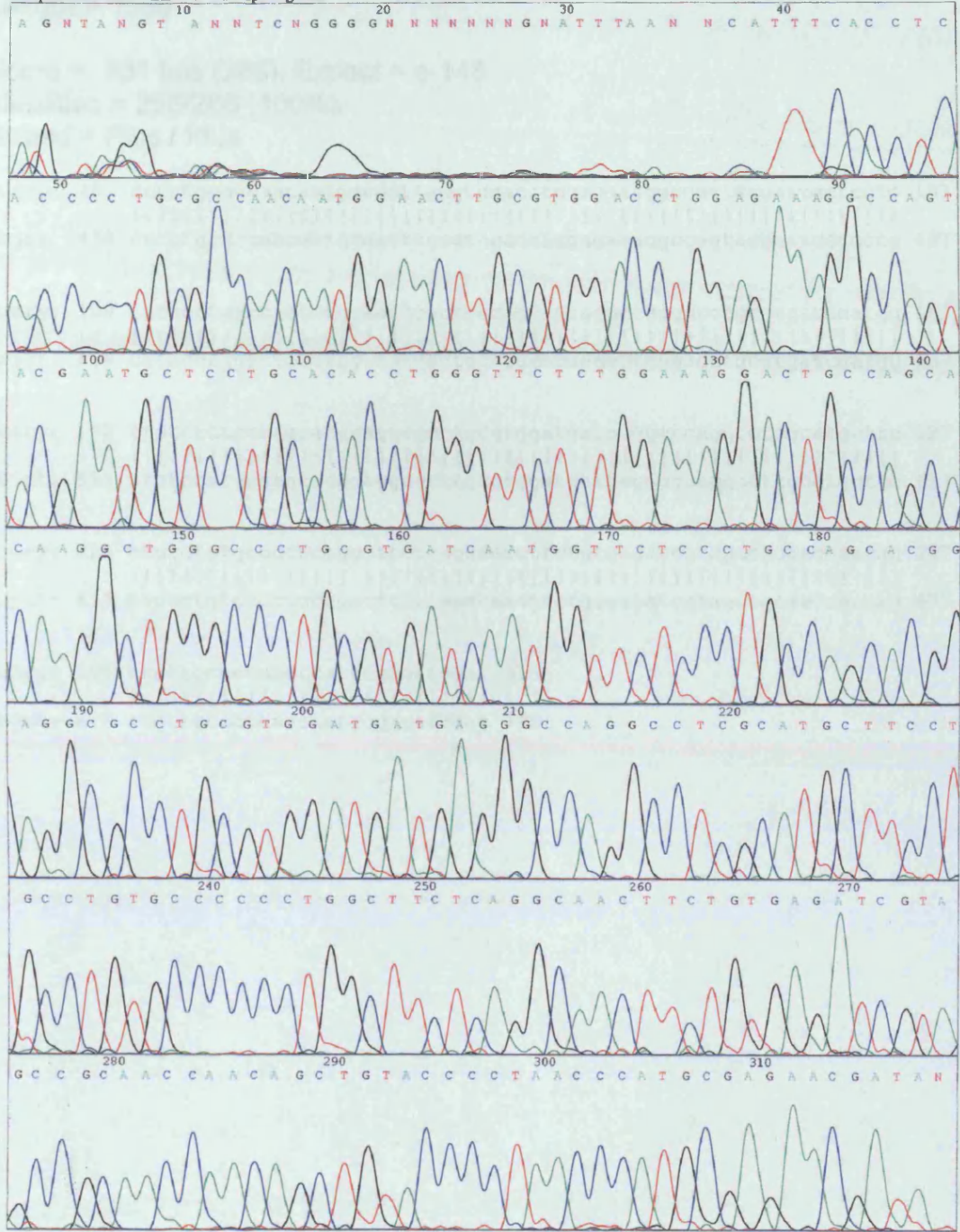
b: *ngfa*





c: pref-1

File: 04-PREF1-S      Lane: 4      Base spacing 9.65      Signal G:53 A:36 T:30 C:64  
Sample: PREF1-S      1147 bases in 13427 scans



gi|309092|gb|L12721.1|MUSADDIFF  
**Mus musculus adipocyte differentiation-associated protein mRNA,**  
complete cds  
Length = 1589

Score = 531 bits (268), Expect = e-148  
Identities = 268/268 (100%)  
Strand = Plus / Plus

Query: 48 ccctgcgccaacaatggaacttgctggacctggagaaaggccagtacgaatgctcctg 107  
|||||  
Sbjct: 438 ccctgcgccaacaatggaacttgctggacctggagaaaggccagtacgaatgctcctg 497

Query: 108 cacacctgggttctctggaaggactgccagcacaaggctgggccctgctgatcaatgg 167  
|||||  
Sbjct: 498 cacacctgggttctctggaaggactgccagcacaaggctgggccctgctgatcaatgg 557

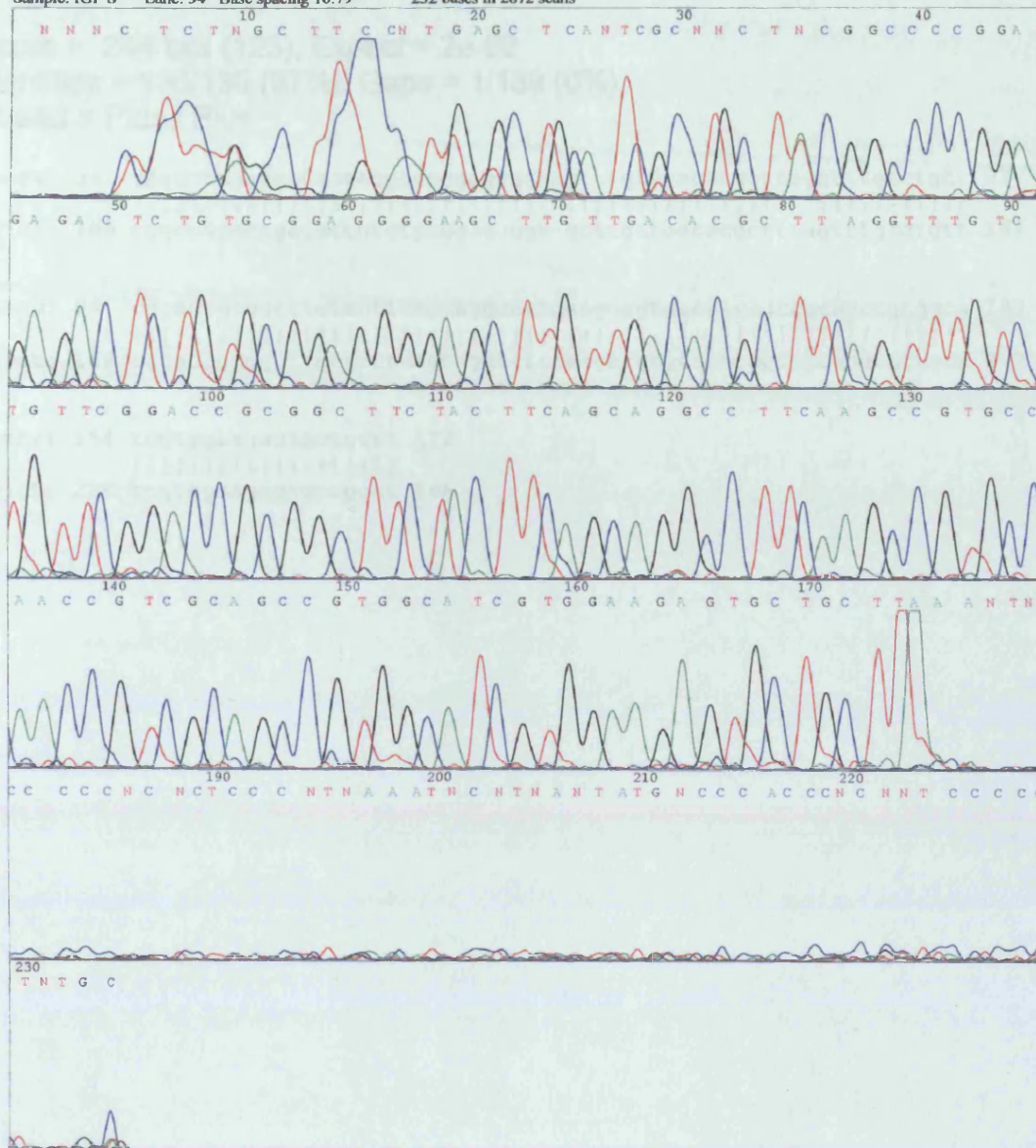
Query: 168 ttctccctgccagcacggaggcgctgctggatgatgaggccaggcctcgcatgcttc 227  
|||||  
Sbjct: 558 ttctccctgccagcacggaggcgctgctggatgatgaggccaggcctcgcatgcttc 617

Query: 228 ctgcctgtgccccctggcttctcaggcaacttctgtgagatcgtagccgcaaccaacag 287  
|||||  
Sbjct: 618 ctgcctgtgccccctggcttctcaggcaacttctgtgagatcgtagccgcaaccaacag 677

Query: 288 ctgtaccocctaaccatgcgagaacgat 315  
|||||  
Sbjct: 678 ctgtaccocctaaccatgcgagaacgat 705

d: *igf-2*

File: 34\*IGF S      Lane: 34      Base spacing 10.79      Signal G:91 A:28 T:39 C:41  
Sample: IGF S      232 bases in 2872 scans



gi|193484|gb|M14951.1|MUSGFII  
Mouse insulin-like growth factor II (IGF-II) mRNA, complete cds  
Length = 1435

Score = 244 bits (123), Expect = 2e-62  
Identities = 136/139 (97%), Gaps = 1/139 (0%)  
Strand = Plus / Plus

Query: 34 cggccccggagagactctgtgcgagggggaagcttggtgacacgcttaggtttgtctggt 93  
|||||  
Sbjct: 109 cggccccggagagactctgtgcgaggggga-gcttggtgacacgcttcagttgtctggt 167

Query: 94 cggaccgcggttctacttcagcaggccttcaagccgtgccaaccgtcgcagccgtggca 153  
|||||  
Sbjct: 168 cggaccgcggttctacttcagcaggccttcaagccgtgccaaccgtcgcagccgtggca 227

Query: 154 tcgtggaagagtgctgctt 172  
|||||  
Sbjct: 228 tcgtggaagagtgctgctt 246

## Reference List

Alarid, E. T., Bakopoulos, N., and Solodin, N. Proteasome-mediated proteolysis of estrogen receptor: a novel component in autologous down-regulation. *Mol.Endocrinol.*, *13*: 1522-1534, 1999.

Ali, S., Metzger, D., Bornert, J. M., and Chambon, P. Modulation of transcriptional activation by ligand-dependent phosphorylation of the human estrogen receptor- $\alpha/\beta$  region. *Embo Journal*, *12*: 1153-1160, 1993.

Anaf, V., Simon, P., Fayt, I., and Noel, J. Smooth muscles are frequent components of endometriotic lesions. *Hum.Reprod.*, *15* : 767-771, 2000.

Anandappa, S. Y., Sibson, R., Platt-Higgins, A., Winstanley, J. H., Rudland, P. S., and Barraclough, R. Variant estrogen receptor alpha mRNAs in human breast cancer specimens [In Process Citation]. *Int.J.Cancer*, *88*: 209-216, 2000.

AndoLu, J., Takahashi, M., Imai, S., Ishihara, R., Kitamura, T., Iijima, T., Takano, S., Nishiyama, K., Suzuki, K., and Maekawa, A. High-yield induction of uterine endometrial adenocarcinomas in Donryu rats by a single intra-uterine administration of N-ethyl- N'-nitro-N-nitrosoguanidine via the vagina. *Japanese Journal Of Cancer Research*, *85*: 789-793, 1994.

Anzick, S. L., Kononen, J., Walker, R. L., Azorsa, D. O., Tanner, M. M., Guan, X. Y., Sauter, G., Kallioniemi, O. P., Trent, M., and Meltzer, P. S. AIB1, a steroid receptor coactivator amplified in breast and ovarian cancer. *Science*, *277*: 965-968, 1997.

Arbuckle, N. D., Dauvois, S., and Parker, M. G. Effects of antioestrogens on the DNA binding activity of oestrogen receptors in vitro. *Nucleic Acids Research*, *20*: (pp 3839-3844), 1992.

Badia, E., Duchesne, M. J., Semlali, A., Fuentes, M., Giamarchi, C., Richard-Foy, H., Nicolas, J. C., and Pons, M. Long-term hydroxytamoxifen treatment of an MCF-7-derived breast

cancer cell line irreversibly inhibits the expression of estrogenic genes through chromatin remodeling. *Cancer Res.*, 60: 4130-4138, 2000.

Barkhem, T., Carlsson, B., Nilsson, Y., Enmark, E., Gustafsson, J. A., and Nilsson, S. Differential response of estrogen receptor alpha and estrogen receptor beta to partial estrogen agonists/antagonists. *Molecular Pharmacology*, 54: 105-112, 1998.

Baum, M. Tamoxifen. *Endocrine-Related Cancer*, 4: 237-243, 1997.

Baum, M. Tamoxifen - the treatment of choice. why look for alternatives? *Br J Cancer*, 78: 1-4, 1998.

Beekman, J. M., Allan, G. F., Tsai, S. Y., Tsai, M. J., and Omalley, B. W. Transcriptional activation by the estrogen-receptor requires a conformational change in the ligand-binding domain. *Molecular Endocrinology*, 7: 1266-1274, 1993.

Bergman, M. D., Schachter, B. S., Karelus, K., Combatsiaris, E. P., Garcia, T., and Nelson, J. F. Up-regulation of the uterine estrogen-receptor and its messenger- ribonucleic-acid during the mouse estrous-cycle - the role of estradiol. *Endocrinology*, 130: 1923-1930, 1992.

Bernstein, L., Deapen, D., Cerhan, J. R., Schwartz, S. M., Liff, J., McGann-Maloney, E., Perlman, J. A., and Ford, L. Tamoxifen therapy for breast cancer and endometrial cancer risk. *J.Natl.Cancer Inst.*, 91: 1654-1662, 1999.

Bhattacharyya, A., Ear, U. S., Koller, B. H., Weichselbaum, R. R., and Bishop, D. K. The breast cancer susceptibility gene BRCA1 is required for subnuclear assembly of Rad51 and survival following treatment with the DNA cross- linking agent cisplatin. *J.Biol.Chem.*, 275: 23899-23903, 2000.

Black, L. J., Jones, C. D., and Falcone, J. F. Antagonism of estrogen action with a new benzothiophene derived antiestrogen. *Life Sci.*, 32: 1031-1036, 1983.

Blanks, R. G., Moss, S. M., McGahan, C. E., Quinn, M. J., and Babb, P. J. Effect of NHS breast screening programme on mortality from breast cancer in England and Wales, 1990-8: comparison of observed with predicted mortality [In Process Citation]. *BMJ*, *321*: 665-669, 2000.

Blumenthal, R. D., Samoszuk, M., Taylor, A. P., Brown, G., Alisauskas, R., and Goldenberg, D. M. Degranulating eosinophils in human endometriosis. *Am.J.Pathol.*, *156*: 1581-1588, 2000.

Boocock, D. J., Maggs, J. L., Brown, K., White, I. N. H., and Park, B. K. Major inter-species differences in the rates of *O*-sulfonation and *O*-glucuronylation of  $\alpha$ -hydroxytamoxifen in vitro: a metabolic disparity protecting human liver from the formation of tamoxifen-DNA adducts. *Carcinogenesis*, in press, 2000.

Brosens, J. J., Barker, F. G., and de Souza, N. M. Myometrial zonal differentiation and uterine junctional zone hyperplasia in the non-pregnant uterus. *Hum.Reprod.Update.*, *4*: 496-502, 1998.

Brzozowski, A. M., Pike, A. C. W., Dauter, Z., Hubbard, R. E., Bonn, T., Engstrom, O., Ohman, L., Greene, G. L., Gustafsson, J.-A., and Carlquist, M. Molecular basis of agonism and antagonism in the oestrogen receptor. *Nature*, *389*: (pp 753-758), 1997.

Bunone, G., Briand, P. A., Miksicek, R. J., and Picard, D. Activation of the unliganded estrogen receptor by egf involves the map kinase pathway and direct phosphorylation. *Embo Journal*, *15*: 2174-2183, 1996.

Bush, T. L. The epidemiology of cardiovascular-disease in postmenopausal women. *Annals Of The New York Academy Of Sciences*, *592*: 263-271, 1990.

Carmichael, P. L., Ugwumadu, A. H. N., Neven, P., Hewer, A. J., Poon, G. K., and Phillips, D. H. Lack of genotoxicity of tamoxifen in human endometrium. *Cancer Res*, *56*: 1475-1479, 1996.

Carmichael, P. L., Sardar, S., Neven, F., VanHoof, I., Ugwumadu, A., Bourne, T., Tomas, E., Hellberg, P., Hewer, A. J., and Phillips, D. H. Detection of DNA adducts in the human endometrium: a lack of evidence. *European Journal Of Cancer*, 34: S66-S67, 1998.

Carmichael, P. L., Sardar, S., Crooks, N., Neven, P., Van Hoof, I., Ugwumadu, A., Bourne, T., Tomas, E., Hellberg, P., Hewer, A. J., and Phillips, D. H. Lack of evidence from HPLC <sup>32</sup>P-post-labelling for tamoxifen-DNA adducts in the human endometrium. *Carcinogenesis*, Vol 20: 339-342, 1999.

Carmichael, P. L., Pole, J. C. M., and Neven, P. Modulation of endometrial transforming growth factor beta (TGF beta) by tamoxifen. *European Journal Of Cancer*, 36: S42-S43, 2000.

Carthew, P., Rich, K. J., Martin, E. A., De Matteis, F., Lim, C. K., Manson, M. M., Festing, M. F., White, I. N. H., and Smith, L. L. DNA damage as assessed by <sup>32</sup>P-postlabelling in three rat strains exposed to dietary tamoxifen: the relationship between cell proliferation and liver tumour formation. *Carcinogenesis*, 16: 1299-1304, 1995.

Carthew, P., Edwards, R. E., Nolan, B. M., Martin, E. A., and Smith, L. L. Tamoxifen associated uterine pathology in rodents: relevance to women. *Carcinogenesis*, 17: 1577-1582, 1996.

Carthew, P., Edwards, R. E., and Nolan, B. M. Depletion of hepatocyte nuclear estrogen receptor expression is associated with promotion of tamoxifen induced GST-P foci to tumours in rat liver. *Carcinogenesis*, 18: 1109-1112, 1997.

Carthew, P., Edwards, R. E., and Nolan, B. M. Uterotrophic effects of tamoxifen, toremifene, and raloxifene do not predict endometrial cell proliferation in the ovariectomized CD1 mouse. *Toxicol.Appl.Pharmacol.*, 158: 24-32, 1999.

Carthew, P., Edwards, R. E., Nolan, B. M., Tucker, M. J., and Smith, L. L. Compartmentalized uterotrophic effects of tamoxifen, toremifene, and estradiol in the ovariectomized Wistar (Han) rat. *Toxicol.Sci.*, 48: 197-205, 1999.

Carthew, P., Edwards, R. E., Nolan, B. M., Martin, E. A., Heydon, R. T., White, I. N., and Tucker, M. J. Tamoxifen induces endometrial and vaginal cancer in rats in the absence of endometrial hyperplasia. *Carcinogenesis*, *21*: 793-797, 2000.

Chae, K., Gibson, M. K., and Korach, K. S. Estrogen receptor stereochemistry: ligand binding orientation and influence on biological activity. *Mol.Pharmacol.*, *40*: 806-811, 1991.

Chae, K., Lindzey, J., McLachlan, J. A., and Korach, K. S. Estrogen-dependent gene regulation by an oxidative metabolite of diethylstilbestrol, diethylstilbestrol-4',4"-quinone. *Steroids*, *63*: 149-157, 1998.

Chaw, Y. F., Crane, L. E., Lange, P., and Shapiro, R. Isolation and identification of cross-links from formaldehyde-treated nucleic acids. *Biochemistry*, *19*: 5525-5531, 1980.

Chen, J. D. and Li, H. Coactivation and corepression in transcriptional regulation by steroid/nuclear hormone receptors. *Critical Reviews In Eukaryotic Gene Expression*, *8*: 169-190, 1998.

Chiarenza, A., Lazarovici, P., Lempereur, L., Cantarella, G., Bianchi, A., and Bernardini, R. Tamoxifen inhibits nerve growth factor-induced proliferation of the human breast cancerous cell line MCF-7. *Cancer Res*, *61*: 3002-3008, 2001.

Claus, E. B., Risch, N., and Thompson, W. D. Genetic analysis of breast cancer in the cancer and steroid hormone study. *Am.J.Hum.Genet.*, *48*: 232-242, 1991.

Cohen, C. J. Tamoxifen and endometrial cancer: Tamoxifen effects on the human female genital tract. *Seminars In Oncology*, *24* : S1-55-S1-64, 1997.

Cohen, I., Beyth, Y., Shapira, J., Tepper, R., Fishman, A., Cordoba, M., Bernheim, J., Yigael, D., and Altaras, M. M. High frequency of adenomyosis in postmenopausal breast cancer patients treated with tamoxifen. *Gynecol.Obstet.Invest*, *44*: 200-205, 1997.

Collins, P. and Webb, C. Estrogen hits the surface [news] [see comments]. *Nat.Med.*, *5*: 1130-1131, 1999.

Cooke, P. S., Buchanan, D. L., Lubahn, D. B., and Cunha, G. R. Mechanism of estrogen action: lessons from the estrogen receptor- alpha knockout mouse. *Biology of Reproduction*, *59*: 470-475, 1998.

Couse, J. F. and Korach, K. S. Reproductive phenotypes in the estrogen receptor-alpha knockout mouse. *Ann.Endocrinol.(Paris)*, *60*: 143-148, 1999.

Coward, P., Lee, D., Hull, M. V., and Lehmann, J. M. 4-Hydroxytamoxifen binds to and deactivates the estrogen- related receptor gamma. *Proc Natl Acad Sci USA*, *98*: 8880-8884, 2001.

Cowley, S. M., Hoare, S., Mosselman, S., and Parker, M. G. Estrogen receptors alpha and beta form heterodimers on dna. *J Biol Chem*, *272*: 19858-19862, 1997.

Cummings, S. R., Eckert, S., Krueger, K. A., Grady, D., Powles, T. J., Cauley, J. A., Norton, L., Nickelsen, T., Bjarnason, N. H., Morrow, M., Lippman, M. E., Black, D., Glusman, J. E., Costa, A., and Jordan, V. C. The effect of raloxifene on risk of breast cancer in postmenopausal women: results from the MORE randomized trial. *Multiple Outcomes of Raloxifene Evaluation. JAMA*, *281*: 2189-2197, 1999.

Dauvois, S., Danielian, P. S., White, R., and Parker, M. G. Antiestrogen ICI 164,384 reduces cellular estrogen receptor content by increasing its turnover. *Proc Natl Acad Sci USA*, *89*: (pp 4037-4041), 1992.

De Souza, A. T., Yamada, T., Mills, J. J., and Jirtle, R. L. Imprinted genes in liver carcinogenesis. *FASEB J.*, *11*: 60-67, 1997.

DevinLeclerc, J., Meng, X., Delahaye, F., Leclerc, P., Baulieu, E. E., and Catelli, M. G. Interaction and dissociation by ligands of estrogen receptor and hsp90: the antiestrogen ru 58668

induces a protein synthesis- dependent clustering of the receptor in the cytoplasm. *Molecular Endocrinology*, 12: 842-854, 1998.

Easton, D. F., Bishop, D. T., Ford, D., and Crockford, G. P. Genetic linkage analysis in familial breast and ovarian cancer: results from 214 families. The Breast Cancer Linkage Consortium. *Am.J.Hum.Genet.*, 52: 678-701, 1993.

Ekena, K., Katzenellenbogen, J. A., and Katzenellenbogen, B. S. Determinants of ligand specificity of estrogen receptor-  $\alpha$ : Estrogen *versus* androgen discrimination. *J Biol Chem*, 273: 693-699, 1998.

El Khissiin, A. and Leclercq, G. Implication of proteasome in estrogen receptor degradation. *FEBS Lett.*, 448: 160-166, 1999.

Evans, R. M. The steroid and thyroid-hormone receptor superfamily. *Science*, 240: 889-895, 1988.

Faccini, J. M., Abbott, D. P., and Paulus, G. J. J. Uterus; Non-neoplastic lesions. *Mouse Histopathology: A Glossary for use in Toxicity and Carcinogenicity Studies*, pp. 158-159. Elsevier, 1990.

Ferenczy, A. Pathophysiology of adenomyosis. *Hum.Reprod.Update.*, 4: 312-322, 1998.

Ferguson, A. T. and Davidson, N. E. Regulation of estrogen receptor alpha function in breast cancer. *Crit Rev.Oncog.*, 8: 29-46, 1997.

Fisher, B., Costantino, J. P., Redmond, C. K., Fisher, E. R., Wickerham, D. L., Cronin, W. M., and NSABP Contributors Endometrial cancer in tamoxifen-treated breast cancer patients: Findings from the National Surgical Adjuvant Breast and Bowel Project (NSABP) B-14. *J Natl Cancer Inst*, 86: 527-537, 1994.

Fisher, B., Costantino, J. P., Wickerham, D. L., Redmond, C. K., Kavanah, M., Cronin, W. M., Vogel, V., Robidoux, A., Dimitrov, N., Atkins, J., Daly, M., Wieand, S., TanChiu, E., Ford, L., and Wolmark, N. Tamoxifen for prevention of breast cancer: Report of the National Surgical Adjuvant Breast and Bowel Project P-1 study. *J Natl Cancer Inst*, 90: 1371-1388, 1998.

Fishman, J., Osborne, M. P., and Telang, N. T. The role of estrogen in mammary carcinogenesis. *Ann.N.Y.Acad.Sci.*, 768: 91-100, 1995.

Fliss, A. E., Benzeno, S., Rao, J., and Caplan, A. J. Control of estrogen receptor ligand binding by Hsp90. *J Steroid Biochem Mol Biol*, 72: 223-230, 2000.

Futamura, M., Arakawa, H., Matsuda, K., Katagiri, T., Saji, S., Miki, Y., and Nakamura, Y. Potential role of BRCA2 in a mitotic checkpoint after phosphorylation by hBUBR1. *Cancer Res.*, 60: 1531-1535, 2000.

Garces, C., Ruiz-Hidalgo, M. J., Bonvini, E., Goldstein, J., and Laborda, J. Adipocyte differentiation is modulated by secreted delta-like (dlk) variants and requires the expression of membrane-associated dlk. *Differentiation*, 64: 103-114, 1999.

Gashler, A. and Sukhatme, V. P. Early growth response protein 1 (Egr-1): prototype of a zinc-finger family of transcription factors. *Prog.Nucleic Acid Res.Mol.Biol.*, 50: 191-224, 1995.

Glass, C. K., Rose, D. W., and Rosenfeld, M. G. Nuclear receptor coactivators. *Current Opinion In Cell Biology*, 9: 222-232, 1997.

Gorski, J., Toft, D., Shyamala, G., Smith, D., and Notides, A. Hormone receptors: studies on the interaction of estrogen with the uterus. *Recent Prog.Horm.Res.*, 24: 45-80, 1968.

Grandien, K., Berkenstam, A., and Gustafsson, J. A. The estrogen receptor gene: promoter organization and expression. *International Journal Of Biochemistry & Cell Biology*, 29: 1343-1369, 1997.

Greaves, P., Goonetilleke, R., Nunn, G., Topham, J., and Orton, T. Two-year carcinogenicity study of tamoxifen in Alderly Park Wistar-derived rats. *Cancer Res*, 53: 3919-3924, 1993.

Greene, G. L., Gilna, P., Waterfield, M., and et al Sequence and expression of human estrogen receptor complementary DNA. *Science*, 231: 1986.

Guo, Y., Greenwood, M. T., Petrof, B. J., and Hussain, S. N. Expression and regulation of protein inhibitor of neuronal nitric oxide synthase in ventilatory muscles. *Am.J.Respir.Cell Mol.Biol.*, 20: 319-326, 1999.

Hall, J. M., Lee, M. K., Newman, B., Morrow, J. E., Anderson, L. A., Huey, B., and King, M. C. Linkage of early-onset familial breast cancer to chromosome 17q21. *Science*, 250: 1684-1689, 1990.

Hard, G. C., Iatropoulos, M. J., Jordan, K., Radi, L., Kaltenberg, O. P., Imondi, A. R., and Williams, G. M. Major differences in the hepatocarcinogenicity and DNA adduct forming ability between toremifene and tamoxifen in female Cr1: CD(BR) rats. *Cancer Res*, 53: 4534-4541, 1993.

Hata, H. and Kuramoto, H. IMMUNOCYTOCHEMICAL DETERMINATION OF ESTROGEN AND PROGESTERONE RECEPTORS IN HUMAN ENDOMETRIAL ADENOCARCINOMA CELLS (ISHIKAWA CELLS). *J Steroid Biochem Mol Biol*, 42: 201-210, 1992.

Hawkins, M. B., Thornton, J. W., Crews, D., Skipper, J. K., Dotte, A., and Thomas, P. Identification of a third distinct estrogen receptor and reclassification of estrogen receptors in teleosts [In Process Citation]. *Proc.Natl.Acad.Sci.U.S.A*, 97: 10751-10756, 2000.

Hebert, C. D., Endo, S., Korach, K. S., Boyd, J., Barrett, J. C., McLachlan, J. A., and Newbold, R. R. Characterization of murine cell lines from diethylstilbestrol-induced uterine endometrial adenocarcinomas. *In Vitro Cell Dev.Biol.*, 28A: 327-336, 1992.

Henderson, B. E. and Feigelson, H. S. Hormonal carcinogenesis. *Carcinogenesis*, 21: 427-433, 2000.

Henderson, V. W., Paganinihill, A., Emanuel, C. K., Dunn, M. E., and Buckwalter, J. G. Estrogen replacement therapy in older women - comparisons between alzheimers-disease cases and nondemented control subjects. *Archives Of Neurology*, 51: 896-900, 1994.

Henderson, V. W. Estrogen, Cognition, and a Women's Risk of Alzheimer's Disease. *American Journal of Medicine*, 103: 11S-18S, 1997.

Hershko, A. and Ciechanover, A. The ubiquitin system. *Annu.Rev.Biochem.*, 67: 425-479, 1998.

Hess, R. A., Bunick, D., Lee, K. H., Bahr, J., Taylor, J. A., Korach, K. S., and Lubahn, D. B. A role for oestrogens in the male reproductive system [see comments]. *Nature*, 390: 509-512, 1997.

HilakiviClarke, L., Cho, E., Onojafe, I., Liao, D. J., and Clarke, R. Maternal exposure to tamoxifen during pregnancy increases carcinogen- induced mammary tumorigenesis among female rat offspring. *CLINICAL CANCER RESEARCH*, 6: 305-308, 2000.

Hilsenbeck, S. G., Friedrichs, W. E., Schiff, R., OConnell, P., Hansen, R. K., Osborne, C. K., and Fuqua, S. A. W. Statistical analysis of array expression data as applied to the problem of tamoxifen resistance. *J Natl Cancer Inst*, 91: 453-459, 1999.

Hirata, S., Shoda, T., Kato, J., and Hoshi, K. The multiple untranslated first exons system of the human estrogen receptor beta (ERbeta) gene. *J.Steroid Biochem.Mol.Biol.*, 78: 33-40, 2001.

Hiroi, H., Inoue, S., Watanabe, T., Goto, W., Orimo, A., Momoeda, M., Tsutsumi, O., Taketani, Y., and Muramatsu, M. Differential immunolocalization of estrogen receptor alpha and beta in rat ovary and uterus. *Journal Of Molecular Endocrinology*, 22: 37-44, 1999.

Holli, K., Valavaara, R., Blanco, G., Kataja, V., Hietanen, P., Flander, M., Pukkala, E., and Joensuu, H. Safety and efficacy results of a randomized trial comparing adjuvant toremifene and tamoxifen in postmenopausal patients with node-positive breast cancer [In Process Citation]. *J.Clin.Oncol.*, 18: 3487-3494, 2000.

Homesley, H. D. Management of endometrial cancer. *Am.J.Obstet.Gynecol.*, 174: 529-534, 1996.

Hong, H., Kohli, K., Trivedi, A., Johnson, D. L., and Stallcup, M. R. GRIP1, a novel mouse protein that serves as a transcriptional coactivator in yeast for the hormone binding domains of steroid receptors. *Proc.Natl.Acad.Sci.U.S.A.*, 93: 4948-4952, 1996.

Horwitz, K. B. and McGuire, W. L. Nuclear mechanisms of estrogen action. *The Journal of Biological Chemistry*, 253: 8185-8191, 1978.

Howell, A., DeFriend, D. J., Robertson, J. F. R., Blamey, R. W., Anderson, L., Anderson, E., Sutcliffe, F. A., and Walton, P. Pharmacokinetics, pharmacological and anti-tumour effects of the specific anti-oestrogen ICI 182 780 in women with advanced breast cancer. *Br J Cancer*, 74: 300-308, 1996.

Howell, A., Osborne, C. K., Morris, C., and Wakeling, A. E. ICI 182,780 (Faslodex): development of a novel, "pure" antiestrogen. *Cancer*, 89: 817-825, 2000.

Huang, A., Leygue, E., Dotzlaw, H., Murphy, L. C., and Watson, P. H. Influence of estrogen receptor variants on the determination of ER status in human breast cancer. *Breast Cancer Res.Treat.*, 58: 219-225, 1999.

Hunter, D. S., Hodges, L. C., Vonier, P. M., Fuchs-Young, R., Gottardis, M. M., and Walker, C. L. Estrogen receptor activation via activation function 2 predicts agonism of xenoestrogens in normal and neoplastic cells of the uterine myometrium. *Cancer Res.*, 59: 3090-3099, 1999.

Hyder, S. M., Stancel, G. M., Chiappetta, C., Murthy, L., Boettger-Tong, H. L., Makela, and S. Uterine expression of vascular endothelial growth factor is increased by estradiol and tamoxifen. *Cancer Res*, 56: (pp 3954-3960), 1996.

Hyder, S. M., Huang, J. C., Nawaz, Z., Boettger-Tong, H., Makela, S., Chiappetta, C., and Stancel, G. M. Regulation of vascular endothelial growth factor expression by estrogens and progestins. *Environ.Health Perspect.*, 108 Suppl 5: 785-790, 2000.

Jazaeri, O., Shupnik, M. A., Jazaeri, A. A., and Rice, L. W. Expression of estrogen receptor alpha mRNA and protein variants in human endometrial carcinoma. *Gynecol.Oncol.*, 74: 38-47, 1999.

Jensen, E. V., Jacobson, H. I., Smith, S., Jungblut, P. W., and De Sombre, E. R. The use of estrogen antagonists in hormone receptor studies. *Gynecol.Invest*, 3: 108-123, 1972.

Jones, P. S., Parrott, E., and White, I. N. H. Activation of transcription by estrogen receptor alpha and beta is cell type- and promoter-dependent. *J Biol Chem*, 274: 32008-32014, 1999.

Jordan, V. C. How is tamoxifen's action subverted? *J Natl Cancer Inst*, 92: 92-94, 2000.

Jordan, V. C. Selective estrogen receptor modulation: A personal perspective. *Cancer Res*, 61: 5683-5687, 2001.

Kangas, L. Agonistic and antagonistic effects of antiestrogens in different target organs. *Acta Oncologica*, 31: (pp 143-146), 1992.

Katsuda, S., Yoshida, M., Watanabe, T., Kuroda, H., AndoLu, J., Takahashi, M., Hayashi, H., and Maekawa, A. Estrogen receptor mRNA in uteri of normal estrous cycling and ovariectomized rats by in situ hybridization. *Proceedings Of The Society For Experimental Biology And Medicine*, 221: 207-214, 1999.

Kierszenbaum, A. L. The 26S proteasome: ubiquitin-mediated proteolysis in the tunnel [In Process Citation]. *Mol.Reprod.Dev.*, 57: 109-110, 2000.

Klinge, C. M., Studinski-Jones, A. L., Kulakosky, P. C., Bambara, R. A., and Hilf, R. Comparison of tamoxifen ligands on estrogen receptor interaction with estrogen response elements. *Mol.Cell Endocrinol.*, 143: 79-90, 1998.

Korach, K. S., Horigome, T., Tomooka, Y., Yamashita, S., Newbold, R. R., and McLachlan, J. A. Immunodetection of estrogen receptor in epithelial and stromal tissues of neonatal mouse uterus. *Proc Natl Acad Sci USA*, 85: (pp 3334-3337), 1988.

Korach, K. S. Insights from the study of animals lacking functional estrogen receptor. *Science*, 266: 1524-1527, 1994.

Koritnik, D. R., Koshy, A., and Hoversland, R. C. 17 beta-estradiol treatment increases the levels of estrogen receptor and its mRNA in male rat liver. *Steroids*, 60: 519-529, 1995.

Kos, M., O'Brien, S., Flouriot, G., and Gannon, F. Tissue-specific expression of multiple mRNA variants of the mouse estrogen receptor alpha gene(1) [In Process Citation]. *FEBS Lett.*, 477: 15-20, 2000.

Koujyo, T., Hatakeyama, S., Yamada, H., Iwabuchi, K., Kajino, K., Ogasawara, K., Onoe, K., and Fujimoto, S. Induction of endometriosis and adenomyosis by transvaginal pituitary transplantation in mice with and without natural killer cell activity. *Am.J.Reprod.Immunol.*, 40: 441-446, 1998.

Krege, J. H., Hodgkin, J. B., Couse, J. F., Enmark, E., Warner, M., Mahler, J. F., Sar, M., Korach, K. S., Gustafsson, J. A., and Smithies, O. Generation and reproductive phenotypes of mice lacking estrogen receptor beta. *Proc.Natl.Acad.Sci.U.S.A*, 95: 15677-15682, 1998.

Kuiper, G. G. J. M., Enmark, E., Peltö-Huikko, M., Nilsson, S., and Gustafsson, J.-A. Cloning of a novel estrogen receptor expressed in rat prostate and ovary. *Proc Natl Acad Sci USA*, *93*: (pp 5925-5930), 1996.

Kuiper, G. G. J. M., Lemmen, J. G., Carlsson, B., Corton, J. C., Safe, S. H., van der Saag, P. T., Van der Burg, P., and Gustafsson, J. Å. Interaction of estrogenic chemicals and phytoestrogens with estrogen receptor  $\beta$ . *Endocrinology*, *139*: 4252-4263, 1998.

Kunz, G., Beil, D., Huppert, P., and Leyendecker, G. Structural abnormalities of the uterine wall in women with endometriosis and infertility visualized by vaginal sonography and magnetic resonance imaging. *Hum.Reprod.*, *15*: 76-82, 2000.

Larsimont, D., Kiss, R., d'Olne, D., de Launoit, Y., Matthei, W., Paridaens, R., Pasteels, J. L., and Gompel, C. Correlation between nuclear cytomorphometric parameters and estrogen receptor levels in breast cancer. *Cancer*, *63*: 2162-2168, 1989.

Lawrence, J. B. and Singer, R. H. Quantitative analysis of in situ hybridization methods for the detection of actin gene expression. *Nucleic Acids Res.*, *13*: 1777-1799, 1985.

Lee, Y. J. and Gorski, J. Estrogen receptor down-regulation is regulated noncooperatively by estrogen at the transcription level. *Molecular And Cellular Endocrinology*, *137*: 85-92, 1998.

Leo, C., Li, H., and Chen, J. D. Differential mechanisms of nuclear receptor regulation by receptor-associated coactivator 3. *J.Biol.Chem.*, *275*: 5976-5982, 2000.

Levenson, A. S. and Jordan, V. C. The key to the antiestrogenic mechanism of raloxifene is amino acid 351 (aspartate) in the estrogen receptor. *Cancer Res*, *58*: 1872-1875, 1998.

Liehr, J. G. Is estradiol a genotoxic mutagenic carcinogen? *Endocr.Rev.*, *21*: 40-54, 2000.

Lim, S. P., Leung, E., and Krissansen, G. W. The beta7 integrin gene (Itgb-7) promoter is responsive to TGF-beta1: defining control regions. *Immunogenetics*, 48: 184-195, 1998.

Lindsay, R. Why do oestrogens prevent bone loss? *Baillieres Clin.Obstet.Gynaecol.*, 5: 837-852, 1991.

Liu, H., Lee, E. S., Los Reyes, A., Zapf, J. W., and Jordan, V. C. Silencing and reactivation of the selective estrogen receptor modulator-estrogen receptor alpha complex. *Cancer Res*, 61: 3632-3639, 2001.

Lommatzsch, M., Braun, A., Mannsfeldt, A., Botchkarev, V. A., Botchkareva, N. V., Paus, R., Fischer, A., Lewin, G. R., and Renz, H. Abundant production of brain-derived neurotrophic factor by adult visceral epithelia. Implications for paracrine and target-derived Neurotrophic functions. *Am.J.Pathol.*, 155: 1183-1193, 1999.

Lopes, U. G., Erhardt, P., Yao, R., and Cooper, G. M. p53-dependent induction of apoptosis by proteasome inhibitors. *J.Biol.Chem.*, 272: 12893-12896, 1997.

Lu, B., Leygue, E., Dotzlaw, H., Murphy, L. J., and Murphy, L. C. Functional characteristics of a novel murine estrogen receptor-beta isoform, estrogen receptor-beta 2 [In Process Citation]. *J.Mol.Endocrinol.*, 25: 229-242, 2000.

Lubahn, D. B., Moyer, J. S., Golding, T. S., Couse, J. F., Korach, K. S., and Smithies, O. Alteration of reproductive function but not prenatal sexual development after insertional disruption of the mouse estrogen receptor gene. *Proc.Natl.Acad.Sci.U.S.A*, 90: 11162-11166, 1993.

MacGregor, J. I. and Jordan, V. C. Basic guide to the mechanisms of antiestrogen action. *Pharmacological Reviews*, 50: (pp 151-196), 1998.

Mai, K. T., Yazdi, H. M., Perkins, D. G., and Parks, W. Pathogenetic role of the stromal cells in endometriosis and adenomyosis. *Histopathology*, 30: 430-442, 1997.

Makela, S., Davis, V. L., Tally, W. C., Korkman, J., Salo, L., Vihko, R., Santti, R., and Korach, K. S. Dietary Estrogens Act through Estrogen Receptor-Mediated Processes and Show No Antiestrogenicity in Cultured Breast Cancer Cells. *Environ. Health Perspect.*, *102*: 572-578, 1994.

Martin, E. A., Rich, K., White, I. N. H., Woods, K. L., Powles, T. J., and Smith, L. L. <sup>32</sup>P-Postlabelled DNA adducts in liver obtained from women treated with tamoxifen. *Carcinogenesis*, *16*: 1651-1654, 1995.

Martin, E. A., Carthew, P., White, I. N. H., Heydon, R. T., Gaskell, M., Mauthe, R. J., Turteltaub, K. W., and Smith, L. L. Investigation of the formation and accumulation of liver DNA adducts in mice chronically exposed to tamoxifen. *Carcinogenesis*, *18*: 2209-2215, 1997.

McCluggage, W. G., Desai, V., and Manek, S. Tamoxifen-associated postmenopausal adenomyosis exhibits stromal fibrosis, glandular dilatation and epithelial metaplasias [In Process Citation]. *Histopathology*, *37*: 340-346, 2000.

McNeil, C. In search of the perfect serm: beyond tamoxifen and raloxifene. *J Natl Cancer Inst*, *90*: 956-957, 1998.

Medlock, K. L., Branham, W. S., and Sheehan, D. M. Effects of toremifene on neonatal rat uterine growth and differentiation. *Biology of Reproduction*, *56*: (pp 1239-1244), 1997.

Metzger, D., Ali, S., Bornert, J. M., and Chambon, P. Characterization of the amino-terminal transcriptional activation function of the human estrogen receptor in animal and yeast cells. *J. Biol. Chem.*, *270* : 9535-9542, 1995.

Misiti, S., Schomburg, L., Yen, P. M., and Chin, W. W. Expression and hormonal regulation of coactivator and corepressor genes. *Endocrinology*, *139*: 2493-2500, 1998.

Mitchell, P. J. and Tjian, R. Transcriptional regulation in mammalian cells by sequence-specific DNA binding proteins. *Science*, *245*: 371-378, 1989.

Mitchner, N. A., Garlick, C., and BenJonathan, N. Cellular distribution and gene regulation of estrogen receptors alpha and beta in the rat pituitary gland. *Endocrinology*, 139: 3976-3983, 1998.

Monje, P., Zanello, S., Holick, M., and Boland, R. Differential cellular localization of estrogen receptor alpha in uterine and mammary cells. *Molecular And Cellular Endocrinology*, 181: 117-129, 2001.

Mosselman, S., Polman, J., and Dijkema, R. ERbeta: Identification and characterization of a novel human estrogen receptor. *FEBS Letters*, 392: (pp 49-53), 1996.

Mourits, M. J., De Vries, E. G., Willemse, P. H., Ten Hoor, K. A., Hollema, H., and Van der Zee, A. G. Tamoxifen treatment and gynecologic side effects: a review. *Obstet.Gynecol.*, 97: 855-866, 2001.

Mueller, M. D., Vigne, J. L., Minchenko, A., Lebovic, D. I., Leitman, D. C., and Taylor, R. N. Regulation of vascular endothelial growth factor (VEGF) gene transcription by estrogen receptors alpha and beta. *Proc.Natl.Acad.Sci.U.S.A*, 97: 10972-10977, 2000.

Nandi, S., Guzman, R. C., and Yang, J. Hormones and mammary carcinogenesis in mice, rats, and humans: a unifying hypothesis. *Proc.Natl.Acad.Sci.U.S.A*, 92: 3650-3657, 1995.

Nawaz, Z., Stancel, G. M., and Hyder, S. M. The pure antiestrogen ICI 182,780 inhibits progestin-induced transcription. *Cancer Res.*, 59: 372-376, 1999.

Nawaz, Z., Lonard, D. M., Dennis, A. P., Smith, C. L., and O'Malley, B. W. Proteasome-dependent degradation of the human estrogen receptor. *Proc.Natl.Acad.Sci.U.S.A*, 96: 1858-1862, 1999.

Newbold, R. R., Bullock, B. C., and McLachlan, J. A. Uterine adenocarcinoma in mice following developmental treatment with estrogens: a model for hormonal carcinogenesis. *Cancer Res.*, 50: 7677-7681, 1990.

Newbold, R. R., Jefferson, W. N., Padilla-Burgos, E., and Bullock, B. C. Uterine carcinoma in mice treated neonatally with tamoxifen. *Carcinogenesis*, *18*: 2293-2298, 1997.

Newbold, R. R., Hanson, R. B., Jefferson, W. N., Bullock, B. C., Haseman, J., and McLachlan, J. A. Increased tumors but uncompromised fertility in the female descendants of mice exposed developmentally to diethylstilbestrol. *Carcinogenesis*, *19*: 1655-1663, 1998.

Newbold, R. R. and Liehr, J. G. Induction of uterine adenocarcinoma in CD-1 mice by catechol estrogens. *Cancer Res.*, *60*: 235-237, 2000.

Newbold, R. R., Banks, E. P., Bullock, B., and Jefferson, W. N. Uterine adenocarcinoma in mice treated neonatally with genistein. *Cancer Res*, *61*: 4325-4328, 2001.

Niederacher, D., An, H. X., Cho, Y. J., Hantschmann, P., Bender, H. G., and Beckmann, M. W. Mutations and amplification of oncogenes in endometrial cancer. *Oncology*, *56*: 59-65, 1999.

Nikov, G. N., Hopkins, N. E., Boue, S., and Alworth, W. L. Interactions of dietary estrogens with human estrogen receptors and the effect on estrogen receptor-estrogen response element complex formation. *Environ.Health Perspect.*, *108*: 867-872, 2000.

Nuttall, M. E., Stroup, G. B., Fisher, P. W., Nadeau, D. P., Gowen, M., and Suva, L. J. Distinct mechanisms of action of selective estrogen receptor modulators in breast and osteoblastic cells [In Process Citation]. *Am.J.Physiol Cell Physiol*, *279*: C1550-C1557, 2000.

Nuttall, M. E., Pendrak, I., Emery, J. G., Nadeau, D. P., Fisher, P. W., Nicholson, T. A., Zhu, Y., Suva, L. J., Kingsbury, W. D., and Gowen, M. Antagonism of oestrogen action in human breast and endometrial cells in vitro: potential novel antitumour agents. *Cancer Chemother.Pharmacol.*, *47*: 437-443, 2001.

O'Regan, R. M., Cisneros, A., England, G. M., MacGregor, J. I., Muenzner, H. D., Assikis, V. J., Bilimoria, M. M., Piette, M., Dragan, Y. P., Pitot, H. C., Chatterton, R., and Jordan, V. C.

Effects of the antiestrogens tamoxifen, toremifene, and ICI 182,780 on endometrial cancer growth [see comments]. *J.Natl.Cancer Inst.*, *90*: 1552-1558, 1998.

Ogawa, S., Inoue, S., Watanabe, T., Hiroi, H., Orimo, A., Hosoi, T., Ouchi, Y., and Muramatsu, M. The complete primary structure of human estrogen receptor  $\beta$  (hER $\beta$ ) and its heterodimerization with ER $\alpha$  *in vivo* and *in vitro*. *Biochemical and Biophysical Research Communications*, *243*: 122-126, 1998.

Onate, S. A., Tsai, S. Y., Tsai, M. J., and O'Malley, B. W. Sequence and characterization of a coactivator for the steroid hormone receptor superfamily. *Science*, *270*: 1354-1357, 1995.

Ota, H., Igarashi, S., and Tanaka, T. Morphometric evaluation of stromal vascularization in the endometrium in adenomyosis. *Hum.Reprod.*, *13*: 715-719, 1998.

Pace, P., Taylor, J., Suntharalingam, S., Coombes, R. C., and Ali, S. Human estrogen receptor beta binds dna in a manner similar to and dimerizes with estrogen receptor alpha. *J Biol Chem*, *272*: 25832-25838, 1997.

Paech, K., Webb, P., Kuiper, G. G. J. M., Nilsson, S., Gustafsson, J. A., Kushner, P. J., and Scanlan, T. S. Differential ligand activation of estrogen receptors er alpha and er beta at ap1 sites. *Science*, *277*: 1508-1510, 1997.

Paganini-Hill, A., Ross, R. K., and Henderson, B. E. Endometrial cancer and patterns of use of oestrogen replacement therapy: a cohort study. *Br.J.Cancer*, *59*: 445-447, 1989.

Pakdel, F., Le Goff, P., and Katzenellenbogen, B. S. An assessment of the role of domain F and PEST sequences in estrogen receptor half-life and bioactivity. *J.Steroid Biochem.Mol.Biol.*, *46*: 663-672, 1993.

Park, J. J., Irvine, R. A., Buchanan, G., Koh, S. S., Park, J. M., Tilley, W. D., Stallcup, M. R., Press, M. F., and Coetzee, G. A. Breast cancer susceptibility gene 1 (BRCA1) is a coactivator of the androgen receptor [In Process Citation]. *Cancer Res.*, *60*: 5946-5949, 2000.

Parker, M. G. Action of 'pure' antiestrogens in inhibiting estrogen receptor action. *Breast Cancer Research & Treatment*, 26: (pp 131-137), 1993.

Pavao, M. and Traish, A. M. Estrogen receptor antibodies: specificity and utility in detection, localization and analyses of estrogen receptor alpha and beta. *Steroids*, 66: 1-16, 2001.

Pearlstone, D. B., Pearlstone, M. M., Vassilopoulou-Sellin, R., and Singletary, S. E. Hormone replacement therapy and breast cancer [see comments]. *Ann.Surg.Oncol.*, 6: 208-217, 1999.

Pelletier, G., Labrie, C., and Labrie, F. Localization of oestrogen receptor alpha, oestrogen receptor beta and androgen receptors in the rat reproductive organs. *J.Endocrinol.*, 165: 359-370, 2000.

Petersen, D. N., Tkalcevic, G. T., KozaTaylor, P. H., Turi, T. G., and Brown, T. A. Identification of estrogen receptor beta(2), a functional variant of estrogen receptor beta expressed in normal rat tissues. *Endocrinology*, 139: 1082-1092, 1998.

Peto, R., Boreham, J., Clarke, M., Davies, C., and Beral, V. UK and USA breast cancer deaths down 25% in year 2000 at ages 20-69 years [letter] [see comments]. *Lancet*, 355: 1822, 2000.

Pettersson, K., Grandien, K., Kuiper, G. G. J. M., and Gustafsson, J.-A. Mouse estrogen receptor beta forms estrogen response element- binding heterodimers with estrogen receptor alpha. *Molecular Endocrinology*, 11: (pp 1486-1496), 1997.

Pettersson, K., Delaunay, F., and Gustafsson, J. A. Estrogen receptor beta acts as a dominant regulator of estrogen signaling [In Process Citation]. *Oncogene*, 19: 4970-4978, 2000.

Philips, A., Chalbos, D., and Rochefort, H. Estradiol increases and anti-estrogens antagonize the growth factor- induced activator protein-1 activity in MCF7 breast cancer cells

without affecting c-fos and c-jun synthesis [published erratum appears in J Biol Chem 1993 Dec 5;268(34):26032]. *J.Biol.Chem.*, 268: 14103-14108, 1993.

Phillips, D. H., Carmichael, P. L., Hewer, A., Cole, K. J., and Poon, G. K. Alpha-hydroxytamoxifen, a metabolite of tamoxifen with exceptionally high DNA-binding activity in rat hepatocytes. *Cancer Res*, 54: 5518-5522, 1994.

Pietras, R. J. and Szego, C. M. Specific binding sites for oestrogen at the outer surfaces of isolated endometrial cells. *Nature*, 265: 69-72, 1977.

Planas-Silva, M. D., Shang, Y. F., Donaher, J. L., Brown, M., and Weinberg, R. A. AIB1 enhances estrogen-dependent induction of cyclin D1 expression. *Cancer Res*, 61: 3858-3862, 2001.

Podsypanina, K., Ellenson, L. H., Nemes, A., Gu, J., Tamura, M., Yamada, K. M., Cordon-Cardo, C., Catoretti, G., Fisher, P. E., and Parsons, R. Mutation of Pten/Mmac1 in mice causes neoplasia in multiple organ systems. *Proc.Natl.Acad.Sci.U.S.A*, 96: 1563-1568, 1999.

Poon, G. K., Cui, Y. C., McCague, R., Lonning, P. E., Feng, R., Rowlands, M. G., and Jarman, M. Analysis of phase 1 and phase 11 metabolites of tamoxifen in breast cancer patients. *Drug Metab Dispos*, 21: 1119-1194, 1995.

Razandi, M., Pedram, A., Greene, G. L., and Levin, E. R. Cell membrane and nuclear estrogen receptors (ERs) originate from a single transcript: studies of ERalpha and ERbeta expressed in Chinese hamster ovary cells. *Mol.Endocrinol.*, 13: 307-319, 1999.

Reich, O., Regauer, S., Urdl, W., Lahousen, M., and Winter, R. Expression of oestrogen and progesterone receptors in low-grade endometrial stromal sarcomas. *Br.J.Cancer*, 82: 1030-1034, 2000.

Rider, V., Carlone, D. L., and Foster, R. T. Oestrogen and progesterone control basic fibroblast growth factor mRNA in the rat uterus. *Journal of Endocrinology*, 154: 75-84, 1997.

Rock, K. L., Gramm, C., Rothstein, L., Clark, K., Stein, R., Dick, L., Hwang, D., and Goldberg, A. L. Inhibitors of the proteasome block the degradation of most cell proteins and the generation of peptides presented on MHC class I molecules. *Cell*, 78: 761-771, 1994.

Roe, E. B., Chiu, K. M., and Arnaud, C. D. Selective estrogen receptor modulators and postmenopausal health. *Adv.Intern.Med.*, 45: 259-278, 2000.

Routledge, E. J., White, R., Parker, M. G., and Sumpter, J. P. Differential Effects of Xenoestrogens on Coactivator Recruitment by Estrogen Receptor (ER) alpha and ERbeta. *J.Biol.Chem.*, 275: 35986-35993, 2000.

Rutanen, E. M., Salmi, A., and Nyman, T. mRNA expression of insulin-like growth factor-I (IGF-I) is suppressed and those of IGF-II and IGF-binding protein-1 are constantly expressed in the endometrium during use of an intrauterine levonorgestrel system. *Mol.Hum.Reprod.*, 3: 749-754, 1997.

Rutanen, E. M. Insulin-like growth factors in endometrial function. *Gynecol.Endocrinol.*, 12: 399-406, 1998.

Rutqvist, L. E., Johansson, H., Signomklao, T., Johansson, U., Fornander, T., and Wilking, N. Adjuvant tamoxifen therapy for early stage breast cancer and second primary malignancies. Stockholm Breast Cancer Study Group. *J.Natl.Cancer Inst.*, 87: 645-651, 1995.

Rutqvist, L. E. Second cancers after adjuvant tamoxifen therapy for breast cancer. *J Natl Cancer Inst*, 88: 1497, 1996.

Saceda, M., Lindsey, R. K., Solomon, H., Angeloni, S. V., and Martin, M. B. Estradiol regulates estrogen receptor mRNA stability. *J Steroid Biochem Mol Biol*, 66: 113-120, 1998.

Saunders, P. T. K., Maguire, S. M., Gaughan, J., and Millar, M. R. Expression of oestrogen receptor beta (ERbeta) in multiple rat tissues visualised by immunohistochemistry. *Journal of Endocrinology*, 154: (pp R13-R16), 1997.

Sauve, F., McBroom, L. D., Gallant, J., Moraitis, A. N., Labrie, F., and Giguere, V. CIA, a novel estrogen receptor coactivator with a bifunctional nuclear receptor interacting determinant. *Mol.Cell Biol.*, 21: 343-353, 2001.

Sbracia, M., Zupi, E., Alo, P., Manna, C., Marconi, D., Scarpellini, F., Grasso, J. A., Di Tondo, U., and Romanini, C. Differential expression of IGF-I and IGF-II in eutopic and ectopic endometria of women with endometriosis and in women without endometriosis. *Am.J.Reprod.Immunol.*, 37: 326-329, 1997.

Schild, H. and Rammensee, H. G. Perfect use of imperfection [news; comment]. *Nature*, 404: 709-710, 2000.

Schwabe, J. W., Neuhaus, D., and Rhodes, D. Solution structure of the DNA-binding domain of the oestrogen receptor. *Nature*, 348: 458-461, 1990.

Seidl, K., Erck, C., and Buchberger, A. Evidence for the participation of nerve growth factor and its low- affinity receptor (p75NTR) in the regulation of the myogenic program. *J.Cell Physiol*, 176: 10-21, 1998.

Seo, H. S., Larsimont, D., Querton, G., El Khissiin, A., Laios, I., Legros, N., and Leclercq, G. Estrogenic and anti-estrogenic regulation of estrogen receptor in MCF-7 breast-cancer cells: comparison of immunocytochemical data with biochemical measurements. *Int.J.Cancer*, 78: 760-765, 1998.

Service, R. F. New role for estrogen in cancer? *Science*, 279: 1631-1633, 1998.

Shang, Y., Hu, X., DiRenzo, J., Lazar, M. A., and Brown, M. Cofactor dynamics and sufficiency in estrogen receptor-regulated transcription. *Cell*, 103: 843-852, 2000.

Shiau, A. K., Barstad, D., Loria, P. M., Cheng, L., Kushner, P. J., Agard, D. A., and Greene, G. L. The structural basis of estrogen receptor/coactivator recognition and the antagonism of this interaction by tamoxifen. *Cell*, 95: 927-937, 1998.

Shughrue, P. J. Estrogen action in the estrogen receptor alpha-knockout mouse: is this due to er-beta? *Molecular Psychiatry*, *3*: 299-302, 1998.

Silva, E. G., Tornos, C. S., and Follen-Mitchell, M. Malignant neoplasms of the uterine corpus in patients treated for breast carcinoma: the effects of tamoxifen. *Int J Gynecol Pathol.*, *13*: 248-258, 1994.

Simpson, B. J. B., Langdon, S. P., Rabiasz, G. J., Macleod, K. G., Hirst, G. L., Bartlett, J. M. S., Crew, A. J., Hawkins, R. A., MacineiraPerez, P. P., Smyth, J. F., and Miller, W. R. Estrogen regulation of transforming growth factor-alpha in ovarian cancer. *J Steroid Biochem Mol Biol*, *64*: 137-145, 1998.

Simpson, E. R., Merrill, J. C., Hollub, A. J., Grahamlarence, S., and Mendelson, C. R. Regulation of estrogen biosynthesis by human adipose-cells. *Endocrine Reviews*, *10*: 136-148, 1989.

Spearow, J. L., Doemeny, P., Sera, R., Leffler, R., and Barkley, M. Genetic variation in susceptibility to endocrine disruption by estrogen in mice. *Science*, *285*: 1259-1261, 1999.

Stenoien, D. L., Mancini, M. G., Patel, K., Allegretto, E. A., Smith, C. L., and Mancini, M. A. Subnuclear trafficking of estrogen receptor-alpha and steroid receptor coactivator-1. *Mol.Endocrinol.*, *14*: 518-534, 2000.

Sun, J., Meyers, M. J., Fink, B. E., Rajendran, R., Katzenellenbogen, J. A., and Katzenellenbogen, B. S. Novel ligands that function as selective estrogens or antiestrogens for estrogen receptor-alpha or estrogen receptor-beta. *Endocrinology*, *140*: 800-804, 1999.

Takama, F., Kanuma, T., Wang, D., Kagami, I., and Mizunuma, H. Oestrogen receptor beta expression and depth of myometrial invasion in human endometrial cancer. *Br.J.Cancer*, *84*: 545-549, 2001.

Tan, J., Paria, B. C., Dey, S. K., and Das, S. K. Differential uterine expression of estrogen and progesterone receptors correlates with uterine preparation for implantation and decidualization in the mouse. *Endocrinology*, *140*: 5310-5321, 1999.

Tcherepanova, I., Puigserver, P., Norris, J. D., Spiegelman, B. M., and McDonnell, D. P. Modulation of estrogen receptor-alpha transcriptional activity by the coactivator PGC-1. *J.Biol.Chem.*, *275*: 16302-16308, 2000.

Tibbetts, T. A., Mendoza-Meneses, M., O'Malley, B. W., and Conneely, O. M. Mutual and intercompartmental regulation of estrogen receptor and progesterone receptor expression in the mouse uterus. *Biol.Reprod.*, *59*: 1143-1152, 1998.

Tikkanen, M. K., Carter, D. J., Harris, A. M., Le, H. M., Azorsa, D. O., Meltzer, P. S., and Murdoch, F. E. Endogenously expressed estrogen receptor and coactivator AIB1 interact in MCF-7 human breast cancer cells. *Proc.Natl.Acad.Sci.U.S.A.*, *97*: 12536-12540, 2000.

Toda, K., Yang, L. X., and Shizuta, Y. Transcriptional regulation of the human aromatase cytochrome P450 gene expression in human placental cells. *J.Steroid Biochem.Mol.Biol.*, *53*: 181-190, 1995.

Tonetti, D. A., Oregan, R., Tanjore, S., England, G., and Jordan, V. C. Antiestrogen stimulated human endometrial cancer growth: laboratory and clinical considerations. *J Steroid Biochem Mol Biol*, *65*: 181-189, 1998.

Tora, L., White, J., Brou, C., Tasset, D., Webster, N., Scheer, E., and Chambon, P. The human estrogen receptor has two independent nonacidic transcriptional activation functions. *Cell*, *59*: 477-487, 1989.

Tsutsui, T. [Mechanisms of estrogen-induced carcinogenesis--detection of DNA adducts in cultured mammalian cells by <sup>32</sup>P-postlabeling]. *Nippon Yakurigaku Zasshi*, *110*: 1-9, 1997.

Turner, C. H., Sato, M., and Bryant, H. U. Raloxifene preserves bone strength and bone mass in ovariectomized rats. *Endocrinology*, 135: 2001-2005, 1994.

Van Den Bermd, G. J., Kuiper, G. G., Pols, H. A., and van Leeuwen, J. P. Distinct effects on the conformation of estrogen receptor alpha and beta by both the antiestrogens ICI 164,384 and ICI 182,780 leading to opposite effects on receptor stability. *Biochem.Biophys.Res.Commun.*, 261: 1-5, 1999.

vanAgthoven, T., vanAgthoven, T. L. A., Dekker, A., vanderSpek, P. J., Vreede, L., and Dorssers, L. C. J. Identification of bcar3 by a random search for genes involved in antiestrogen resistance of human breast cancer cells. *Embo Journal*, 17: 2799-2808, 1998.

VandenBermd, G. J. C. M., Kuiper, G. G. J. M., Pols, H. A. P., and VanLeeuwen, J. P. T. M. Distinct effects on the conformation of estrogen receptor alpha and beta by both the antiestrogens ICI 164,384 and ICI 182,780 leading to opposite effects on receptor stability. *Biochem Biophys Res Comm.*, 261: 1-5, 1999.

Vladusic, E. A., Hornby, A. E., Guerra-Vladusic, F. K., Lakins, J., and Lupu, R. Expression and regulation of estrogen receptor beta in human breast tumors and cell lines. *ONCOLOGY REPORTS*, 7: 157-167, 2000.

Wakeling, A. E. and Valcaccia, B. Antioestrogenic and antitumour activities of a series of non-steroidal antioestrogens. *J.Endocrinol.*, 99: 455-464, 1983.

Wakeling, A. E. and Bowler, J. ICI 182,780, a new antioestrogen with clinical potential. *J Steroid Biochem Mol Biol*, 43: (pp 173-177), 1992.

Webb, P., Nguyen, P., Valentine, C., Lopez, G. N., Kwok, G. R., McInerney, E., Katzenellenbogen, B. S., Enmark, E., Gustafsson, J. A., Nilsson, S., and Kushner, P. J. The estrogen receptor enhances AP-1 activity by two distinct mechanisms with different requirements for receptor transactivation functions. *Mol.Endocrinol.*, 13: 1672-1685, 1999.

Webb, P., Nguyen, P., Valentine, C., Weatherman, R. V., Scanlan, T. S., and Kushner, P. J. An Antiestrogen-responsive Estrogen Receptor-alpha Mutant (D351Y) Shows Weak AF-2 Activity in the Presence of Tamoxifen. *J.Biol.Chem.*, 275: 37552-37558, 2000.

Weihua, Z., Saji, S., Makinen, S., Cheng, G., Jensen, E. V., Warner, M., and Gustafsson, J. A. Estrogen receptor (ER) beta, a modulator of ERalpha in the uterus. *Proc.Natl.Acad.Sci.U.S.A*, 97: 5936-5941, 2000.

White, I. N. H., De Matteis, F., Davies, A. M., Smith, L. L., Crofton-Sleigh, C., Venitt, S., Hewer, A., and Phillips, D. H. Genotoxic potential of tamoxifen and analogues in female Fischer F344/N rats, DBA/2 and C57Bl/6 mice and in human MCL-5 cells. *Carcinogenesis*, 13: 2197-2203, 1992.

White, I. N. H. The tamoxifen dilemma. *Carcinogenesis*, 20: 1153-1160, 1999.

Wijayaratne, A. L., Nagel, S. C., Paige, L. A., Christensen, D. J., Norris, J. D., Fowlkes, D. M., and McDonnell, D. P. Comparative analyses of mechanistic differences among antiestrogens. *Endocrinology*, 140: 5828-5840, 1999.

Wijayaratne, A. L. and McDonnell, D. P. The human estrogen receptor-alpha is a ubiquitinated protein whose stability is affected differentially by agonists, antagonists, and selective estrogen receptor modulators. *J.Biol.Chem.*, 276: 35684-35692, 2001.

Wooster, R., Neuhausen, S. L., Mangion, J., Quirk, Y., Ford, D., Collins, N., Nguyen, K., Seal, S., Tran, T., Averill, D., Fields, P., Marshall, G., Narod, S., Lenoir, G. M., Lynch, H., Feunteun, J., Devilee, P., Cornelisse, C. J., Menko, F. H., and et al Localization of a breast cancer susceptibility gene, BRCA2, to chromosome 13q12-13. *Science*, 265: 2088-2090, 1994.

Wormke, M., Stoner, M., Saville, B., and Safe, S. Crosstalk between estrogen receptor alpha and the aryl hydrocarbon receptor in breast cancer cells involves unidirectional activation of proteasomes [In Process Citation]. *FEBS Lett.*, 478: 109-112, 2000.

www. National Osteoporosis Soc. 1997. Ref Type: Internet Communication

www. Cancer Research Campaign. 2000. Ref Type: Internet Communication

www. Imperial Cancer Research Fund. 2000. Ref Type: Internet Communication

Xu, L., Glass, C. K., and Rosenfeld, M. G. Coactivator and corepressor complexes in nuclear receptor function. *Curr.Opin.Genet.Dev.*, 9: 140-147, 1999.

Xu, Z. and Clark, J. Characterization of uterine cytosol and nuclear sex steroid receptors in aging female ICR mice. *Proc.Chin Acad.Med.Sci.Peking.Union Med.Coll.*, 5: 207-212, 1990.

Yamashita, S., Newbold, R. R., McLachlan, J. A., and Korach, K. S. Developmental pattern of estrogen receptor expression in female mouse genital tracts. *Endocrinology*, 125: 2888-2896, 1989.

Yang, N. N., Bryant, H. U., Hardikar, S., Sato, M., Galvin, R. J., Glasebrook, A. L., and Termine, J. D. Estrogen and raloxifene stimulate transforming growth factor-beta 3 gene expression in rat bone: a potential mechanism for estrogen- or raloxifene-mediated bone maintenance. *Endocrinology*, 137: 2075-2084, 1996.

Yang, N. N., Venugopalan, M., Hardikar, S., and Glasebrook, A. Identification of an estrogen response element activated by metabolites of 17beta-estradiol and raloxifene. *Science*, 273: (pp 1222-1225), 1996.

Yang, X. and Lippman, M. E. BRCA1 and BRCA2 in breast cancer. *Breast Cancer Res.Treat.*, 54: 1-10, 1999.

Yoshii, A., Koji, T., Ohsawa, N., and Nakane, P. K. In-situ localization of ribosomal-rnas is a reliable reference for hybridizable rna in tissue-sections. *Journal Of Histochemistry & Cytochemistry*, 43: 321-327, 1995.

Young, L. J., Wang, Z. X., Donaldson, R., and Rissman, E. F. Estrogen receptor alpha is essential for induction of oxytocin receptor by estrogen. *Neuroreport*, *9*: 933-936, 1998.

Zhou, Y., Chorich, L., Mahesh, V. B., and Ogle, T. F. Regulation of estrogen receptor protein and mRNA by estradiol and progesterone in rat uterus. *J. Steroid Biochem. Molec. Biol.*, *46*: 687-698, 1993.

Zhou, Y., Matsuda, M., Sakamoto, S., and Mori, T. Changes in Uterine Microvessels as a Possible Pathogenic Factor in the Development of Adenomyosis Induced by Pituitary Grafting in Mice. *Acta Histochem. Cytochem.*, *32*: 387-391, 1999.

Zhu, B. T. and Conney, A. H. Functional role of estrogen metabolism in target cells: review and perspectives. *Carcinogenesis*, *19*: 1-27, 1998.